

FIRST

International Conference on Circular Economy and Sustainable Ecosystem

2024

Unlocking the Potential for Green Recovery

Conference Proceedings





The Open University of Sri Lanka



The Open University of Sri Lanka

Department of Mechanical Engineering

Proceedings

First International Conference on Circular Economy and Sustainable Ecosystem

IC²ESE 2024

November 21 - 22

Colombo, Sri Lanka

© Department of Mechanical Engineering, The Open University of Sri Lanka

All rights reserved. No part of this publication may be reproduced, stored in a retrieval system, or transmitted in any form or by any means—electronic, mechanical, photocopying, recording, or otherwise—without prior written permission from the Department of Mechanical Engineering, The Open University of Sri Lanka.

All articles included in these proceedings have been reviewed and accepted for publication. The responsibility for the content of each article lies solely with the respective authors.

Message from the Vice Chancellor

Dear Delegates, Scholars, and Esteemed Guests,

It is with great pleasure and a sense of responsibility that I welcome you to the International Conference on Circular Economy and Sustainable Ecosystem (IC²ESE 2024). This event, organized by the Department of Mechanical Engineering of the Open University of Sri Lanka (OUSL) in collaboration with the German Academic Exchange Service (DAAD), and National Science Foundation of Sri Lanka (NSF) serves as a significant platform for global thought leaders, researchers, practitioners, and policymakers to unite and address some of the most pressing challenges of our time.



The theme of IC²ESE 2024 resonates deeply with the collective urgency to reimagine how we produce, consume, and coexist within our finite planetary boundaries. The integration of circular economy principles with sustainable ecosystem management is no longer a mere aspiration but a necessity for securing the well-being of future generations.

I am particularly proud to highlight the collaborative efforts behind this conference. The partnership between the Department of Mechanical Engineering and DAAD underscores the value of international cooperation in fostering innovation and driving impactful change. The diversity of perspectives and expertise represented here promises to contribute profoundly to advancing knowledge and actionable solutions in this critical area.

As Vice Chancellor, I am honoured to support this conference, recognizing its alignment with our institutional commitment to fostering interdisciplinary collaboration and nurturing innovative solutions to global challenges. I encourage each of you to engage fully in the discussions, exchange ideas, and forge meaningful connections that extend beyond the confines of this event.

Let us take this opportunity not only to discuss but also to act upon the transformative strategies that will shape a more resilient and sustainable future. I wish you a productive and inspiring conference and look forward to the outcomes that will emerge from your collective wisdom and dedication.

Warm regards,

Snr. Prof. P. M. C. Thilakarathne

Vice Chancellor The Open University of Sri Lanka Sri Lanka

Message from the Conference Chair

It is with great pleasure that I, as the Conference Chair, present the successful conclusion of the international conference on Circular Economy and Sustainable Ecosystem, IC2ESE 2024 – A Transformative Step Towards a Greener Future. This conference is a significant milestone and a key outcome of the EU-funded Capacity Building in Higher Education project EUSL-Energy (Europe–Sri Lanka Capacity Building in Energy Circular Economy), which was implemented from 2020 to 2023.



Among the many achievements of the EUSL-Energy project is the launch of a joint Master's degree program titled Master of Science in Energy for

Circular Economy (MECE), collaboratively developed by four Sri Lankan universities. The program has already attracted more than 450 students across its first three cohorts, reflecting its strong relevance and demand. A key task within the project was also to organize an international conference to disseminate project outcomes and ensure the long-term sustainability of the initiative. IC2ESE 2024 is the direct outcome—and indeed, the enduring success—of that vision.

The conference, jointly organized with the German Academic Exchange Service (DAAD), was held on the 21st and 22nd of November 2024. It brought together leading academics, industry professionals, and policymakers to explore innovative pathways for green recovery and sustainable development. Discussions underscored the critical importance of circular economic principles in addressing global environmental and energy challenges.

The keynote sessions highlighted the nexus of sustainable engineering and education, presented pioneering research in green technologies, and shared advancements in renewable energy systems and circular living. These were complemented by a series of specialized technical sessions, engaging workshops, and a field visit, offering participants a comprehensive and enriching experience.

As we celebrate the success of IC2ESE 2024, I am pleased to announce that preparations are already underway for IC2ESE 2025, scheduled to take place on the 11th and 12th of December 2025. We warmly invite you to participate in next year's conference as we continue to foster collaboration and innovation for a greener, more sustainable future.

Torsten Fransson, CEO, EXPLORE Energy Sweden AB Prof. Em. Chair Heat and Power Technology [KTH], Sweden

Message from DAAD Regional Office New Delhi

On behalf of the German Academic Exchange Service (DAAD), I am delighted to extend my heartfelt congratulations to the Faculty of Engineering at The Open University of Sri Lanka for organizing the IC2ESE International Conference on Circular Economy and Sustainable Ecosystem (IC2ESE 2024).

As a proud co-sponsor of this significant event, DAAD is deeply committed to fostering academic and scientific exchange between Germany and countries worldwide, including Sri Lanka. Conferences such as IC2ESE



2024 provide an invaluable platform for academics, researchers, policymakers, and industry leaders to engage in meaningful dialogue on pressing global issues. The theme of this year's conference - the transformative potential of the circular economy resounds strongly with DAAD's mission to promote sustainability and innovation in education and research.

We are excited to see this hybrid event bring together participants from varied disciplines and places, creating opportunities to share insights and co-develop solutions for building resilient, sustainable ecosystems. It is through such collaborations that we can address global challenges and inspire the next generation of changemakers.

We commend the Faculty of Engineering for its vision and dedication in hosting this conference and look forward to the impactful discussions and partnerships it will foster.

Wishing all participants an enriching and successful IC2ESE 2024!

Warm regards,

Apoorv Mahendru Deputy Director & Head of Marketing DAAD Regional Office, New Delhi

Message from Conference Co-chair

It is with immense pride and gratitude that I welcome you all to the International Conference on Circular Economy and Sustainable Ecosystem (IC2ESE), hosted by the Mechanical Engineering Department of the Faculty of Engineering Technology, The Open University of Sri Lanka.

As a grantee of the DAAD Research Ambassadors Program, I initially envisioned hosting an Early Career Research Day to empower and support emerging researchers in this vital field. However, recognizing



the global importance of climate and environmental sciences, this initiative has been elevated into a fully-fledged international conference. This transformation allows us to address a broader audience and facilitate the exchange of knowledge and ideas on a global platform.

I extend my heartfelt appreciation to our distinguished keynote speakers, whose valuable insights and experience sharing enrich this conference and inspire us all. My gratitude also goes to the authors for their impactful research contributions, the dedicated committee members for their tireless efforts in organizing this event, and to all participants for their enthusiastic engagement, which breathes life into our discussions.

IC2ESE stands as a testament to our collective commitment to addressing the pressing challenges of waste management, energy management and environmental sustainability. I am confident this conference will foster meaningful collaborations and drive innovative solutions for a sustainable future.

Thank you all for contributing to the success of this event. Wishing you a rewarding and inspiring conference experience.

Warm regards,
Dr. (Mrs.) S. N. C. M. Dias
Conference Co-Chair
DAAD Research Ambassador for Sri Lanka

Message from the Conference Secretary

It is my great pleasure to welcome you to the International Conference on Circular Economy and Sustainable Ecosystem (IC2ESE 2024). As the Conference Secretary, I am proud to have been part of the dedicated team that worked hard to bring this important event to life.

IC2ESE 2024 provides an excellent platform for researchers, academics, industry leaders, and policymakers from around the world to share their knowledge, experiences, and innovative solutions. The focus on integrating circular economy principles with sustainable ecosystem practices is both timely and necessary, as the world faces urgent environmental and resource challenges.



Organizing a conference of this scale requires the tireless effort of many individuals and organizations. I sincerely thank our conference chair, co-chairs, coordinator, committee members, reviewers, sponsors, and all others who contributed to making this event a reality. I also express my deep appreciation to the authors and participants whose active involvement gives meaning to our work.

I encourage you to use this opportunity to network, exchange ideas, and form collaborations that will continue beyond this conference. Together, we can work towards a more resilient, resource-efficient, and sustainable future.

I wish you all a successful and inspiring conference experience.

Warm regards,
Eng. Dr. D. H. R. J. Wimalasiri
Conference Secretary
International Conference on Circular Economy and Sustainable Ecosystem (IC2ESE 2024)

Message from the Conference Coordinator

It is with great pride and anticipation that I welcome you to the International Conference on Circular Economy and Sustainable Ecosystem (IC2ESE 2024). As the Conference Coordinator and Head of the Department of Mechanical Engineering at The Open University of Sri Lanka, I am delighted to be a part of this impactful initiative.



This conference, hosted under the theme 'Unlocking the Potential for Green Recovery', addresses the urgent global need for

sustainable practices. It serves as a vital platform for researchers, industry experts, and policymakers to converge and explore strategies to integrate circular economy principles with ecosystem management. By fostering meaningful discussions, IC2ESE 2024 aims to inspire actionable solutions that address environmental challenges while promoting economic resilience.

The Department of Mechanical Engineering has taken a leading role in organizing this event in collaboration with esteemed partners such as the German Academic Exchange Service (DAAD) and the National Science Foundation of Sri Lanka (NSF). These partnerships reflect our commitment to advancing research, innovation, and education in sustainable development.

As the conference unfolds, I encourage all participants to actively engage in sessions, share insights, and collaborate on interdisciplinary approaches to address pressing global challenges. The collective expertise and diverse perspectives gathered here have the potential to pave the way for transformative solutions that will benefit both society and the environment.

I would like to express my heartfelt gratitude to the organizing committee, sponsors, and contributors whose dedication has made this conference possible. Let us use this opportunity to strengthen our commitment to building a sustainable future for generations to come.

I wish you all a productive and enriching experience at IC2ESE 2024.

Warm regards,

Eng. H. D. N. S. Priyankara Conference Coordinator Senior Lecturer / Head Department of Mechanical Engineering The Open University of Sri Lanka

Organizing Committee

Conference Chair: Torsten Fransson, CEO, EXPLORE Energy Sweden AB

(Prof. Em. Chair Heat and Power Technology [KTH, Sweden])

Conference Co-Chairs: Prof. N. S. Senanayake, Dr. Chamila Dias

Conference Secretary: Dr. Ruminda Wimalsiri

Conference Coordinator: Eng. H. D. N. S. Priyankara

Scientific Committee: Editorial and Publication Committee

Dr. Chamila Dias (Chair) Prof. N.S. Senanayake (Chair)

Prof. N. S. Senanayake Dr. Chamila Dias

Dr. Ravindu Lokuliyana Dr. KAC Udayakumar

Dr. Isuru Wijewardana Dr. B. G. D. A. Madushanka

Eng. Duminda Wijewardena Eng. Ruchira Abeyweera

Dr. Upuli Perera Dr. Sepalika Welikala

Dr. Sumith Baduge (UOR)

Ms. Hemali Pasqual

Dr. Duleeka Gunarathne (UOM) Dr. P. T. R. Dabare

Eng. Lekha Bakmeedeniya (UOP) Eng. Kamani Sylva

Publicity Committee Logistics Committee

Dr. P. T. R. Dabare (Chair) Dr. B. G. D. A. Madushanka (Chair)

Mr. Lakmal Perera Ms. Sumudu Jathunarachchi

Mr. Kosala Karunasena Eng. Lakmal Perera

Mr. Isuru Premarathne Eng. Ruchira Abeyweera

Mr. Nishantha Pathirana Ms. Prasadini Attapathu

Ms. Deema Danajanie

Mr. Akalanka Manchanayake

Keynote Speakers

Keynote Speaker 1: Dr. -Ing. Ranahansa Dasanayake

Keynote Speaker 2: Prof. Shiromi Karunarathne – Net-Zero Buildings

Keynote Speaker 3: Prof. Ajith De Alwis –Emerging Energy Technologies and Innovations

Keynote Speaker 4: Dr. Mayuri Wijayasundara - Circular Economy towards Energy

Web Master: Mr. Kanishka Indrajith Thennakoon

Conference Website: www.eusl.edu.lk/ic2ese/

Panel of Reviewers

Prof. N. S. Senanayaka

Mr. I. P. T. S. Wickramasooriya

Dr. B. G. D. Madushanka

Dr. Ruminda Wimalasiri

Dr. Rasika Perera

Mr. Ruchira Abeyweera

Dr. Sumith Baduge

Dr. KC Udayakumar

Ms. Sumudu Jathunarachchi

Dr. Chamila Dias

Dr. I. Aththanayaka

Dr. R. Lokuliyana

Prof. Saminda Fernando

Mr. D. C. Wijewardene

Ms. Nimalie Tennakoon

Mr. H. D. N. S. Priyankara

Dr. Ganila Paranawithana

Mr. Nipun Tantrigoda

Mr. H. S. Lakmal Perera

Ms Samantha Manawadu

Ms. Kamani Sylva

Prof. Shiromi Karunaratne

Dr. Chandana Jayawardana

Mr. P. D. SarathChandra

Mr. B. G. A. Dinesh

Dr. Thushara Subasinghe

Prof. Sanja Gunawardana

Dr. W. A. L. Nivanthi

Dr. Duleeka Gunarathne

Dr. Kasun De Silva

Dr. K. Jayawickrama C Kumara

Dr. Thushari Silva

Dr. Sewwandhi Chandrasekara

Prof. Anbahan Ariyadurai

Dr. Priyantha Bandara

Eng. Sugnada Somasundara

Prof. Shantha Egodoge

Eng. Ravi De Mel

Dr. Uthpala Jayawardana

Prof. Bandunee Athapattu

Prof. Saman Yapa

Dr. P. T. R. Dabare

Content

Μ	lessage from the Vice Chancellori
Μ	lessage from the Conference Chairii
Μ	lessage from DAAD Regional Office, New Delhiiii
	lessage from Conference Co- hairiv
Μ	lessage from the Conference Secretaryv
Μ	lessage from the Conference Coordinatorvi
0	rganizing Committeevii
Р	anel of Reviewersviii
1.	Solar and Wind-Based 6 kW Energy Module for Emergency Use1
	A. J. Mohamed Hijas, Chaminda Ranaweera
2.	Advances, Challenges, and Future Perspectives in Supercapacitor Developments for Electric Vehicles
	U. L. I. Udayantha, S. M. A. V. S. Tennakoon, S. N. C. M. Dias
3.	Performance Comparison of Dye-Sensitized Solar Cells Using <i>Elaeocarpus serratus</i> Red Leaf Dye Extracted with Various Polar Solvents
	S. Davisan, K. S. A. Panditharathna, C. N. Nupearachchi, and V. P. S. Perera
4.	Comprehensive Life Cycle Assessment of Hybrid and Electric Vehicles: Framework to Evaluate Sustainability in the Sri Lankan Context
	Bhanuka Samarasinghe, Anuradhi Rajapaksha
5.	Classification of End-Energy use in Wathupitiwala Export Processing Zone to Analyze the Feasibility of Switching to Alternative Energy Sources
	C. W. M. D. Chandrasekara, L. T. Jayasuriya, R. L. K. Lokuliyana ³
6.	Characterization and Analysis of Cellulose Extracted from Salvinia molesta 51 A. R. Abeyweera, A. M. P. B. Samarasekara
7.	Numerical Simulation of Stable 2D/3D Mixed-dimensional Perovskite Solar Cells with High Power Conversion Efficiency58
	W. G. A. Pabasara, U. K. D. M. Akmal, G. A. Sewvandi ¹
8.	Global Preparedness in Mitigating Environmental Impacts Of Renewable Energy 66 Nisitha Thushan Perera
9.	Lifecycle Impact Analysis of a Traditionally Manufactured Cotton Batik Shirt in Sri Lanka– Case Study77
	K. M. G. L. Karunarathna, T. D. Amarasooriya

Solar and Wind-Based 6 kW Energy Module for Emergency Use

A.J Mohamed Hijas1*, Chaminda Ranaweera2

¹General Directorate of Endowments, Ministry of AWQAF, Department of Investment, Doha, Qatar, ²National Grid Bristol, BS2 0TB, United Kingdom

hijasahi@yahoo.com*, charanaweera@yahoo.com

Abstract

Small-scale renewable energy systems are becoming more popular due to the recent development of small-scale energy technologies. The integration of these different technologies, forming a hybrid system, can be a realistic alternative to conventional fossil-fuel-powered engines for providing energy on a small scale, which could be a solution for addressing increasing global energy demand. An optimal design and analysis of the "Solar and Windbased 6 kW Energy Module for Emergency Use" (EMEU) are presented in this paper. This study aims to develop a standalone portable power system that provides electricity in refugee camps during the recovery from natural disasters or emergencies. In this study, a mobile container comprising solar, wind, and energy storage systems is designed to provide electricity for 100 Refugee Housing Units (RHU) in disaster situations. The preliminary analysis was done for the site Kalmatiya at Hambantota District in Sri Lanka. Demand forecasting of 100 RHUs was analyzed, and the daily and hourly load curves were developed accordingly. A detailed study of monthly wind potential is conducted for the selected location using hourly (every ten minutes) measured wind speed data at 25 m height for one year. The detailed Solar PV potential is analyzed by using PV-Sol simulation software. The cost and energy produced for solar and wind modules were estimated for several combinations to select the optimum combination to form a 6 kW EMEU. The optimum combination to meet the energy demand with an utterly renewable system is a 9.3 kW solar PV Module and a 6 kW wind module with a 28 kWh energy storage system for the particular site condition. The result is significant in mitigating the environmental issues compared to using only diesel engines; the amount of reduction of CO₂ by using the complete renewable system is 13.8 tons per annum.

Keywords: Energy Module for Emergency Use, Integration of Wind Energy and Solar PV

1 Introduction

Small-scale renewable energy systems are becoming more popular due to the recent development of small-scale energy technologies and the global increase in energy demand. Integration of these different technologies, forming a hybrid system, can be a realistic alternative to conventional fossil fuel-powered engines to provide energy in small communities. Among these energy systems, the renewable ones, such as wind, solar, and biomass, are even more attractive due to rising fossil fuel prices and environmental impacts [1, 2]. So far, vast renewable energy resources such as wind and solar have not been sufficiently harnessed for electricity generation in Sri Lanka. The combinations of different types of renewable energy, such as wind and solar, coupled with energy storage units, such as batteries and gas/diesel engines as backup, provide a stand-alone energy system.

According to the wind energy resource atlas of Sri Lanka developed by the National Renewable Energy Laboratory (NREL) of the United States, there are $5,000~\rm km^2$ of windy areas with good to excellent wind resource potential in Sri Lanka. The windy area represents about 6% of the total land area of Sri Lanka, and this windy area could support $24,000~\rm MW$ [3]

Sri Lanka is situated close to the equator, therefore receives an abundant supply of solar radiation year-round. Solar radiation over the island does not show a marked seasonal variation, though significant spatial differentiation could be observed between the lowlands and mountain regions. Over most parts of the flat dry zone, which accounts for two-thirds of the land area, solar radiation varies between $4.5 - 6.0 \, \text{kWh/m}^2/\text{day}$. Solar radiation levels remain as low as $2.0 - 3.5 \, \text{kWh/m}^2/\text{day}$ over the high plains of hill country due to the significant cloud cover over most parts of the day [4]. Thus, a substantial potential exists in the dry zone of Sri Lanka for harnessing solar energy.

The main objective of this study is to design a small hybrid solar PV/wind/energy storage electrical system for the emergency energy module. The design of the electrical system includes finding the optimum combination of wind and solar PV for a typical location in Sri Lanka while considering the actual possible generation from the wind turbine and solar PV modules. In this work, a wind and solar-based 6 kW energy module called "mobile container" is proposed with a focus on providing electricity for emergency needs in Sri Lanka.

2 Literature Review

2.1 Hybrid Energy System Using Wind and PV Solar

In the study [5], designing and analysing the "Electric Power System of an Emergency Energy Module", it mobile system is designed for power supply in refugee camps and during the recovery of natural disasters. It is an independent power system comprising solar, wind, and biomass-based power generation and control. The design and analysis of the electric power system is mainly focused on increasing the renewable energy efficiency of the system while saving excess power on the battery bank and controlling the battery discharging.

According to another study [6], small-scale renewable energy systems are becoming more popular due to the recent development of small-scale energy technologies and the global increase in energy demand. A renewable hybrid energy system consists of two or more energy sources, power conditioning equipment, a controller, and an optional energy storage system. These hybrid energy systems are becoming popular in remote areas with power generation applications due to advancements in renewable energy technologies and a substantial rise in the prices of petroleum products.

One of the options for building isolated power systems is by hybridizing renewable power sources like wind, solar, micro-hydro, etc., along with appropriate energy storage [7]. The simple and novel methodology proposed is based on the principles of process integration. It finds the minimum battery capacity when the availability and ratings of various renewable resources, as well as load demand, are known. The battery sizing methodology is used to determine the sizing curve and thereby the feasible design space for the entire system.

2.2 Wind Data Analysis and Resource Estimation

2.2.1 The method of Bin

There are several ways to summarize the data concisely, allowing for an evaluation of the wind resource or wind power production potential of a specific site [8]. The method of bins provides a way to summarize wind data and to determine expected turbine productivity. The data must first be separated into the wind speed intervals or bins in which they occur. It is most convenient to use the same size bins.

2.2.2 Weibull probability density function

Use of the Weibull probability density function requires knowledge of two parameters: k, a shape factor, and c, a scale factor. The Weibull probability density function and the cumulative distribution function are given by [8]

$$F(U) = 1 - \exp\left(-\left(\frac{U}{c}\right)^k\right)$$

for the Weibull distribution, it is possible to determine the average velocity as follows [8]

$$\overline{U} = c \Gamma \left(1 + \frac{1}{k} \right)$$

Where $\Gamma(x) = \text{gamma function} = \int_0^\infty e^{-t} t^{x-1} dt$

2.2.3 Wind Turbine Energy Production Estimates Using Statistical Techniques

For a given wind regime probability density function, p(U), and a known turbine power curve, Pw(U), the average wind turbine power, $\overline{P}w$, is given by

$$\bar{P}_{\rm w} = \int_0^\infty {\rm Pw} \, ({\rm U}) \, p({\rm U}) \, dU$$

assuming a constant value for drive train efficiency, another expression for the average wind machine power is given by

$$\bar{P}_{\rm w} = \frac{1}{2} \rho \pi R^2 \eta \int_0^\infty C_p(\lambda) U^3 p(U) dU$$

tip speed ratio $-\lambda$ radius of the wind rotor -R drive train efficiency $-\eta$

2.3 Study of Wind Turbine

A 1kW wind mill with its controller and inverter is used for the wind power generating module for the EEM selected.

Specifications

• Model: FD1000

Type: 3 blades upwindRotor diameter: 3.0m

Start-up wind speed: 2.5m / s (5.6mph)
Cut-in wind speed: 3m/s (6.7mph)
Rated wind speed: 9m/s (20.1mph)

Rated power: 1000 W
Maximum power: ~1300 W

Furling wind speed: 12m/s (27mph)Over speed protection: auto furl

Generator: permanent magnet alternator

• Output form: 48VDC nominal

2.4 Study of Solar PV Module

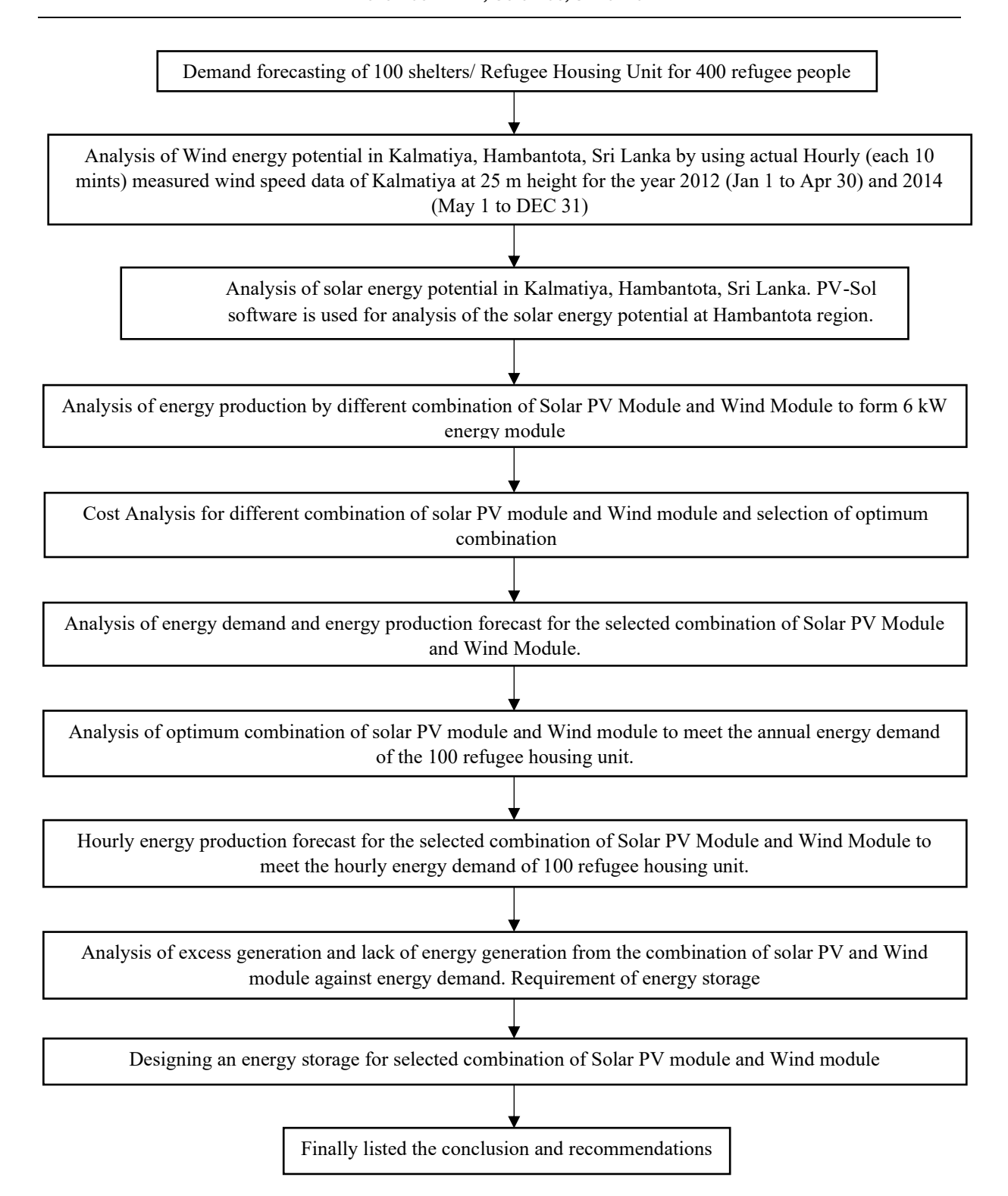
Jinko JKM465 M-7RL3 solar module is selected for the design, which has a lifetime of 25 years and a 20.71% efficiency. Electrical characteristics of Jinko JKM465 M-7RL3 in standard test conditions are given in the following Table 01

Table 01 Electrical characteristics of Jinko JKM465 M-7RL3 in standard test conditions

Maximum Power (Pmax)	465Wp
Maximum Power Voltage (Vmp)	43.18V
Maximum Power Current (Imp)	10.77A
Open-circuit Voltage (Voc)	51.92V
Short-circuit Current (Isc)	11.59A
Module Efficiency (%)	20.17%
Maximum system voltage	1000/15000VDC
Dimension	2182 x 1029 x 40 mm

3 Methodology

This study adopts a systematic approach to designing a hybrid solar PV and wind energy system for emergency energy use. The methodology is structured to achieve the objective of determining the optimal combination of solar PV and wind modules while ensuring the energy needs of refugee housing units are met effectively. This methodology ensures a data-driven, analytical approach to optimizing hybrid solar PV and wind energy systems for emergency applications



4 Demand Forecasting of 100 Shelters for 400 Refugee People

Reference to the shelter and settlement guidelines by the European Commission and the shelter design catalogue 2016 by UNHCR, the minimum required electric power requirements for the Refugee Housing Unit (RHU) were collected.

One 10 W LED light and 50 W power socket for mobile chargers are considered for one Refugee Housing Unit (RHU). The office is equipped with LED lights, a power outlet for a laptop, and a mini refrigerator for medical Aid. According to the study, the modern mini fridges are working 30% - 50% of the time if the fridge is not opened frequently [9].

5W LED lights are selected for outdoor lighting outside of each refugee housing unit. 20 units of common toilets are illuminated with 5W LED light and 5W small ventilation fan.

a. Hourly Load Curve of 100 Refugee Housing Units (RHU)

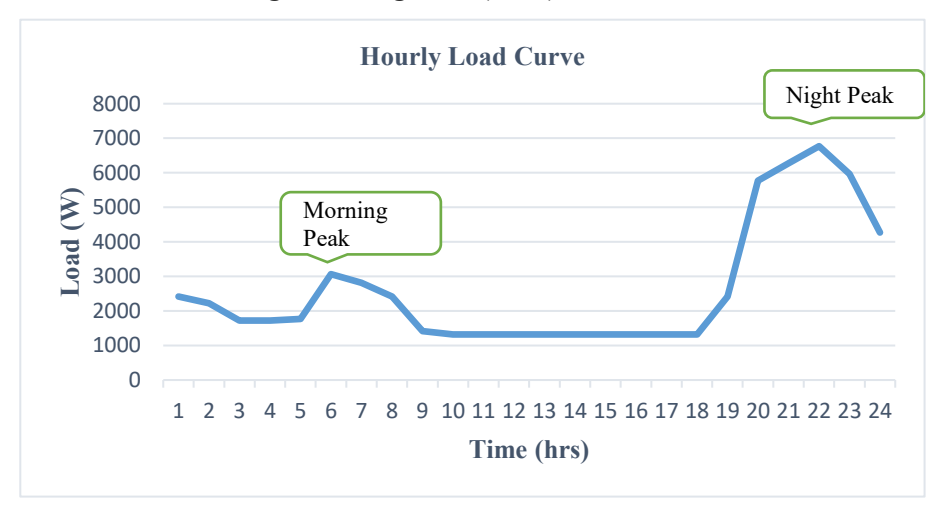


Fig. 1 The Hourly Load Curve of 100 Refugee Housing Units (RHU)

Fig. 1 illustrates the hourly load curve of 100 Refugee Housing Units (RHU). The morning peak load is thought to result from people waking up and preparing for work or morning activities; therefore, the indoor lights in the RHUs are turned on, and more phones are connected to outlets for charging. These electrical devices connected to the power system contribute to the morning peak load.

Daytime load is assumed as the base load. Laptops, refrigerators, a minimum number of ventilation fans, and outdoor and indoor lights connected to the power system cause daytime load.

The night peak load is assumed to be due to outdoor lighting, indoor lighting, ventilation fans, people coming back from work, and plugging more phone chargers into the sockets.

5 Estimation of Wind Energy Potential in Kalmatiya, Hambantota. Sri Lanka

According to the National Renewable Energy Laboratory NREL, the wind power class for Kalmatiya is class 4 with an average wind speed of 7-7.5 m/s at 50 m height [3] and solar resource Annual 4.50-05 (kWh/m²/day) according to the NREL Map [4].

Hourly (each 10 minutes) measured wind speed data of Kalmatiya at 25 m height for the year 2012 (Jan 1 to Apr 30) and 2014 (May 1 to DEC 31) are used for the analysis (Source: Sustainable Energy Authority of Sri Lanka). The wind energy potential of each month has been calculated separately

The probability distribution of wind speeds, actual power output from the wind turbine, and capacity factor of the FD 1000 wind turbines were analyzed for each month separately for the one-year period.

Step 01 - Separated the hourly (every 10 minutes) wind speed data for each month from the annual hourly wind speed data

Step 02 - Create a bin that consists of different wind speeds from 0 to 25 m/s. By using the histogram function in Excel, we created the frequency of different wind speeds from the 10-minute wind speed data for each month.

Step 03 - Create the percentage of fractions of different wind speeds and draw the histogram, which shows the probability of distribution of wind speed for each month.

Step 04 - Create the Weibull distribution with the mean speed of each month, assuming the shape factor k=2, then calculate the scale factor, c, from the following equation [8].

$$\overline{U} = c \Gamma \left(1 + \frac{1}{k} \right)$$

$$c = \frac{\overline{U}}{e^{\left(\Gamma\left(1 + \frac{1}{k}\right)\right)}}$$

Where
$$\Gamma(x) = \text{gamma function} = \int_0^\infty e^{-t} t^{x-1} dt$$

By using values of shape factor k and scale factor c, create the Weibull distribution function in Excel for each wind speed bin and draw the Weibull distribution on the existing wind speed histogram.

Step 05 - Find the wind power density for each wind speed by using the wind speed and Weibull distribution value for each wind speed in the bin from the following equation [8].

Wind power density = (½ * air density * wind speed ^3 * Weibull distribution value) W/m²

Step 06 - Adjusting the shape factor k value to match the Weibull distribution curve with the existing wind speed histogram by comparing average wind power density from the Weibull method and the direct method.

Step 07 - Multiplying the wind power density for each speed with the wind turbine swept area and the power coefficient of the wind turbine will give the actual power output from the wind turbine each month.

$$Cp = \frac{power\ extracted\ by\ the\ turbine}{total\ wind\ power}$$

The Highest wind potential is recorded at Kalmatiya in July.

Fig. 2 demonstrates the wind speed probability density function. The Weibull parameter (k), which describes the breadth of distribution of wind speed over the month, is 3.19, and the scale factor (c) is 7.10 m/s. The average wind power density for July at Kalmatiya is 214.79 W/m². The capacity factor of the FD 1000 wind turbine is 46%.

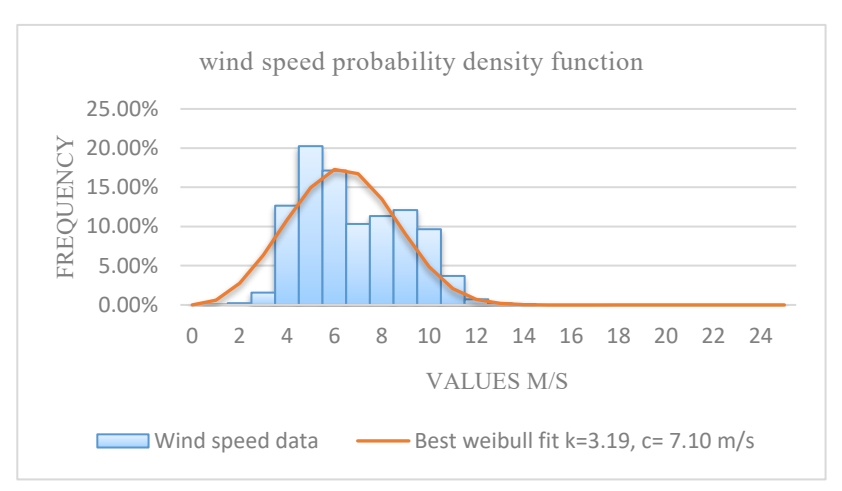


Fig. 2 The wind speed probability density function

Table 2 presents a summary of the wind energy potential estimation at Kalmatiya at a height of 25 m.

Table 2 The summary of the estimation of wind energy potential at Kalmatiya at 25 m height

S.No	Month	Wind Power Density(W/m ²)	Capacity factor
1.	January	54.34	12%
2.	February	51.96	11%
3.	March	39.34	09%
4.	April	53.87	12%
5.	May	99.34	22%
6.	June	172.64	38%
7.	July	214.79	46%
8.	August	148.95	33%
9.	September	112.72	25%

10.`	October	56.84	12%
11.	November	40.52	09%
12	December	27.54	06%

6 Solar Energy Potential in Hambantota. Sri Lanka

According to solar Resource Assessment for Sri Lanka and Maldives by National Renewable Energy Laboratory NREL, annual solar resource at Hambantota is 4.50 - 05 (kWh/m²/day) [4].

PV-Sol software is used for analysis of the solar energy potential at Hambantota region. 1.4 kW PV module and 10 years' solar data's used to analysis the possible solar PV generation. The table 3 below shows the monthly possible energy generation by a selected 1.4 kW PV module. Jinko JKM465M-7RL3 solar module is selected for the design.

Month	Total solar Irradiation (kWh/m²)	Energy generated by solar PV module (kWh)	Capacity Factor
January	160.25	178.12	0.18
February	149.70	171.58	0.17
March	172.10	192.46	0.19
April	161.82	164.01	0.16
May	153.11	131.65	0.13
June	144.34	127.01	0.13
July	151.12	133.49	0.13
August	161.73	158.06	0.16
September	153.24	167.21	0.17
October	157.70	178.45	0.18
November	134.13	149.76	0.15
December	145.62	160.82	0.16

Fig. 3 shows the monthly energy production for a 1.4 kW PV module at Hambantota. The chart is taken from the PV Sol software simulation result for the modeling of a 1.4 kW Solar PV module system.



Fig. 3 Monthly energy production for a 1.4 kW PV module at Hambantota

7 Analysis of Cost and Energy Production by Different Combinations of Solar PV Modules and Wind Modules

7.1 Analysis of Energy Production by Different Capacities of Solar PV Modules

The energy production forecast for different capacities of solar PV modules was obtained from PVsol software modeling and simulation to determine the optimal combination of solar PV modules and wind modules for a 6 kW emergency energy module.

Table 4 below shows the summary of the energy generated by different capacities of solar PV modules. The energy generated by different PV modules is taken from the PV Sol software simulation outputs.

Month	Energy generated by 1.4 kW PV	Energy generated by 2.3 kW PV	Energy generated by 3.3 kW PV	Energy generated by 4.2 kW PV	Energy generated by 5.2 kW PV
	Module (kWh)				
January	178.12	315.05	408.23	552.61	722.28
February	171.58	289.73	382.31	521.17	664.38
March	192.46	318.93	446.19	579.39	753.69
April	164.01	255.80	409.81	483.10	658.40
May	131.65	217.61	338.04	412.77	575.16
June	127.01	212.65	316.71	389.76	537.47
July	133.49	221.91	336.80	414.53	570.55
August	158.06	248.49	396.88	471.42	646.14
September	167.21	269.99	399.66	495.43	659.55
October	178.45	301.45	408.95	547.41	703.74
November	149.76	260.70	345.92	461.87	603.88
December	160.82	282.11	372.73	498.42	661.64

Table 4 Summary of the energy generated by different capacities of solar modules

7.2 Analysis of Energy Production by Different Combinations of Wind Modules

A summary of the energy generated by different capacities of wind turbine modules is shown in Table 5. The outputs of the estimation of Wind Energy Potential in Kalmatiya, Hambantota. Sri Lanka is used to form different capacities and energy production of different wind modules

Month	Energy	Energy	Energy	Energy	Energy
	generated by				
	1kW Wind	2kW Wind	3kW Wind	4 kW Wind	5 kW Wind
	Module (kWh)				
January	85.80	171.60	257.40	343.20	429.00
February	77.00	154.00	231.00	308.00	385.00
March	63.86	127.72	191.58	255.44	319.30
April	84.90	169.80	254.70	339.60	424.50
May	161.20	322.40	483.60	644.80	806.00
June	272.10	544.20	816.30	1088.40	1360.50
July	340.07	680.14	1020.21	1360.28	1700.35
August	241.80	483.60	725.40	967.20	1209.00
September	177.30	354.60	531.90	709.20	886.50
October	92.07	184.14	276.21	368.28	460.35
November	63.60	127.20	190.80	254.40	318.00
December	43.71	87.42	131.13	174.84	218.55

Table 5 Summary of the energy generated by different capacities of the Wind Turbine module

7.3 Cost Analysis for Different Combinations of Solar PV Modules and Wind Modules

The cost analysis is shown in Table 6 below to find the optimum combination of different capacities of solar PV modules and wind modules to form a 6 kW emergency energy module for Sri Lankan coastal conditions by

considering the cost and energy produced by solar PV modules and wind modules. Five different combinations of solar PV modules and wind modules were taken into consideration for the analysis.

The CEB Long Term Generation Expansion Plan 2020 – 2039 document's Investment Plan for Major Wind & Solar Developments (Base Case), 2020-2039 [12] is used for the cost analysis of the wind module and solar module. The cost included only the pure construction cost of power plants and excluded the cost for feasibility, EIA, pre-construction, detailed design, etc.

Combination			Annual Energy	Approximate	
	Solar PV Module (kW)	Wind Module (kW)	yield (kWh)	Implementation cost (LKR)	
Α	1.4 kW	5 kW	10429.65	1,209,596.50	
В	2.3 kW	4 kW	10008.04	1,128,879.46	
С	3.3 kW	3 kW	9672.43	1,061,823.62	
D	4.2 kW	2 kW	9234.72	981,106.57	
E	5.2 kW	1 kW	9460 31	914050 72	

Table 6 Summary of the cost analysis of different combinations of Solar PV and wind modules

As per analysis of the wind and solar energy potential distribution, analysis of energy produced by different combinations of wind and solar PV modules and cost analysis, the best combination for the 6 kW energy module for emergency use is combination B which is the combination of 2.3 kW solar PV module and 4 kW wind turbine.

8 Analysis of Energy Production Forecast for Combination of 2.3 kW Solar PV Module and 4 kW Wind Module.

Table 7 below shows the energy generation of the optimum combination of solar PV and wind module to form the 6 kW emergency energy module at Kalmatiya, Hambantota, Sri Lanka.

The total annual energy generation from the optimum combination of 2.3 kW solar PV and 4 kW wind module is 10,008.4 kWh, but the annual energy demand forecasting of 100 Refugee Housing Units (RHU) is 22,995 kWh. So, the optimum combination of solar and wind modules can share 44% of the total annual energy demand of the refugee housing unit.

Month	Total solar Irradiation	Energy generated by 2.3 kW PV Module		
	(kWh/m ²)	(kWh)	height (m/s)	by 4kW Wind Module (kWh)
January	160.25	315.05	3.69	343.2
February	149.70	289.73	3.86	308.00
March	172.10	318.93	3.39	255.44
April	161.82	255.80	3.64	339.60
May	153.11	217.61	4.59	644.80
June	144.34	212.65	5.89	1088.40
July	151.12	221.91	6.36	1360.28
August	161.73	248.49	5.50	967.20
September	153.24	269.99	4.86	709.20
October	157.70	301.45	3.62	368.28
November	134.13	260.70	3.37	254.40
December	145.62	282.11	2.88	174.84
Annual	1844.9	3194.4	4.30	6813.64

Table 7 Energy generation of an optimum combination of solar PV and Wind module

8.1 Analysis of Optimum Combination of Solar PV Module and Wind Module to Meet the Annual Energy Demand of The 100 Refugee Housing Unit.

The approach of the analysis is to find the capacity of the solar PV module for different sizes of the wind module. The average annual energy generation from a 1 kW wind module is 1703.41 kWh, and the average capacity factor for the solar PV module is 0.16. The solar PV module capacity to meet the energy demand is calculated by using the average capacity factor for the solar PV module at the selected location. Table 10 shows the different combinations of solar PV modules and wind modules to meet the demand of 100 RHUs and their total cost of each combination.

The optimum combination of solar PV Module and Wind Module to meet the demand is 6 kW wind module and 9.11 kW solar PV Module with considering solar and wind potential analysis and the cost. Our target is not only to minimize the cost but also to utilize green energy to fulfill our energy demand, hence the combination F selected, which produces almost equal energy from solar, wind modules, and the cost is competitive compared to other combinations.

Wind Module Capacity (kW)	Energy Generated by Wind Module (kWh/year)	Energy Needed to Be Generated by Solar PV Module to Meet the Demand (kWh/year)	Solar PV Module Capacity (kW) Combination		Approximated Implementation cost for a combination of solar PV and Wind Module (LKR)
1	1703.41	21291.59	15.19	A – 1 kW, 15.19 kW	2,278,931
2	3406.82	19588.18	13.98	B – 2 kW, 13.98 kW	2,316,570
3	5110.23	17884.77	12.76	C – 3 kW, 12.76 kW	2,354,208
4	6813.64	16181.36	11.54	D – 4 kW, 11.54 kW	2,391,847
5	8517.05	14477.95	10.33	E – 5 kW, 10.33 kW	2,429,486
6	10220.46	12774.54	9.11	F – 6 kW, 9.11 kW	2,467,125
7	11923.87	11071.13	7.90	G – 7 kW, 7.90 kW	2,504,764
8	13627.28	9367.72	6.68	H - 8 kW, 6.68 kW	2,542,403
9	15330.69	7664.31	5.47	I – 9 kW, 5.47 kW	2,580,041
10	17034.10	5960.90	4.25	J – 10 kW,4.25 kW	2,617,680

Table 10 Different combinations of solar PV and wind modules to meet the demand

8.2 Hourly Energy Production Forecast and Demand for the Combination of 9.3 kW Solar PV Module and 6 kW Wind Module.

The hourly annual energy generated by the 6 kW wind module is calculated for a year. PV Sol software is used to model the 9.3 kW Solar PV Module, and hourly energy generated data is taken from the simulation.

The hourly energy demand for the 100 refugee housing units is compared against the hourly energy production from the combination of 9.3 kW Solar PV Module and 6 kW Wind Module, and the excess energy generation and lack of energy generation from the combination of Solar PV and Wind module. So, the requirement for an energy storage battery bank is proposed. The excess energy produced needs to be stored, and energy needs to be transferred from energy storage units to meet the energy demand.

9 Designing Energy Storage for 9.3 kW Solar PV Module and 6 kW Wind Module

Capacity

Factor Solar

Wind

0.11

0.12

0.09

0.12

0.22

The lowest capacity factor offering month is December for the combination of Solar and Wind Energy resources; therefore, the analysis is carried out for December. The average hourly electricity demand and the possible average electricity generation from solar and wind are calculated for this analysis.

7	Jan	Feb	Mar	Apr	May	Jun	Jul	Aug	Sep	Oct	Nov	Dec
	0.18	0.17	0.19	0.16	0.13	0.13	0.13	0.16	0.17	0.18	0.15	0.16

0.38

0.46

0.33

0.25

0.12

0.09

0.06

Table 11. Monthly capacity factor for the solar and wind at Kalmatiya, Hambantota

(a) Hourly Electricity Generation from a Combination of 9.3 kW PV Module and 6 kW Wind Module in A Selected Week in December

A typical one-week energy demand for 100 refugee housing units (RHU) and energy generation from 12th December to 18th December by a combination of 9.3 kW solar PV module and 6 kW wind module is used to find the battery energy storage requirement.

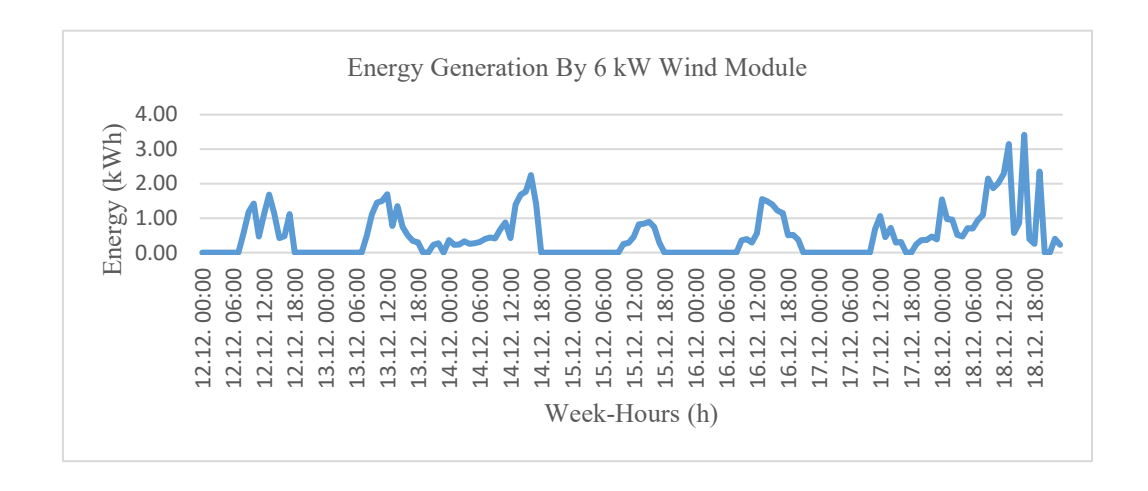


Fig. 4 Hourly electricity generation from a 6 kW Wind module in a selected week in December

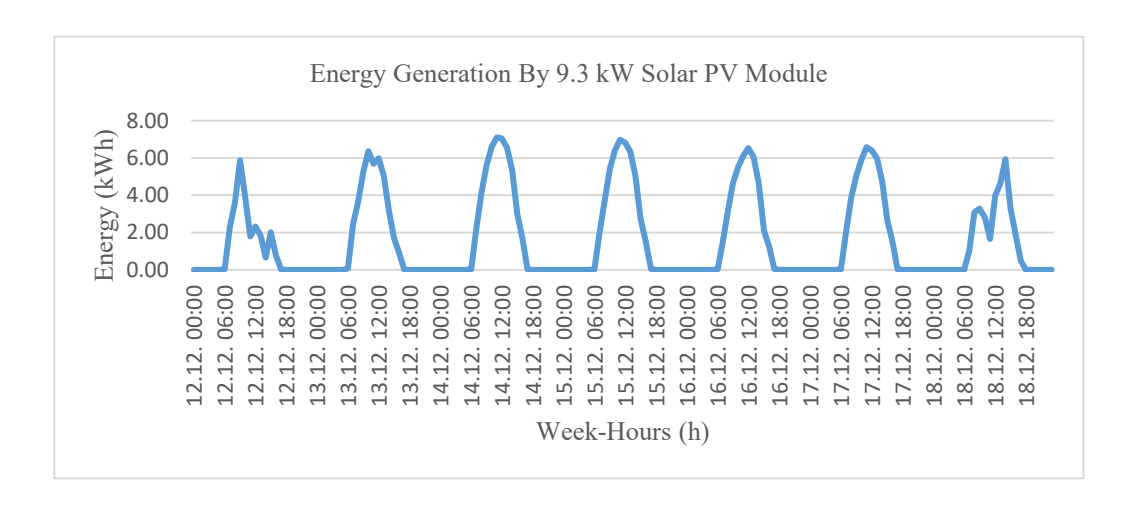


Fig. 5 Hourly electricity generation from 9.3 kW Solar PV and 6 kW Wind module in the selected week in December

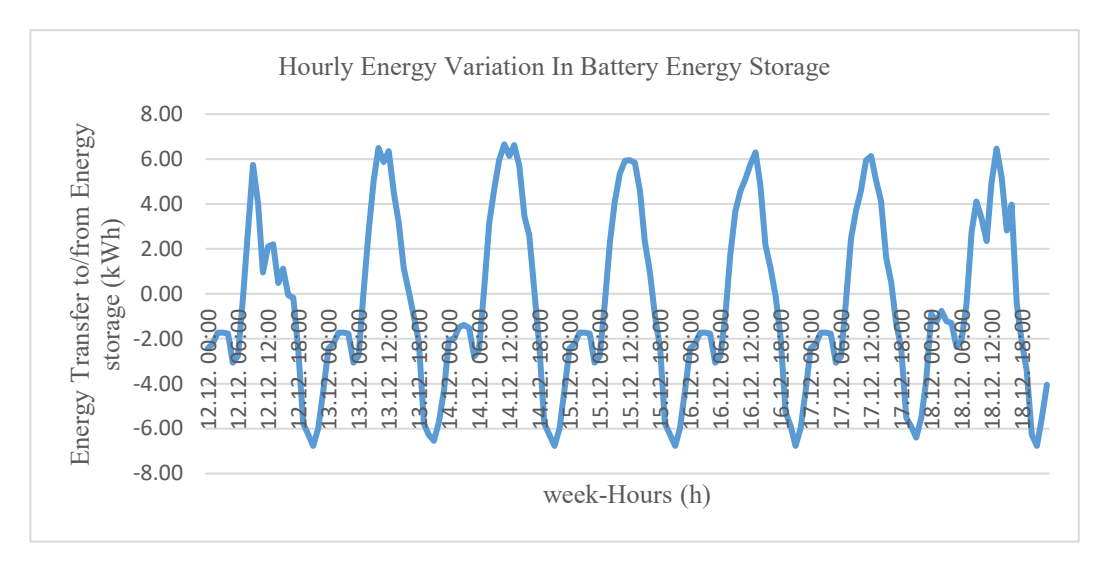


Fig. 6 Hourly electricity generation from 9.3 kW Solar PV and 6 kW Wind module in the selected week in December

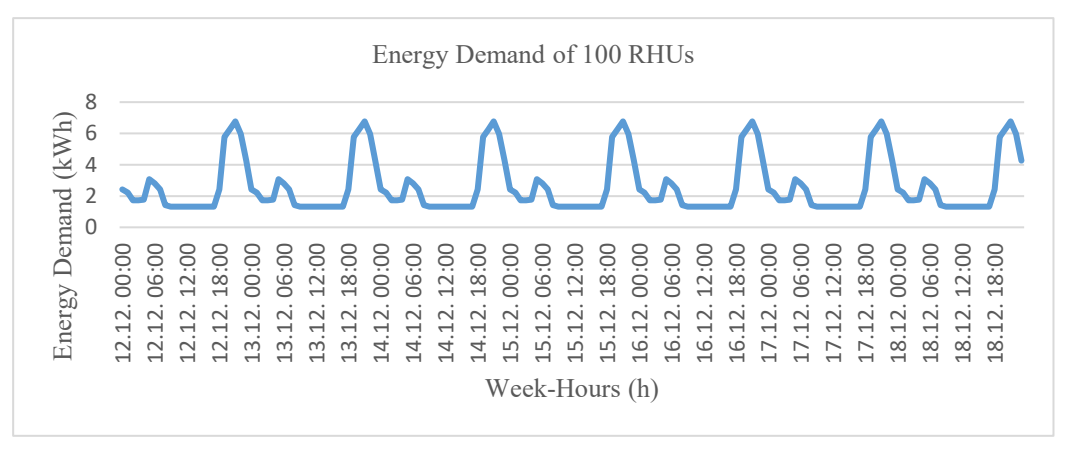


Fig. 7 Hourly Average Energy Demand Variation for a selected Week in December

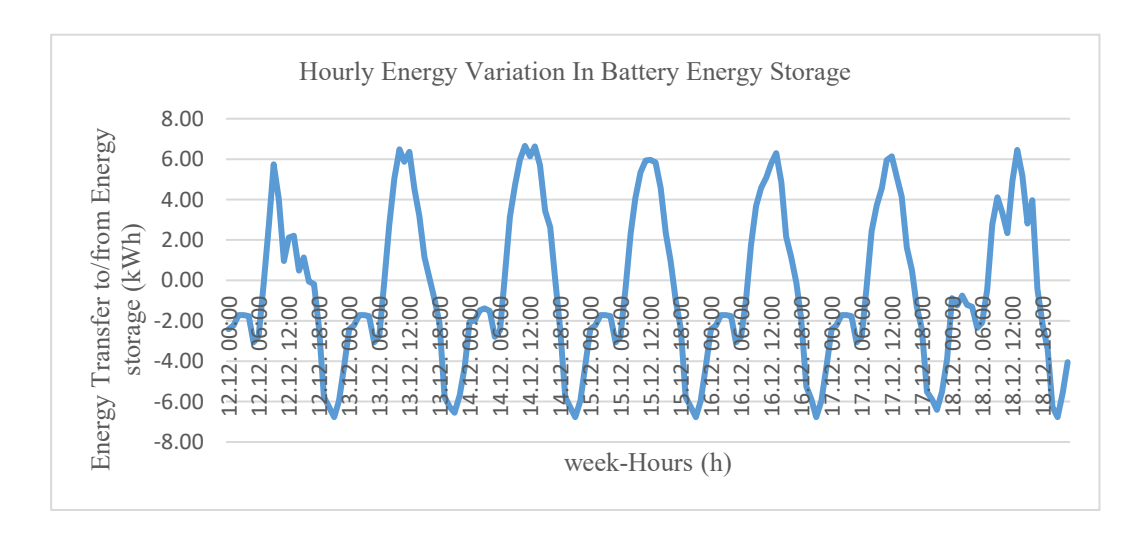


Fig. 8 Hourly Average Energy Storage and Discharge Variation for a selected Week in December

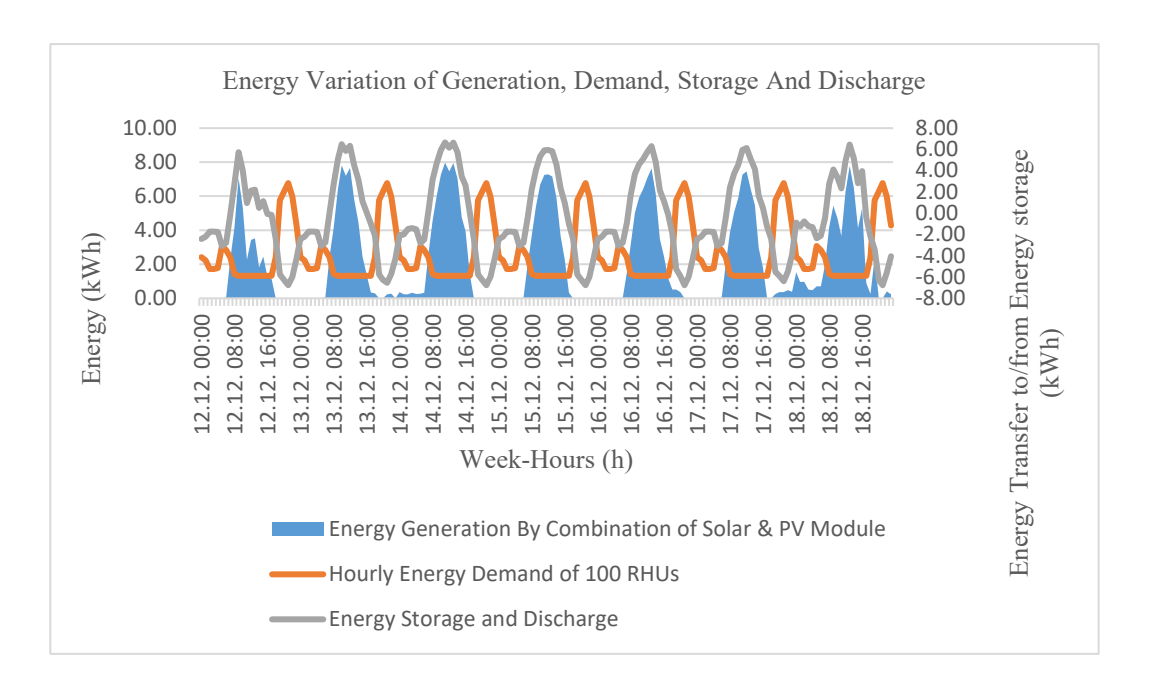


Fig. 9 Hourly Averaged Energy Generation, Demand, Storage, and Discharge Variation for a selected week in December

(b) Summary of the Analysis

Referring to the hourly averaged energy generation, demand, storage, and discharge variation for a week in December from 12th December to 18th December, it was observed that the maximum energy needed to be transferred from energy storage is 28 kWh. Therefore, the energy storage capacity requirement for the implementation of a renewable system with a 9.3 kW solar PV installation and a 6 kW wind power installation is 28 kWh.

Date and Duration	Energy Transfer From / To Energy Storage (kWh)			
12.12. 08:00 To 13.12. 07:00	-27.98			
13.12. 08:00 To 14.12. 07:00	-9.79			
14.12. 08:00 To 15.12. 07:00	-2.52			
15.12. 08:00 To 16.12. 07:00	-11.78			
16.12. 08:00 To 17.12. 07:00	-11.08			
17.12. 08:00 To 18.12. 07:00	-7.11			

Table 16 Energy transfer From/To energy storage for the selected week

10 Discussion

Considering the wind and solar energy potential distribution, analysis of Energy produced by different combinations of wind module and solar PV module, and the cost analysis, the best combination to construct a 6 kW Energy Module for Emergency Use is a combination of a 2.3 kW solar PV module and a 4 kW wind turbine.

The total annual energy generation from the optimum combination of solar and wind modules is 10,008.4 kWh but the annual energy demand forecast of 100 RHUs is 22,995 kWh. So, the 6 kW EEM combination of solar and wind modules can share 44% of the total annual energy demand of 100 RHUs.

The 6 kW EEM can be used with a combination of an 8 kVA auto-start diesel backup generator in order to meet the demand, which can be an alternative solution for complete conventional fuel-powered energy generators.

The amount of CO₂ produced by conventional diesel fuel is 0.6 kg for 1 kWh [13]. Hence, the reduction of CO₂ by using a combination of solar and wind-based 6 kW EEM with a backup generator to provide energy for 100 RHUs is 6 tons per annum.

The solution to meet the demand of 100 RHUs with a complete renewable system is a combination of 9.3 kW solar PV module and 6 kW wind module with a 28 kWh energy storage system. The amount of reduction of CO₂ by using a complete renewable system is 13.8 tons per annum.

11 Conclusion

The new trends in the energy sector mainly concern energy security and sustainable development across the globe. The role of renewable energy has therefore become ever more significant. The developed countries are already on track to walk out of the fossil fuel era and are focusing mainly on the areas of renewable energy technologies and energy efficiency. Through this study summary of the renewable energy potential of Sri Lanka was given. It was identified that Sri Lanka has the potential power generation of wind and solar energy. The southern part of the southern coastal and western coastal areas is suitable for wind and solar power generation. The actual measured site data of wind speed and solar irradiation have been used for the analysis and calculations. The analysis work has been carried out considering that the system supplies its maximum power capacity of solar and wind modules continuously, and no reactive components were considered in the system. The solution to meet the demand of 100 RHUs with a complete renewable system is a combination of 9.3 kW solar PV module and 6 kW wind module with a 28 kWh energy storage system.

References

- [1] P. Nema, R. Nema and S. Rangnekar, "A current and future state of art development of hybrid energy system using wind and PV-solar: A review," Renewable and Sustainable Energy Reviews, vol. 13, no. 8, p. 2096–2103, 2009.
- [2] B. Wichert, "PV-diesel hybrid energy systems for remote area power generation A review of current practice and future developments," Renewable and Sustainable Energy Reviews, vol. 1, no. 3, p. 209–228, 1997.
- [3] Wind Energy Resource Atlas of Sri Lanka and the Maldives, D. Elliott, M. Schwartz, G. Scott, S. Haymes, D. Heimiller, R. George. National Renewable Energy Laboratory, August 2003, page 49
- [4] Solar Resource Assessment for Sri Lanka and the Maldives, Dave Renne, Ray George, Bill Marion, Donna Heimiller. National Renewable Energy Laboratory, August 2003, page 16.
- [5] C. Ranaweera, Electric power system of an emergency energy module, Stockholm: Department of Energy Technology, KTH, Royal Institute of Technology, 2012.
- [6] P. Nema, R. Nema and S. Rangnekar, "A current and future state of art development of hybrid energy system using wind and PV-solar: A review," Renewable and Sustainable Energy Reviews, vol. 13, no. 8, p. 2096–2103, 2009.
- [7] E. Sreeraj, K. Chatterjee and S. Band, "Design of isolated renewable hybrid power systems," Solar Energy, vol. 84, no. 7, p. 1124–1136, 2010.
- [8] J.F Manwell's, J.G Mc Gowan, A. L. Rogers, Wind Energy Explained. Theory, Design and Application 2010, Chapter 2, Second edition, WILEY
- [9] "How many watts does a mini fridge use" Accessed on: Sep. 18. 2020. [Online]. Available: https://smartkitchenimprovement.com/how-many-watts-does-a-mini-fridge-use/
- [10] "CEB Annual report 2018 PDF" Accessed on: Sep. 18. 2020. [Online]. Available: https://ceb.lk/publication-media/annual-reports/en
- [11] "Study report on electricity demand curve and system peak reduction 2012 PDF" Accessed on: Sep. 18. 2020. [Online]. Available: https://www.pucsl.gov.lk/wp-content/uploads/2020/06/2012-STUDY-REPORT-ON-ELECTRICITY-DEMAND-CURVE-AND-SYSTEM-PEAK-REDUCTION.pdf
- [12] "CEB Long Term Generation Expansion Plan 2020 2039" Accessed on: Sep. 18. 2020. [Online]. Available: https://ceb.lk/publication-media/planing-documents/77/en
- [13] M.V.P. Geetha Udayakanthi, "Design of a wind-solar hybrid power generation systems in Sri Lanka, Department of Energy Technology, KTH, Royal Institute of Technology, 2015.

Advances, Challenges, and Future Perspectives in Supercapacitor Developments for Electric Vehicles

U. L. I. Udayantha^{1*}, S. M. A. V. S. Tennakoon¹, S. N. C. M. Dias²

¹Department of Mechanical and Manufacturing Technology, Faculty of Technology, Wayamba University of Sri Lanka, Sri Lanka, ²Center for Environmental Studies and Sustainable Development, The Open University of Sri Lanka, Sri Lanka

ishanudayantha8@gmail.com*

Abstract

Next-generation EVs need advanced energy storage devices for sustainable performance and energy efficiency. Despite this, SCs offer enormous potential due to their magnificent charging and discharging rates. This review presents recent advancements in SCs by addressing key issues on electrode materials, electrolytes, and new nanostructuring techniques boosting their performance. SCs, especially for EV applications, have become very useful in power management. They can deliver quick bursts of energy to the traction drive to enhance acceleration and recover energy during braking for extended vehicle range and overall efficiency. Despite their huge potential, SCs face several challenges that must be addressed. Those are the limitations to energy density, thereby restricting the amount of energy they can store, high production costs, and safety concerns related to their operation under various conditions. The prospects of SCs in EVs are bright, and research is underway to develop new materials that can provide higher energy density and life. Besides, more advanced manufacturing processes to bring down the cost and integration with smart technologies will make an SC more versatile and effective in supporting the next generation of electric vehicles.

Keywords: Supercapacitors (SCs), Electric vehicles (EVs), Energy storage, Electrode materials, Power management

1 Introduction

EVs are becoming an attractive alternative to petroleum-driven cars, especially with the urge for cleaner and more sustainable means of transport. Contrary to conventional gasoline-powered vehicles, EVs run on electric power, which is supplied through batteries; therefore, energy storage forms an integral part of their performance [1]. Efficient energy storage solutions will be required to maximize EV range, efficiency, and overall effectiveness [2]. Among other energy storage technologies, SCs are getting attractive due to their higher power density and faster charging/discharging capabilities. Therefore, amid the soaring demand for EVs, further development in SC technology is becoming imperative so that its performance can be improved by better association with the existing battery systems to provide a more efficient and reliable drive experience [3]. They are a new generation of energy storage devices that can deliver high power within a very short period of time. Contrary to conventional batteries that store energy through electrochemical reactions, SCs store and release their energy through electrostatic fields and can charge or discharge much faster [4]. What makes them especially useful in EV applications is their ability to provide instant, powerful surges, for example, when the vehicle is accelerating or undergoes regenerative braking [5]. In recent years, advances in SC technology have aimed at improving their energy density and, more recently, incorporating them into existing battery systems to enhance overall vehicle performance [6]. Certainly, as EVs continue to evolve, SCs will become more essential in solving power management difficulties and increasing driving range, showing promise for more efficient and sustainable electric transportation [7]. This paper is a review intended to present a big picture of the current development status, ongoing challenges, and prospects of SCs for EV applications. It reviews the recent innovations in SC technology, covering new electrode materials and electrolytes, and nano-structuring techniques. The review explores the practical applications of SCs in EVs regarding power management and interfacing with their battery systems. This review also underlines some major challenges the industry has to face, like the limitations of energy density, cost, and safety concerns. The following will also bring some interesting insight into the future directions of SC research and development in general, toward pushing for more efficient and sustainable energy storage devices in EV applications.

2 SC Basics

SCs are known by the names of ultracapacitors or electrochemical capacitors, which store and discharge energy via electrostatic interactions and not via chemical reaction [8]. It consists of two electrodes soaked in an electrolyte, which may be liquid, gel, or solid. If a voltage has been imposed, the accumulation of positive charges on one electrode and negative charges on the other will form an electric field across the electrolyte. This process allows SCs to store large amounts of energy in a very short time and release it instantaneously [9]. Unlike the traditional battery systems, which store energy through electrochemical reactions, SCs offer high power density with rapid charge-discharge cycles, making them suited for applications that require quick spurts of energy, such as acceleration in an electric vehicle or regenerative braking [10]. There are three types of SCs, which the energy

storage process could classify: electrochemical double-layer capacitors (EDLCs), pseudocapacitors, and hybrid SCs [11]. EDLCs store energy through electrostatic interaction between the charged surfaces of the electrodes and the electrolyte. Perfection is achieved both in power density and cycling stability. The devices use materials like activated carbon with high surface areas to maximize energy storage [12]. In pseudocapacitors, faradaic redox reactions occur at the electrode surface, giving them a higher energy density than EDLCs. They mostly utilize transition metal oxides or conductive polymers as their electrodes [13]. Hybrid SCs combine characteristics from EDLC and pseudocapacitors by incorporating various electrodes and electrolytes to have high energy density while enabling rapid power delivery. Such a combination only makes sense if it derives the strength of each type, so hybrid SCs have all the potential to become promising in application fields where both high power and energy storage are required, like in EVs [4,14]. SCs differ from traditional batteries by the following three features: energy density, power density, and cyclic stability. Energy density, which designates the amount of energy stored per unit mass or volume, is lower in SCs compared with batteries [9]. This limits the SCs' application for long-term energy storage since they usually store less energy of a given size. In contrast, the power density—the rate at which energy is delivered or absorbed—is very high in SCs. They can release or absorb energy in a very short time relative to a battery and thus fit perfectly in applications involving fast acceleration, like acceleration and braking systems of EVs [15,16]. They have better cyclic stability; they can bear more charge-discharge cycles without appreciable degradation compared to batteries. This added strength prolongs their operational life and reduces the time spent on maintenance. The batteries are appropriate in cases of storing huge amounts of energy over long periods, while the SCs are useful in cases of high power delivery and very long cycle life; hence, they are complementary technologies in an EV [17].

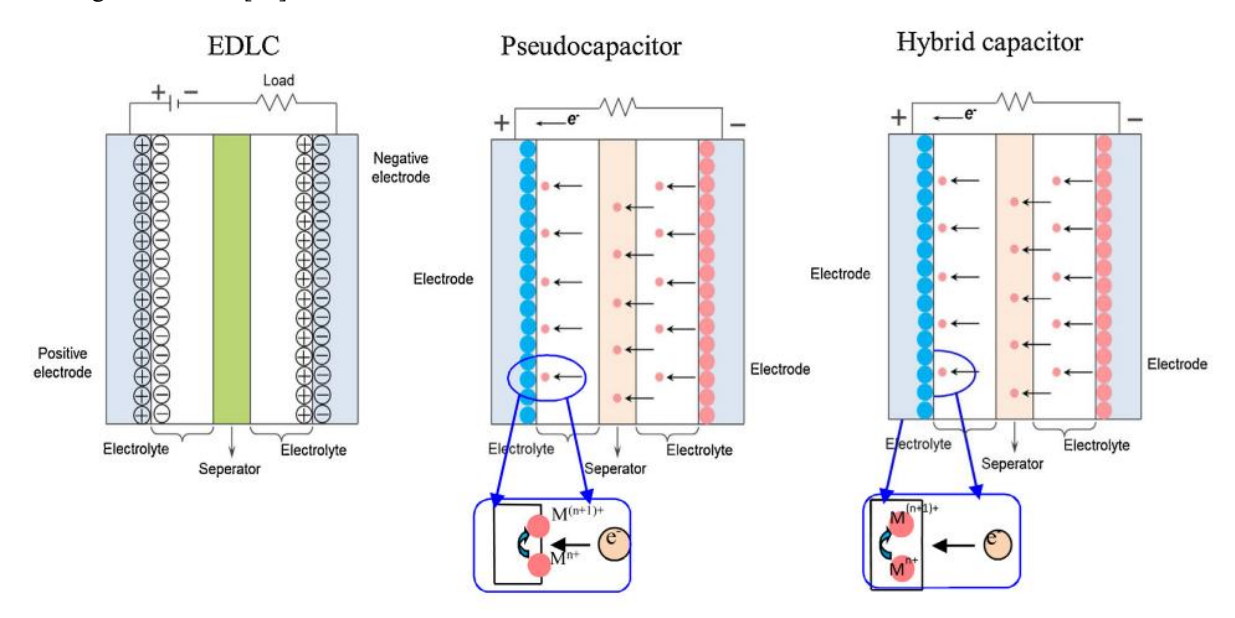


Fig. 1 Schematic representation of three SC types - EDLC showcasing electrostatic charge storage, Pseudocapacitors highlighting redox reactions at the electrode surface, and Hybrid Capacitor combining the features of both EDLC and pseudocapacitors for enhanced energy and power density [18]

3 Advances in SC Technology

3.1 Electrode Materials

In a real sense, SC performance is heavily dependent on the choice of electrode materials. Among transition metal oxides are manganese oxide and cobalt oxide, which largely display high pseudocapacitance and offer improved energy storage and power delivery. Such materials will improve the overall performance by offering extra charge storage through redox reactions [19]. Conductive polymers, like polyaniline and polypyrrole, have high electrical conductivity and specific capacitance to raise the energy density of SCs. In addition to their high flexibility and processability in film or other shapes, they are also applied to this application. [20]. Carbon-based materials such as graphene, activated carbon, and carbon nanotubes are also used due to their large surface areas and electrical conductivity. High power density and quick charging/discharging rates are possible to achieve in graphene due to its excellent conductivity and large surface area [21]. The most popular is activated carbon, which has a large surface area and is low-cost. Carbon nanotubes, on the other hand, have high strength and conductivity. Each type of electrode material has some unique benefits to SCs; thus, ongoing research is focused on optimizing these materials for improved performance, higher energy density, and reduced cost if they are to find their application in EVs [22].

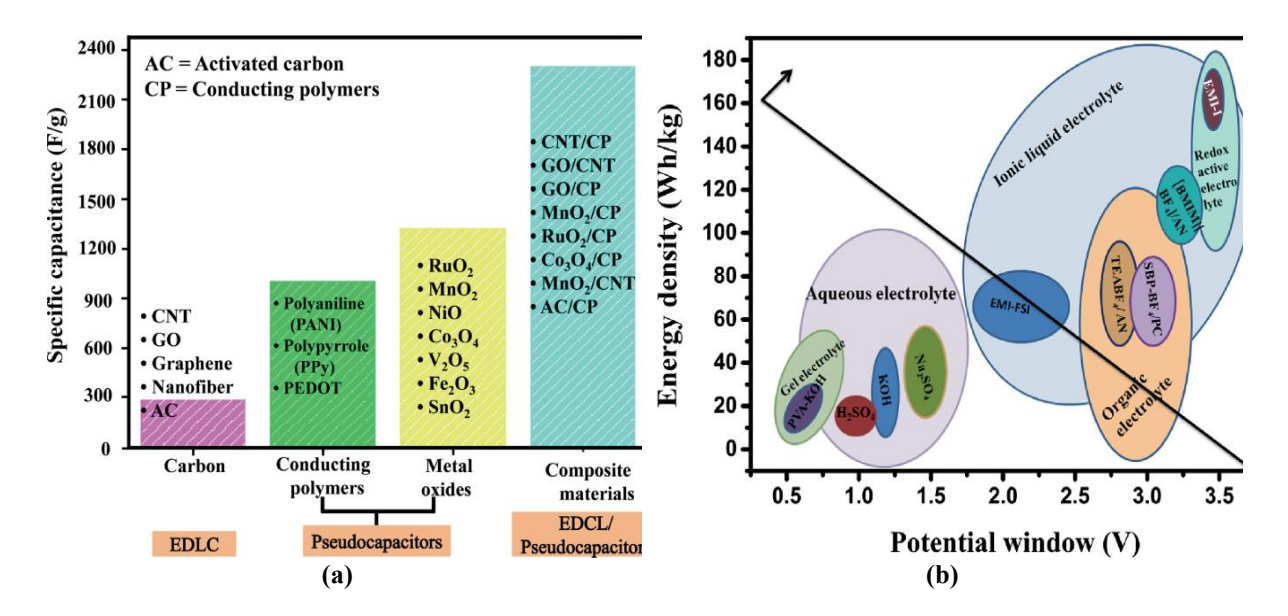


Fig. 2 (a) Comparing the Specific Capacitance of Various Electrode Materials (b). Energy Density vs. Potential Window: Exploring SCs with Different Electrolytes [23]

3.2 Electrolytes

However, the choice of electrolyte determines the performance and safety of SCs. For example, aqueous electrolytes such as sulfuric acid or potassium hydroxide have low costs and high ionic conductivity. These materials provide quite reasonable performance and stability, but are limited to a narrow voltage window, which sets a restriction on the overall energy density of SCs [24]. Organic electrolytes, like those based on organic solvents and salts, provide an extended voltage range and higher energy density than aqueous electrolytes. Their fields of application are cases where larger energy densities and broader temperature stabilities are necessary [25]. Ionic liquid electrolytes are liquids at room temperature, composed of salts, and exhibit high thermal stability and large electrochemical windows, making them highly suitable for very demanding applications, but also more costly [26]. Among the ones being developed, solid-state electrolytes stand out as very promising due to their beneficial combination of both energy density and safety from the elimination of liquid electrolytes. They are still under research and have some potential to improve the performance and life expectancy of SCs [27]Each category of electrolytes has different advantages and limitations, and current research is underway to further optimize these materials for better SC efficiency in EV applications.

3.3 Nano-structuring Techniques

Nano-structuring techniques are vital to improving the performance of SCs with the improvement of electrode materials. The surface area of nanostructured electrodes made of nanoparticles, nano-rods, and nanowires is higher than the volume counterparts. It offers an increased surface area to store more charges and faster charge-discharge rates, which are enormously important for high-performance SCs [28]. Some standard methods of fabricating these nanostructures include electrospinning and chemical vapor deposition. Additionally, surface modification techniques have been employed to enhance the performance of electrodes [29]. Coating, doping, and functionalization techniques are expected to enhance various electrodes' conductivity stability and electrochemical properties. For instance, electrode coatings with conductive polymers or metals significantly improve the overall performance and durability. [30]. Such advances in nano-structuring and surface modification will culminate in the development of SCs: higher energy density, better power delivery, and extended cycle life, making them increasingly more suitable for use in EVs [31].

4 Applications for SCs in EVs

While the theoretical advancement of SC technology looks promising, it is far from satisfactory from a practical performance viewpoint. For instance, some works on integrating SCs into EVs showed enhanced acceleration and regenerative braking efficiency. However, only a few quantitative analyses have been done to determine the amount of energy recovered by braking or specific enhancement in the battery's cycle life with SCs. Case studies,

such as implementing hybrid energy storage systems in commercial EVs or pilot tests in public transport fleets, will help identify cost-benefit trade-offs and operational challenges. These practical perspectives would round out the performance understanding of SCs and facilitate their transition from research to industry.

4.1 Power Management

Effective power management in the SC to optimize its performance is necessary for electric vehicles. For example, systems for energy recovery, such as regenerative braking, capture, and store energy typically wasted during vehicle braking. This recovered energy is then stored in SCs, where it can be rapidly released to support acceleration and thus overall enhance energy efficiency [3]. An additional area of importance is in load balancing, where SCs help in spreading power to be available across a wide array of vehicle systems, therefore reducing pressure on the primary battery and increasing life duration [32]. In addition, SCs are used as peak power devices that provide a temporary burst of high power, which is necessary for either acceleration or other high-demand situations. SCs support the central battery by providing this peak power, enabling the latter to work more efficiently, thereby improving the vehicle's performance. All these power management functions are important in enhancing the efficiency and responsiveness of EVs and thereby underline the important role that SCs play in the newer technology of EVs [7,33].

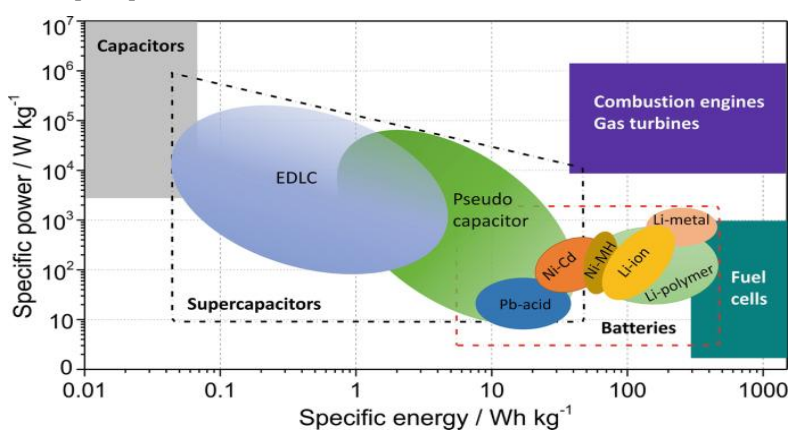


Fig. 2 Ragone plot comparing modern electrochemical energy storage systems, conventional capacitors, and internal combustion engines and turbines. This plot illustrates the energy and power density of each system, showcasing their performance differences [34]

4.2 Integration with Battery Systems

Now, what constitutes a technological advancement in EVs is integrating SCs with battery systems known as Hybrid Energy Storage Systems. HESS incorporates high energy density from the batteries and rapid power delivery and lifespan from the SCs. The integration means that a battery can accomplish the primary tasks of energy storage and retain long-term power for driving, while the SCs are designed to handle the short injections of power, like that required by acceleration or regenerative braking [33,35,36]. Such an arrangement will not only improve energy utilization but also relieve stress from the battery, which may result in extended life and better vehicle efficiency [37]. Other than providing a smoothing effect to the power demands, SCs reduce the rate of degradation experienced by the batteries, hence improving their performance and prolonging their lives. This synergism between the SCs and batteries offers better energy management for the EVs, hence improving their general efficiency and reliability [3].

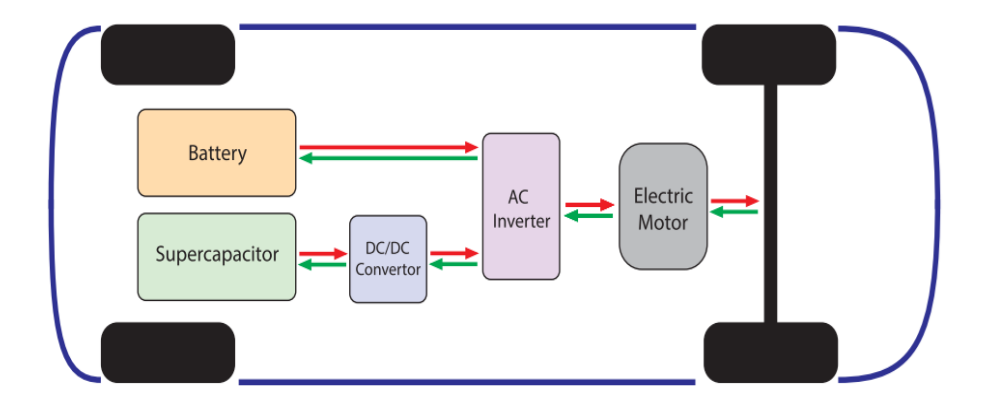


Fig. 3 Electric vehicle powertrain dynamics - Red arrows illustrate the discharge of stored electric energy, powering the wheels through electrical systems. Green arrows demonstrate regenerative braking, where energy from the wheels recharges the storage system. Blue arrows depict the power exchange between different device types [38]

5 Challenges in SC Development for EVs

The development of SCs for EVs faces several challenges, including limitations in energy density compared with batteries, which restrict the driving range. The high cost of advanced electrode materials is another hurdle to large-scale application. The environmental impact of synthesizing electrode and electrolyte materials further complicates scalability, which requires sustainable and cost-effective manufacturing processes.

5.1 Energy Density Limitations

One of the most significant drawbacks of SCs is that, compared to conventional batteries, their energy density is very low. Energy density is an area where researchers focus on several strategies. First of all, the improvement in the electrode material can be implemented by using advanced nano-materials and composites, which increase the surface area and pave the way for more charge storage [39]. The major increase in the energy density might be had from the incorporation of high-capacity materials, for instance, transition metal oxides or conductive polymers [40]. Another way is to optimize electrolyte formulations that can help in increasing the operating voltage window and directly boosting the energy storage capacity [41]. Develop hybrid systems where the supercapacitors can be mixed with other energy storage technologies, such as batteries, to bridge the gap in energy density and leverage the strengths of each technology [42]Thus, the present research focuses, in addition to other strategies, on making SCs more competitive in terms of energy density, thereby improving their suitability for EVs and other high-performance applications.

Table 1. Comparison of Key Characteristics: SCs, Lead-Acid Batteries, and Li-Ion Batteries

Characteristics	SC	Lead-Acid	Li-Ion	
Specific Energy Density (Wh kg ⁻¹)	0.05 - 5 [43]	30 – 50 [43]	75 - 200 [43]	
			100 - 200 [44]	
			150 – 350 [36]	
Specific Power Density (W kg ⁻¹)	~100000 [43]	75 -300 [43]	150 – 315 [43]	
		180 [44]	500 – 2000 [36]	
Energy Capital Cost (\$/kWh)	300 - 2000 [43]	200 – 400 [43]	600 - 2500 [43]	
Power Capital Cost (\$/kW)	100 – 300 [43]	300 – 600 [43]	1200 – 4000 [43]	
Life Cycles	50000 [43]	500 – 1000 [43]	1000 - 10000	
		2000 – 4500 [36]	[43]	
			1500 – 4500 [36]	
Overall Efficiency	0.75 - 0.83 [36]	0.70 - 0.90 [43]	0.80 - 0.85 [43]	
		0.70 - 0.75 [36]	0.85 - 0.95 [36]	
Operation Temperature Range (°C)	-40 to 50 [45]	-5 to 40 [46]	-30 to 60 [33]	

The table compares the key characteristics of SCs, lead-acid batteries, and the current leading batteries for Li-ion electric vehicles. Indeed, this low specific energy density $(0.05-5 \text{ Wh kg}^{-1})$ makes them unsuitable for long-range, but at the same time, SCs excel in quick acceleration applications where the specific power density is high $(\sim 100,000 \text{ W kg}^{-1})$ [10]. The basic features of lead-acid batteries yield average energy and power densities, which

make them very cost-effective for energy storage (\$200–400/kWh) and power delivery (\$300–600/kW). On the other hand, Li-ion batteries show a high value of about 75–350 Wh kg⁻¹ of energy density and an even wider power density range of 150 to 2000 W kg⁻¹, but they cost more in price, with ranges of the order \$600–2500/kWh for energy and \$1200–4000/kW for power [47,48]. Concerning life cycles, SCs lead, with up to 50,000 cycles in comparison to Li-ion batteries, representing 1,000–10,000, followed by lead-acid batteries, which complete 500–1,000 cycles. Efficiency varies; SCs range from 75% to 83%, lead-acid from 70% to 90%, and Li-ion from 80% to 95% [49]. The temperature range for SCs is the widest, from -40°C to 50°C, which makes the batteries versatile; for lead-acid, it is the narrowest, -5°C to 40°C, while for Li-ion, it is good at -30°C to 60°C [45]. The other comparison that will be useful is in showing the trade-offs in energy density versus power density, cost, life cycles, efficiency, and temperature range between the technologies, and how the technologies can meet the various EV applications [50].

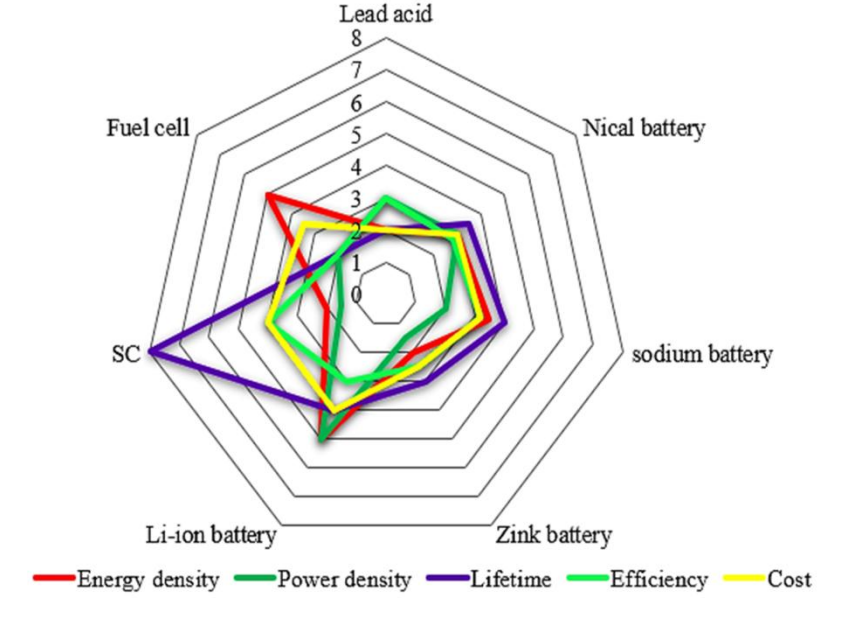


Fig. 4 Comparing batteries and SCs - This chart highlights the key differences between batteries and SCs in terms of energy storage, power delivery, and performance characteristics [23]

5.2 Cost and Scalability

One of the key development challenges of SCs for EV applications is their cost and scalability. The high-performance SC relies on materials that can be quite expensive. Indeed, some advanced nanomaterials and rare or rather expensive metals are required [16]. Moreover, the manufacturing processes for producing the required materials and the assembling procedure for SCs may become complex and correspondingly expensive. For example, the high-quality synthesis of graphene or conducting polymers often requires intricate and costly techniques [51]. Cheaper materials and process simplification are ways researchers are working to ensure that these issues are solved. This is through the search for alternative materials that are more abundant, offering comparable performance at cheaper costs, and bringing about improved production methods to raise efficiency and reduce related costs [52]. Issues on scaling while maintaining quality are another challenge; moving from the laboratory scale to the commercial scale calls for massive investment in infrastructure. It is expected that, by working on these lines, SCs will become more economically viable and widely accessible, therefore finding enhanced adoption in EVs[2].

5.3 Safety and Stability

In any case, an SC for use in an electric vehicle should be developed to guarantee its safety and stability. One of the major technical challenges to overcome is thermal management because an SC can easily heat up in high-power delivery and fast charge/discharge cycles. High temperatures are known to cause performance degradation, decrease longevity, and make these devices unsafe [53]. Effective thermal management strategies would be needed, which involve heat-dissipating materials or designing advanced cooling systems to ensure the operational safety and reliability of SCs [10]. Operational safety concerns detailed that SCs should be resistant to mechanical stress, overcharge and short-circuit events; if not properly taken care of, they may lead to a predisposition to failure or even accidents [39]Researchers are working on enhancing the stability of SCs by designing materials that can withstand extreme conditions and safety issues. This will make SCs a reliable and secure way of storing energy in EVs.

6. Future Perspectives and Emerging Trends

6.1 Next-Generation Materials

Next-generation materials will play a vital role in developing SC technology, particularly in its application in EVs. Many researchers are investigating emerging materials and composites to enhance SC performance. For example, these new types of carbon materials, like graphene and carbon nanotubes, have very high electrical conductivities and large surface areas that can tremendously enhance energy and power densities. [54]. Researchers are, therefore, working on advanced metal oxides and conductive polymers to ensure charge storage and stability, more so than conventional materials. Hybrid materials combining the classes of various materials are also under study to make them appropriate to ensure the strengths of each component are developed. For instance, mixing carbon-based materials with a metal-organic framework can create a high-performance characteristic electrode. The intention is that SC technology can be pushed to its limits by such types of innovative materials and composites [55]. New material types, such as carbon aerogels and MXenes, have also shown great promise, reaching energy densities comparable to lithium-ion batteries in initial tests. Research collaborations across industries and academic institutions are accelerating the optimization of these materials for scalable and cost-effective production.

6.2 Advanced Manufacturing Techniques

Advanced manufacturing methods are revolutionizing SC production, opening up new opportunity areas concerning efficiency and scalability. One such technique is 3D printing, which allows for the precise fabrication of complicated electrode structures and custom-designed components. With the possibility of making intricate designs through this method, improvement in the performance and functionality of SCs can be realized [56]. 3D printing enables researchers to test a wide range of materials and geometries, resulting in the development of new, highly innovative electrode architectures that raise energy storage and power delivery [57]. Another high-throughput technique is roll-to-roll manufacturing, in which long, flexible substrates are continuously processed to produce SC components in large quantities. This technique is mainly used to fabricate SCs that are flexible, lightweight, and easily integrated into many applications [58]. This gives both methods huge cost, materials usage, and production speed advantages when developing more efficient SCs and promoting their commercial use in EVs. Large-scale SC fabrication is being adapted for roll-to-roll processing, significantly reducing the fabrication cost while maintaining consistency in performance. Additive manufacturing methods, such as 3D printing, also provide a route to customized design for specific EV applications.

6.3 Smart SCs

In this regard, smart SCs have been said to be the key development in EV energy storage in the future. The SCs become increasingly intelligent and reactive when real-time conditions are introduced by integrating the IoT and artificial intelligence [59]. IoT sensors inside the SCs can track several parameters, such as temperature, voltage, and charge status, continuously providing data on their performance [60]. AI algorithms can analyze this data to predict potential issues, optimize charge-discharge cycles, and ensure peak efficiency during the operation of SCs. The predictive maintenance ability identifies and solves problems before they become failures, thus improving reliability and lifetime [61,62]. However, AI-driven optimization goes a step further to dynamically adjust the performance of the SC concerning the vehicle's driving conditions and, therefore, improves overall efficiency and energy management [59]. The marriage of IoT and AI in SCs thus catapults energy storage for EVs a quantum leap into intelligence and adaptivity. IoT-enabled SCs will also predict performance issues and enhance operational efficiency, revolutionizing energy management.

7. Conclusion

SCs have become one of the critical technologies for EVs since they can deliver enormous power rapidly and efficiently. While they are excellent in quick energy supply and improving vehicle performance, several challenges remain to be improved. Among them, there is an increase in energy density, cost reduction, and strengthening of safety and stability. However, progress in materials, new manufacturing processes, and smart technologies is showing the way forward to better supercapacitors. SCs will probably develop a more efficient and reliable electric vehicle by making these improvements. Further research and innovation will be required to solve these challenges and to fully exploit the potential of SCs in electric transport.

References

- [1] U. Eberle and R. Von Helmolt, "Sustainable transportation based on electric vehicle concepts: A brief overview," *Energy Environ. Sci.*, vol. 3, no. 6, pp. 689–699, 2010, doi: 10.1039/c001674h.
- [2] M. A. Hannan, M. M. Hoque, A. Mohamed, and A. Ayob, "Review of energy storage systems for electric vehicle applications: Issues and challenges," *Renew. Sustain. Energy Rev.*, vol. 69, no. September 2015, pp. 771–789, 2017, doi: 10.1016/j.rser.2016.11.171.

- [3] E. Faggioli, P. Rena, V. Danel, X. Andrieu, R. Mallant, and H. Kahlen, "Supercapacitors for the energy management of electric vehicles," *J. Power Sources*, vol. 84, no. 2, pp. 261–269, 1999, doi: 10.1016/S0378-7753(99)00326-2.
- [4] W. Raza *et al.*, "Recent advancements in supercapacitor technology," *Nano Energy*, vol. 52, no. June, pp. 441–473, 2018, doi: 10.1016/j.nanoen.2018.08.013.
- [5] Q. Y. Zhang and J. Huang, "Research on regenerative braking energy recovery system of electric vehicles," *J. Interdiscip. Math.*, vol. 21, no. 5, pp. 1321–1326, 2018, doi: 10.1080/09720502.2018.1498047.
- [6] M. Z. Iqbal, M. M. Faisal, and S. R. Ali, "Integration of supercapacitors and batteries towards high-performance hybrid energy storage devices," *Int. J. Energy Res.*, vol. 45, no. 2, pp. 1449–1479, 2021, doi: 10.1002/er.5954.
- [7] M. E. Choi, J. S. Lee, and S. W. Seo, "Real-time optimization for power management systems of a battery/supercapacitor hybrid energy storage system in electric vehicles," *IEEE Trans. Veh. Technol.*, vol. 63, no. 8, pp. 3600–3611, 2014, doi: 10.1109/TVT.2014.2305593.
- [8] A. C. Forse, C. Merlet, J. M. Griffin, and C. P. Grey, "New perspectives on the charging mechanisms of supercapacitors," *J. Am. Chem. Soc.*, vol. 138, no. 18, pp. 5731–5744, 2016, doi: 10.1021/jacs.6b02115.
- [9] K. V. G. Raghavendra *et al.*, "An intuitive review of supercapacitors with recent progress and novel device applications," *J. Energy Storage*, vol. 31, no. June, p. 101652, 2020, doi: 10.1016/j.est.2020.101652.
- [10] S. Liu, L. Wei, and H. Wang, "Review on the reliability of supercapacitors in energy storage applications," *Appl. Energy*, vol. 278, no. June, p. 115436, 2020, doi: 10.1016/j.apenergy.2020.115436.
- [11] T. Brousse *et al.*, "Materials for electrochemical capacitors," *Springer Handbooks*, pp. 495–561, 2017, doi: 10.1007/978-3-662-46657-5_16.
- [12] T. Morimoto, K. Hiratsuka, Y. Sanada, and K. Kurihara, "Electric double-layer capacitor using organic electrolyte," *J. Power Sources*, vol. 60, no. 2, pp. 239–247, 1996, doi: 10.1016/S0378-7753(96)80017-6.
- [13] T. Gu and B. Wei, "Fast and stable redox reactions of MnO2/CNT hybrid electrodes for dynamically stretchable pseudocapacitors," *Nanoscale*, vol. 7, no. 27, pp. 11626–11632, 2015, doi: 10.1039/c5nr02310f.
- [14] M. F. El-Kady *et al.*, "Engineering three-dimensional hybrid supercapacitors and for high-performance integrated energy storage," *Proc. Natl. Acad. Sci. U. S. A.*, vol. 112, no. 14, pp. 4233–4238, 2015, doi: 10.1073/pnas.1420398112.
- [15] D. B. Robinson, "Optimization of power and energy densities in supercapacitors," *J. Power Sources*, vol. 195, no. 11, pp. 3748–3756, 2010, doi: 10.1016/j.jpowsour.2009.12.004.
- [16] S. Huang, X. Zhu, S. Sarkar, and Y. Zhao, "Challenges and opportunities for supercapacitors," *APL Mater.*, vol. 7, no. 10, 2019, doi: 10.1063/1.5116146.
- [17] N. Vukajlović, D. Milićević, B. Dumnić, and B. Popadić, "Comparative analysis of the supercapacitor influence on lithium battery cycle life in electric vehicle energy storage," *J. Energy Storage*, vol. 31, no. February, p. 101603, 2020, doi: 10.1016/j.est.2020.101603.
- [18] M. Dai, D. Zhao, and X. Wu, "Research progress on transition metal oxide based electrode materials for asymmetric hybrid capacitors," *Chinese Chem. Lett.*, vol. 31, no. 9, pp. 2177–2188, 2020, doi: 10.1016/j.cclet.2020.02.017.
- [19] Y. Wang, J. Guo, T. Wang, J. Shao, D. Wang, and Y. W. Yang, "Mesoporous transition metal oxides for supercapacitors," *Nanomaterials*, vol. 5, no. 4, pp. 1667–1689, 2015, doi: 10.3390/nano5041667.
- [20] Z. Xu *et al.*, "Investigation on the role of different conductive polymers in supercapacitors based on a zinc sulfide/reduced graphene oxide/conductive polymer ternary composite electrode," *RSC Adv.*, vol. 10, no. 6, pp. 3122–3129, 2020, doi: 10.1039/c9ra07842h.
- [21] S. Bose, T. Kuila, A. K. Mishra, R. Rajasekar, N. H. Kim, and J. H. Lee, "Carbon-based nanostructured materials and their composites as supercapacitor electrodes," *J. Mater. Chem.*, vol. 22, no. 3, pp. 767–784, 2012, doi: 10.1039/c1jm14468e.
- [22] Z. Liu, S. Zhang, L. Wang, T. Wei, Z. Qiu, and Z. Fan, "High-efficiency utilization of carbon materials for supercapacitors," *Nano Sel.*, vol. 1, no. 2, pp. 244–262, 2020, doi: 10.1002/nano.202000011.
- [23] K. K. Kar, Springer series in materials science 300 handbook of nanocomposite supercapacitor materials IV. 2023. [Online]. Available: https://doi.org/10.1007/978-3-031-23701-0

- [24] M. Z. Iqbal, S. Zakar, and S. S. Haider, "Role of aqueous electrolytes on the performance of electrochemical energy storage device," *J. Electroanal. Chem.*, vol. 858, p. 113793, 2020, doi: 10.1016/j.jelechem.2019.113793.
- [25] J. Cao, J. Tian, J. Xu, and Y. Wang, "Organic Flow Batteries: Recent Progress and Perspectives," *Energy and Fuels*, vol. 34, no. 11, pp. 13384–13411, 2020, doi: 10.1021/acs.energyfuels.0c02855.
- [26] H. Liu and H. Yu, "Ionic liquids for electrochemical energy storage devices applications," *J. Mater. Sci. Technol.*, vol. 35, no. 4, pp. 674–686, 2019, doi: 10.1016/j.jmst.2018.10.007.
- [27] Y. Yang, T. Zhu, C. Chi, L. Liu, J. Zheng, and X. Gong, "All-Solid-State Asymmetric Supercapacitors with Novel Ionic Liquid Gel Electrolytes," *ACS Appl. Electron. Mater.*, vol. 2, no. 12, pp. 3906–3914, 2020, doi: 10.1021/acsaelm.0c00759.
- [28] S. Verma, S. Arya, V. Gupta, S. Mahajan, H. Furukawa, and A. Khosla, "Erratum: Performance analysis, challenges and future perspectives of nickel based nanostructured electrodes for electrochemical supercapacitors (J Mater Res Technol (2021) 11 (564-599) DOI: 10.1016/j.jmrt.2022.04.037)," *J. Mater. Res. Technol.*, vol. 18, p. 5452, 2022, doi: 10.1016/j.jmrt.2021.01.027.
- [29] C. Guan and J. Wang, "Recent Development of Advanced Electrode Materials by Atomic Layer Deposition for Electrochemical Energy Storage," *Adv. Sci.*, vol. 3, no. 10, pp. 1–23, 2016, doi: 10.1002/advs.201500405.
- [30] L. Jiang *et al.*, "Electropolymerization of camphorsulfonic acid doped conductive polypyrrole anti-corrosive coating for 304SS bipolar plates," *Appl. Surf. Sci.*, vol. 426, pp. 87–98, 2017, doi: 10.1016/j.apsusc.2017.07.077.
- [31] D. S. Achilleos and T. A. Hatton, "Surface design and engineering of hierarchical hybrid nanostructures for asymmetric supercapacitors with improved electrochemical performance," *J. Colloid Interface Sci.*, vol. 447, pp. 282–301, 2014, doi: 10.1016/j.jcis.2014.12.080.
- [32] A. Turksoy, A. Teke, and A. Alkaya, "A comprehensive overview of the dc-dc converter-based battery charge balancing methods in electric vehicles," *Renew. Sustain. Energy Rev.*, vol. 133, no. August, p. 110274, 2020, doi: 10.1016/j.rser.2020.110274.
- [33] K. C. Divya and J. Østergaard, "Battery energy storage technology for power systems-An overview," *Electr. Power Syst. Res.*, vol. 79, no. 4, pp. 511–520, 2009, doi: 10.1016/j.epsr.2008.09.017.
- [34] Q. Zhen, S. Bashir, and J. L. Liu, *Nanostructured Materials for Next-Generation Energy Storage and Conversion: Advanced Battery and Supercapacitors*. 2019. doi: 10.1007/978-3-662-58675-4.
- [35] J. Cao and A. Emadi, "A new battery/ultracapacitor hybrid energy storage system for electric, hybrid, and plug-in hybrid electric vehicles," *IEEE Trans. Power Electron.*, vol. 27, no. 1, pp. 122–132, 2012, doi: 10.1109/TPEL.2011.2151206.
- [36] B. Zakeri and S. Syri, "Electrical energy storage systems: A comparative life cycle cost analysis," *Renew. Sustain. Energy Rev.*, vol. 42, pp. 569–596, 2015, doi: 10.1016/j.rser.2014.10.011.
- [37] R. Carter, A. Cruden, and P. J. Hall, "Optimizing for efficiency or battery life in a battery/supercapacitor electric vehicle," *IEEE Trans. Veh. Technol.*, vol. 61, no. 4, pp. 1526–1533, 2012, doi: 10.1109/TVT.2012.2188551.
- [38] M. Khalid, A review on the selected applications of battery-supercapacitor hybrid energy storage systems for microgrids, vol. 12, no. 23. 2019. doi: 10.3390/en12234559.
- [39] J. Yan, Q. Wang, T. Wei, and Z. Fan, "Recent advances in design and fabrication of electrochemical supercapacitors with high energy densities," *Adv. Energy Mater.*, vol. 4, no. 4, 2014, doi: 10.1002/aenm.201300816.
- [40] C. Guan *et al.*, "Iron oxide-decorated carbon for supercapacitor anodes with ultrahigh energy density and outstanding cycling stability," *ACS Nano*, vol. 9, no. 5, pp. 5198–5207, 2015, doi: 10.1021/acsnano.5b00582.
- [41] L. Cheng *et al.*, "Accelerating Electrolyte Discovery for Energy Storage with High-Throughput Screening," *J. Phys. Chem. Lett.*, vol. 6, no. 2, pp. 283–291, 2015, doi: 10.1021/jz502319n.
- [42] L. Kouchachvili, W. Yaïci, and E. Entchev, "Hybrid battery/supercapacitor energy storage system for the electric vehicles," *J. Power Sources*, vol. 374, no. June 2017, pp. 237–248, 2018, doi: 10.1016/j.jpowsour.2017.11.040.
- [43] H. Chen, T. N. Cong, W. Yang, C. Tan, Y. Li, and Y. Ding, "Progress in electrical energy storage system: A critical review," *Prog. Nat. Sci.*, vol. 19, no. 3, pp. 291–312, 2009, doi: 10.1016/j.pnsc.2008.07.014.

- [44] P. Nikolaidis and A. Poullikkas, "A comparative review of electrical energy storage systems for better sustainability," *J. Power Technol.*, vol. 97, no. 3, pp. 220–245, 2011, [Online]. Available: http://papers.itc.pw.edu.pl/index.php/JPT/article/view/1096/776
- [45] R. Esr, *Influence of temperature on supercapacitor performance*, vol. 25. 2015. doi: 10.1007/978-3-319-20242-6 4.
- [46] F. Rahman, S. Rehman, and M. A. Abdul-Majeed, "Overview of energy storage systems for storing electricity from renewable energy sources in Saudi Arabia," *Renew. Sustain. Energy Rev.*, vol. 16, no. 1, pp. 274–283, 2012, doi: 10.1016/j.rser.2011.07.153.
- [47] Y. Ding, Z. P. Cano, A. Yu, J. Lu, and Z. Chen, "Automotive Li-Ion Batteries: Current Status and Future Perspectives," *Electrochem. Energy Rev.*, vol. 2, no. 1, 2019, doi: 10.1007/s41918-018-0022-z.
- [48] L. Li *et al.*, "Carbon-based materials for fast charging lithium-ion batteries," *Carbon N. Y.*, vol. 183, pp. 721–734, 2021, doi: 10.1016/j.carbon.2021.07.053.
- [49] H. D. Yoo, E. Markevich, G. Salitra, D. Sharon, and D. Aurbach, "On the challenge of developing advanced technologies for electrochemical energy storage and conversion," *Mater. Today*, vol. 17, no. 3, pp. 110–121, 2014, doi: 10.1016/j.mattod.2014.02.014.
- [50] J. Wen, D. Zhao, and C. Zhang, "An overview of electricity powered vehicles: Lithium-ion battery energy storage density and energy conversion efficiency," *Renew. Energy*, vol. 162, pp. 1629–1648, 2020, doi: 10.1016/j.renene.2020.09.055.
- [51] M. Wang and Y. X. Xu, "Design and construction of three-dimensional graphene/conducting polymer for supercapacitors," *Chinese Chem. Lett.*, vol. 27, no. 8, pp. 1437–1444, 2016, doi: 10.1016/j.cclet.2016.06.048.
- [52] M. Isachenkov, S. Chugunov, I. Akhatov, and I. Shishkovsky, "Regolith-based additive manufacturing for sustainable development of lunar infrastructure An overview," *Acta Astronaut.*, vol. 180, no. January, pp. 650–678, 2021, doi: 10.1016/j.actaastro.2021.01.005.
- [53] M. Al Sakka, H. Gualous, J. Van Mierlo, and H. Culcu, "Thermal modeling and heat management of supercapacitor modules for vehicle applications," *J. Power Sources*, vol. 194, no. 2, pp. 581–587, 2009, doi: 10.1016/j.jpowsour.2009.06.038.
- [54] R. R. Salunkhe *et al.*, "Nanoarchitectured graphene-based supercapacitors for next-generation energy-storage applications," *Chem. A Eur. J.*, vol. 20, no. 43, pp. 13838–13852, 2014, doi: 10.1002/chem.201403649.
- [55] W. Du *et al.*, "Advanced metal-organic frameworks (MOFs) and their derived electrode materials for supercapacitors," *J. Power Sources*, vol. 402, no. May, pp. 281–295, 2018, doi: 10.1016/j.jpowsour.2018.09.023.
- [56] J. Sun *et al.*, "Printable nanomaterials for the fabrication of high-performance supercapacitors," *Nanomaterials*, vol. 8, no. 7, pp. 1–24, 2018, doi: 10.3390/nano8070528.
- [57] F. Zhang *et al.*, "3D printing technologies for electrochemical energy storage," *Nano Energy*, vol. 40, no. August, pp. 418–431, 2017, doi: 10.1016/j.nanoen.2017.08.037.
- [58] F. C. Krebs, J. Fyenbo, and M. Jørgensen, "Product integration of compact roll-to-roll processed polymer solar cell modules: Methods and manufacture using flexographic printing, slot-die coating and rotary screen printing," *J. Mater. Chem.*, vol. 20, no. 41, pp. 8994–9001, 2010, doi: 10.1039/c0jm01178a.
- [59] R. Wang, M. Yao, and Z. Niu, "Smart supercapacitors from materials to devices," *InfoMat*, vol. 2, no. 1, pp. 113–125, 2020, doi: 10.1002/inf2.12037.
- [60] K. Balachander, A. Amudha, and M. Mansoor Ali, "IoT Based Control of Hybrid Energy Storage System for an Electric Vehicle using Super Capacitor and Battery," *J. Phys. Conf. Ser.*, vol. 1979, no. 1, 2021, doi: 10.1088/1742-6596/1979/1/012032.
- [61] Y. Zhou *et al.*, "Hybrid genetic algorithm method for efficient and robust evaluation of remaining useful life of supercapacitors," *Appl. Energy*, vol. 260, no. May 2019, p. 114169, 2020, doi: 10.1016/j.apenergy.2019.114169.
- [62] M. Uno and K. Tanaka, "Accelerated charge-discharge cycling test and cycle life prediction model for supercapacitors in alternative battery applications," *IEEE Trans. Ind. Electron.*, vol. 59, no. 12, pp. 4704–4712, 2012, doi: 10.1109/TIE.2011.2182018.

Performance Comparison of Dye-Sensitized Solar Cells Using *Elaeocarpus* serratus Red Leaf Dye Extracted with Various Polar Solvents

S. Davisan*, K.S.A. Panditharathna, C. N. Nupearachchi, and V.P.S. Perera

Department of Physics, Faculty of Natural Sciences, The Open University of Sri Lanka s.day.vision0407@gmail.com

Abstract

To address the growing global energy demand, the transition to renewable energy, particularly to solar energy, is essential due to its benefits to the Socio-Economic level of society. Dye-sensitized solar cells (DSSCs) have garnered interest in their flexibility, lightweight properties, and cost-effectiveness among solar technologies. This research aims to improve DSSC efficiency by optimizing the extraction of natural pigments from *Elaeocarpus serratus* red leaves using various solvents. The choice of solvent is critical in determining the interaction between natural dyes and the TiO₂ layer, influencing DSSC performance. In this study, dyes were extracted by suspending leaves in solvents of varying polarities, including distilled water, ethanol, isopropyl alcohol, acetone, cyclohexanone, and ethyl acetate, over 24 hours at room temperature. The extracted dyes were used in DSSCs, and their photovoltaic performance was evaluated under a 100 mW/cm² LED light source. Ethanol emerged as the most effective solvent, achieving the highest efficiency (0.786%) and short-circuit current density (3.036 mA/cm²). UV-Visible absorption analysis revealed the presence of pigments like chlorophylls, carotenoids, and anthocyanins, highlighting the influence of solvent polarity on pigment extraction. This study identified ethanol as the best solvent for natural dye extraction, offering a promising approach to enhance DSSC performance and advance sustainable solar energy technologies.

Keywords: Elaeocarpus serratus, SL Olive, Weralu, Red Leaf, polarity solvent

1 Introduction

Energy is a critical component in virtually all processes and activities across the universe. It plays a pivotal role in sustaining life, enabling movement and work, driving various processes, generating power, impacting economies, and fostering technological and industrial advancement. Over recent centuries, particularly throughout the 20th and into the 21st century, there has been a significant shift in energy consumption and demand. This shift is a result of industrial advancements, population growth, and evolving technologies [1].

Energy sources are primarily categorized into two types: nonrenewable and renewable. The use of nonrenewable energy sources, such as coal, oil, and natural gas, has been linked to several substantial drawbacks affecting the environment, human health, and economic stability [2].

The environmental consequences of relying on nonrenewable sources include air pollution, emissions of greenhouse gases, water pollution, and land degradation. From a health perspective, the pollution from these energy sources can lead to respiratory problems, cardiovascular diseases, and other health issues. Economically, the volatility of nonrenewable energy prices and their finite nature pose significant risks and sustainability challenges, potentially hindering innovation and economic transition toward greener alternatives [2] [3] [4].

Researchers are currently focused on identifying and formulating alternative and effective strategies to address these issues. The shift towards renewable energy sources, including solar, wind, and hydroelectric power, offers potential solutions to many existing problems. Utilizing renewable energy provides a cleaner, more sustainable alternative that can greatly diminish dependency on nonrenewable resources, thus alleviating environmental, health, and economic issues, and fostering a more sustainable future [5].

Solar energy is one of the most easily available and eco-friendly renewable energy sources. Solar energy can be converted into electrical energy by using photovoltaic cells. Solar cell technology has significantly advanced over time, resulting in the development of various generations of solar cells, each distinguished by unique characteristics and efficiency levels. The first generation, known as crystalline silicon solar cells, and the second generation solar cells are categorized as thin-film solar cells. The primary materials utilized in this generation include amorphous silicon (a-Si), cadmium telluride (CdTe), and copper indium gallium selenide (CIGS).

The third generation encompasses a diverse array of emerging photovoltaic technologies, many of which are still under development or research. These technologies aim to surpass the efficiency constraints of conventional materials while reducing production costs. Notable examples of third-generation solar cells include organic photovoltaic cells (OPVs), dye-sensitized solar cells (DSSCs), perovskite solar cells, and quantum dot solar cells. The focus in developing third-generation solar cells lies in utilizing low cost materials and innovative processes that could potentially exceed the efficiency limitations of traditional silicon-based solar cells and mitigate both costs and environmental impacts [6] [7] [8] [9].

Dye-sensitized solar cells (DSSCs), also known as Grätzel cells, represent a unique class of solar cells that mimic the natural process of photosynthesis [10]. The fundamental architecture of dye-sensitized solar cells (DSSCs) is composed of four main components: photoanode, a dye layer, an electrolyte, and a counter electrode.

The photoanode of DSSCs typically comprises transparent conductive oxide (TCO) glass, which is coated with a porous layer of titanium dioxide (TiO_2) nanoparticles. This TiO_2 layer serves as a semiconductor, facilitating the crucial processes of light absorption and photovoltaic conversion.

The electrolyte, which can be either liquid or solid, contains a redox couple, usually iodide/triiodide. It occupies the interstitial space between the photoanode and the cathode. Its primary role is to transport electrons back to the dye molecules after they have traveled through the external circuit, thus maintaining the continuity of the electric current.

Positioned opposite the photoanode, the counter electrode is generally coated with platinum or another catalytic material. This electrode is critical for facilitating the regeneration of the redox mediator within the electrolyte, completing the electrical cycle necessary for cell operation.

Sensitization of the TiO₂ occurs through its coating with light-absorbing dye, which captures sunlight and generates electrons. Commonly, ruthenium-based dyes are employed due to their effective light-absorption properties. However, research is also focusing on organic dyes and other alternatives that could offer advantages in terms of cost and spectral response. In the dye extracting process, solvents play major roles.

The choice of extraction solvent for natural dyes is crucial in determining the strong interaction between the dye molecules and the TiO₂ layer in dye-sensitized solar cells (DSSCs). Various natural sources can be utilized to extract pigments to be used as photosensitizers in DSSCs, making them cost-effective and sustainable alternatives. These natural dyes typically contain pigments such as anthocyanins, chlorophylls, carotenoids, and flavonoids, though most natural dyes consist of only a few primary pigments. The efficiency of DSSCs is influenced by the composition of these pigments and the interaction strength between the dye molecules and TiO₂ nanoparticles. This interaction is governed by multiple factors affecting the anchoring groups in the extracted dye molecules, which are critical for charge transport and separation within the cells. As such, these anchoring groups play a significant role in the photoconversion efficiency of DSSCs, and the extraction solvent greatly impacts the characteristics of these groups within the dye solution [11].

Each component is integral to the DSSC's operation, contributing to its potential as an alternative to conventional photovoltaic technologies. In dye-sensitized solar cells (DSSCs), the process begins when sunlight shines on dye molecules, leading to the absorption of photons. This event excites the molecules, causing them to release electrons. These electrons are then propelled into the conduction band of the titanium dioxide (TiO₂), from where they move through the TiO₂ to the transparent conductive oxide (TCO) glass, eventually reaching the external circuit.

Dye-sensitized solar cells (DSSCs) present multiple advantages, positioning them as an attractive alternative to conventional photovoltaic technologies. These advantages include their low cost, flexibility, and lightweight nature, efficient performance under diffuse lighting conditions, various aesthetic options, straightforward manufacturing process, and environmental friendliness. Each of these attributes contributes to the growing interest in DSSCs for diverse applications, ranging from portable electronics to integrated building solutions.

Ongoing research and development are significantly improving the performance and durability of dye-sensitized solar cells (DSSCs), marking them as pivotal in the global movement towards sustainable energy solutions.

The objective of this study is to explore how different solvents affect the Photo-Conversion Efficiency (PCE) of natural dyes extracted from *Elaeocarpus serratus* leaves, which are then used to construct low-cost Natural Dye-Sensitized Solar Cells (DSSCs). The DSSCs were successfully assembled using dye extracts from the red leaves of Elaeocarpus serratus as photosensitizers. The extraction was carried out using a variety of solvents, including distilled water, ethanol, isopropyl alcohol, ethyl acetate, acetone, and cyclohexanone.

2 Methodology

2.1 Materials

P-25 TiO₂ Nano particles, PEG 400, Triton X-100, 0.1M HNO₃, FTO glass plates, Ethanol, Isopropyl alcohol, Distilled Water, Aceton, Cyclohexanone, Ethyl Acetate, iodine (I₂), potassium iodide (KI), acetonitrile, and ethylene carbonate, *Elaeocarpus serratus* red leaf

2.2 Preparation of Photocathode

2.2.1 Preparation of dye

Fresh red leaves of *Elaeocarpus serratus*, commonly known as Olive or Weralu in Sri Lanka, were collected and cut into small pieces. One gram of these leaves was then extracted using solvents with varying polarities, including distilled water (D.W.), ethanol (EtOH), isopropyl alcohol (IPA), acetone, cyclohexanone, and ethyl acetate. The extraction was carried out in separate beakers at room temperature for 24 hours. Afterward, the natural dyes obtained from the SL Olive red leaves were filtered and poured into individual sample bottles. [12].

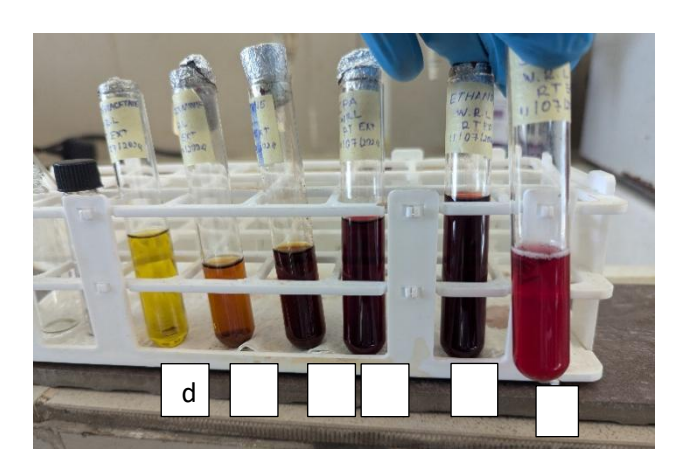


Fig. 1 Elaeocarpus serratus red leaf (a) D. Water extraction (b) Ethanol extraction (c) Isopropyl alcohol extraction (d) Ethyl Acetate extraction (e) Aceton extraction (f) Cyclohexanone extraction

2.2.2 FTO Cleaning Process

The following method was employed to clean 2 cm x 1 cm pieces of Fluorine-doped Tin Oxide (FTO) glass plates. Initially, the FTO plates were subjected to a five-minute ultrasonic bath containing distilled water and liquid soap. This was followed by a further sonication of five minutes using distilled water and several drops of concentrated H_2SO_4 . Subsequently, the plates were boiled in isopropyl alcohol within a beaker at $80^{\circ}C$. After boiling, the FTO plates were air-dried using a low-heat hair dryer, and their conductivity was assessed using a conductivity meter [12].

2.2.3 Preparation of TiO₂ Paste

To formulate the TiO2 paste, 0.25 g of 20 nm TiO2 powder was mixed with 0.1 ml of 0.1M HNO3, a drop of Triton-X 100, and a drop of PEG 400. The mixture was stirred until a thick paste was achieved. This paste was then uniformly applied to the conductive surface of the FTO glass plates using the doctor blade technique. Following application, the plates were sintered at 450°C for 30 minutes in a furnace and allowed to cool.

The TiO2-coated glass plates were subsequently immersed in individual test tubes filled with dye solutions, which were prepared from Elaeocarpus serratus red leaf dye extraction.

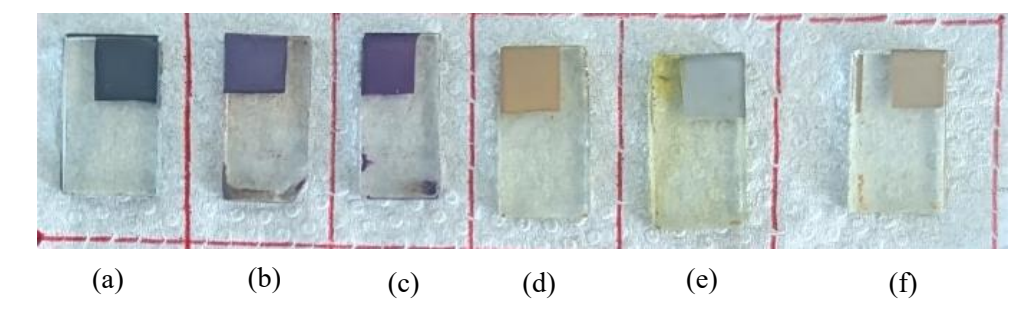


Fig. 2 Dye-coated film (a) D. Water (b) Ethanol (c) Isopropyl alcohol (d) Ethyl Acetate (e) Aceton (f) Cyclohexanone

2.2.4 Development of DSSCs

A key component of a dye-sensitized solar cell (DSSC) is the electrolyte. In this study, a liquid I_2/I_3 electrolyte was prepared by dissolving 0.127 g of iodine (I_2) and 0.83 g of potassium iodide (KI) in a mixture of acetonitrile

and ethylene carbonate, following an 8:2 ratio, to a total volume of 10 ml in a volumetric flask [13]. The solution was stirred continuously for five hours to ensure complete dissolution of the solids.

The assembly of the DSSC involved a dye-coated TiO2 film deposited on fluorine-doped tin oxide (FTO) glass, serving as the anode, and a platinum (Pt)-coated glass plate as the cathode. These components were aligned side by side and secured with crocodile clips. The prepared liquid electrolyte was then introduced into the capillary space between the two electrodes.

2.3 DSSC Characterization

The UV-visible absorption spectra of Elaeocarpus serratus dye were examined utilizing a Spectrophotometer across the wavelength range of 400 - 800 nm. Moreover, the photovoltaic characteristics of the Dye-Sensitized Solar Cell (DSSC) were assessed, encompassing parameters such as open circuit voltage (V(OC)), short circuit current (I(SC)), short circuit current density (J(SC)), fill factor (FF), efficiency (η), series resistance (R(S)), and shunt resistance (R(Sh)). These assessments were performed using the computerized PK-I-V 100 I-V analyzer, under the illumination of an LED light source with an intensity of 100 mW/cm².

3 Results and Discussion

Plant-derived pigments hold significant potential for dye-sensitized solar cells (DSSCs) due to their environmental advantages and strong light absorption properties. These natural compounds, responsible for the colors in flowers, fruits, and leaves, are effective in the photovoltaic processes central to DSSCs. Pigments in plants fall into two main categories: photosynthetic pigments like chlorophylls and carotenoids, which are crucial for capturing light energy, and protective pigments such as anthocyanins, which shield the plant from UV radiation and herbivores [14] [15].

In the case of Elaeocarpus serratus, the green color of the leaves is mainly due to chlorophyll pigments, vital for photosynthesis. As the leaves age or face stress, chlorophyll breaks down, revealing carotenoids, which provide yellow, orange, and red hues while protecting against photodamage. Anthocyanins, which can appear red, purple, or blue depending on pH levels, often emerge in leaves that turn red, offering protection from UV radiation and herbivores [16].

The choice of extraction solvent is crucial in determining how these natural dyes interact with the TiO₂ layer in DSSCs, impacting their effectiveness. Natural dyes, including chlorophylls, carotenoids, and anthocyanins, are cost-effective and sustainable alternatives to synthetic dyes. Their efficiency in solar cells depends on the pigment composition and the interaction strength between dye molecules and TiO₂ nanoparticles. The anchoring groups in the dye molecules, which are influenced by the solvent used, are key to charge transport and separation, affecting the overall photoconversion efficiency [11].

The diverse pigments found in plants like Elaeocarpus serratus not only contribute to their visual appeal but also offer valuable resources for sustainable energy solutions. Their ability to absorb light efficiently makes them ideal candidates for natural sensitizers in DSSCs, presenting a promising alternative to conventional synthetic dyes.

Fig. 3 shows the picture of Elaeocarpus serratus leaves, and the chemical structures of these pigments are illustrated in Fig. 4.



Fig. 3 Picture of the *Elaeocarpus serratus* leaves

$$\begin{array}{c} \text{CH}_3\text{ CH}_3 & \text{CH}_3 & \text{CH}_3 & \text{CH}_3 \\ \text{OH} & \text{CH}_3 & \text{CH}_3 & \text{CH}_3 & \text{CH}_3 \\ \text{OH} & \text{OH} & \text{OH} & \text{OH} \\ \text{OH} & \text{OH} & \text{OH} & \text{OH} \\ \text{CH}_3\text{CH}_2 & \text{N} & \text{OCH}_3 & \text{CH}_3 \\ \end{array}$$

Fig. 4 Structures of pigments in leaves (a) Xanthophyll (Carotenoid), (b) Cyanidin (Anthocyanin), (c) Chlorophyll a, (d) Flavonoid [17]

3.1 Photovoltaic Measurement of the DSSCs

Photovoltaic parameters were determined for dye-sensitized solar cells (DSSCs) using a PK-IV 100 analyzer. under a light intensity of 100 mW/cm^2 .

Fig. 5 presents the correlation between the open-circuit voltage and short-circuit current density for DSSCs that employed different polarity solvent extracts from mature red Elaeocarpus serratus leaves. Table 1 shows the photovoltaic parameter measurement of the Dye-sensitized solar cells

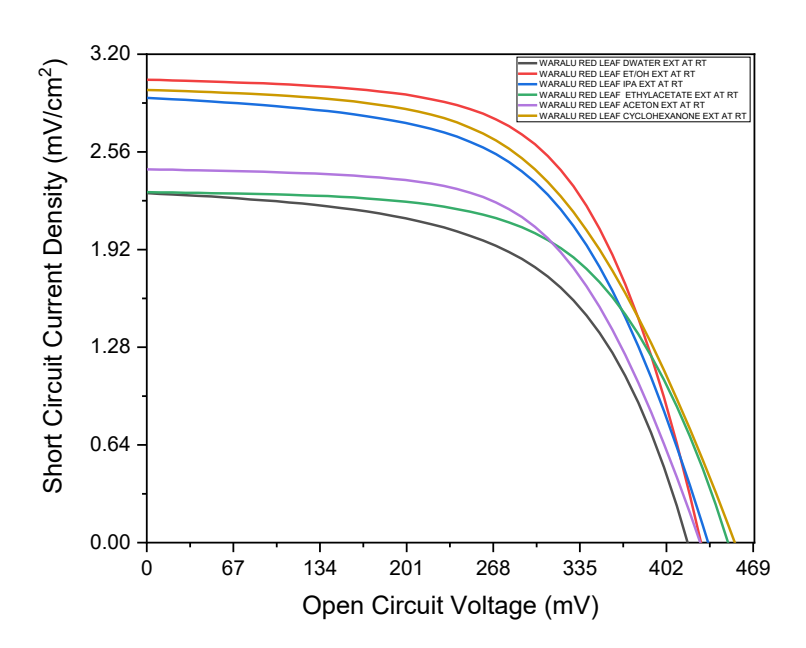


Fig. 5 The relationship between open circuit voltage (V) and short circuit current density (J)

Table 1 Photovoltaic Measurements of the DSSCs

	Open circuit voltage (V(OC)) mV	Short Circuit Current Density (J(SC)) mA/cm ²	Fill Factor	Efficiency (η)
D. Water	418.4	2.290	0.566	0.542
Ethanol	428.7	3.032	0.605	0.786
IPA	434.2	2.914	0.561	0.709
Ethyl acetate	449.6	2.297	0.598	0.618
Aceton	428.1	2.446	0.593	0.621
Cyclohexanone	454.8	2.966	0.544	0.734

3.2 UV-Visible characteristics

The UV-visible absorption, characteristic of various pigments, acts as a distinctive identifier. Chlorophyll absorbs blue-violet and red-blue light, while carotenoids absorb blue-green and violet light, reflecting yellow, red, and orange hues. Flavonoids, including anthocyanins, contribute to a spectrum of colors in plants, with heightened absorption in ultraviolet and blue-green wavelengths and reflection in the blue and violet ranges [17] [18].

Spectrophotometry assesses pigment types by measuring transmitted light, revealing absorbed wavelengths. Extracting and analyzing plant pigments in a spectrophotometer unveils absorbed light wavelengths.

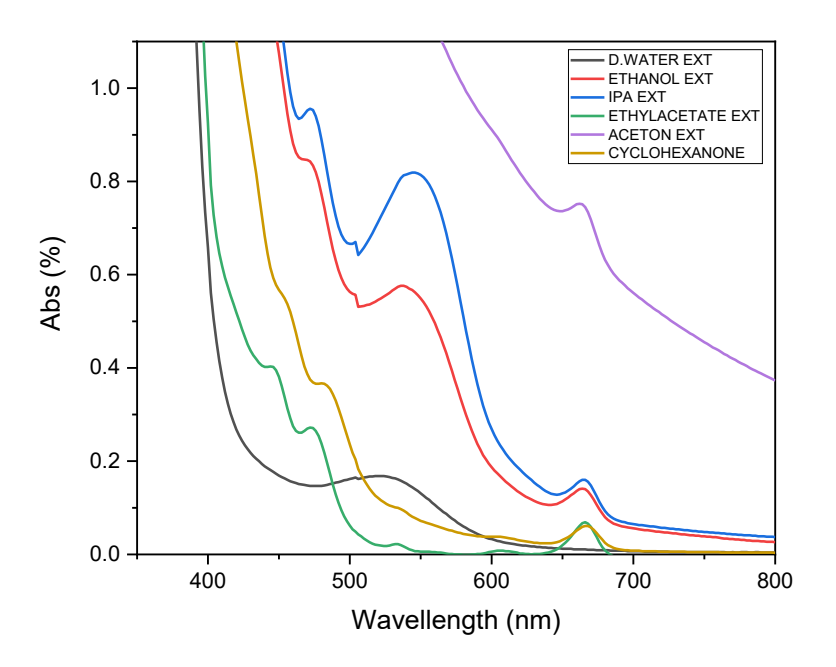


Fig. 6 Absorption spectrum of the Elaeocarpus serratus red leaf in different solvents

In this research study, natural dye was extracted from Elaeocarpus serratus red leaf in different polarity solvents such as Ethanol, Isopropyl alcohol, Distilled Water, Aceton, Cyclohexanone, Ethyl Acetate at room temperature for 24 hours.

Absorption spectrum of the different solvent dye extracts is evaluated by using a UV-Visible spectrophotometer in the range of 400 nm to 800 nm. Fig. 6 shows the UV-Visible absorption spectrum of the *Elaeocarpus serratus* red leaf. Table 2 describes the absorption spectrum wavelengths of each solvent extraction, and Table 3. Describe the unique absorption spectrum wavelengths of the natural pigments.

Table 2 Absorb wavelengths for each solvent extract

Extraction	Abs Wavelength (nm)
D. Water	522.67 nm
Ethanol	663.6 nm, 538.4nm & 471.0 nm
IPA	665.4 nm, 545.0 nm & 471.1 nm
Ethyl acetate	666.7nm 534. 47 nm & 472.5 nm
Aceton	661.8 nm
Cyclohexanone	666.7 nm & 482.6 nm

Table 3 Absorbance wavelengths of the plant pigments

Plant Pigment	Abs Wavelength (nm)
Chlorophyll	425, 470, 606, 640, 660
Carotenoids	450 – 455
Anthocyanin	510 to 520
Xanthophylls	435, 494

It is evident from spectroscopic data that the Dye extract in deionized water contains anthocyanin. The reason for the higher performance of DSSCs dye coated with ethanol extract may be due to the presence of all the pigments, as evident from the absorption spectra. Dye in isopropyl alcohol also shows a similar spectrum. The dye extracted into cyclohexanone seems to contain chlorophylls and carotenoids mainly, and still has comparable efficiency to the ethanol extract, which is an important inference.

4 Conclusion

The study successfully evaluated the effectiveness of various polar solvents in extracting natural dyes from the red leaves of *Elaeocarpus serratus* to be used in dye-sensitized solar cells (DSSCs). Among the tested solvents, Isopropyl alcohol, Distil Water, Aceton, Cyclohexanone and Ethyl Acetate, ethanol achieving the highest efficiency of 0.786% and a short-circuit current density of 3.036 mA/cm². Cyclohexanone showed the open-circuit voltage 454.8 mV and a short-circuit current density of 2.966 mA/cm², resulting in a good efficiency of 0.734%. IPA also performed well with a V(OC) of 434.2 mV, J(SC) of 2.914 mA/cm², and efficiency of 0.709%, making it a strong alternative to ethanol. Acetone produced a V(OC) of 428.1 mV, J(SC) of 2.446 mA/cm², and efficiency of 0.621%, while ethyl acetate showed a V(OC) of 449.6 mV, J(SC) of 2.297 mA/cm², and efficiency of 0.618%. Distil Water had the lowest performance, with a V(OC) of 418.4 mV, J(SC) of 2.290 mA/cm², fill factor of 0.566, and efficiency of 0.542%, highlighting its limitations for DSSC applications. This indicates that ethanol is the most effective solvent for dye extraction from Elaeocarpus serratus red leaves in DSSC applications.

The UV-Visible absorption spectra revealed that the extracted pigments primarily consisted of chlorophylls, carotenoids, and anthocyanins, with characteristic absorption peaks corresponding to these pigments. This spectral data underscores the importance of solvent polarity in optimizing the extraction process for specific pigments that contribute to the overall efficiency of DSSCs.

The photovoltaic measurements further highlighted the influence of solvent choice on key parameters such as open-circuit voltage, fill factor, and resistances, both series and shunt. The superior performance of DSSCs fabricated with ethanol-extracted dyes can be attributed to the optimal absorption and electron transfer properties of the extracted pigments.

Overall, this research demonstrates the critical role of solvent selection in enhancing the efficiency of DSSCs through effective pigment extraction. The findings provide valuable insights for future studies aimed at improving the performance of DSSCs using natural dyes, promoting the development of more sustainable and cost-effective solar energy technologies.

References

- [1] M. S. D. A. M. A. S. Md kashif Gohar Deshmukh, "Renewable energy in the 21st century: A review," *Materials Today*, pp. 1756 1759, 2023.
- [2] B. Freedman, Environmental Science, 2018.
- [3] S. A. R. M. U. D. S. H. A. I. Muhammed Ramzan, "Environmental cost of non-renewable energy and economic progress: DO ICT and financial development mitigate some burden," *Journal of Cleaner Production*, vol. 333, 2022.
- [4] acciona, "SUSTAINABILITY For all," acciona, [Online]. Available: https://www.activesustainability.com/renewable-energy/environmental-impact-of-non-renewable-energies/? adin=11734293023.
- [5] C. R. C. D. Y. R. V. S. D. K. S. J. S. K. S. K. Krishna Kumar Jaiswal, "Renewable and sustainable clean energy development and impact on social, economic, and environmental health," *Energy Nexus*, vol. 7, 2022.
- [6] Park, N.G, "Perovskite solar cells: an emergining photovoltaic technology," *Materials today*, vol. 18, no. 2, pp. 65-72, 2015.
- [7] Wöhrle D.and Meissner D, "Organic solar cells," Advanced Materials, vol. 3, no. 3, pp. 129-138, 1991.
- [8] Aroutiounian V, Petrosyan S, Khachatryan A and Touryan K, "Quantum dot solar cells," *Journal of Applied Physics*, vol. 89, no. 4, pp. 2268-2271, 2001.
- [9] O'Regan B and Gratzel M, "A low-cost, high-efficiency soler cell based on dye-sensitized colloidal TiO2 films," *Natural*, pp. 737-740, 1991.
- [10] M, O'Regan B and Gratzel, "Alow-cost, high-efficiency solar cell based on dye-sensitized colloidal TiO2 films," *Natural journal*, pp. 737-740, 1991.
- [11] Y. U. R. R. Sabarikirishwaran Ponnambalam, "Effect of Natural Dye Solvent Extraction on the Efficiency of Dye Sensitive Solar Cells from Leaf Biomass of Sandoricum koetjape and Syzygium samarangense," *Wast and Biomass Valorization*, 2023.
- [12] P. V. a. A. G. Davisan. S, "Fabrication of Dye-Sensitized Solar Cell Using Natural Dye Extracted from Elaeocarpus serratus Red Leaf," in *IPSL Proceeding 39th Technical Session*, 2023.
- [13] Wickramasinghe G.C, Jayathilaka D.L.N and Perera V.P.S, "Construction of Dye Sensitized Solar Cell Using Natural Dye Extraction from Petals of Erabadu Flower," *OURS*, 2017.
- [14] T. K. A. A. Oluwaseun Adedokun, "Review on Natural Dye-Sensitized Solar Cells (DSSCs)," *International Journal of Engineering Technologies IJET*, vol. 2, 2016.
- [15] Sjursnes B.J., Kvittinegn L. & Schmid R., "Normal and Reversed-Phase Thin Layer Chromatography of Green Leaf extract," *J. Chem. Edu*, Vols. 92, 1, pp. 1993-196, 2015.
- [16] G. A. A. V. P. S. Davisan, "Fabrication of Dye-Sensitized Solar Cell using mixtures of Natural dye Extraction from Elaeocarpus Serratus Red and Green leaves," in *Institute of Physics Sri Lanka*, 2024.
- [17] Sousa C, "Anthocyanins, Carotenoids and Chlorophylls in Edible Plant Leaves Unveiled by Tandem Mass Spectrometry," *Foods*, 2022.
- [18] S. Wakim, "Absorption of Light," in LibreTexts BIOLOGY.
- [19] [Online]
- [20] J. C. D. V. J. B. W. Eduardo Narbona, "Painting the green canvas: how pigments produce flower colours," *The Biochemist*, 2021.

Comprehensive Life Cycle Assessment of Hybrid and Electric Vehicles: Framework to Evaluate Sustainability in the Sri Lankan Context

Bhanuka Samarasinghe^{1*}, Anuradhi Rajapaksha²

¹ The Open University of Sri Lanka, Sri Lanka, ²Monash University, Australia bhanuka.samarasinghe5@gmail.com*, Anuradhi.RajapakshaVithanage@monash.edu

Abstract

Environmental pollution caused by conventional internal combustion engine vehicles is a global challenge the world faces. Hybrid and electric vehicles with less or zero emissions are potential solutions to these negative environmental impacts. However, with the increasing demand for hybrid/electric vehicles, evaluating the true environmental impact and sustainability of these technologies, considering their entire life cycle, from the production and operation stage to end-of-life disposal, is essential. This paper presents a framework to evaluate the environmental impacts of conventional, hybrid, and electric vehicles, mainly focusing on the Sri Lankan vehicle market. The study discusses the key life cycle stages, including fuel and electricity consumption, routine maintenance, and vehicle end-of-life disposal. The findings emphasize the importance of evaluating the entire vehicle life cycle and highlight the need for improved recycling technologies and green energy solutions to achieve true sustainability for hybrid and electric vehicles.

Keywords: Life Cycle Analysis, Hybrid Vehicles, Electric Vehicles, Environmental Impact, Sustainability

1 Introduction

The burning of fossil fuels for energy began around the Industrial Revolution. According to The Energy Institute's Statistical data [1], fossil fuel is the most used energy resource in the world, and CO₂ emissions from the combustion of fossil fuels are the largest source of energy-related greenhouse gas (GHG) emissions, contributing around 87% of the total emissions. This excessive GHG emission results in global warming and thereby negatively affects the climate, ecosystem, human health, agriculture, etc. [2,3] The use of sustainable and environmentally friendly technologies has gained significant attention to overcome these environmental challenges. Transportation, a main user of fossil fuels and contributor to greenhouse gas emissions, plays a major role when designing such solutions. Hybrid vehicles and electric vehicles are such promising, environmentally friendly technologies that have come into the transportation market in the recent past.

Hybrid vehicles feature an internal combustion engine and an electric motor that utilizes electricity stored in battery packs. These two sources of power give the hybrid vehicle the ability to run on either of them: at low speeds or idling, using the electric motor, while at higher speeds or more demanding driving conditions, relying on an internal combustion engine. This combination of an internal combustion engine and an electric motor enhances fuel efficiency and reduces emissions in hybrid vehicles. On the other hand, electric vehicles are fully powered using an electric motor and a large battery, resulting in zero emissions while driving. With global net-zero GHG emission targets and a climate-neutral by 2050 strategy [4], there is a rapid increase in hybrid and electric vehicle usage in the world [5]. This trend is visible in Sri Lanka with the policies and tax releases introduced by the government and the economic benefits that hybrid and electric vehicles offer during their operation phase.

Environmental Life Cycle Analysis (eLCA) is a tool that evaluates the environmental aspects and potential environmental impacts throughout a product's life cycle from raw material acquisition through material processing and transportation, manufacturing, distribution, consumption, reuse or recycling, and final disposal (i.e., cradle-to-grave approach) [6]. With the trends in green transportation, it is essential to evaluate the environmental footprint of hybrid and electric vehicles using strategies like eLCA and find whether those types of vehicles are truly environmentally friendly when analyzed considering their full life cycle. Briefly, we can divide the life cycle of a vehicle into 5 phases: production, assembly, transportation/use, maintenance, and disposal. By examining each phase, we can assess whether hybrid and electric vehicles are truly environmentally friendly or if their advantages are outweighed by the environmental cost of manufacturing and disposal.

Many studies have been done to assess the environmental impact of hybrid and electric vehicles at different phases [7-12]. These studies conclude that compared to conventional vehicles, although hybrid/electric vehicles help to reduce global warming in the use phase due to less or zero emission, they significantly affect the environment by increasing human toxicity, freshwater eco-toxicity, eutrophication and metal depletion impacts etc. during the manufacturing and disposal phases. These negative effects arise from the raw or rare earth material extraction, energy-intensive processes, etc., in the manufacturing phase and challenges in battery disposal and recycling. This study aims to provide a comprehensive framework to evaluate the environmental footprint of hybrid and electric vehicles using eLCA, especially focusing on the Sri Lankan market.

2 Environmental Life Cycle Analysis of Hybrid and Electric Vehicles

2.1 Environmental Life Cycle Analysis (eLCA)

eLCA is a technique introduced by the ISO 14040 and ISO 14044 - Environmental Management standards to increase the awareness of the importance of environmental protection, and the possible impacts associated with both manufactured and consumed products to identify opportunities to improve environmental performance, inform decision makers to take required actions and measures, and identify eco-friendly products etc. [6] It is a systematic approach to assess to environmental impacts associated with all stages of a product's life, from raw material extraction to disposal at end-of-life, and hence known as a "cradle-to-grave" analysis. By considering the entire life cycle, this technique helps manufacturers, consumers, and policymakers to identify the stages where environmental impacts are more significant, allowing for more informed decision-making and the development of sustainable strategies for production, consumption, and waste management.

According to the standards, Life Cycle Analysis (LCA) typically includes four phases: the definition of the goals and scope of the study, the preparation of a life cycle inventory (an inventory of inputs and outputs), the impact assessment, and finally, the interpretation. However, as shown in Fig.1, LCA is an iterative methodology, where refining these phases is required when proceeding forward.

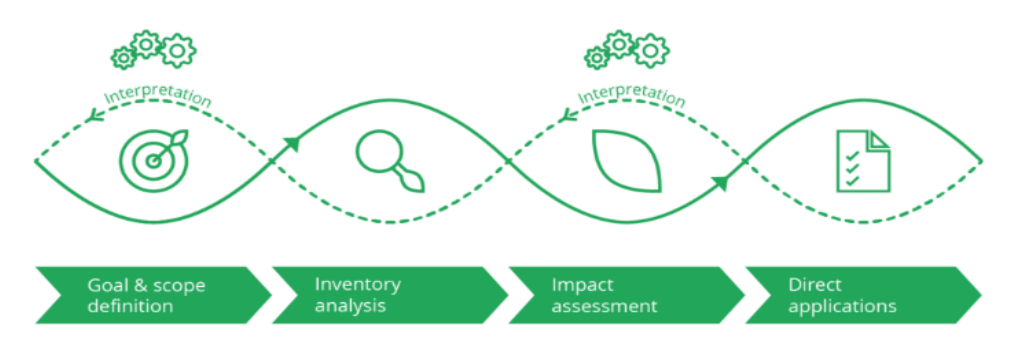


Fig. 1 The iterative LCA methodology (Source: [13])

2.1.1 Goal & Scope Definition

The first phase, goal and scope definition, is a qualitative step that sets the foundation for the entire assessment, defining its purpose, boundaries, and intended outcomes. Determining why the assessment is being conducted and what decisions are intended to inform (product comparison, environmental certification, regulatory compliance, etc.) comes under the goal. This phase also includes defining the functional unit and system boundaries (cradle-to-grave, cradle-to-gate, or gate-to-gate, etc.).

2.1.2 Inventory Analysis

This phase focuses on collecting and quantifying data related to the environmental inputs and outputs of the product. Environmental inputs include resources taken out from the environment to put into the product's life cycle, such as raw materials, energy, and water. Conversely, environmental outputs mean the emissions to the environment, waste generation, etc. This phase of LCA can be carried out in 3 major steps,

- 1. Constructing a detailed flowchart including phases of the product life cycle according to the system boundaries.
- 2. Data collection (both inputs and outputs) for all phases identified in step 1.
- 3. Calculating environmental loads (resource use and pollutant emission) of the product.

2.1.3 Impact Assessment

In this phase, potential environmental impacts such as global warming, acidification, eutrophication, ecotoxicity, human toxicity, resource depletion, etc., are evaluated based on inventory analysis. This step allows us to understand the sustainability challenges associated with each phase of the product's life cycle.

2.1.4 Interpretation

In the final phase of the LCA, results from all phases are considered together and analyzed, considering the uncertainties of the applied data and the assumptions that have been made throughout the study.

2.2 Framework for eLCA of Conventional, Hybrid, and Electric Vehicles

2.2.1 Goal & Scope Definition

The goal of this eLCA is to compare the environmental impacts of hybrid and electric vehicles with conventional internal combustion engine-operated vehicles. A system boundary can be decided based on the data collection, and as a starting point, the most available vehicle type can be selected (e.g., 4-seater passenger car). The presented framework will focus on the vehicle's life cycle from the production stage to the end-of-life stage, adapting to a cradle-to-grave approach. Fig. 2 presents a life cycle structure and boundaries that can be applied to a vehicle [14].

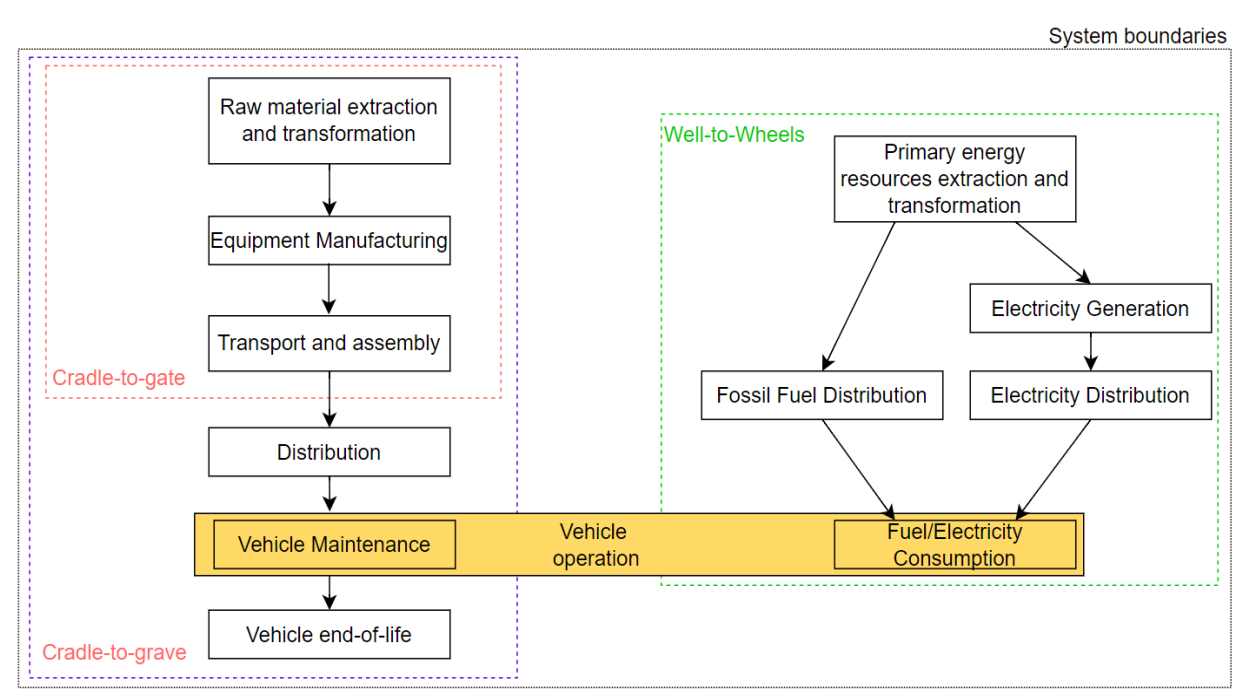


Fig. 2 Life cycle structure and boundaries for the proposed eLCA

2.2.2 Inventory Analysis

Based on the flowchart given in Fig.2, environmental inputs and outputs should be collected for each block. Here, for a detailed analysis, the main blocks can be divided into subblocks and analyzed. Table 1 briefly shows the possible data that can be collected under each block.

Table 1 Inventory analysis tasks for the proposed eLCA

Raw material extraction and transformation	Identify the raw materials required (e.g., metals for battery and body components, rubber for tyres) Quantify the energy used for mining, extraction, and processing of raw material (e.g., electricity, fuels)	
	Record emissions from raw material extraction and transformation processes (e.g., CO2, NOx, SOx from mining machinery, and refining)	
	Collect data on water use, land use, and any hazardous chemicals used in extraction and transformation processes	
Equipment manufacturing	Identify the manufacturing processes involved (e.g., battery assembly, vehicle frame construction)	

	Quantify energy consumption during manufacturing (e.g., electricity for machining)	
	Record emissions from industrial processes	
	Assess material losses, scrap generation, and waste disposal during manufacturing	
	Quantify fuel consumption and emissions from transporting materials to the assembly plant (e.g., fuel use in trucks, trains, ships)	
Transport and Assembly	Record energy and emissions associated with vehicle assembly (e.g., electricity use, process emissions)	
	Collect data on packaging materials used in transport and their disposal	
Distribution	Quantify fuel consumption and emissions during vehicle distribution to dealers or end-users (e.g., shipping from factory to destination)	
Distribution	Track any environmental impacts of any packaging and shipping containers used in the distribution process	
Primary Energy Resource Extraction and Transformation	Quantify the energy and emissions associated with extracting fossil fuels (e.g., coal, oil) for electricity generation and fuel production	
	Include emissions from mining, refining, and processing energy resources (e.g., CO ₂ , Methane)	
	Analyze water and land use associated with energy extraction processes	
Electricity Generation and Distribution	Quantify emissions from electricity generation for charging hybrid or electric vehicles (e.g., power plants burning fossil fuels, renewable energy inputs)	
Distribution	Record transmission and distribution losses in electricity grids	
Fossil Fuel Distribution	Analyze pipeline losses, and fuel transportation impacts (e.g., tanker trucks, ships)	
Fuel/ Electricity Consumption	Quantify the fuel and electricity consumption during vehicle operation over its lifetime	
(Vehicle Operation)	Record emissions from internal combustion engine use (e.g.: CO ₂ , NO ₂ , SO ₂ , particulate matter)	
Vehicle Maintenance	Quantify materials and energy required for routine vehicle maintenance (e.g., oil changes, battery replacements, tyre wear)	
	Record waste generated from maintenance activities (e.g., used oil, replaced parts)	
Vehicle End-of-Life	Analyze the disposal or recycling of vehicle components (e.g., batteries, metals, plastics)	
	Quantify energy use and emissions from recycling processes (e.g., re-melting of metals, dismantling operations)	
	Record environmental impacts from landfilling or incinerating non-recyclable materials	

Most of this data can be collected from industry reports and databases, energy sector reports, environmental impact databases, electricity generation data from the national grid, standardized emission data from manufacturers and testers, recycling industry reports, etc.

2.2.3 Impact Assessment

After performing the inventory analysis, the impact assessment phase translates the collected data into meaningful environmental impacts. Referring to the handbook for recommendations for life cycle impact assessment, provided by the "International Reference Life Cycle Data System" (ILCD) [15], the following are some environmental impact categories that can be assessed for a vehicle eLCA based on the inventory analysis.

- 1. Climate change based on Global Warming Potential (GWP)
- 2. Human toxicity based on Comparative Toxic Unit (CTU)
- 3. Acidification
- 4. Ecotoxicity
- 5. Resources (water, mineral, fossil, etc.) depletion based on consumption

Environmental inputs and outputs found from the inventory analysis for each block in the flow chart can be classified into the above categories. Then, based on the available data, the contribution to different impact categories can be quantified.

2.2.4 Interpretation

In the final phase, results from the impact assessment can be analyzed to obtain a conclusion about the vehicle's overall environmental impact and a comparison between different types of vehicles. Based on the conclusions, recommendations can be provided to reduce the negative environmental effects from different stages of the vehicle life cycle.

3 Discussion

As we focus more on the Sri Lankan market, some of the life cycle stages discussed in the above section are less significant. For example, the Sri Lankan vehicle market mainly depends on imports, and it is not necessary to consider the stages in the cradle-to-gate boundary if we focus only on the environmental impacts that happen in Sri Lanka. Therefore, in this section, we will focus on the life cycle stages, which significantly impact on environment and occur in Sri Lanka.

3.1 Fuel/Electricity consumption during vehicle operation

In the context of Sri Lanka's vehicle market, fuel and electricity consumption during operation is a critical factor in determining the overall environmental impact of vehicles. Conventional vehicles in Sri Lanka mainly run on gasoline or diesel, which contributes to the country's dependence on fossil fuels. According to databases [16,17], transport accounts for a significant portion of fossil fuel consumption in Sri Lanka. Fuel consumption of these vehicles basically depends on the type and size of vehicle, age, accumulated distance travelled, maintenance condition, etc., and are relatively fuel-inefficient compared to hybrids and electric cars. Traffic congestion in urban areas like Colombo further increases this fuel consumption and leads to higher CO2 emissions per kilometer. Additionally, conventional vehicles also emit other pollutants like NO2 and particulate matter, contributing to urban air pollution. In contrast, hybrid vehicles are more fuel efficient due to their combined operation of ICE and electric motors. Electric vehicles rely entirely on electricity, which drastically reduces tailpipe emissions. However, the environmental impact of this electricity consumption depends on the source of electricity. In Sri Lanka, a significant proportion of electricity still comes from fossil fuels, although there is a growing share of renewables, especially hydropower. For instance, according to the Ceylon Electricity Board (CEB, 2022 [17]), around 50% of the grid electricity comes from renewable energy sources, primarily hydropower, with the remainder generated from coal and oil. Therefore, the indirect emissions from electric vehicles depend on the energy mix used for charging.

To conduct a detailed eLCA of these vehicles in the Sri Lankan context, fuel consumption data can be sourced from national energy databases from CEB, transport sector reports conducted by 3rd parties, etc., and emission data can be obtained from vehicle manufacturers and emission testing agencies.

3.2 Vehicle Maintenance

Vehicle maintenance is another critical aspect in the life cycle of conventional, hybrid, and electric vehicles. Proper maintenance not only affects vehicle lifespan and performance but also influences environmental outcomes such as energy use and material consumption over the vehicle's life cycle. Maintenance for ICE conventional vehicles involves routine tasks like oil changes, air filter replacements, and engine tuning. These tasks consume various materials and generate hazardous waste, contributing to environmental impacts. For instance, conventional

vehicles require frequent oil changes, typically every 5,000 km, which generates used motor oil as hazardous waste. According to [18], the disposal and recycling is not well-regulated in Sri Lanka, often leading to soil and water contamination. Additionally, the energy involved in manufacturing replacement parts and fluids (such as motor oil and coolant) contributes indirectly to environmental impacts. Over a vehicle's lifetime, this adds to its overall carbon footprint.

Hybrid vehicles share many maintenance needs with conventional vehicles but require additional checks for battery management systems and periodic battery replacement based on driving conditions and usage. Electric vehicles (EVs) require minimal maintenance due to the absence of ICE components, eliminating the need for oil changes and reducing exhaust system repairs. Lithium-ion batteries in EVs last 8-10 years or 150,000-200,000 km before requiring replacement. Additionally, electric vehicles use regenerative braking, which reduces wear on traditional brakes and extends the lifespan of brake pads and rotors.

To incorporate maintenance phases into an eLCA, data on resource usage, energy consumption, and waste generation can be sourced from emission test centers, vehicle service records, recycling facilities, and environmental impact reports.

3.3 Vehicle End-of-Life

The end-of-life (EOL) phase of a vehicle includes the dismantling, recycling, or disposal of various vehicle components. The EOL phase for conventional vehicles in Sri Lanka typically involves the recycling of metal components, such as steel from the chassis and Aluminum from engine blocks, which reduces the need for raw material extraction and lowers the environmental impact of producing new metal. However, managing non-metal components and hazardous fluids, such as used motor oil and coolant, remains problematic due to improper disposal practices, leading to soil and water contamination.

Hybrid vehicles add complexity to the EOL phase with their Lithium-Ion or Nickel-metal hybrid batteries, which contain valuable rare earth materials like Lithium, Cobalt, and Nickel. Despite the recyclability of metals, Sri Lanka's underdeveloped battery recycling infrastructure often results in improper battery disposal. Similarly, hybrid vehicles' advanced electronics require specialized recycling processes to recover valuable materials from circuit boards. Electric vehicles (EVs) face even greater challenges due to larger and more complex battery systems. While Lithium-Ion battery recycling is a growing industry globally, limited recovery rates and the absence of local recycling facilities in Sri Lanka result in reliance on exports or landfilling, further exacerbating environmental issues. EVs, however, offer opportunities for resource recovery, as they contain high-value materials that could be efficiently reclaimed with improved recycling technologies.

For an eLCA end-of-life phase, data on recycling rates, disposal practices, and resource recovery can be obtained from local recycling industries, environmental agencies, and global case studies. Addressing Sri Lanka's infrastructural gaps, particularly in battery recycling, and developing sustainable EOL strategies are essential for minimizing environmental impacts and supporting a circular economy for vehicles.

Conclusion

This paper provides a comprehensive evaluation framework for assessing the environmental sustainability of hybrid and electric vehicles (HEVs) compared to conventional vehicles in the context of Sri Lanka using Environmental Life Cycle Analysis (eLCA). By systematically examining the critical life cycle stages; operation, maintenance, and end-of-life, this study highlights the significant environmental impacts associated with hybrid and electric vehicles compared to conventional internal combustion engine vehicles.

While hybrid and electric vehicles significantly reduce emissions during their operational phase, particularly in urban environments, the environmental burdens of their production and end-of-life phases, especially concerning battery manufacturing and recycling, pose notable challenges. These challenges are amplified in the Sri Lankan context due to the country's reliance on fossil fuels for electricity generation and limited recycling infrastructure for advanced vehicle components.

Key insights emphasize the need for a comprehensive approach to sustainability that extends beyond operational emissions. Policies encouraging renewable energy integration into the national grid, investments in local recycling technologies, and the adoption of sustainable materials in vehicle manufacturing are crucial. Furthermore, fostering a circular economic framework for end-of-life vehicle components, particularly batteries, is essential for mitigating environmental impacts.

Future research should focus on collecting localized life cycle inventory data and exploring alternative battery technologies to better adapt to Sri Lanka's unique energy and infrastructure landscape. Addressing these gaps will pave the way for sustainable transportation solutions that align with global net-zero emission goals and support Sri Lanka's transition to a greener economy.

References

- [1] "Statistical Review of World Energy," Energy Institute. Accessed: Aug. 06, 2024. [Online]. Available: https://www.energyinst.org/statistical-review/resources-and-data-downloads
- [2] Barbir, F., Veziroğlu, T.N., and Plass H.J., Jr.: Environmental damage due to fossil fuels use. Int. J. Hydrogen Energy, 15(10), pp.739-749, (1990)
- [3] Judkins, R.R., Fulkerson, W. and Sanghvi, M.K.: The dilemma of fossil fuel use and global climate change. Energy & fuels, 7(1), pp.14-22 (1993)
- [4] "2050 long-term strategy", European Commission. Accessed: Aug 06, 2024. [Online]. Available: https://climate.ec.europa.eu/eu-action/climate-strategies-targets/2050-long-term-strategy en
- [5] "The Global Electric Vehicle Market In 2024", Virta. Accessed: Aug. 06, 2024. [Online]. Available: https://www.virta.global/global-electric-vehicle-market
- [6] Environmental management Life cycle assessment Requirements and guidelines. International Organization for Standardization. Accessed: Aug. 10, 2024. [Online]. Available: https://www.iso.org/obp/ui/#iso:std:iso:14044:ed-1:v1:en
- [7] Hawkins, T.R., Gausen, O.M. and Strømman, A.H.: Environmental impacts of hybrid and electric vehicles—a review. The International Journal of Life Cycle Assessment, 17, pp.997-1014 (2012)
- [8] Tagliaferri, C., Evangelisti, S., Acconcia, F., Domenech, T., Ekins, P., Barletta, D. and Lettieri, P.: Life cycle assessment of future electric and hybrid vehicles: A cradle-to-grave systems engineering approach. Chemical Engineering Research and Design, 112, pp.298-309 (2016)
- [9] Lombardi, L., Tribioli, L., Cozzolino, R. and Bella, G.: Comparative environmental assessment of conventional, electric, hybrid, and fuel cell powertrains based on LCA. The International Journal of Life Cycle Assessment, 22, pp.1989-2006 (2017)
- [10] Pipitone, E., Caltabellotta, S. and Occhipinti, L.: A life cycle environmental impact comparison between traditional, hybrid, and electric vehicles in the European context. Sustainability, 13(19), p.10992 (2021)
- [11] Zhao, E., Walker, P.D. and Surawski, N.C.: Emissions life cycle assessment of diesel, hybrid and electric buses. Proceedings of the Institution of Mechanical Engineers, Part D: Journal of Automobile Engineering, 236(6), pp.1233-1245 (2022)
- [12] Verma, S., Dwivedi, G. and Verma, P.: Life cycle assessment of electric vehicles in comparison to combustion engine vehicles: A review. Materials Today: Proceedings, 49, pp.217-222 (2022)
- [13] L. Golsteijn, "LCA basics: Life Cycle Assessment Explained," PRé Sustainability, Jul. 17, 2022. Accessed: Aug. 20, 2024. [Online]. Available: https://pre-sustainability.com/articles/life-cycle-assessment-lca-basics/
- [14] Naranjo, G.P.S., Bolonio, D., Ortega, M.F. and García-Martínez, M.J.: Comparative life cycle assessment of conventional, electric and hybrid passenger vehicles in Spain. Journal of cleaner production, 291, p.125883 (2021)
- [15] "International Reference Life Cycle Data System (ILCD) Handbook- Recommendations for Life Cycle Impact Assessment in the European context", European Commission. Accessed: Aug. 20, 2024. [Online]. Available: https://eplca.jrc.ec.europa.eu/uploads/ILCD-Handbook-Recommendations-for-Life-Cycle-Impact-Assessment-in-the-European-context.pdf
- [16] Dhar, S. and Munshi, T.: Assessment of Skills and Knowledge Gap in Energy Efficiency within the Transport Sector in Sri Lanka Energy (2021)
- [17] Sugathapala, T.: Fuel Economy of Light Duty Vehicles in Sri Lanka (2015)
- [18] "Used Engine Oil Recycling: Challenges and Opportunities PurePath," PurePath, May 21, 2024. Accessed: Aug. 23, 2024. [Online]. Available: https://www.purepathtech.com/used-engine-oil-recycling-challenges-and-opportunities
- [19] Kaya, M.: State-of-the-art lithium-ion battery recycling technologies. Circular Economy, 1(2), p.100015 (2022)

Classification of end-energy use in Wathupitiwala Export Processing Zone to analyze the feasibility of switching to alternative energy sources

C.W.M.D. Chandrasekara¹, L. T. Jayasuriya^{2*}, R. L. K. Lokuliyana³

¹Brandix Apparel Solutions (Pvt) Ltd, Mirigama. ²Department of Electrical and Electronic Technology, Faculty of Technology, Rajarata University of Sri Lanka, ³Department of Mechanical Engineering, Faculty of Engineering Technology, The Open University of Sri Lanka.

ltjayasu@tec.rjt.ac.lk

Abstract

This study examines the end-energy consumption patterns of the Wathupitiwala Export Processing Zone (WEPZ) in Sri Lanka and examines the viability of the switch to renewable energy sources. The research measures the energy use data of various industries in the area, and in this way, it reveals the main areas of consumption and the possibilities for efficiency improvements. It also studies the possibility of using renewable energy sources such as solar PV, wind, hydrogen fuel cells, and waste-to-energy in the zone's operations. The analysis shows that electricity is the principal energy source, with air conditioning and production machinery sectors being the major end-users. The research depicts the economic benefits of Solar PV installations, as well as the deficiencies of wind power and hydrogen fuel cells, which are restrained by weather conditions and location, and financial barriers. Waste-to-energy, which is less competitive at the present time, may have growth opportunities in the future for the WEPZ. The study concludes by affirming that fusion of energy sources has the potential to mitigate GHG emissions while also adding to the security and positively influencing environmental sustainability and long-run energy supply. It will act as a key steppingstone for WEPZ and all the other related areas in Sri Lanka that will need to evolve toward a low-carbon and more resilient energy future.

Keywords: Fuel Switching, Energy Consumption, Alternative Energy, Feasibility Assessment

1 Introduction

Industrial parks in Sri Lanka are vital as they offer infrastructure and accommodation to a wide range of industries for manufacturing activities. These industries require various energy sources to function, thus accounting for Greenhouse gas (GHG) emissions. For instance, the manufacturing and construction sector in 2019 contributed to 1. 03 MtCO2e. Industrial growth in Sri Lanka was followed by the establishment of the WEPZ in 1997-98 by the Board of Investors (BOI), which provided duty-free facilities to industrialists and developed infrastructure facilities for investors. The industries included in the WEPZ are apparel, food & beverages, packaging materials & accessories, each of which has its energy intensity. It is essential to gain detailed knowledge of the type of energy used by these factories, their usage, and the effects on the environment. While some factories have undertaken energy audits and analysed their energy profile and emissions, others have not yet undertaken such an exercise. These bring about the chances of shifting to clean production processes and the use of renewable energy sources. Due to financial issues, the economic crisis for industries has been a problem globally, and one of the consequences has been the price to pay for fossil-based energy systems. Diesel scarcity has affected transport arrangements for employees, the movement of finished goods, and raw material movements. The adoption of new and renewable sources of power can, to some extent, reduce the effects of such trophies, and future operations will be more stable.

The purpose of this research is twofold: the first is to examine the end-energy consumption of factories in the WEPZ in Sri Lanka and the second is to determine the sources of the additional energy in Sri Lanka and the possibility of the additional energy sources being incorporated into the factories' operations given the scalability of the process. The expected output includes coming up with an end-energy consumption profile for the export processing zone, identifying energy wastage areas, and proposing efficiency gains. The research will also aim at finding other potential sources of energy that can be used to meet energy demand, and a possible report on how they can be harnessed.

2 Brief Literature Review

Industrial sites or parks are a common feature with different capacities, facilities, and management across countries worldwide, clustering intensive industrial activities in a tract of land. Global attention on industrial parks and their sustainability transfers has been increasing in recent years, as these have become significant contributors to the industrial sector and contribute more than 50% of national industrial output [1]. Industrial Park development in Sri Lanka was launched along with the open economic policy in 1978. In industrial parks, energy consumption is responsible for GHG emissions and shareable energy infrastructure. Efficient, resilient, and sustainable

infrastructure is a crucial pathway to greening industrialization. Previous studies indicated that energy infrastructure accounted for an average of 75% of direct GHG emissions from industrial parks [2].

The Paris Agreement serves as the foundation for the planning and implementation of decarbonizing carbonintensive sectors in most developed countries. Replacing fossil fuels with renewable energy resources reduces the impact of the emissions of harmful substances into the environment. A reliable project of future energy demand is an essential requirement for planning and formulating policies to provide a sustainable energy supply and switching to alternative energy sources for industrial parks. End-use in industrial parks energy demand illustrated that among the industrial sub-sectors, the energy demand of food beverage and tobacco, textile & leather, chemical rubber & plastics, mechanical engineering & metallurgy, and wood products & papers will be increased [3]. An end-use energy analysis is to identify energy apportioning and use of energy in air conditioning, lifting, lighting, equipment, and others while saving energy and reducing cost comprise. The Building Energy Intensity is calculated to compare the consumption levels of buildings. This is a crucial challenge among building designers, engineers, and decision-makers, to reduce the electricity demand, thus providing monetary savings, greenhouse gas and other pollutant reductions, and improved energy security [4]. Building characteristics, compositions, lifestyles, and equipment are recognized as the main factors influencing energy consumption, which has been a subject of extensive exploration. Energy consumption is measured according to energy sources to impose fees & taxes. ISO 12655:2013 is an international standard for measuring the energy use of buildings that classifies building energy consumption into heating, cooling, domestic hot water, ventilation, lighting, appliance, lift, and auxiliary facilities. Measurement systems are used to evaluate energy consumption by end-use [5][6].

During the end-use energy calculations, it is required to extract key components from the total consumption to avoid explicit modelling dependencies on time of day and on working versus non-working days. Least squares fitting for outside temperature and natural illumination dependency proceeds independently for each hour of the day. Cubic polynomials model dependencies on Steadman's apparent temperature and log-scale illumination. Subsequently, multiple regression models were used to quantitatively analyze the valid determinants of each enduse energy [7]. Renewable energy has gained public attention as a solution to the interlinked problems of economic crisis, volatile energy prices, insecure fossil fuel supplies, and global climate change. Fossil fuels, geothermal energy, and nuclear power exploit highly concentrated, mined resources and convert them to useful energy in power plants or refineries. However, those are highly dependent on intermediate suppliers and commodity markets. Solar, wind, and biomass energy are independent sources that are highly diffuse, ambient energy from the sun or wind, and these are cleaner products. Encouraging the use of renewable energy sources has an impact on the development of responsible environmental management. A hydrogen fuel cell is an energy converter device that produces electricity via the electrochemical reaction, with water as the by-product. The application of fuel cells is strongly related to the economic aspect, including local and infrastructure costs, making it more relevant to implement in a developed country [8].

3 Methodology

The research aims to identify the energy consumption patterns of industries located within the industrial site, where the majority of energy usage occurs. A comprehensive questionnaire was developed to gather relevant information on various aspects, including industry type, industry capacity, energy sources, consumption patterns, applications of energy, and potential areas for optimizing energy consumption in Wathupitiwala EPZ.

A mathematical analysis was conducted based on collected data to rationalize energy consumption concerning the types of energy sources utilized. Mathematical models were employed to identify energy consumption patterns across various industry categories, and a comprehensive evaluation was undertaken to explore potential opportunities. This analysis will inform the identification of opportunities to implement alternative energy sources, particularly renewable energy sources. The suitability and applicability of renewable energy sources for industries in Wathupitiwala EPZ were critically assessed. Geometric, economic, and technical feasibility analyses were performed on alternative energy sources to determine the most appropriate solutions for actual industrial needs, thus clarifying their viability and efficiency. The study concluded with a clear identification of the benefits and risks associated with natural energy sources within the industrial park. Moreover, these alternative energy sources were tested, and their compatibility with real industrial needs was evaluated.

4 Summary of the Analysis

Twenty-four factories utilize various energy sources in their manufacturing processes, leading to greenhouse gas emissions accounted for by the organization. Energy consumption for product manufacturing is classified as direct consumption, while administrative activities such as security, meal provision, and transportation are categorized as indirect energy consumption. Common energy sources identified among the factories include electricity, furnace oil, biomass, and LPG. A questionnaire was created to gather historical data from the factories, encompassing

energy sources, production capacity, and energy usage to examine the relationship between production, energy consumption patterns, and energy sources for each organization. Data collection faced limitations due to non-operational factories, and the lack of energy monitoring mechanisms, resulting in data gathered from only twelve organizations for the initial analysis.

Energy sources against consumption are plotted in Fig. 1, which gives a brief overview of each organization using what type of energy sources.

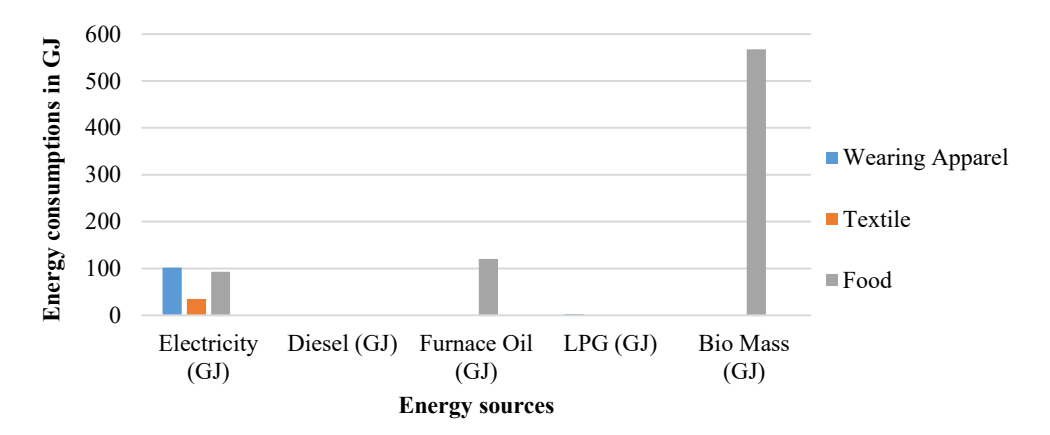


Fig. 1 Energy sources against consumption.

Fig. 1 gives information about the energy consumption of key industry categories operating in the Wathupitiwala EPZ, where historical data is available. It can be identified as electrical energy used by all four industry categories. Multiple organizations use electricity, and it can be analyzed in detail considering industry categorization and consumption. Electrical energy consumption in the wearing apparel industry category was plotted against production output to gain further understanding. Organizations are referred to as units and numbered sequent Unit 1, Unit 2, Unit 3 & Unit 4. Unit 1 has almost twice as many operating sewing machines compared to Unit 2. Unit 3 only caters to warehousing and pre-production operations of the garments before moving into the sewing operation. This includes cutting, molding, and kitting operations with higher production capacity. Unit 4 only caters the seamless garment manufacturing with heat presses and fabric bonding machines. Table 1 provides information on the machines used at these four units. Energy intensity depends on the number of machines in operation.

	Unit 1	Unit 2	Unit 3	Unit 4
Sewing machines	✓	✓	-	✓
Heat transfer machines	✓	✓	-	✓
Mini electric boilers	✓	✓	-	✓
Heat press machines	-	-	=	✓
Molding machines	-	-	✓	=
Auto cutters	-	-	✓	-
Spreaders	-	-	✓	-
Laser cutters	-	-	✓	✓
Piping cutters	-	-	✓	-
Band knifes	✓	✓	✓	✓

Table 11 Machine mix of wearing apparel factories.

Fig. 2 shows the energy consumption drop during the year 2020. Compared with the production output, it represents a sudden rise. Background stories supported the deviation in the plot, as 2020 was impacted by the COVID-19 pandemic, factory operations were altered with lockdowns, and operational demand was reduced. The apparel sector faces difficulties in production, sales, and sudden moves on product type changes cause abnormalities.

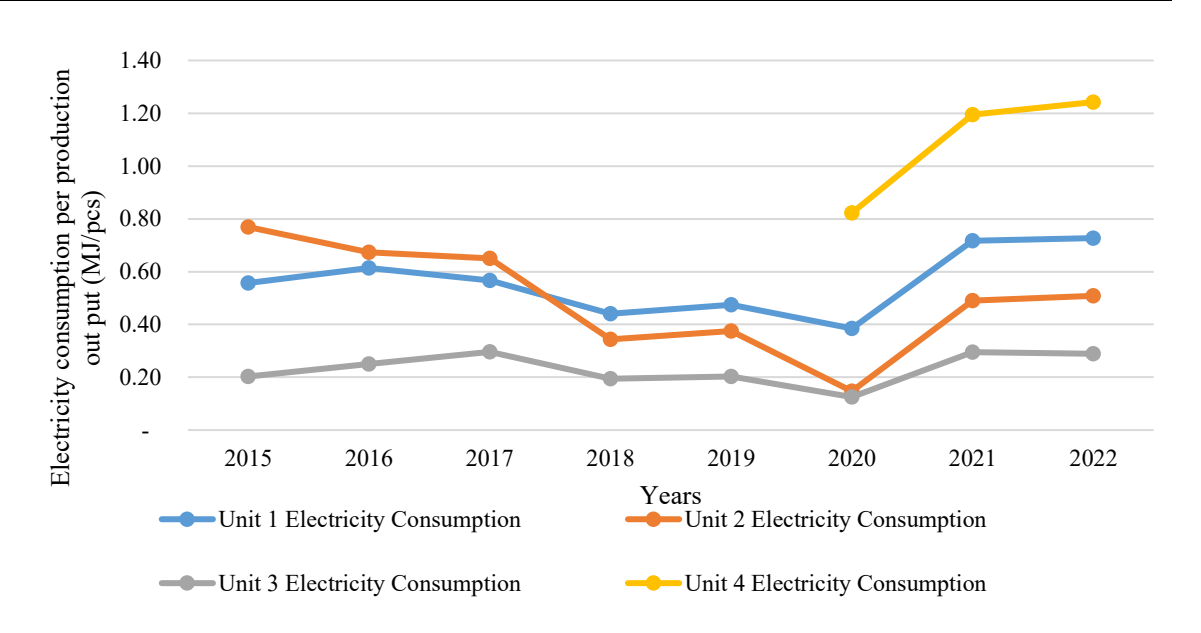


Fig. 2 Comparison of wearing apparel factories.

Electrical energy consumption in food processing industry-related factories was analysed with historical data, where they represent Unit 8, Unit 9 & Unit 10 in Fig. 3. Unit 8 consists of a large-scale operation with 3 nos. of (Ultra High Temperature) UHT machines. UHT is a complex manufacturing process incorporated with a sequence of machinery that consumes more electrical energy. Unit 8 has recorded power consumption through power analyzers over the period. From the observation of the power analyzer recorded data pattern, the October to December period represents a continuous data set analyzed in Fig. 4. A Gradual increase in this quarter can be seen, specifically in the month of December. This is basically due to the seasonal market demand.

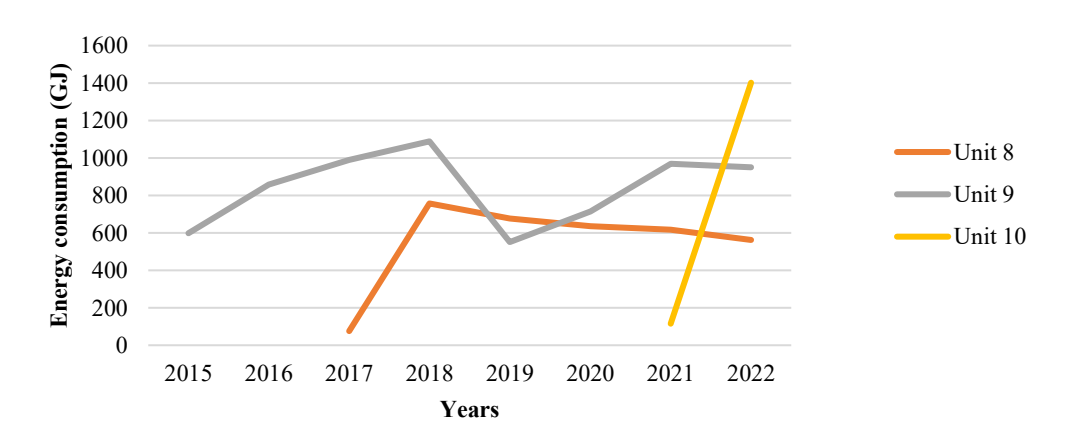


Fig. 3 Electrical energy use (GJ) comparison in food processing factories

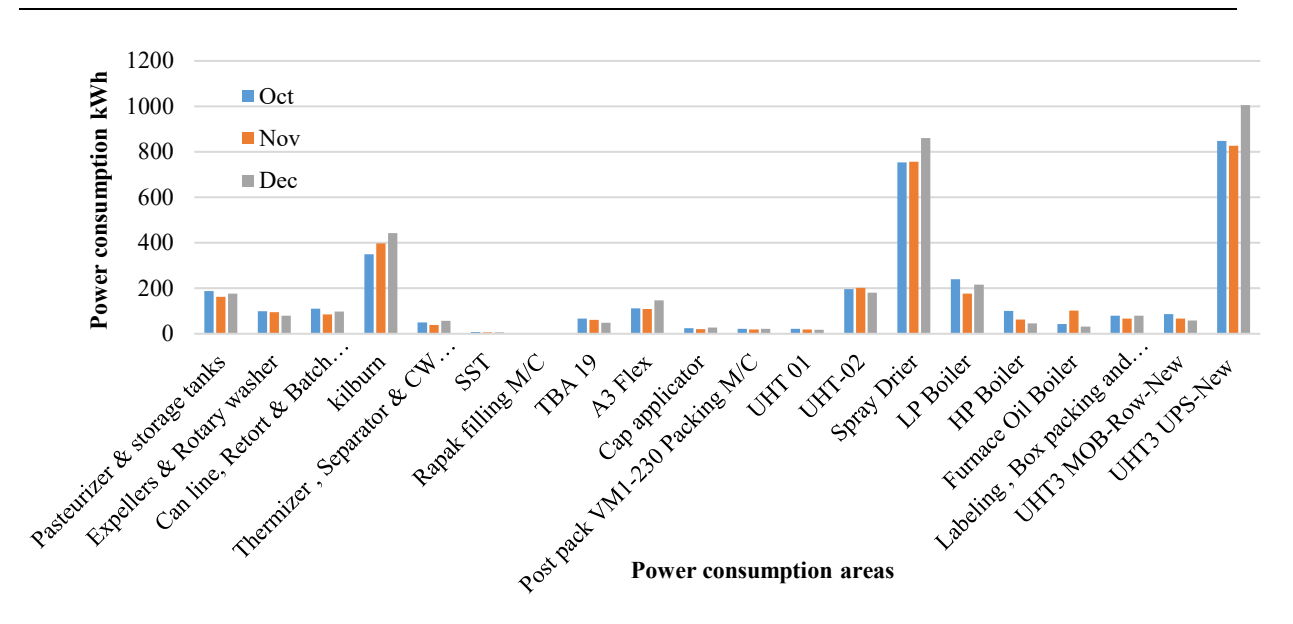


Fig. 4 Power consumption of different production areas in Unit 8

Electrical energy conversions and end use were analysed according to the collected data. Compared to the industry categorization, end-use categories for electrical energy are as per below,

- Lighting lighting systems in production floor, office areas, task lighting, street lighting
- **Production machines** electricity consumption of sewing machines, different types of cutters, etc.
- Heating machines heat seal, heat press, Molding, ovens, burners, UHT
- Steam generation mini electric boilers.
- Compressed air generation compressors, dryers
- Air conditioning central air conditioning systems, package type air conditioners, split type air conditioners, dehumidifiers
- Ventilation ceiling fans, wall-mounted fans, industrial fans, exhaust fans, forced ventilators.
- Refrigeration refrigerators, bottle coolers, cool rooms, cool boxes
- Cooking rice steamers, industrial blenders, grinders, choppers,
- Other this section considers electrical energy uses that cannot be easily recognized in the above-specified categories. This includes the energy consumption of workshop tools for different activities, pumps used for ad hoc works, and electricity used for construction activities of the sites and events such as musical shows.

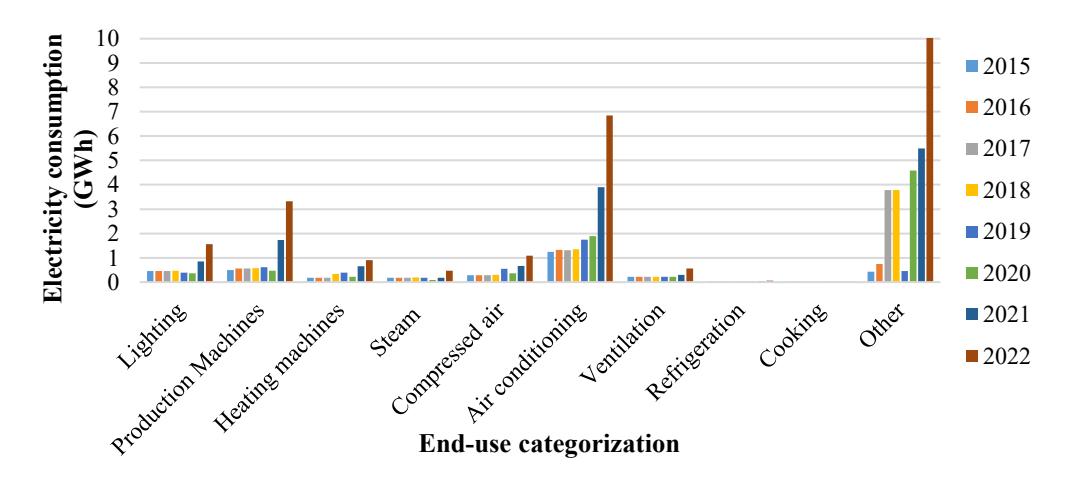


Fig. 5 Electricity consumption analysis.

According to Fig. 5, from the defined end-use categories, air conditioning systems consume the highest portion of electrical energy. Production machinery and lighting systems consume electrical energy accordingly to the second and third highest. For a better understanding of the electrical energy use of the above categorization, each category is compared within the industrial type.

According to Fig. 6, there can be a slight reduction in energy consumption for lighting during the 2018 - 2019 period because of converting fluorescent bulbs to LED bulbs. Compared to Units 2 and 4, Units 1 and 3 consume a higher portion of electricity for lighting. This is due to two reasons Unit 1 and Unit 3 have larger floor areas and several light fixtures installed to meet the expected lux level defined by the factory ordinance for specific operation. Unit 3 has a variety of operations and requires higher lux levels as inspection & cutting operations are performed, which need physical inspection verification.

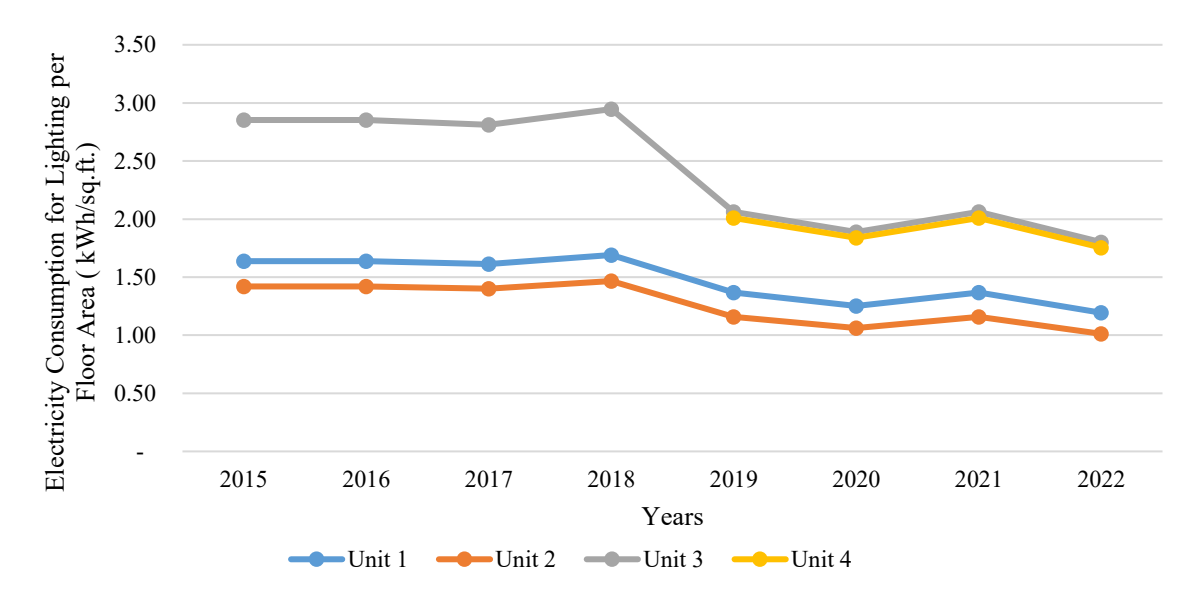


Fig. 6 Electricity consumption (solid lines) for lighting comparison in the wearing apparel category by floor area (dotted line).

The end energy consumption of electrical energy is represented in Fig. 7 for Unit 1, Unit 2, Unit 3, and Unit 4. There can be a significant reduction from 2020, due to the impact of the COVID pandemic.

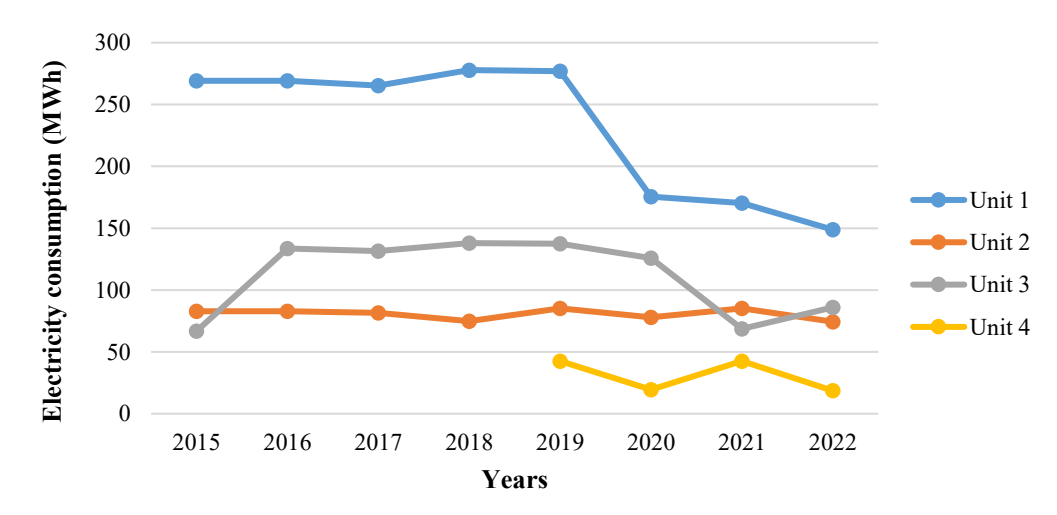


Fig. 7 Electricity consumption for production machines comparison in the wearing apparel category.

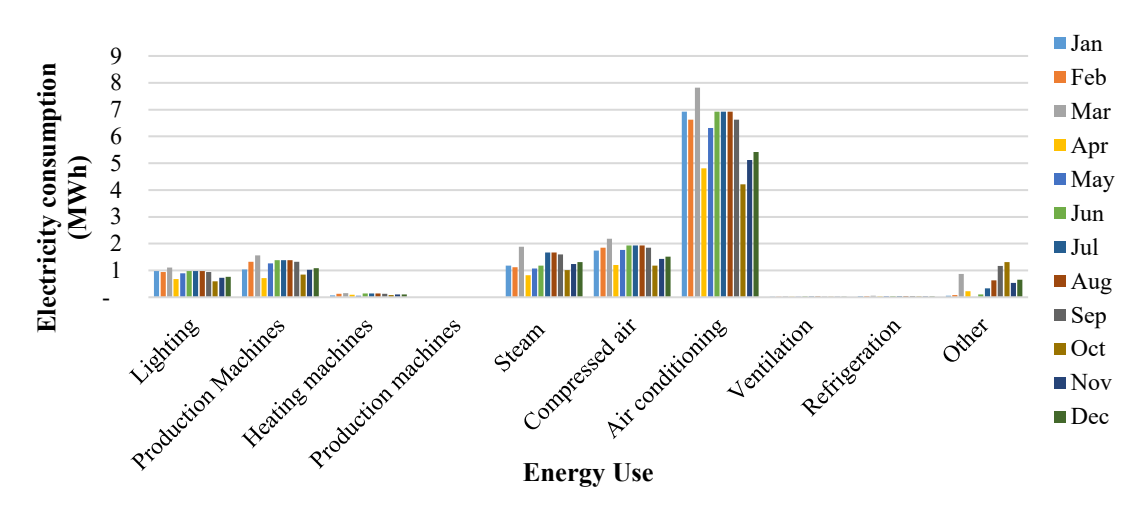


Fig. 8 Unit 1- 2022 full-year energy use classification.

Electricity consumption of production machines (example analysis for Unit 1 is given in Fig. 8) and production output of the year 2022 were compared to get a better understanding. There are abnormal behaviors identified in May-June & Nov-Dec months as electricity consumption by production machines remains higher, but produced pieces is lower. Finding the root cause concludes that reworks of the pieces caused additional operations but did not generate countable output, which deviates from the relationship between electricity consumption and output. This kind of behavior incurred financial losses to the organization.

Biomass is used for steam generation at food processing factories in the zone, as there are different end uses including indirect heating, drying, cooling & finishing operations. Indirect heating includes making hot water, boiling milk, and hot water jacketing to maintain the temperature of the distribution networks & storage tanks of chocolate & other mixtures. Unit 7 & Unit 8, which are manufacturing food products, widely use steam generated through biomass. Figs. 9 and 10 give information on the energy consumption of the food processing industry categorization.

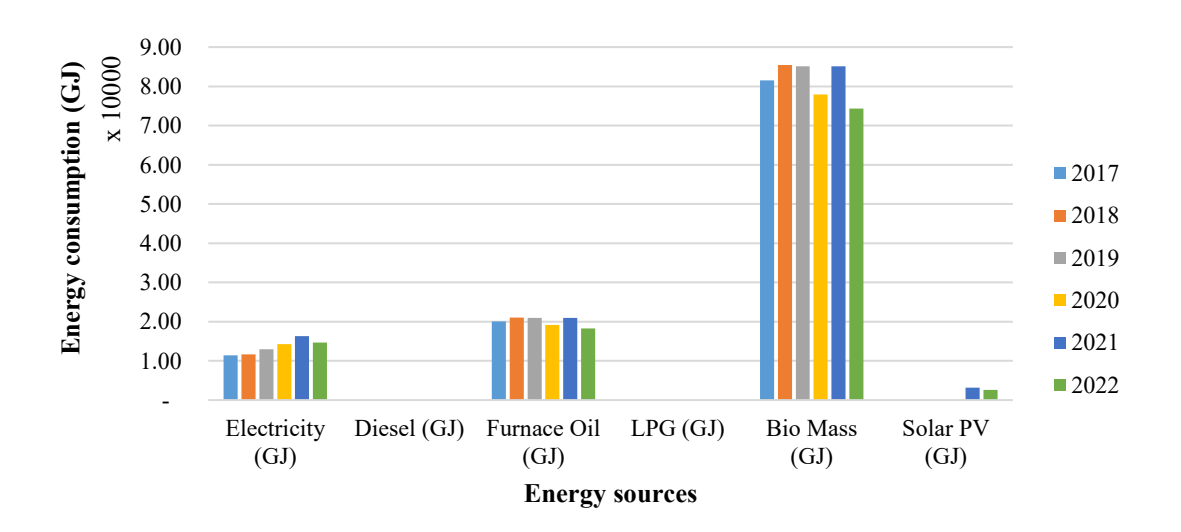


Fig. 9 Energy consumption by sources at Unit 7

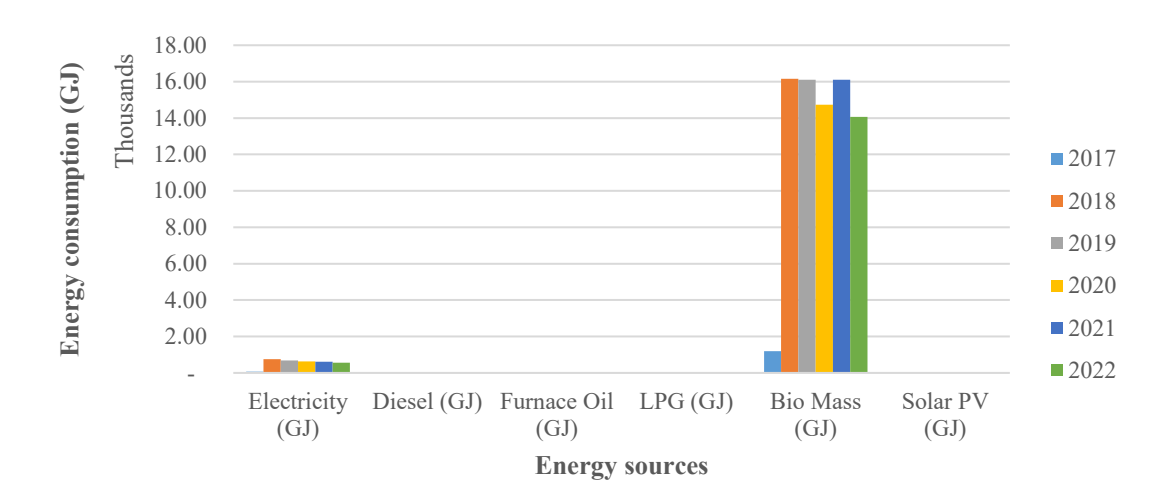


Fig. 10 Energy consumption by sources at Unit 8

Energy consumption is at the average level, and there cannot be major variations. Also, the impact of the COVID pandemic during 2020 is negligible compared with other industry categorizations, especially the wearing apparel category, as discussed earlier, because the food processing operations depend on machines rather than people, compared to the apparel sector. Applications of the steam generated through biomass are different and specific to the operation process, causing difficulties in the end energy use comparison between organizations. According to the collected data, furnace oil is only consumed at Unit 7, which is for steam generation.

LPG is consumed for cooking purposes by most of the organizations in the WEPZ, where there are no consumption tracking mechanisms implemented. The lack of recorded data creates difficulties in the analysis and forecasting.

4.1 Alternative energy sources for Wathupitiwala EPZ

Analysis concluded that a widely consumed energy source is electricity where it needs to find alternative energy sources.

4.1.1 Solar Energy

Solar PV generation has emerged as a prominent and sustainable solution to meet the increasing electricity demand. Harnessing the power of sunlight, solar PV technology converts solar energy directly into electricity using semiconductor materials. This renewable energy source offers different advantages, including abundant availability, minimal environmental impact, and the potential for decentralized power generation.

Organizations found that the return on investment of Solar PV systems is higher, and the move toward renewable energy sources and trends is happening. Electricity generated by the solar PV system is supplied to the CEB. WEPZ has a global horizontal irradiation daily as 5.2 kWh/m2 and a photovoltaic potential daily of 4.0 kWh/kWp, which is a good number over the period, referring to the global solar atlas. Therefore, this industrial site can generate higher electricity with a Solar PV system, where organizations plan to install roof-mounted Solar PV systems on their premises.

Fig. 11 represents the growth of grid-connected electricity generation through Solar PV systems by organizations located in the industrial site. We can consider changes in environmental aspects, such as increased rainfall days and CEB network interruptions, as challenges for the continuity of Solar PV generation, where it can identify a remarkable generation drop in 2022 compared to 2021.

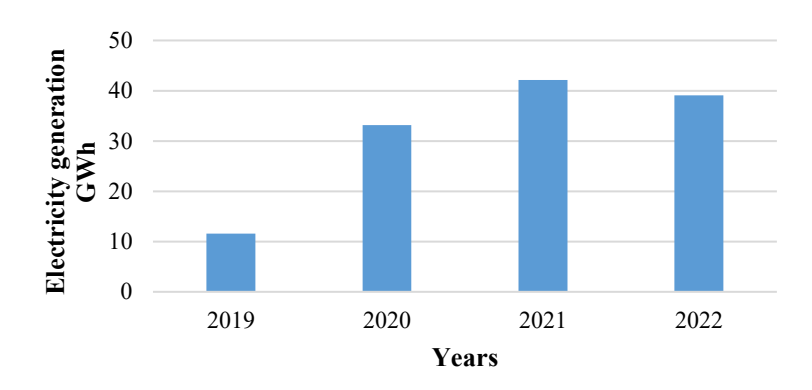


Fig. 11 Solar PV Electricity generation (GWh) by the organizations in the zone.

A roof-mounted solar PV system can expand over 86,400 m², supporting approximately 43,200 solar panels with a total generation capacity of 17 MW. The system requires 85 inverters (200 kW each), with a total capital cost of LKR 1.47 billion. The site receives 4.64 kWh/m²/day of solar insolation, generating an estimated 67,470.8 kWh/day or 24.3 GWh/year. With CEB purchasing electricity at LKR 34.50/kWh, annual revenue is projected at LKR 837.99 million, resulting in a payback period of around 2 years. Converting 150 streetlamps to solar-powered units would cost LKR 5.25 million, saving LKR 2.96 million annually, with a payback period of 2 years.

4.1.2 Wind Energy

Global Wind Atlas was developed with the data collection to provide information on wind speeds and patterns, allowing for an assessment of the wind resource potential in different regions. According to the information on the global wind atlas, at 100 m height, wind speed 4.73 m/s and mean power density 100 W/m² around the area WEPZ is located do not meet the minimum threshold required for efficient and cost-effective wind energy generation. Since the location is not close to the coastal area, the wind speed will be lower and will not meet expectations. Also, well minimum clearance space required for wind turbines cannot be accommodated within the zone. Therefore, wind energy is not a viable alternative energy source for this study.

4.1.3 Hydrogen fuel cell

The hydrogen fuel cell is a developing technology that can be applied as an alternative energy source for industrial parks. Hydrogen fuel cells hold great promise for the lighting sector rather than other applications as fuel for automobiles and many others. It offers an eco-friendly and sustainable alternative to conventional power sources.

Hydrogen fuel cells can be utilized to power a wide range of devices, from small-scale lighting fixtures to larger installations in residential, commercial, and industrial settings. Fuel cells can be coupled with energy-efficient LED lighting systems to maximize energy savings and extend the operational life of the lighting fixtures. The combination of hydrogen fuel cells and LEDs provides a sustainable and long-lasting solution, reducing both electricity consumption and GHG emissions.

Though hydrogen fuel cells have these advantages as an alternative energy source, their pricing is not yet competitive to make a change in the energy market. This will impact the feasibility of the application as an alternative energy source. Considering the initial investment and the advanced technology required, it can be concluded that fuel cell storage-based power generation is not a viable alternative energy source for WEPZ.

4.1.4 Waste-to-Energy

The solid waste consists of fabric offcuts, fabric dust, and mixed waste collected at the BOI dump yard and those sent for incineration or landfill. Solid waste collection over the last 3 years was analysed and represented in summary in the following Fig. 12.

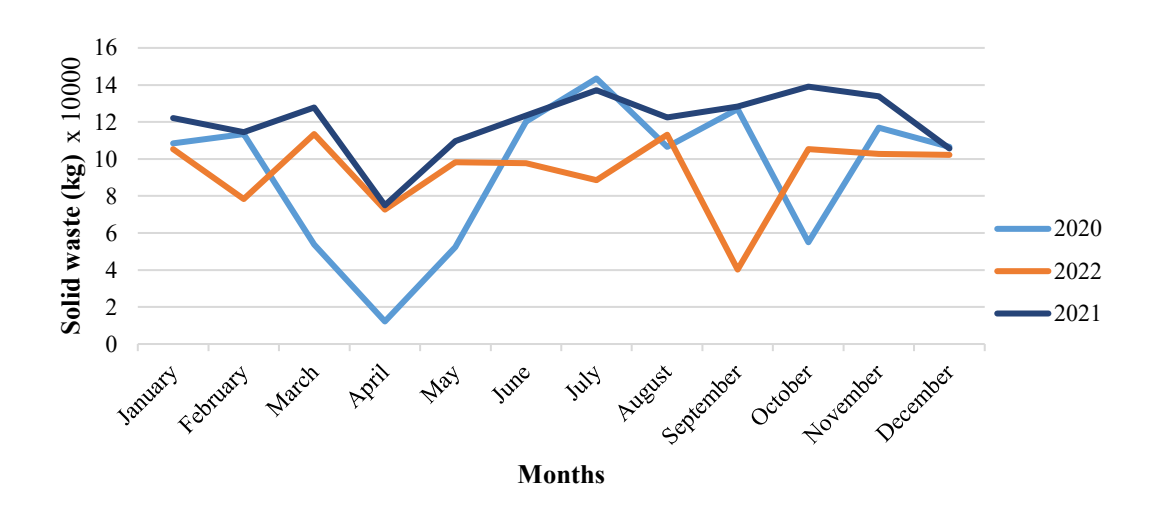


Fig. 12 Total solid waste disposal over the past 3 years.

A waste-to-energy plant could potentially manage the 100,000 kg of solid waste collected monthly (approximately 3,333 kg/day or 138 kg/hr). This waste stream is primarily composed of fabric off-cuts (80%) with a calorific value of 15.5 MJ/kg. The plant, with a capacity of 3 metric tons per day, would be able to generate around 1.5 MWh of electricity daily, amounting to 600 MWh annually, based on the estimate that 0.5 MWh can be generated from one ton of solid waste.

The investment required for such a plant, sourced from China, is calculated at \$250 per annual ton capacity, leading to a total investment cost of \$300,000 for a plant capable of handling 1,200 tons annually. The O&M costs are projected to be \$17 per ton, equating to an annual O&M cost of \$20,400.

LCOE for this waste-to-energy plant is calculated at \$0.534 per kWh, or 179.88 LKR per kWh, assuming 8,760 operating hours per year. Given that the cost to produce electricity from this plant is significantly higher than the price of electricity sold in the current market, the economic feasibility of generating profit through the sale of electricity from the waste-to-energy plant is low under current conditions.

5 Conclusion

The present study has provided a detailed analysis of the end-energy consumption patterns and the potential adoption of renewable energy within WEPZ. It also emphasized that quite a considerable opportunity for energy saving and reduction of related emissions through targeted interventions is available.

Electricity consumption in the zone is dominated by sectors such as air conditioning and production machinery, meaning that energy-efficient technologies and practices would be highly relevant in these areas. Besides, external events such as the COVID-19 pandemic have shown the importance of building resilience in energy systems and supply chains.

While solar PV presents a strong case for renewable energy integration with attractive financial returns, there are clear limitations regarding how far wind energy and hydrogen fuel cells could go in meeting this objective. A diversified approach toward the sourcing of energy, therefore, must be undertaken. The economics of the waste-to-energy solution do not sound very encouraging at this moment. However, the idea is worth giving more time as technology improves, along with the change in market forces.

The evidence from this study, therefore, acts as a roadmap upon which WEPZ and other industrial zones could diversify into sustainable and resilient energy futures. Energy efficiency, utilization of renewable energy, and deploying the latest technologies in such zones would substantially reduce environmental degradation and improve energy security and help develop a greener economy.

Abbreviations

AFC - Alkaline Fuel Cells

BEI – Building Energy Index

BOI – Board of Investment

CEB - Ceylon Electricity Board

CHP - combined heat and power

CNC - Computer Numerical Control

FCV - Fuel Cell Vehicles

GHG - Greenhouse Gas

ISO - International Standard Organization

LED - Light Emitting Diode

LPG - Liquid Petroleum Gas

LCOE - The Levelized Cost of Electricity

NWSDB - National Water Supply and Drainage Board

O&M – Operational and maintenance

PAFC – Phosphoric Acid Fuel Cell

PEM – Proton Exchange Membrane

PV - Photovoltaic

SOFC - Solid Oxide Fuel Cells

UHT - Ultra High Temperature

WEPZ - Wathupitiwala Export Processing Zone

Acknowledgment

My gratitude goes to the participants who volunteered their time and insights, as their contributions were crucial to the empirical foundation of this work. I am grateful to WEPZ, BOI Sri Lanka and all organizations based in the zone for providing the necessary resources, facilities, and support that made this research possible. I am truly fortunate to have had such a remarkable network of individuals by my side, and I remain deeply grateful for their contributions.

References

- [1] Guo, Y., Tian, J., & Chen, L. (2020). Managing energy infrastructure to decarbonize industrial parks in China. *Nature Communications*, 11(1). https://doi.org/10.1038/s41467-020-14805-z
- [2] Bhattarai, N., Bajracharya, I., (2015). Industrial sector's energy demand projections and analysis of Nepal for sustainable national energy planning process of the country. *Journal of the institute of Engineering*, 11(1):50-66.
- [3] McNeil, M. A., Karali, N., & Letschert, V. (2019). Forecasting Indonesia's electricity load through 2030 and peak demand reductions from appliance and lighting efficiency. *Energy for Sustainable Development*, 49, 65–77. https://doi.org/10.1016/j.esd.2019.01.001
- [4] Moghimi, S., Azizpour, F., Mat, S., Lim, C. H., Salleh, E., & Sopian, K. (2013). Building energy index and end-use energy analysis in large-scale hospitals—case study in Malaysia. *Energy Efficiency*, 7(2), 243–256. https://doi.org/10.1007/s12053-013-9221-y
- [5] Hobby, J. D., & Tucci, G. H. (2011). Analysis of the residential, commercial, and industrial electricity consumption. https://doi.org/10.1109/isgt-asia.2011.6167087
- [6] Soo Jin Lee, You Jeong Kim, Hye Jin, Kim, Sung Im, Soo Yeon Ha, & Song, S.-Y. (2019). Residential End-Use Energy Estimation Models in Korean Apartment Units through Multiple Regression Analysis. *Energies*, *12*(12), 2327–2327. https://doi.org/10.3390/en12122327
- [7] Xie, Y., & Azlin. (2022). Factors Affecting Residential End-Use Energy: Multiple Regression Analysis Based on Buildings, Households, Lifestyles, and Equipment. *Buildings*, *12*(5), 538–538. https://doi.org/10.3390/buildings12050538
- [8] Baharuddin, N. A., Wan Yusoff, W. N. A., Abd Aziz, A. J., & Mohd Tahir, N. N. (2021). Hydrogen fuel cells for sustainable energy: Development and progress in selected developed countries. *IOP Conference Series: Materials Science and Engineering*, 1078(1), 012011. https://doi.org/10.1088/1757

Characterization and Analysis of Cellulose Extracted from Salvinia molesta

A. R. Abeyweera*, A.M.P.B. Samarasekara

Department of Materials Science and Engineering, University of Moratuwa, Kattubedda, Sri Lanka. abeyashani16@gmail.com

Abstract

Salvinia molesta, an aggressive aquatic weed, poses a significant threat to global water bodies by rapidly invading and disrupting ecosystems, leading to substantial environmental and economic impacts. Traditional methods for controlling this invasive species, ranging from biological and physical to chemical strategies, often prove ineffective over time, costly, and labor-intensive. Recent research suggests that microcellulose, a material renowned for its unique properties, offers promising alternatives. This study investigates the extraction of highpurity cellulose from Salvinia molesta through a comprehensive pretreatment process. The process involved Soxhlet extraction, followed by alkaline treatment and bleaching, aimed at isolating cellulose from the weed's biomass. Chemical analysis of the plant material revealed the average composition of 25.4% cellulose, 11.9% hemicellulose, 3.3% lignin, and 19.5% ash content, with a moisture content of 46.8% in the fresh sample. The extracted cellulose was rigorously characterized using Fourier Transform Infrared Spectroscopy (FTIR) to confirm its chemical structure and Scanning Electron Microscopy (SEM) to detail its morphology. The FTIR results affirmed the successful isolation of cellulose with minimal residual impurities, while SEM provided insight into its structural integrity. The findings highlight the successful extraction of high-quality cellulose from Salvinia molesta, demonstrating its potential for diverse applications in materials science, environmental management, and other fields. This study not only proposes a sustainable solution for managing the invasive Salvinia molesta but also explores innovative ways to repurpose this invasive species into valuable materials.

Keywords: Salvinia molesta, cellulose, eco-friendly, sustainable, aquatic weed

1 Introduction

Salvinia molesta, a rapidly proliferating aquatic plant, presents significant environmental and socioeconomic challenges on a global scale. This invasive species disrupts essential ecosystem services, including transportation, hydropower generation, and fishing, leading to severe consequences for local economies and biodiversity. Traditional control methods, biological, physical, and chemical, while commonly employed, are not only costly and labor-intensive but also fail to deliver sustainable long-term solutions [1] [2]. Moreover, the disposal of Salvinia biomass, which is often managed through landfilling, exacerbates environmental problems by contributing to secondary contamination through nutrient leaching and the emission of greenhouse gases [3][4]. Effective management of Salvinia molesta, therefore, requires an integrated approach that combines existing technologies with innovative research to develop practical, sustainable solutions [5] [6].

One promising alternative is the valorization of *Salvinia* biomass as a feedstock for producing high-value materials, particularly due to its high cellulose content and rapid growth, which does not compete with arable land. The production of cellulose from this renewable plant source offers both economic and environmental benefits, making it a viable option for addressing the invasive plant problem. Cellulose, which is derived from lignocellulosic biomass, can be produced through various mechanical, biological, and chemical processes. Mechanical methods such as ball milling and high-pressure homogenization are known for their efficiency but are energy intensive. Enzymatic hydrolysis, while effective in breaking down cellulose, tends to be slow and costly. Acid hydrolysis, particularly with hydrochloric acid, stands out as it yields high-quality cellulose microcrystals, making it a preferred method for cellulose extraction [7][8].

In the context of Salvinia molesta, the synthesis of cellulose presents a novel and sustainable approach to managing this invasive species. This study focuses on the extraction and characterization of cellulose from Salvinia molesta using a combination of alkaline pretreatment and delignification methodologies. These processes are known for their effectiveness in breaking down the complex lignocellulosic structure of plant biomass, allowing for the isolation of high-purity cellulose. The resultant cellulose exhibits promising properties for various applications, particularly in biomedical engineering and renewable energy sectors. The study not only highlights the economic and environmental advantages of this approach but also contributes to the growing body of research on utilizing invasive species as a resource rather than a waste product.

This comprehensive investigation into the characterization of cellulose isolated from Salvinia molesta contributes significantly to the field of materials science, where there is a growing interest in renewable and sustainable resources. The findings from this study could inform future research and drive innovation in industrial applications, promoting the use of natural resources to address environmental challenges.

2 Methodology

2.1 Materials

Salvinia molesta was obtained from Thalangama tank in Kaduwela, Sri Lanka, situated at 6°53'16.99"N latitude and 79°56'50.10"E longitude. The experimental procedures involved the use of toluene (99%), ethanol (97%), potassium hydroxide (97%), hydrogen peroxide (50%), acetone, sodium hydroxide, sulfuric acid (98%), and barium chloride solution, all of analytical grade.

2.2 Cellulose Extraction and Purification

Salvinia went through a comprehensive cleaning process, commencing with sequential washes using tap water and distilled water to effectively eliminate any residues of soil, sand, and debris. Subsequently, the air-dried Salvinia underwent a meticulous grinding procedure to produce a fine powder using a grinder, followed by sieving to ensure uniformity, and subsequent storage within a sealed plastic bag for further analysis. An exact measure of thirty grams of the powdered substance was carefully dispensed into a porous thimble and sealed with pristine cotton wool. A mixture containing 300 ml of toluene and 150 ml of ethanol in a 2:1 ratio was employed to extract the crushed Salvinia powder through deployment of a Soxhlet extractor, maintained at a temperature of 75 °C for a duration of 6 hours. Following this, the powder underwent a dewaxing process and was subsequently neutralized through ethanol washing, before being subjected to a two-hour drying period within an oven adjusted to 60 °C [9].

The dewaxed powder was then subjected to an alkaline treatment process utilizing 2% and 5% potassium hydroxide at a temperature of 90 °C, while being continuously agitated on a magnetic stirrer. This treatment process was repeated twice for each percentage, with a specific 1:20 (g/ml) ratio of the dewaxed sample to the alkaline treatment solution. The sample was meticulously rinsed with distilled water to achieve pH neutrality after each treatment [10]. Following the alkaline treatment, the dried sample underwent a bleaching process entailing the utilization of 50% hydrogen peroxide (H2O2). This process involved using a 1:20 (g/ml) sample-to-solvent ratio and was repeated twice at 90°C for a 2-hour duration, with continuous swirling throughout. The sample was neutralized by rinsing with distilled water during each bleaching step and subsequently subjected to a 2hour drying phase within an oven set at 60°C[11].

2.3 Characterization

2.3.1 Chemical Composition

The chemical composition of Salvinia molesta was determined using the Yang method. The ash content and moisture content were assessed in accordance with ASTM standards 2007 and 2003, respectively.

2.3.2 Fourier Transform Infrared Spectroscopy (FTIR)

An FTIR (Bruker ALPHA) machine was used to analyze the chemical structure of the extracted cellulose. Spectra were obtained from 24 scans, utilizing a 4 cm-1 resolution, spanning the 4000-400 cm-1 range in transmittance mode. Identification of characteristic absorption bands facilitated the confirmation of cellulose presence and the elimination of non-cellulosic components.

2.3.3 Scanning Electron Microscopy (SEM)

The investigation of the materials' structural alterations, morphological structure, and surface properties was conducted employing scanning electron microscopy (SEM) utilizing an EVO 18 apparatus manufactured by Carl Zeiss AG, Germany. The samples were prepared with a coating of gold sputter, and an accelerating voltage of 15 kV was applied for the assessment.

3 Results and Discussion

3.1 Chemical Composition

The average chemical composition of Salvinia molesta was analyzed to understand the distribution of key components, which is critical for assessing its potential as a source of cellulose. The results, summarized in Table 1, show that the weed contains a significant amount of moisture, making up 46.8% of the fresh sample. The cellulose content is relatively high at 25.4%, indicating that Salvinia molesta is a viable source of cellulose for various applications. Several studies have identified Salvinia molesta as a promising source of cellulose, with a cellulose content ranging from 20% to 30%, depending on the growth conditions and harvesting time. The cellulose fibers are primarily composed of glucose units, which can be converted into various bioproducts such as bioethanol, biodegradable plastics, and other sustainable materials. The relatively high cellulose content 25.4% suggests that Salvinia molesta can be efficiently utilized for applications in material science and green chemistry, supporting previous findings by [12]-[13] that highlight the weed's viability as a cellulose source.

Table 1 The chemical constituent of Salvinia molesta

Constituent	Composition in grammes per 100 grammes of dried weed (%)
Moisture (fresh)	46.8
Cellulose	25.4
Hemicellulose	11.9
Lignin	3.3
Ash content	19.5

Hemicellulose, comprising about 11.9% of the dried weed, consists of various polysaccharides such as xylans, mannans, and arabinoxylans, which are crucial in determining the mechanical properties of the plant cell walls. According to [14]Hemicellulose in aquatic plants like Salvinia molesta contributes to the flexibility and resilience of the cell wall, which in turn affects the extraction process of cellulose. The presence of hemicellulose, while necessary for the structural integrity of the plant, may require mild alkaline or enzymatic pretreatment for efficient cellulose isolation. Lignin content in Salvinia molesta is relatively low, around 3.3%, compared to terrestrial plants, which often contain 15-30% lignin. The low lignin content is beneficial for cellulose extraction since less energy and fewer chemicals are needed to break down the lignin structure. Lignin is a complex aromatic polymer that provides rigidity to plants, but its low presence in Salvinia molesta aligns with findings, who noted that aquatic weeds generally contain less lignin, making them easier to process for cellulose extraction [15][16].

The ash content of Salvinia molesta is relatively high at 19.5%, indicating a significant amount of inorganic minerals like calcium, magnesium, potassium, and silica. These minerals can affect the thermal stability and behavior of the material during pyrolysis or combustion processes. The high ash content might be advantageous in application- suggest that the mineral-rich nature of Salvinia molesta may also enhance its potential as a soil conditioner or fertilizer after pyrolysis. Salvinia molesta also contains extractives such as tannins, polyphenols, and various organic acids, which can contribute to its biological activity and potential use in pharmaceuticals, dyes, and other industrial applications. The extractives content can vary, but they are typically in the range of 5-10% of the dry weight. These components can influence the overall efficiency of cellulose extraction processes and may require additional pre-treatment steps for removal, as indicated by [17]. Overall, the chemical composition data indicate that Salvinia molesta has a relatively high cellulose content with manageable levels of hemicellulose and lignin, making it a promising raw material for cellulose extraction. The high moisture content and ash content should be taken into account when processing the material, as they may impact both the extraction efficiency and the thermal stability of the derived cellulose.

3.2 Fourier transform infrared spectroscopy

The FTIR analysis of Salvinia molesta provided a detailed chemical profile of the plant material, revealing key structural and compositional insights. The spectrum shown in Fig. 1, a broad and intense peak in the 3500 to 3000 cm⁻¹ range, is indicative of O-H stretching vibrations [18]. This peak is attributed to hydroxyl groups from aliphatic alcohols and adsorbed water, suggesting extensive hydrogen bonding within the plant's structure. The broad nature of these peaks underscores the high moisture content and the potential for significant hydrogen bonding interactions, which may affect the material's interaction with chemical treatments and influence its processing behavior.

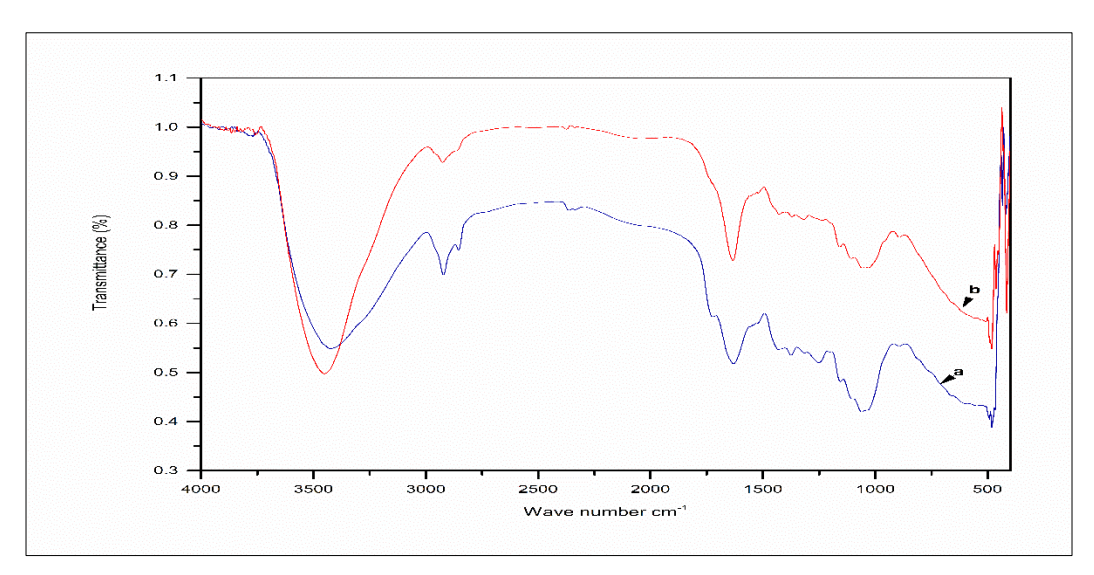


Fig.1 Comparison spectra of (a)raw, (b). extracted cellulose

In the 3000 to 2800 cm⁻¹ range, the FTIR spectrum exhibited peaks corresponding to C-H stretching vibrations. These peaks are associated with alkanes and other hydrocarbon chains, suggesting the presence of organic compounds such as fatty acids and waxes [19]. These hydrocarbon groups contribute to the overall hydrophobic nature of the plant material, which can impact the efficiency of chemical treatments and modifications.

A significant peak observed at 1060 cm⁻¹ in the 1270 to 1050 cm⁻¹ range corresponds to C-O stretching vibrations for the C-O-C ether group [19]. This peak provides insights into the presence of cellulose and other polysaccharides in Salvinia molesta. The increase in intensity of this peak following chemical treatments indicates a higher cellulose content due to the removal of non-cellulosic components like lignin and hemicellulose. This enhancement in cellulose content is crucial for applications that require higher cellulose purity, such as in bio-composites or biodegradable materials.

Peaks in the 3000 to 2850 cm⁻¹ range, associated with C-H stretching in alkenes and aromatics, highlight the presence of these functional groups in the plant. The peak around 2000 cm⁻¹ suggests the presence of triple bond groups, which may indicate cross-linking within the cellulose network or interactions with other organic molecules. The significant C-O band absorption peaks between 1300 and 1000 cm⁻¹ reveal the presence of esters, which could be a result of esterification reactions or naturally occurring esterified compounds in the plant material[20]. Lignin and hemicellulose, identified by peaks in the 2923 to 2920 cm⁻¹ range, were present in the raw and dewaxed samples but were notably absent after chemical treatments[21]-[22]. This disappearance confirms the effectiveness of the chemical treatments in isolating cellulose by removing these non-cellulosic components.

A consistent peak around 1630 cm⁻¹, attributed to O-H bending from absorbed water, indicates that water is retained throughout the extraction process. Peaks at approximately 1370 cm⁻¹ and 1420 cm⁻¹, corresponding to C-H bending and CH₂ bending in the pyranose ring of cellulose, confirm the presence of cellulose's structural framework. After bleaching, a peak around 1030 cm⁻¹, associated with C-O-C vibrations in the pyranose ring, verifies the persistence of the cellulose structure despite the treatment. Additionally, a characteristic peak at approximately 890 cm⁻¹, related to the β-glycosidic linkage between glucose units in cellulose, was distinctly observed in the bleached sample, indicating that the glycosidic bonds crucial for cellulose integrity remain intact[23]. Overall, the FTIR analysis elucidates the chemical and structural transformations occurring in Salvinia molesta during processing. The observed changes in peak intensities and the presence or absence of specific functional groups provide a comprehensive understanding of the material's composition and the effectiveness of the chemical treatments. These findings underscore the potential for utilizing Salvinia molesta in applications requiring high-purity cellulose or modified cellulose materials.

3.3 Scanning Electron Microscopy

The SEM image (Fig. 2) of the cellulose extracted from Salvinia molesta after the bleaching stage offers a detailed examination of the material's morphology, revealing a network of fibrils that are characteristic of well-isolated micro cellulose. The image, taken at a magnification of 5000x and an accelerating voltage of 20.00 kV, shows a fibrillar structure that is both highly intricate and interconnected. The SEM image of the bleached cellulose extracted from Salvinia molesta provides a clear visual representation of the material's microstructural characteristics, showcasing the effects of the sequential de-waxing, alkaline, and bleaching treatments. The dewaxing stage, involving solvent extraction with ethanol and toluene mixture, effectively removed surface

impurities and waxes, leading to a clean, exposed fiber surface. This initial step is crucial for enhancing the subsequent chemical treatments by ensuring that cellulose fibers are accessible for further processing. Following de-waxing, the alkaline treatment with potassium hydroxide (KOH) further refined the material by dissolving hemicellulose and partially breaking down lignin, which binds the cellulose fibers. The SEM image reveals a fibrillated structure, indicative of the removal of non-cellulosic components, resulting in the liberation of individual cellulose fibers.

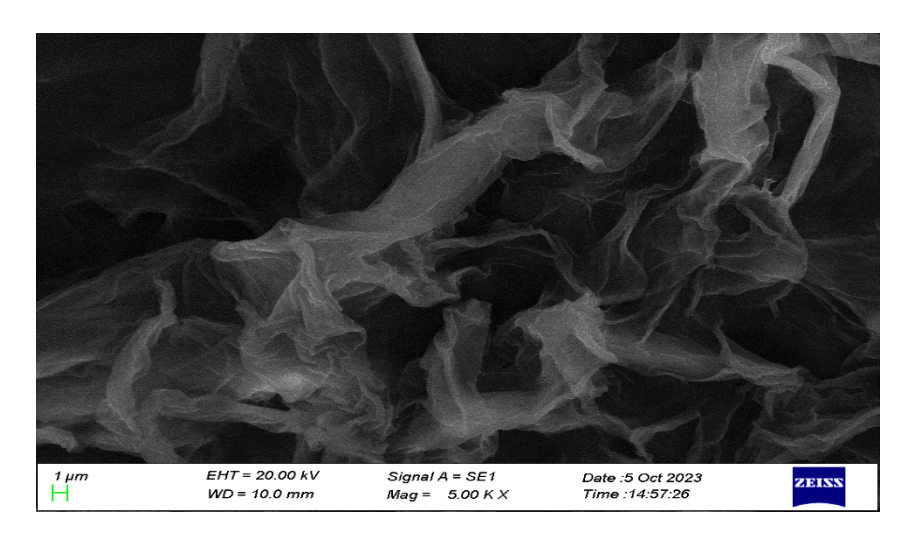


Fig.2 SEM image of the cellulose extracted sample

The visible network of fibers, with a relatively uniform diameter and distribution, suggests an efficient removal of lignin and hemicellulose, confirming the effectiveness of the alkaline treatment. The subsequent bleaching process, using hydrogen peroxide or sodium hypochlorite, removed any remaining lignin and colorants, yielding a high-purity, white cellulose. This is evident in the SEM image, where the fibers appear distinct, separated, and free of impurities, with minimal agglomeration. The well-defined fibrillar network seen in the image highlights the success of the entire extraction process, which culminates in a highly purified cellulose material suitable for advanced applications. The morphological features observed, such as the fine, web-like structure and uniform fiber size, indicate that the pretreatment stages effectively prepared the material for use in various fields. The fibrils appear thin, wrinkled, and layered, indicative of the successful removal of non-cellulosic components such as lignin, hemicellulose, and other impurities during the pretreatment processes. This wrinkled and layered texture is consistent with the morphology observed in other studies of microcellulose, where chemical treatments like bleaching result in the breakdown of non-cellulosic matter, leaving behind a predominantly cellulose structure [24][25].

The fibrils are loosely entangled, forming a porous and fibrous network. This structure is beneficial for various applications, as the high surface area provided by the porous network enhances the material's interaction with other substances, which is particularly advantageous in composite materials and filtration systems. The integrity of the fibrils, despite the rigorous chemical treatments, speaks to the robustness of the cellulose, which is essential for maintaining the desired mechanical properties in final applications [26].

Furthermore, the absence of large, irregular particles or debris in the SEM image suggests a high level of purity in the extracted cellulose. The effectiveness of the bleaching process is evident in the uniformity of the fibril network, which indicates that the cellulose has been thoroughly cleaned of residual impurities. This level of purity is critical for high-performance applications where the presence of lignin or hemicellulose could adversely affect the material properties [27]. The consistent size and distribution of the fibrils in the image also suggest that the extraction process was well-controlled, resulting in a homogeneous cellulose product. This homogeneity is vital for ensuring that the material can be reliably used in various industrial applications, from reinforcing agents in bio-composites to the development of environmentally friendly materials [28].

In summary, the SEM image underscores the successful isolation and purification of cellulose from Salvinia molesta, highlighting the potential of this invasive species as a valuable source of micro cellulose. The detailed morphological features observed in the image align with those reported in similar studies, confirming the effectiveness of the extraction process and the suitability of the material for high-value applications in materials science and beyond.

4 Conclusions

This study successfully demonstrated the potential of Salvinia molesta as a sustainable source of high-purity cellulose, offering a novel solution to the ecological and economic challenges posed by this invasive aquatic weed. The average chemical composition analysis revealed a significant cellulose content of 25.4% with a relatively low lignin content of 3.3%, underscoring its suitability for cellulose extraction. Fourier Transform Infrared Spectroscopy (FTIR) results confirmed the effective removal of non-cellulosic components, as evidenced by the distinct cellulose peaks. Additionally, Scanning Electron Microscopy (SEM) provided detailed insights into the morphology of the extracted cellulose, revealing a well-structured network of fibrils with minimal impurities, further validating the success of the extraction process. The observed fibrillar network in the SEM images highlights the structural integrity and high surface area of the cellulose, making it a promising material for various applications.

These findings underscore the viability of using Salvinia molesta as a raw material for producing micro cellulose, which holds significant potential in fields such as biomedical engineering, renewable energy, and advanced materials science. By transforming an environmental problem into a valuable resource, this research contributes to the development of sustainable materials and presents an innovative approach to environmental management. Future research should focus on optimizing the extraction process to enhance cellulose purity and explore additional applications for the derived microcellulose, potentially broadening its utility across various industrial sectors. The outcomes of this study not only address the pressing issue of Salvinia molesta proliferation but also open up new avenues for sustainable materials development.

References

- [1] N. Hussain, T. Abbasi, and S. A. Abbasi, "Vermiremediation of an invasive and pernicious weed salvinia (Salvinia molesta)," *Ecol. Eng.*, vol. 91, pp. 432–440, Jun. 2016, doi: 10.1016/j.ecoleng.2016.03.010.
- [2] J. A. Coetzee and M. P. Hill, "Salvinia molesta D. Mitch. (Salviniaceae): Impact and control," *CAB Rev. Perspect. Agric. Vet. Sci. Nutr. Nat. Resour.*, vol. 15, no. 33, Jul. 2020, doi: 10.1079/PAVSNNR202015033.
- [3] C. S. Kariyawasam, L. Kumar, B. K. Kogo, and S. S. Ratnayake, "Long-term changes of aquatic invasive plants and implications for future distribution: A case study using a tank cascade system in sri lanka," *Climate*, vol. 9, no. 2, pp. 1–18, Feb. 2021, doi: 10.3390/cli9020031.
- [4] P. Chathura Dineth Perera, "Review of major abundant weeds of cultivation in Sri Lanka Goldenrods invasion in Central Europe-drivers of invasion and eradication methods View project Review of major abundant weeds of cultivation in Sri Lanka," *Int. J. Sci. Res. Publ.*, vol. 5, no. 5, 2014, [Online]. Available: www.ijsrp.org
- [5] J. A. Doeleman, "Biological Control of Salvinia molesta in Sri Lanka: An Assessment of Costs and Benefits."
- [6] A. Setiadi *et al.*, "Economical Performances and Cholesterol Profiles due to the Incorporation of Salvinia molesta in the Diets of Kampong Chicken," *Trop. Anim. Sci. J.*, vol. 43, no. 4, pp. 347–353, 2020, doi: 10.5398/tasj.2020.43.4.347.
- [7] Michael Jacob Ioelovich, "Microcellulose Vs Nanocellulose A Review," World J. Adv. Eng. Technol. Sci., vol. 5, no. 2, pp. 001–015, Mar. 2022, doi: 10.30574/wjaets.2022.5.2.0037.
- [8] M. Rahimi Kord Sofla, R. J. Brown, T. Tsuzuki, and T. J. Rainey, "A comparison of cellulose nanocrystals and cellulose nanofibres extracted from bagasse using acid and ball milling methods," *Adv. Nat. Sci. Nanosci. Nanotechnol.*, vol. 7, no. 3, Sep. 2016, doi: 10.1088/2043-6262/7/3/035004.
- [9] M. Shahid Nazir, B. Ari Wahjoedi, A. Wahid Yussof, and M. Azmuddin Abdullah, "MCC from OPEFB," 2013.
- [10] Y.-R. Seo, J.-W. Kim, S. Hoon, J. Kim, J. H. Chung, and K.-T. Lim, "Cellulose-based Nanocrystals: Sources and Applications via Agricultural Byproducts," *J. Biosyst. Eng*, vol. 43, no. 1, pp. 59–71, 2018, doi: 10.5307/JBE.2018.43.1.059.
- [11] A. Safina Aridi, C. Nyuk Ling, N. Akmal Ishak, N. Nadiah Mohammad Yusof, M. Fikry Mohamed Ahmed, and Y. Aniza Yusof, "Structural FTIR analysis of cellulose functional groups isolated from Leucaena leucocephala pods using different bleaching agents."
- [12] S. Nawaj Alam, B. Singh, and A. Guldhe, "Aquatic weed as a biorefinery resource for biofuels and value-

- added products: Challenges and recent advancements," *Clean. Eng. Technol.*, vol. 4, p. 100235, 2021, doi: 10.1016/j.clet.2021.100235.
- [13] A. Ganguly, P. K. Chatterjee, and A. Dey, "Studies on ethanol production from water hyacinth A review," *Renew. Sustain. Energy Rev.*, vol. 16, no. 1, pp. 966–972, 2012, doi: 10.1016/j.rser.2011.09.018.
- [14] V. K. Gupta and M. G. Tuohy, Biofuel technologies: Recent developments, no. 26. 2014. doi: 10.1007/978-3-642-34519-7.
- [15] M. Moozhiyil and J. Pallauf, "Chemical Composition of the Water Fern, Salvinia molesta, and Its Potential as Feed Source for Ruminants."
- [16] P. K. Mani, "BIOCHEMICAL AND BIOTECHNOLOGICAL INVESTIGATIONS ON THE WATER-FERN SALVINIA MOLESTA MITCHELL. IN PARTIAL FULFILMENT OF THE REQUIREMENTS FOR THE DEGREE OF DOCTOR OF PHILOSOPHY in PLANT BIOCHEMISTRY AND BIOTECHNOLOGY UNDER THE FACULTY OF MARINE SCIENCES," 1998.
- [17] M. I. Choudhary, N. Naheed, A. Abbaskhan, S. G. Musharraf, H. Siddiqui, and Atta-ur-Rahman, "Phenolic and other constituents of fresh water fern Salvinia molesta," *Phytochemistry*, vol. 69, no. 4, pp. 1018–1023, 2008, doi: 10.1016/j.phytochem.2007.10.028.
- [18] W. R. Kunusa, I. Isa, L. A. R. Laliyo, and H. Iyabu, "FTIR, XRD and SEM Analysis of Microcrystalline Cellulose (MCC) Fibers from Corncorbs in Alkaline Treatment," in *Journal of Physics: Conference Series*, Institute of Physics Publishing, Jun. 2018. doi: 10.1088/1742-6596/1028/1/012199.
- [19] M. Asrofi, H. Abral, A. Kasim, and A. Pratoto, "XRD and FTIR Studies of Nanocrystalline Cellulose from Water Hyacinth (*Eichornia crassipes*) Fiber," *J. Metastable Nanocrystalline Mater.*, vol. 29, no. August, pp. 9–16, 2017, doi: 10.4028/www.scientific.net/jmnm.29.9.
- [20] N. D. Kambli, V. Mageshwaran, P. G. Patil, S. Saxena, and R. R. Deshmukh, "Synthesis and characterization of microcrystalline cellulose powder from corn husk fibres using bio-chemical route," *Cellulose*, vol. 24, no. 12, pp. 5355–5369, Dec. 2017, doi: 10.1007/s10570-017-1522-4.
- [21] R. Md Salim, J. Asik, and M. S. Sarjadi, "Chemical functional groups of extractives, cellulose and lignin extracted from native Leucaena leucocephala bark," *Wood Sci. Technol.*, vol. 55, no. 2, pp. 295–313, Mar. 2021, doi: 10.1007/s00226-020-01258-2.
- [22] L. A. S. Costa, D. de J. Assis, G. V. P. Gomes, J. B. A. Da Silva, A. F. Fonsêca, and J. I. Druzian, "Extraction and Characterization of Nanocellulose from Corn Stover," in *Materials Today: Proceedings*, Elsevier Ltd, 2015, pp. 287–294. doi: 10.1016/j.matpr.2015.04.045.
- [23] A. Ratnakumar, A. M. P. B. Samarasekara, D. A. S. Amarasinghe, and L. Karunanayake, "Characteristics of Natural Cellulose Fibres Extracted from Sri Lankan Rice Straw Varieties," *Trop. Agric. Res.*, vol. 31, no. 3, p. 72, Jun. 2020, doi: 10.4038/tar.v31i3.8398.
- [24] W. Chen, H. Yu, Y. Liu, P. Chen, M. Zhang, and Y. Hai, "Individualization of cellulose nanofibers from wood using high-intensity ultrasonication combined with chemical pretreatments," *Carbohydr. Polym.*, vol. 83, no. 4, pp. 1804–1811, 2011, doi: 10.1016/j.carbpol.2010.10.040.
- [25] G. Chinga-carrasco, "Microscopy and computerized image analysis of wood pulp fibres multi-scale structures," *Microsc. Sci. Technol. Appl. Educ.*, no. level 1, pp. 2182–2189, 2010.
- [26] R. J. Moon, A. Martini, J. Nairn, J. Simonsen, and J. Youngblood, "Cellulose nanomaterials review: Structure, properties and nanocomposites," *Chem. Soc. Rev.*, vol. 40, no. 7, pp. 3941–3994, Jun. 2011, doi: 10.1039/c0cs00108b.
- [27] Y. Habibi, L. A. Lucia, and O. J. Rojas, "Cellulose nanocrystals: Chemistry, self-assembly, and applications," *Chem. Rev.*, vol. 110, no. 6, pp. 3479–3500, 2010, doi: 10.1021/cr900339w.
- [28] I. Siró and D. Plackett, "Microfibrillated cellulose and new nanocomposite materials: A review," *Cellulose*, vol. 17, no. 3, pp. 459–494, 2010, doi: 10.1007/s10570-010-9405-y.

Numerical Simulation of Stable 2D/3D Mixed-dimensional Perovskite Solar Cells with High Power Conversion Efficiency

W.G.A. Pabasara* 1,2, U.K.D.M. Akmal¹, G.A. Sewvandi¹

¹Department of Materials Science and Engineering, University of Moratuwa, Sri Lanka, ²Department of Engineering Technology, University of Ruhuna, Kamburupitiya. Sri Lanka

Abstract

Over the past few decades, solar power has evolved into a sustainable and affordable source of energy, surpassing other renewable energy sources. Perovskite Solar Cells (PSCs) have emerged as a powerful photovoltaic technology due to their remarkable features, including higher efficiency and cost-effectiveness. The perovskite material itself exhibits superior properties, including higher absorption coefficients, adjustable band gaps, and long charge carrier lifetimes. However, conventional 3D perovskite solar cells suffer from instabilities upon exposure to elevated temperatures and moisture, hindering commercialization. 2D perovskite materials demonstrate a higher stability level than their 3D counterparts, but their efficiency is relatively low. Therefore, 2D/3D mixed-dimensional PSCs have been developed to overcome these challenges and achieve balanced performance and long-term stability simultaneously. In this report, Ruddlesden-Popper phase BA2MAn-1PbnI3n+1 2D perovskite material has been incorporated into MAPbI3 and built new device architecture of FTO/ZnO/MAPbI3/BA2MAn-1PbnI3n+1/Cu2O /Au. The performance of the PSCs was optimized through a numerical modeling approach. At the thickness of $0.1 \mu m$ of 2D absorber layer and $1 \mu m$ of the 3D absorber layer, the PSCs achieved 24.76% and 24.88% efficiency for n=3 and n=4 respectively. Our analysis indicates that the incorporation of 2D/3D mixed-dimensional PSC yields high throughput while ensuring the prolonged operational stability of the solar cell.

Keyword: numerical simulation, stability, efficiency, 2D perovskites, mixed-dimensional solar cells, SCAPS 1D

1 Introduction

Global energy consumption is increasing at an unprecedented rate, with rapid population growth and industrialization. It is estimated that global power demand will triple by 2050, even the timely conservation measures are implemented[1]. The limited availability of fossil fuel sources is challenging for energy supply, underscoring the urgent need for renewable and sustainable energy sources. The negative effects of fossil fuels, such as air pollution and greenhouse gas emissions, have become pressing environmental concerns, elucidating the requirements of energy alternatives. In recent decades, solar power has garnered tremendous attention all over the world as a clean and sustainable energy source, providing solutions for the dual challenges of increasing energy demand and climate change. In the current scenario, silicon (Si) based solar cells exhibit the best photovoltaic efficiency and dominate the photovoltaic market. However, the widespread adoption of Si-based solar cells is limited by their high production cost and environmental concerns[2].

PSCs are one of the leading photovoltaic technologies (PV), exhibiting superior power conversion efficiency (PCE) with a simple and affordable fabrication process [3]. The commonly used 3D perovskites have gained vast attention because of their outstanding optoelectronic characteristics, such as a greater absorption coefficient, enhanced carrier transportation, and adjustable bandgap.

Over the past decade, the PCE of PSC has achieved remarkable advancement, increasing by nearly 20% due to rapid technological progress of the photovoltaic field. When introducing perovskite in 2009, the PCE was 3.8% and by 2013, it surpassed 15%, highlighting the rapid early growth of PCS technology. Following this trajectory, over 23% efficiency was attained in 2018. Now it has passed 25% PCE in the laboratory scale, demonstrating substantial progression. It will continuously grow due to diverse advancements and optimization efforts [4]. A remarkable achievement in photovoltaic technology was reported by the Chinese Academy of Sciences, producing a PSC with a peak efficiency rating of 26.1%. The third-party certified PCE of this device is 25.2%, demonstrating that PSCs are now achieving efficiency levels comparable to silicon solar cells. ABX3 is the standard chemical formula of perovskites. Here, A is denoted as monovalent cations such as methylammonium [MA+: CH3NH3+), formamidine [FA+], Cesium (Cs+), or their blend. B is divalent cations, usually metals, such as Pb2+, Sn2+, Ge2+, or a blend of these. Monovalent anions are indicated by X, typically halides, including I-, Br-, Cl-, or a mixture of them. Current research outcomes indicated that Pb-based perovskites are favorable in achieving higher efficiency levels, making them the predominant selection in the field[5]. However, these materials are highly susceptible to degradation due to heat, UV radiation, moisture, and ion migration, which degrade the stability of the devices, creating a barrier to commercialization[6]. Researchers have explored multiple strategies to overcome stability issues without disturbing the performance of 3D PSCs, including encapsulation, modifying composition, and incorporating additives.

^{*}ayomiwalaqedara@gmail.com, mudithaakmal@gmail.com, qalhenagea@uom.lk

The experiments have proved that the stability of 2D PSCs is far better than 3D structures [7]. 2D perovskite materials are represented by (RNH3)2(A)n-1BnX3n+1, where R is a large organic cation, A, B, X, n are a monovalent cation, a divalent metal cation, a halide anion, and the number of perovskite layers, respectively. The organic cation functions as a spacer cation between the inorganic perovskite layers, which form a layered structure with alternating organic and inorganic components. The thickness of the perovskite layer is defined by the n value. When the values of n are increasing, it approaches the 3D perovskite structure. The outstanding stability of twodimensional perovskites can be credited to their distinctive molecular arrangement featuring strong hydrogen bonding between inorganic and organic layers and the improved resistance of organic layers to moisture and intense light exposure. Ruddlesden-Popper (RP), Dion-Jacobson (DJ), and Alternation cation in the interlayer space perovskites (ACI) are the most prevailing 2D perovskite types. Therefore, new avenues are opened to combine 2D perovskite materials with 3D to boost stability without compromising performance. The mixed 2D/3D perovskite structures are an emerging research frontier that still faces unsolved issues but also holds great potential for improvements. Depending on the chemical structure of 2D perovskite material, including the substitute groups and chain lengths in organic layers, the stability can be varied. Moreover, numerous 2D perovskite materials exist that have not yet been explored for their potential to boost the stability of 3D structures. These materials present opportunities for investigating stability enhancements in 3D PSCs. The main concern for these mixed-dimensional structures is balancing enhanced stability and the high efficiency of PSCs. Therefore, it is essential to choose 2D perovskites that have greater resistance to moisture and heat and 3D perovskites with superior carrier generation and transportation.

For instance, Grancini et al. found a 2D/3D bilayer PSC with n-i-p configuration, which has an efficiency of 14.6% with 1-year stability through incorporating (5-ammoniumvaleric acid iodide)2PbI4 2D, which functions as a protective layer against moisture to 3D perovskite. Zhou et al. presented enhanced carrier lifespan and lower charge carrier recombination 2D/3D mixed dimensional PSCs with n-i-p structure offering an efficiency of 21.49%. Liu et al, developed an n-i-p architecture mixed-dimensional perovskite with a PCE of 22.1%. The inclusion of fluorinated 2D perovskite enhances hole extraction and reduces the carrier recombination to achieve enhanced efficiency. Further, this hybrid system is able to retain nearly 90% of its original efficiency after exposure to moisture and simulated sunlight for 1000h. These results reflect that the efficiency of 2D/3D bilayer PCSs depends on the types of 2D perovskites and cell architectures.

The numerical simulation-based studies on PSC optimization are emerging research areas that facilitate identifying the highly stable perovskite materials and optimizing solar cells. Computational simulation studies provide valuable insights into the performance of different cell structures and determine the effects of the different parameters on the performance and the prolonged stability of solar cells [8]. These studies facilitate selecting the appropriate materials for the layers, including the HTL and ETL, and thereby optimize the PCE and other performance characteristics. Sneha Chausia et al have conducted a theoretical investigation of 2D/3D mixed-dimensional solar cell with the architecture of FTO/TiO2/CH3NH3PbI3/PeDAMAPb4I16/Spiro-OMeTAD. In this piece of research, SCAPS 1D software was employed to perform the simulation. They analyzed the effect of properties of different layers on the performance of the device structure and optimized PSC, achieving 26.03% efficiency[9]. In another study, 2D/3D mixed-dimensional PSC with an inverted device configuration: ITO/NiOx/BA2MAn-1PbnI3n+1/MAPbI3/ZnO/Al was simulated using SCAPS 1D. PCE of 24.75% was achieved by optimizing the absorber layer and charge transport layer properties (Joyprokash Chakrabartty et al, 2021).

In this research, BA2MAn-1PbnI3n+1 has been employed as the 2D perovskite material due to its proven stability under external environmental conditions. BA+ (n-butylammonium cation) based 2D perovskite series (n=2 to 4) were developed in 2015, and this perovskite shows a more confined layered structure. It shows less efficiency; however, it could withstand moisture environments for 2 months. In another experimental study, it has been proved that the capability of BA2MAn-1PbnI3n+1 boosts the operation stability of the MAPbI3 perovskite while keeping enhanced efficiency. Y. Wang et al presented that BA2PbI4 2D perovskite-based 2D/3D hybrid solar cell with 18% PCE and this cell retained 78% of its original efficiency after 132 days [10]. Exclusively, as the n value increases, the band gap and exciton binding energy (Eb) will be decreased to the level of a 3D perovskite, leading to an enhancement of the PCE but a decrease of stability [11]. The optimum n value to achieve balanced stability is in between 3 and 5 [12]. In this research, it is proposed a new n-i-p device architecture FTO/ZnO/MAPbI3/BA2MAn-1PbnI3n+1/Cu2O/Au. has not been explored previously. To attain balanced stability and efficiency, the devices were simulated for n=3 and 4. It is expected to develop a PSC with enhanced stability by incorporating 2D perovskite materials along with stable electron transport materials.

2 Methodology for designing and simulating the proposed device

This research is expected to simulate 2D/3D mixed-dimensional solar cell (FTO/ZnO/MAPbI3/BA2MAn-1PbnI3n+1/Cu2O /Au) using SCAPS 1D software and optimize the absorber layer thicknesses to achieve maximum power conversion efficiency. In the simulation, a neutral defect layer was included at the interfaces of HTL/perovskite and the ETL/perovskite layers in the designed device configuration. The front contact electrode

was made of Fluorine-doped tin oxide (FTO), while Cu2O was utilized as the HTL, BA2MAn-1PbnI3n+1/MAPbI3 (n = 3 and 4) as perovskite active absorber materials, ZnO as the ETL, and Gold (Au) as the back contact cathode material, as depicted in Fig. 1. Cu2O was selected as HTL due to its proven stability over the conventional HTL materials such as Spiro-OMeTAD [13]. HTL materials like PEDOT: PSS and poly-TPD are abundantly used in perovskite solar cells; however, those are in the preliminary stage of growth, and some concerns with their acidity and hygroscopic characteristics lead to poor structural stability [14]. Cu2O is an inorganic material that has shown inherent stability against moisture and thermal degradation, whereas organic materials such as Spiro-OMeTAD are more prone to degradation under external environmental conditions. Tung-Han Chuang presented that PSCs using Cu2O as the HTL have retained around 98.3% of their original efficiency after 1000 hours of operation, indicating superior long-term stability [15]. Inorganic metal oxides such as ZnO, TiO2, and SnO2 are among the well-known ETLs in PSCs. ZnO is a widely used ETL in solar cells and has gained widespread attention due to its well-matched energy levels and comparably enhanced electron mobility to other metal oxide ETLs, remarkably enhancing electron extraction performance and minimizing recombination. Additionally, the ZnO as ETL in solar cells offers advantages over other metal oxide-based HTLs as affordable manufacturing, flexibility, and stronger hole-blocking characteristics, leading to the overall enhancement of the performance of PSCs[16].

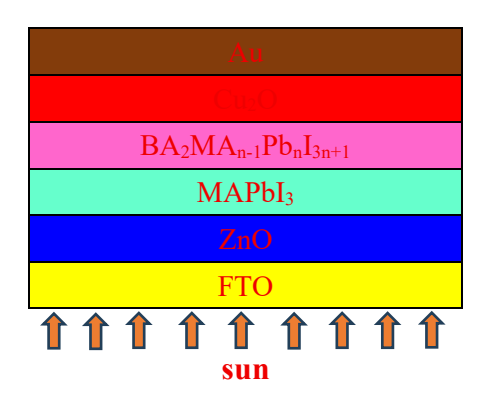


Table 22. Details of optical and electrical parameters of cell architecture.

S/No	Description of the parameter	FTO	MAPbI ₃	$BA_2MA_2Pb_3I_{10}$	BA ₂ MA ₃ Pb ₄ I ₁₃	ZnO	Cu ₂ O
1	Thickness (µm)	0.5	varied	varied	varied	0.06	0.03
2	Band gap (eV)	3.5	1.55	1.85	1.6	3.3	2.22
3	Electron affinity (eV)	4	6.90	3.5	3.87	4.1	3.40
4	Dielectric permeability relative	9	6.50	5.7	5.9	9	7.11
5	VB effective density of state (states/cm³/eV)	2.2x10 ¹⁸	2.75x 10 ¹⁸	7.6x10 ¹⁷	7.24x10 ¹⁷	4 x 10 ¹⁸	2.02x 10 ¹⁷
	CB effective density of state (states/cm3/eV)	1.8x10 ¹⁹	3.9 x 10 ¹⁸	1.33 x 10 ¹⁸	1.5 x 10 ¹⁸	1x 10 ¹⁹	3.0 x 10 ²⁰
6	Hole thermal velocity (cms ⁻²)	1x10 ⁷	1x10 ⁷	$1x10^{7}$	1x10 ⁷	1x10 ⁷	1x10 ⁷
	Electron thermal velocity (cms ⁻²)	$1x10^{7}$	1x10 ⁷	$1x10^{7}$	1x10 ⁷	1x10 ⁷	1x10 ⁷
7	Hole mobility (cm²/Vs)	20	11.8	0.8	1.4	100	30
	Electron mobility (cm²/Vs)	10	11.8	0.8	1.4	25	30
8	Shallow uniform donor density (cm ⁻³)	1015	1x10 ⁹	0	0	1x10 ¹⁸	0
	Shallow uniform donor density (cm ⁻³)	0	1x10 ⁹	0	0	0	$1x10^{18}$
9	ElectronCapture cross section (cm²)	1x10 ⁻¹⁵	1x10 ⁻¹⁵	1x10 ⁻¹⁵	1x10 ⁻¹⁵	1x10 ⁻¹⁵	1x10 ⁻¹⁵

10	Hole Capture cross section (cm ²)	1x10 ⁻¹⁵	1x10 ⁻¹⁵	1x10 ⁻¹⁵	1x10 ⁻¹⁵	1x10 ⁻¹⁵	1x10 ⁻¹⁵
11	Defect density	$1x10^{15}$	8.05x10 ¹³	2x10 ¹⁴	2x10 ¹⁴	1x10 ¹⁵	1x10 ¹⁵

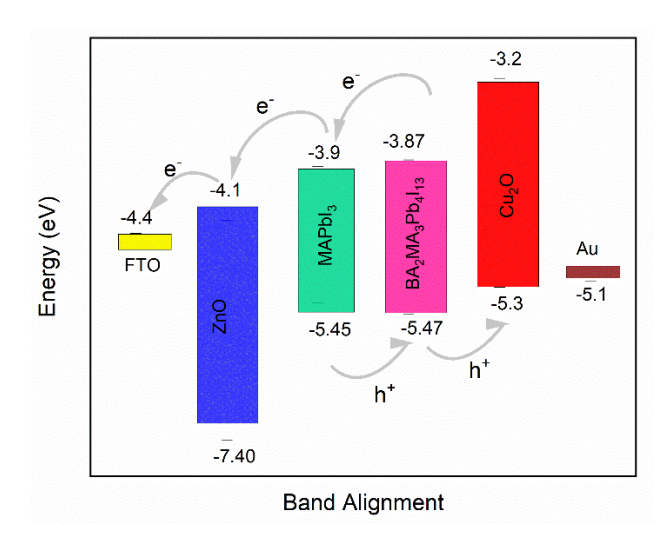
The proposed PSC design was simulated by employing SCAPS 1D simulation software. It is built by the Department of Electronics and Information Systems (ELIS) of the University of Gent in Belgium. It is commonly used in the simulation of optoelectronic devices, particularly for solar cells, due to its capability of solving the Continuity equation and the Poisson equation, allowing an accurate forecast of the output of photovoltaic devices[17]. The presented cell structure was drawn in the software, and simulation was performed using the drift-diffusion model at 300K temperature upon one sun illumination (AM1.5G, 100 mW/cm-2). The parameters used in SCAPS-1D simulations for the different absorber materials, transport layers, and electrodes were adopted from previously published reports, as depicted in Table 1 [9][18].

3 Results and Discussion

3.1 Band alignment

Band alignment is a crucial factor in charge transportation across the absorbed materials and charge transportation layer, ultimately affecting the effectiveness of the photovoltaic devices. Band alignment determines potential barriers that charge carriers must overcome to transit between absorber material and charge transportation materials. Optimal band alignment can reduce these barriers, thereby improving carrier mobility and overall device performance. Moreover, poor band alignment can induce interface states that trap charge carriers, which increase the recombination rates, reducing the device efficiency. The band diagram of the proposed PSC in Fig. 2 demonstrates the operating principle of the proposed solar cell with the HOMO (Highest Occupied Molecular Orbital) and LUMO (Lowest Unoccupied Molecular Orbital) energy of each layer.

As illustrated in Fig.2, the well-aligned valence band energy of Cu2O with the valence band energy of perovskite absorber layers facilitates rapid transportation of photo-induced holes to the back contact. The conduction band of Cu2O and absorber layers offers a substantial band offset, preventing the flow of electrons towards the Au electrode. Similarly, photo-induced electrons efficiently transfer to the FTO due to the favorably aligned conduction bands of the absorb layer and ZnO.



3.2 Impact of absorber layer thickness on solar cell efficiency and performance

The PCE of PSCs is greatly influenced by perovskite layer thickness, defect density within the absorber layer, and charge transportation characteristics of the used materials [19]. Importantly, the thickness of the perovskite layer is crucial for PSCs, as it directly affects the absorbed percentage of the solar irradiance by the perovskite material. For instance, a thin perovskite layer only absorbs a relatively small percentage of incident photons compared to the thick layers, resulting in generation of low photocurrent generation. Conversely, the relatively thick absorber layers can cause substantial carrier recombination losses, which detrimentally impact the PSC's performance. Based on experimental findings, for this analysis, 2D perovskite layer thickness varied from 0.1 μ m to 1 μ m, while 3D perovskite layer thickness varied from 0.1 μ m to 2 μ m with an increment of 0.1 μ m. Absorber layer defect density was kept unchanged at 2 × 1014 cm-3 as mentioned in the experimental reports. First, the 2D perovskite layer thickness (BA2MAn-1PbnI3n+1) was changed, keeping the 3D perovskite layer (MAPbI3) thickness at

0.4 µm as mentioned in the literature [18]. Fig. 3 indicates the behavior of PV characteristics, including PCE, VOC, JSC, and FF in relation to the thickness of BA2MAn-1PbnI3n+1 2D perovskite layer.

According to the findings, $0.1~\mu m$ of BA2MAn-1PbnI3n+1 produces maximum PCE, and with further increase in the thickness, PCE starts to decrease. Therefore, the PCE of the proposed 2D/3D hybrid PSC was maximized at the optimum thickness of $0.1~\mu m$ of the 2D layer. Then, for 3D layer thickness, it was optimized to keep the 2D layer thickness constant at $0.1~\mu m$ and varying the MAPbI3 thickness from $0.1~\mu m$ to $2\mu m$. The behavior of PV parameters with thickness variation is illustrated in Fig. 4. PCE of the proposed devices rises with the thickness of the MAPbI3 layer until $1\mu m$ thickness and then begins to decline with further increases in the MAPbI3 layer thickness, as depicted in Fig. 4a. At $1\mu m$ thickness, the BA2MA2Pb3I10/MAPbI3 device shows 24.76% of maximum efficiency, while BA2MA3Pb4I13/MAPbI3 device shows 24.88% of maximum efficiency.

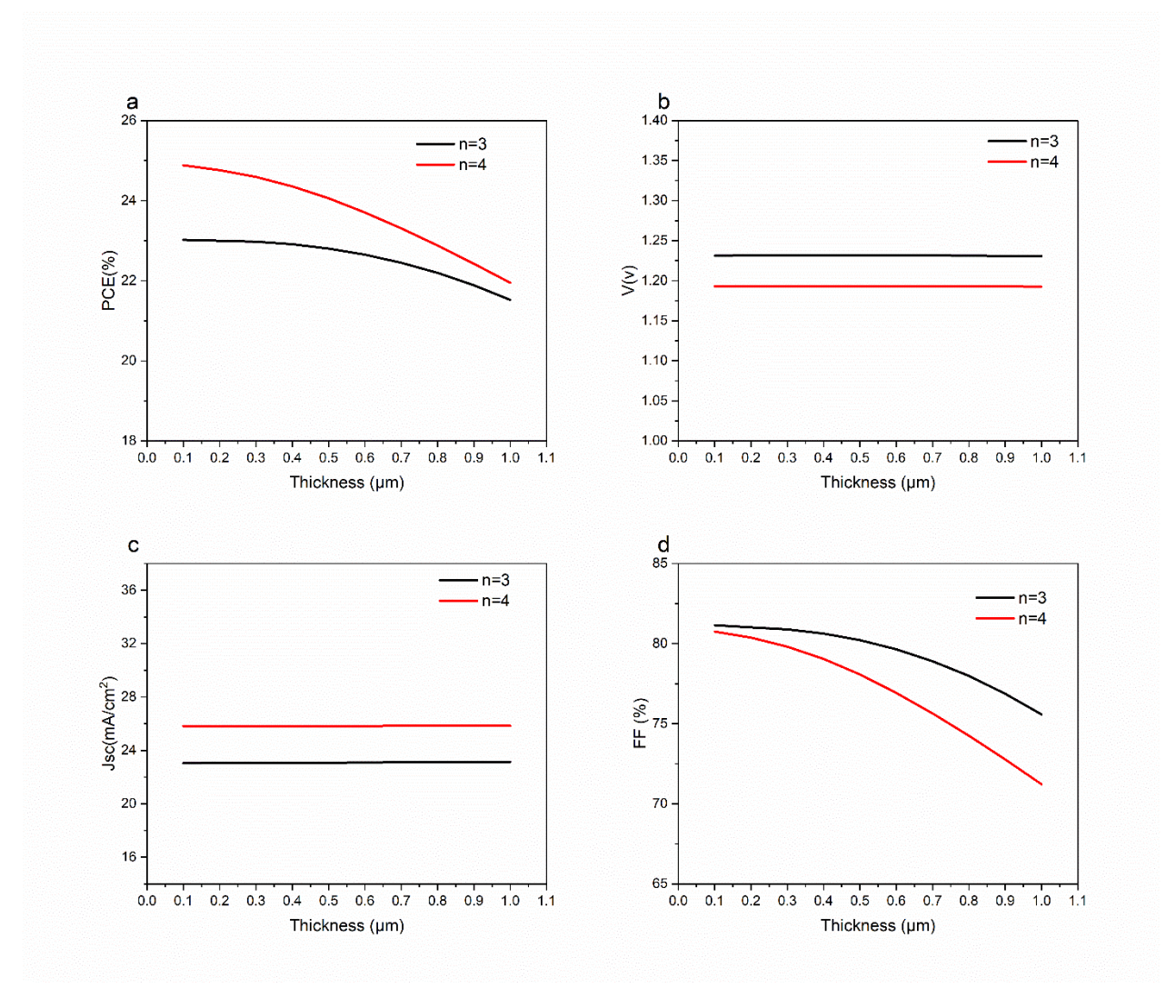


Fig. 11.a) efficiency b) Voc (c), J_{SC} (d) FF as a function of BA₂MA_{n-1}PbnI3_{n+1} absorber layer thickness.

When considering the 2D perovskite layer, it has a limited contribution in light absorption compared to the 3D perovskite layer due to its relatively higher bandgap. So, as the thickness of the 2D layer increases, the PCE gradually declines, primarily because thicker layers hinder charge transport and intensify recombination losses [18]. The relatively stable Jsc is due to the protective function of the 2D layer and the dominant role of the 3D layer in light absorption.

The reasons behind the behavior of PV parameters with 3D perovskite layer thickness can be attributed to absorption changes happening due to the thickness variations. The relatively thin absorber layer has reduced absorption in the long wavelength region, which limits the creation of charge carrier pairs. When thickening the perovskite absorber layer, it enhanced the absorption of long wavelengths, leading to improved exciton pair generation. However, when the thickness continues to increase beyond a critical thickness value, a greater portion

of the solar spectrum can be absorbed, which increases electron-hole pair generation. In this case, these excitons are required to travel to a greater distance, increasing the likelihood of carrier recombination. [20]. Consequently, power conversion efficiency declines after the thickness surpasses a critical threshold, as illustrated in Fig. 3a and 4a. As depicted in Fig. 3b, VOC remains relatively stable when increasing the perovskite thickness. This consistency can be related to the specific band gaps of the perovskite materials. The thickness increment has a negative impact on the FF, which declines with the thickness. When increasing the thickness of the active perovskite layer, the series resistance of the PSC also enhances. When the thickness of the perovskite layer rises, the series resistance within the PSC also tends to increase. This resistance originates from different internal components, including the perovskite material and its interfaces with electrodes and charge transport layers [18]. Increased series resistance tends to decrease the current flow through the PSC, which adversely impacts the fill factor.

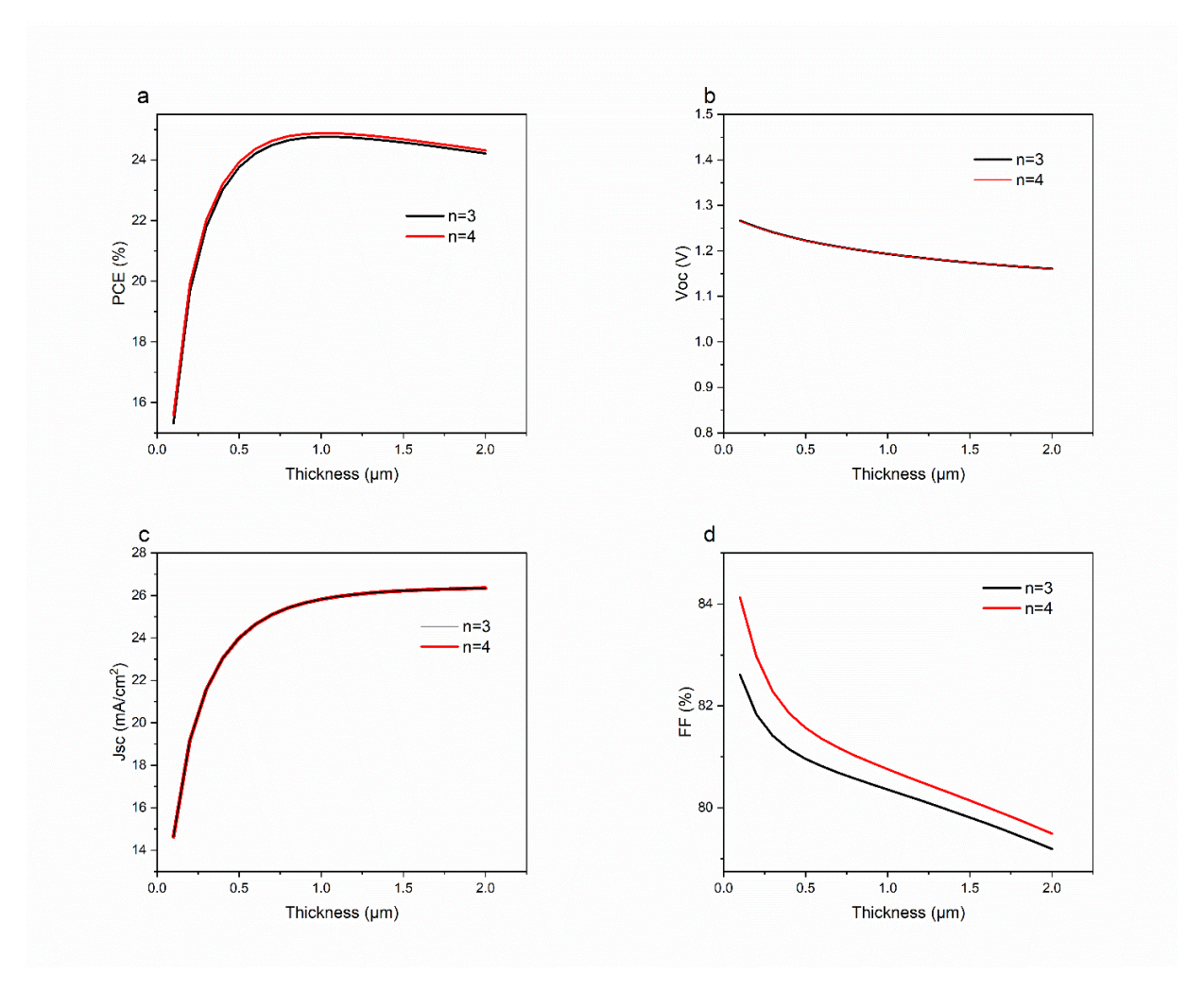


Fig. 22 a) PCE b) V_{OC} (c), J_{SC} (d), FF as a function of MAPbI₃ absorber layer thickness

In the proposed 2D/3D hybrid devices, Voc of BA2MA2Pb3I10/ MAPbI3 (n=3) devices is greater than the value BA2MA3Pb4I13/MAPbI3 (n=4) device. This can be attributed to the higher band gap value of BA2MA2Pb3I10 device. The higher band gap values are favorable for radiative recombination. In this process, the recombination of electrons and holes can occur with photon emission, which facilitates maintaining higher potential difference across the solar cell. Therefore, Voc increases when enhancing the bandgap. Further, this can be linked to the densities of the valence band (Nv) and the conduction band (Nc) [18].

The density of states (N =NC*NV) of BA2MA2Pb3I10 is lower than BA2MA3Pb4I13 perovskite material. Therefore BA2MA2Pb3I10/MAPbI3 absorber layer-based 2D/3D hybrid device shows a greater value of VOC. Conversely, PCE of BA2MA3Pb4I13/MAPbI3 is greater than BA2MA2Pb3I10/MAPbI3 due to the band gap of BA2MA3Pb4I13 being lower than BA2MA2Pb3I10, leading to enhanced absorption of long wavelengths of the solar spectrum and thus improving JSC. In the case of 2D layer thickness variation, the properties of the 2D layer, including bandgap, carrier mobility, and recombination rates, directly affect the device performance. Therefore,

there is a significant difference in photovoltaic parameters of n= and n=4, leading to larger gaps in PCE, Voc, Jsc, and FF compared to 3D layer thickness variation. In the scenario of 3D thickness variation, the 2D layer thickness is kept at a very low thickness of 0.1 μ m, and the effect of the 2D layer on charge transport and light absorption is minimal. Here, the 3D layer dominates both charge transport and light absorption. Under these circumstances, the properties of the 2D layer have a smaller effect on photovoltaic parameters, minimizing the performance gap between n=3 and n=4 plots. These results highlight the primary role of the 2D perovskite layer as a protective barrier.

I-V characteristics of the proposed devices for optimum perovskite absorber layer thickness values are plotted in Fig. 5. The two I-V curves almost overlap as per the Fig.. The main reason for this is the contribution of the 3D perovskite material to the system performance. While the 2D perovskite material boosts the stability of the solar cell and enhances some optoelectronic properties, the overall cell performance is dominated by the MAPbI3 3D perovskite material. Therefore, the difference of n values might not be sufficient to make a significant change in the performance of PSC [21].

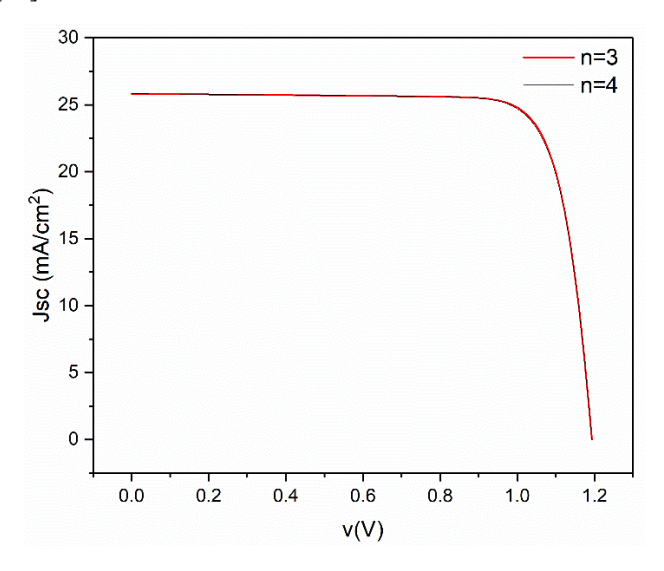


Fig. 33. I-V characteristics of optimized devices

4 Conclusion

Upon exposure to external environmental factors like heat, moisture, and UV, the 3D perovskite materials tend to degrade, reducing the overall performance. 2D perovskite materials, which are low-dimensional perovskite, show excellent stability against external environmental factors relative to the 3D materials. However, their performance is lower than the 3D perovskite solar cells. The approach of integrating 2D perovskite material with 3D materials is an innovative way to enhance stability without compromising performance. In this piece of research, SCAPS 1D-based simulation study was conducted to investigate the performance of 2D/3D mixed-dimensional PSC with a new device architecture; FTO/ZnO/BA2MAn-1PbnI3n+1/MAPbI3/Cu2O/Au. BA2MAn-1PbnI3n+1 was selected as the 2D material due to its proven stability in experimental results. Cu2O and ZnO were selected as HTL and ETL, respectively, as their superior stability relative to the other conventional charge transportation materials. The proposed configuration shows favorable band alignment, facilitating effective charges for carrier transportation, reducing recombination losses. The effect of the absorber layer thicknesses (n=3 and 4) was investigated to optimize the device performance. According to the simulation findings, at the thickness of 0.1 µm of 2D layer and 1 µm of 3D layer, maximum PCE of 24.76% and 24.88% were recorded by BA2MA2Pb3I10/MAPbI3 and BA2MA3Pb4I13/MAPbI3 layer-based devices, respectively. This study provides valuable insight into designing and optimizing 2D/3D mixed-dimensional PSC that could be beneficial for the fabrication of PSC with balanced efficiency and stability at the laboratory scale in a minimal effort and costeffective manner.

Acknowledgments

The authors sincerely recognize Prof. Marc Burgelman and his team at the University of Gent, Belgium, for creating, maintaining, and freely distributing the SCAPS-1D software, which was essential in performing the solar cell simulations in this research.

References

- [1] Danladi, E., Dogo, D. S., Michael, S. U., Uloko, F. O., & Salawu, A. O. (2021). Recent advances in modeling of perovskite solar cells using SCAPS-1D: Effect of absorber and ETM thickness. East European Journal of Physics, 2021(4), 5–17
- [2] Rathore, N., Panwar, N. L., Yettou, F., & Gama, A. (2021). A comprehensive review of different types of solar photovoltaic cells and their applications. *International Journal of Ambient Energy*, 42(10), 1200–1217.
- [3] Mahmud, M. A., et al. (2022). Origin of efficiency and stability enhancement in high-performing mixed dimensional 2D-3D perovskite solar cells: A review. *Advanced Functional Materials*, 32(3), 1–26.
- [4] Yu, Y., Xia, J., & Liang, Y. (2022). Basic understanding of perovskite solar cells and passivation mechanism. *AIP Advances*, 12(5).
- [5] Chowdhury, T. A., Bin Zafar, M. A., Sajjad-Ul Islam, M., Shahinuzzaman, M., Islam, M. A., & Khandaker, M. U. (2023). Stability of perovskite solar cells: Issues and prospects. *RSC Advances*, 13(3), 1787–1810
- [6] Wang, R., Mujahid, M., Duan, Y., Wang, Z. K., Xue, J., & Yang, Y. (2019). A review of perovskites solar cell stability. *Advanced Functional Materials*, 29(47)
- [7] Zhang, W., et al. (2023). Enhanced stability of carbon-based perovskite solar cells by using n-butylamine to assemble 2D capping layer. *Organic Electronics*, 115, 106757
- [8] Abedini-Ahangarkola, H., Soleimani-Amiri, S., & Gholami Rudi, S. (2022). Modeling and numerical simulation of high efficiency perovskite solar cell with three active layers. *Solar Energy*, 236, 724–732.
- [9] Chaurasia, S., et al. (2024). Highly efficient and stable Dion–Jacobson (DJ) 2D-3D perovskite solar cells with 26% conversion efficiency: A SCAPS-1D study. *Journal of Physics and Chemistry of Solids*, 191, 112038.
- [10] Wang, Y., et al. (2020). Unveiling the guest effect of N-butylammonium iodide towards efficient and stable 2D-3D perovskite solar cells through sequential deposition process. *Chemical Engineering Journal*, 391, 123589.
- [11] Yu, H., et al. (2021). Thermal and humidity stability of mixed spacer cations 2D perovskite solar cells. *Advanced Science*, 8(12).
- [12] Choi, H.-S., & Kim, H.-S. (2020). 3D/2D bilayered perovskite solar cells with enhanced stability and performance. *Materials*, 13(17).
- [13] Pellegrino, A. L., et al. (2022). A low temperature growth of Cu₂O thin films as hole transporting material for perovskite solar cells. *Materials*, 15(21).
- [14] Mehrabian, M., Taleb-Abbasi, M., & Akhavan, O. (2024). Using Cu₂O/ZnO as two-dimensional hole/electron transport nanolayers in unleaded FASnI₃ perovskite solar cells. *Materials*, 17(5).
- [15] Chuang, T. H., et al. (2023). Highly stable and enhanced performance of p-i-n perovskite solar cells via cuprous oxide hole-transport layers. *Nanomaterials*, 13(8).
- [16] Kumar, A., et al. (2023). Enhanced efficiency and stability of electron transport layer in perovskite tandem solar cells: Challenges and future perspectives. *Solar Energy*, 266, 112185.
- [17] Mandadapu, U. (2017). Simulation and analysis of lead-based perovskite solar cell using SCAPS-1D. Indian *Journal of Science and Technology*, 10(1), 1–8.
- [18] Chakrabartty, J., Islam, M. A., & Reza, S. (2021). Performance analysis of highly efficient 2D/3D bilayer inverted perovskite solar cells. *Solar Energy*, 230, 195–207.
- [19] Jiang, X., et al. (2020). Dion-Jacobson 2D-3D perovskite solar cells with improved efficiency and stability. *Nano Energy*, 75, 104892
- [20] Mohammed, M. K. A., et al. (2023). Harnessing the potential of Dion-Jacobson perovskite solar cells: Insights from SCAPS simulation techniques. *Journal of Alloys and Compounds*, 963, 171246.
- [21] Kabir, E., Kumar, P., Kumar, S., Adelodun, A. A., & Kim, K. H. (2018). Solar energy: Potential and future prospects. *Renewable and Sustainable Energy Reviews*, 82, 894–900.

Global Preparedness in Mitigating Environmental Impacts Of Renewable Energy

Nisitha Thushan Perera

Mechanical Engineering Department, Faculty of Engineering Technology, The Open University of Sri Lanka s24006836@eusl.edu.lk

Abstract

Global warming is currently the most alarming issue, owing to the overuse of non-renewable energy sources for daily use. The article addresses three important questions about the role of the renewable energy sector in combating global warming and the world's efforts to mitigate renewable energy's environmental impact. The first section describes the negative environmental impact of the renewable energy sector. Intermittency, large-scale project impact, resource consumption, and trash generation are major issues in the renewable energy business. The second section evaluates the aforementioned difficulties and the application of the circular economy idea to address them. In this section, the essay delves into circular economic principles that can help address these difficulties and lessen the negative impacts of renewable energy products and materials. In the third section, the article focuses on government policies, regulations, guidelines, and initiatives that aim to reduce the environmental impact of the renewable energy sector. The main objectives are to focus on identification of the environmental challenges linked to the renewable energy sector, assessing how the circular economy principles can help to overcome these challenges, investigation of the current and past policies and regulations that aid in mitigating renewable energy systems, and evaluating the integration potential into sustainable development goals 7 and 12. The paper is a review of previous studies related to the renewable energy sector. The integration of Sustainable Development Goal 7 and Sustainable Development Goal 12 within the collaboration of the circular economy concept is the best method to achieve a net-zero world by 2030.

Keywords: Global warming, Renewable energy, Circular economy, Intermittency, Sustainable Development Goals (SDGs)

1 Introduction

Fighting global warming has emerged as one of today's most pressing challenges. Global warming is a serious issue that must be addressed by the renewable energy sector in order to create a more sustainable and environmentally friendly future. One of the primary causes is the depletion of nonrenewable resources used to power our daily lives. The greatest method to combat global warming is to promote the renewable energy sector. The use of fossil fuels is the major cause of the global warming catastrophe [2]. The use of fossil fuels to generate energy, such as coal, petroleum, and natural gas, has a significant impact on the Earth's structure. In recent decades, humans have improved their quality of life by inventing machines, vehicles, and factories. However, this requires a significant amount of energy, leading to the burning of fossil fuels [2].

To generate energy, fossil fuels such as coal, petroleum, and natural gas are burned, resulting in the release of greenhouse gases. Greenhouse gases include carbon dioxide, chlorofluorocarbons, methane, nitrous oxide, etc. These gases significantly contribute to global warming by absorbing sunlight and returning excess heat to the atmosphere. The greenhouse effect ensures that excess heat does not escape the atmosphere, causing temperatures to rise and so affecting the global climate [1]. Greenhouse gases act like a blanket, making the Earth warmer than it would otherwise be [39].

Climate change is also one of the most critical impacts of global warming. Global climate change and rising sea levels pose a significant threat. Climate change has led to a shift in weather patterns worldwide. Extreme weather can do significant damage to the Earth's environment. The chart below shows the rise in temperature during the last few decades.

Climate change is a long-term shift in the average meteorological conditions that characterize Earth's local, regional, and global climates. Changes cause a wide range of observed results, all of which are referred to by the same term [40]. Here are some of the ecosystem changes due to climate change.

- 1. Increase of temperature
- 2. Increase in ocean temperature
- 3. Ice and glaciers melting
- 4. Unpredictable changes of the earth ecosystem
- 5. Extreme weather conditions

The picture below was extracted from NASA page. It shows Norway's Ålfotbreen glacier melting faster in Recent Summers [40].



Fig. 1 Norway's Ålfotbreen Glacier Melting Faster in Recent Summers

Transitioning to renewable energy is critical to reducing global carbon emissions and mitigating climate change. By addressing the environmental issues associated with renewable technologies and implementing enabling laws, the world will advance toward a much more sustainable and low-carbon future. This is because renewable energy sources have a significantly lower carbon footprint than other energy sources. However, there are some additional negative effects on the ecology. Wildlife disruption, massive projects, aquatic environment impacts, resource extraction, intermittency, backup power, visual and aural consequences, and emissions during the construction phase are some of the difficulties that have been raised concerning renewable energy.

The Sustainable Development Goal 7 (SDG 7) demands that governments provide cheap, sustainable energy to their citizens. SDG 12 emphasizes the importance of government policies, ethics, norms, and regulations in ensuring sustainable energy consumption and production. Sustainable Development Goals 7 and 12 emphasize the importance of renewable energy in achieving a cleaner, greener future. Renewable energy has a significant role in reducing global warming.

This study aims to highlight the environmental issues associated with the renewable energy sector and explore the possibility of circular economic concepts in reacting appropriately to such concerns. This study also aims to determine how far present and previous laws and regulations have contributed to decreasing the negative environmental consequences of renewable energy systems. Finally, it examines the feasibility of incorporating such efforts into Sustainable Development Goals 7 and 12 to achieve sustainable and responsible energy production and use.

The renewable energy business is being implemented by all, but none is taking into account the waste generated or the ecosystem's damage. Accurately identifying these detrimental effects and taking the appropriate steps to mitigate them are crucial. This article examines numerous solutions for mitigating the negative environmental implications of renewable energy technologies such as wind, solar, hydropower, and biofuels [3]. For this article, three research questions have been identified.

- 1. Is the world prepared to mitigate the negative environmental impact of the renewable energy sector?
- 2. Is the circular economy concept the best way to mitigate the negative impacts of the renewable energy sector?
- 3. What are the policies, programs, rules, and regulations that can be implemented to mitigate the environmental impacts of the renewable energy sector?

2 Research Questions

2.1 Is the world prepared to mitigate the negative environmental impact of the renewable energy sector?

While renewable energy is crucial for reducing global warming, it can also have detrimental environmental repercussions. It is critical to refer to past literature reviews, articles, YouTube videos, workshops, and books to identify the obstacles and negative repercussions related to the renewable energy business. This evaluation will highlight the main issues encountered.

2.1.1 Intermittency of renewable energy sources

Renewable energy sources are heavily reliant on global weather patterns [19]. Consider solar panels, solar panels cannot generate electricity during inclement weather conditions. Insufficient sunlight or cloudy weather can prevent solar panels from producing power at night [20]. Uncertainties are a key issue while using renewable energy.

Wind power is widely used throughout the world. Although wind power has numerous benefits, intermittency remains a significant challenge [7]. The growing popularity of intermittent wind generation has technical and economic implications for power networks [21]. The uncertain nature of solar and wind energy can lead to an irregular supply of electricity [9],[10]. Furthermore, the disruption of wildlife by wind turbines and solar panels is an ecological concern [11],[12]. Operators are less motivated to integrate wind power into their systems due to the current conditions. Tidal power generates electricity from water moving under tidal forces. "Tidal Power - Energy Education" describes this method of generating electricity as a dispatchable source [22]. The power title method is unpredictable, which is why tidal energy is not commonly employed globally [23]. Many tidal power systems are not available on an industrial scale; hence, tidal energy accounts for a tiny fraction of world energy today [43].

2.1.2 Large-scale energy projects and habitat disruption

Due to the energy issue, many countries are adopting and implementing large-scale renewable energy projects. Large-scale renewable energy projects raise the need for land. Any wind turbine installation project will require a significant quantity of land. These wind turbines are big, and they have a considerable impact on the nearby ecosystem and wildlife habitats. In terms of habitat modification, unexpectedly, the major hazard to the biodiversity region is the collision of birds and bats with the wind generated, as well as the downdraught generated by this spring's barotrauma blades [24].

Large-scale hydropower projects have a tremendous impact on the worldwide environment. Hydropower projects require enormous areas for construction. In these hydroelectric projects, individuals must construct dams and hydropower plants that require enormous regions [13]. In terms of habitat degradation, hydropower plants and dams have the potential to flood broad upstream areas, fragmenting habitats and affecting ecosystems and species [14]. Habitats must relocate as a result of dam construction initiatives. Moragolla dam construction is a wonderful illustration of this. The construction of the Moragolla dam and underground penstocks caused substantial dangers to the endangered green Labeo fish species at the project site Moragolla Dam [25]. This case resulted in construction delays and significant costs for the project.

2.1.3 Resource consumption to make energy efficient products

Renewable energy production requires a large quantity of raw materials. Particularly rare raw material resources are required for its manufacturing operations [4],[5]. The advancement of battery storage technology in electric vehicles provides strategic advantages in particular countries [37]. Silicon is by far the most common semiconductor used in solar cells, accounting for around 95% of the modules supplied today. It is also the second most prevalent mineral on the planet, behind oxygen [27]. Other raw materials commonly used in the production of solar panels include glass, aluminum, silicon, copper, and plastic [28].

According to a National Renewable Energy Laboratory research (Table 30), wind turbines are primarily constructed of steel (66-79% of total turbine mass), fiberglass, resin, or plastic (11-16%), iron or cast iron (5-17%), and aluminum (0-2%) [26]. The table below shows you the materials used in wind turbines.

				OEM			
Turbine make	Micon	Nordex	Micon	Vestas	Vestas	Vestas	Vestas
Turbine model	NM52	N-62	NM72	V82 1.65	V90 2.0	V100 2.0	V110 2.0
Nameplate capacity	0.9 MW	1.3 MW	1.5 MW	1.65 MW	2.0 MW	2.0 MW	2.0 MW
Hub height	60.7 m*	69 m	80 m	78 m	80 m	80 m	80 m
Rotor diameter	52.2 m	62 m	72 m	82 m	90 m	100 m	110 m
			M	ass (kg per k	(W)		
Steel	111.2	104.5	110.1	96.3	82.2	83.9	92.2
Fiberglass/resin/plastic	18.8	23.8	20.9	18.2	16.0	14.1	14.2
Iron/cast iron	7.2	17.3	8.7	17.8	20.5	13.3	13.3
Copper	1.6	1.5	1.2	1.8	0.9	0.6	0.7
Aluminum	N/A	N/A	N/A	1.9	2.1	1.7	1.9
Total	139.9	148.2	141.7	138.9	124.0	115.0	124.0
			% of]	Total Turbin	ne Mass		
Steel	79%	71%	78%	69%	66%	73%	74%
Fiberglass/resin/plastic	13%	16%	15%	13%	13%	12%	11%
Iron/cast iron	5%	12%	6%	13%	17%	12%	11%
Copper	1%	1%	1%	1%	1%	1%	1%
Aluminum	N/A	N/A	N/A	1%	2%	1%	2%
Total	99.2%	99.4%	99.4%	97.8%	98.0%	98.7%	98.5%

Table 30. Condensed Bill of Materials for Wind Turbines Used in Analysis

Sources: Liberman (2003); Vestas (2006); Garrett and Ronde (2011); Razdan and Garrett (2015a, 2015b)

Fig. 2 Condensed Bill of Materials For Wind Turbines

Materials used in dam construction might range from soil to rock, steel to concrete, influencing the total environmental impact of the undertaking [29]. The world's largest dam is the "Three Gorges Dam". The Three Gorges

Dam, a straight-crested concrete gravity construction, is 2,335 meters (7,660 feet) long and has a maximum height of 185 meters (607 feet). It has 28 million cubic meters (37 million cubic yards) of concrete and 463,000 metric tons of steel in its design [6],[30].

2.1.4 Waste generation from renewable energy products.

To ensure a sustainable future, it's crucial to effectively manage waste from renewable products [8]. Solar and wind farms generate waste for the environment. However, it is insignificant when compared to other waste fluxes. Between 2016 and 2050, solar waste creation would be 54 to 160 million tons, representing less than one-tenth of e-waste streams and at least 99.6% less than coal ash and municipal garbage [31]. According to Pu Liu and Clare Barlow, global cumulative turbine waste by 2050 will be roughly 42 million tons, which is comparable to solar power [32]. The chart below shows the cumulative waste generated through different sources.

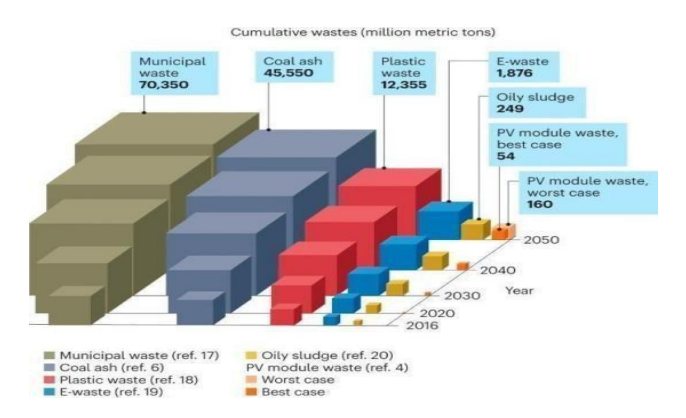


Fig. 3 How much waste do solar panels and wind turbines produce

According to statistics, trash output from these items is lower than other waste flows, yet it is vital to reduce the ways to build a sustainable future.

2.2 Is the circular economy concept the best way to mitigate the environmental impacts of the renewable energy sector?

Transitioning to a circular economy can significantly cut carbon emissions and waste from renewable energy products. Renewable energy products and equipment are expected to develop dramatically in the next three decades. This will generate a large amount of waste for the environment. This is why these materials must be recycled; otherwise, the entire ecosystem will collapse. Adaptation to the circular economy is necessary, and it is currently the best approach. In a circular economy, parts and materials have many life cycles and re-entry points into the market because they are methodically recovered, reused, and manufactured [33].

Embracing the circular economy maximizes material utilization, eco-friendliness, recycling, and waste management. Building suitable infrastructure is crucial to reducing the negative environmental implications of renewable energy [18]. The World Economic Forum identified three key circular economic concepts for the energy transition [34].

- 1. Recycling can conserve critical materials
- 2. Adaptation towards low-carbon circular materials
- 3. Design and develop circular economic structures

2.2.1 Recycling and conserving critical minerals

The primary goal of transitioning to renewable energy is to reduce the use of fossil fuels. Transitioning to solar, wind, hydrogen, biogas, and geothermal electricity consumes significant amounts of key minerals. The International Energy Agency estimates that reaching net zero by 2040 will necessitate a six-fold increase in mineral imports; some critical elements involved, such as lithium, may rise at rates more than 40 times current levels. Nickel and cobalt consumption will increase by more than 20 times. The price of lithium has already risen to a record \$50,000 per ton in February 2021, up from \$10,000 the previous year, with demand increasing, if not galloping [34].

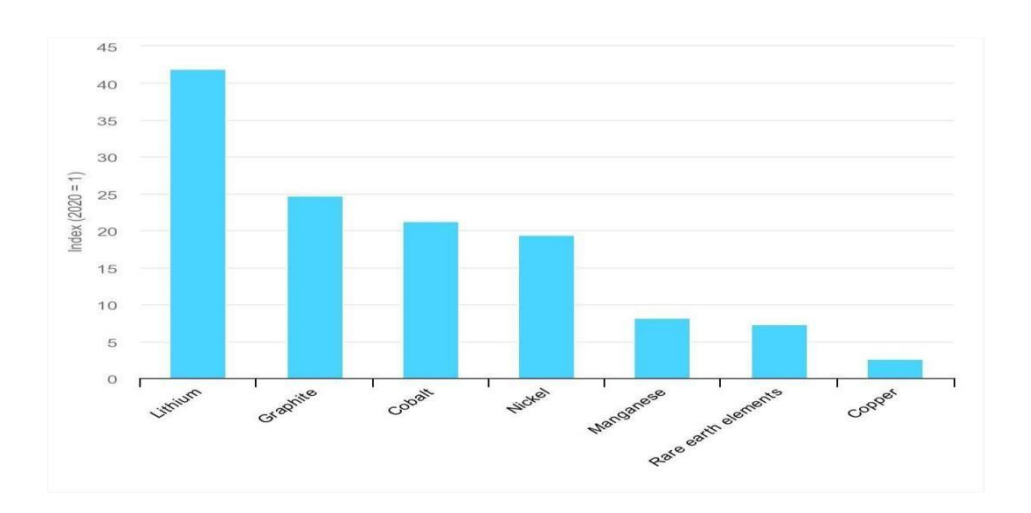


Fig.4 Growth in demand for selected minerals from clean energy technologies, 2040 relative to 2020 (multiples). Source: The Role of Critical Minerals in Clean Energy Transitions, International Energy Agency (2021).

Mining these resources presents a tremendous challenge to the Earth's environment. To lessen the carbon impact of raw material exploitation, humanity must consider sustainability and circular economic concepts. The renewable energy sector has complex challenges. Transitioning to a circular economy reduces reliance on mining, ensures long-term materials, and promotes recycling to recover previously used materials. The most commonly utilized materials include neodymium, tantalum, lithium, cobalt, manganese, graphite, and copper. Currently, just 1% of neodymium is recycled, while other metals in electronics—tantalum, lithium, cobalt, and manganese—critical to the transition have similarly weak recycling rates [34].

2.2.2 Adaptation to low-carbon circular materials.

The goal is to reduce carbon emissions from manufacturing and install renewable energy products. Stakeholders must adopt low-carbon materials. Improving the quality of locally produced products is crucial for reducing the carbon footprint. This reduces the impact of extracting row materials from industrial, construction, or client locations. This cost-effective solution will reduce transportation's impact and contribute to a more sustainable and economic future. According to a World Economic Forum analysis, components used in the production of electric cars are predicted to account for 60% of all lifetime emissions by 2040, up from 18% in 2020, when electric vehicles will dominate [35].

The circular economy will be able to provide low-carbon products like recycled aluminum, which emit up to 95% less CO2 than metal manufacturing from raw materials [17]. As a result, using secondary materials in energy transition infrastructure will move the world closer to achieving net-zero emissions [35].

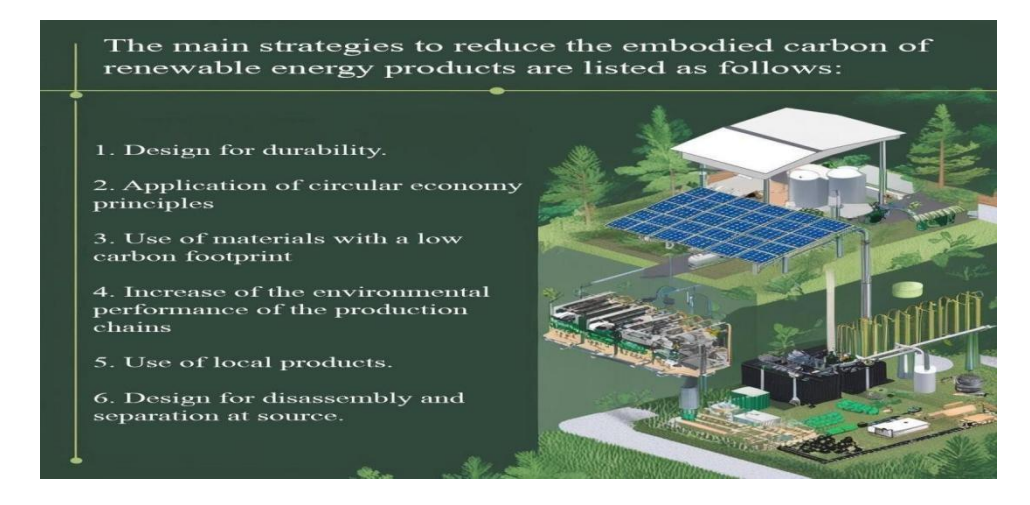


Fig. 5 The main strategies to reduce the embodied carbon of renewable energy products

2.2.3 Design and develop circular economic structures

The circular economy would be built on closed loops that ensure raw materials, components, and products preserve their quality and value for as long as possible. It tends to foster waste reduction through resource efficiency. Furthermore, such a process should be powered by renewable energy sources in order to reduce environmental effects and ensure sustainability. Ultimately, this should result in a regenerative economy that benefits business, society, and the environment [36].

Adaptation to circular economic principles throughout the design stage is key. This is the ideal time to consider long-term recyclable and assembly products for the market. The demand for renewable products is increasing tremendously. Companies are increasingly focusing on circular economy concepts, as illustrated by the following examples.

- The Ajax Dutch football club's stadium built a storage facility equivalent to the hourly electricity consumption of 7,000 families utilizing used Nissan Leaf batteries. On sunny days, the club can now store energy to power the entire stadium during evening games as well as feed it into the local power system [53].
- Siemens Gamesa has launched what it calls the world's first recyclable offshore wind turbine blade. The "Recyclable Blade" is ready for commercial use in the offshore wind industry, and Siemens Gamesa has already signed agreements with three customers [54].

2.3 What are the policies, programs, rules, and regulations that can be implemented to mitigate the environmental impacts of the renewable energy sector?

Mitigating the environmental repercussions of the renewable energy sector is a major concern for everyone right now. Policies, programs, rules, and regulations are critical for achieving this. These policies, regulations, and regulatory frameworks can be applied to a variety of areas. Which have been recognized by past books and papers. The most important thing is to raise people's awareness of the availability of renewable energy sources. It is possible to do this by implementing Sustainable Development Goal 7. This objective provides reliable, resilient, sustainable, and cheap clean energy to everyone on the planet. These guidelines and regulations allow Newmarket to consult with stakeholders as well as consumers. It's time to bring new policies and build awareness among consumers and stakeholders to mitigate the environmental impacts of the renewable energy sector. This is the moment to reform and establish a sustainable civilization for future generations.

Environmental policies in the renewable energy sector will develop initiatives to reduce energy consumption during operation, hence minimizing waste and recycling it. Not only that, but there are numerous benefits to these environmental policies and programs. According to previous researchers' papers, these are the things found to execute environmental rules and regulations in the renewable energy business

2.3.1 Create an obligatory or compulsory rule requiring all energy projects to do an environmental impact assessment.

The government must play a significant role in including the community and sharing Environmental Impact Assessment (EIA) knowledge with everyone. The essential point is that the government must mandate this EIA. It will undoubtedly lessen the environmental impact of the renewable energy industry. The EIA includes five key stages. Where an EIA is necessary, an Environmental Assessment Impact Report must be completed and submitted along with the development permit application. The public will be able to comment. This ensures that you have an opportunity to participate in the decision-making process [46].

Stage	What's involved
1. Screening	Deciding if an EIA is required
2. Scoping	Deciding what needs to be covered in the assessment and reported in the 'EIA Report'
3. Preparing the EIA Report	The EIA report has to include the likely significant environmental effects of the development
4. Making an application and consultation	The EIA Report and development application must be publicised (including electronic advertisement), interested parties and the public must be given an opportunity to give their views on it
5. Decision making	The EIA Report and any comments made on it must be taken into account by the competent authority before they decide whether to give consent for the development. The decision notice has to be published
6. Post decision	The developer starts any monitoring required by the competent authority.

Fig. 6 Stages of the EIA process

2.3.2 Implementing new guidelines for the land and property use of renewable energy sector projects is critical.

Considerable-scale renewable energy projects require a considerable quantity of land space. This can disrupt biodiversity and ecological sensitivity in site regions. Wildlands, natural ecosystems, and endangered species have a significant impact on these large-scale renewable energy sources. It is necessary to create and implement new criteria for these renewable energy projects.

Renewable energy development using energy zones is an important strategy for successfully managing land and storage problems [47]. Renewable energy development connects with a wide range of planning regulations and zoning bylaws, including groundwater resource preservation, urban design, rural resources, and natural heritage systems. In return, because so many distinct technologies interact with the legislative and regulatory framework, effective management across such broad sectors necessitates a matrix management approach. The technique helps to understand how various technologies interact and overlap with existing policy and regulatory landscapes. A practical example of such an approach is 'The Crosswalk', established by the Community Energy Knowledge-Action Partnership, which is a tool for coordinating policies and regulations across departments to promote the development of renewable energies in a coherent and integrated manner [48].

2.3.3 Implementing regulations for recycling operations in the renewable energy sector.

Most renewable energy products generate trash at the end of their useful life. These products end up in landfills as waste, which is a serious issue for the environment and biodiversity. The trash generated by solar panels and wind turbines is particularly significant. Recycling initiatives must be implemented in order to effectively manage garbage. These waste management regulations should be implemented using circular economy concepts. It will help to decrease and manage the waste that is generated by renewable energy products. The government has to address tricky regulations for these recycling projects. Here is an example. The government must prepare quality regulations for these recycling programs. Here's an example. Germany, the Netherlands, Austria, and Finland have already prohibited the disposal of blades in landfills, with more European countries anticipated to follow suit by 2025 [49].

2.3.4 Implementation of the community engagement and the research development sector

Raise awareness of Sustainable Development Goal 7 and its benefits to the community. Also, raise awareness of Sustainable Development Goal 12 of responsible consumption and production. These two sustainable development goals are interconnected. Social media plays a significant role in raising awareness about sustainable products in the renewable energy sector. For example, the solar industry is currently experiencing rapid growth. Stakeholders begin marketing campaigns on social media sites, which generates positive buzz for the solar energy business. Community engagement towards the renewable energy sector has three main advantages [50].

- It promotes trust between project developers and the community.
- Community participation has the potential to significantly minimize opposition to renewable energy projects.
- It builds community support for renewable energy projects.

Research and development are critical in the renewable energy sector. Renewable energy development projects primarily address key climate change challenges while also reducing greenhouse gas emissions, as well as providing the community with a secure and resilient clean energy infrastructure. Investing in the research and development process is necessary since discovering the most environmentally friendly renewable goods is vital. Providing grants and funding for research and development of new technologies that reduce the environmental impact of renewable energy is important.

Summary

Global warming and climate change are the most serious calamities we are facing today. To solve these issues, the ideal solution is to transition to renewable energy sources. The renewable energy sector offers everyone reliable, resilient, sustainable, and affordable clean energy (SDG 7) [15]. The 12th SDG will contribute to responsible energy consumption and production [16]. The Sustainable Development Goals 7 and 12 are inextricably intertwined. This indicates that these two targets will have a considerable impact on global renewable energy infrastructure. The question is whether the world is prepared to counteract the negative environmental impact of the renewable energy sector. This article discusses some negative environmental implications of the renewable energy sector. They are intermittent renewable energy sources, large-scale energy product projects and habitat disruption, resource consumption to manufacture energy-efficient products, and waste generation from renewable energy products.

The intermittent nature of renewable energy sources has diverse effects on the environment. The first issue is that stakeholders attempt to build large-scale projects, which create significant environmental damage. The fundamental point is that stakeholders have a negative attitude toward investing in the renewable energy sector due to its intermittency. When interest rates drop, stakeholders begin to invest in nonrenewable resources. Because it is more cost-effective and affordable than other renewable sources. Intermittency is a significant factor that promotes nonrenewable energy resources. Intermittency will hurt the environment. Large-scale renewable energy projects cause habitat disruption, natural forest destruction, and damage to wildlife. To prevent that, finding alternatives to large energy products is a must. For example, the construction building must be built according to green building standards, which will help to provide natural ventilation and light to the house. It will save the owner's electricity or energy consumption. The research and development section plays a key role in identifying alternatives for these energy products, as well as in managing trash [51],[52].

When considering waste management in the renewable energy sector, it is important to remember that it does not produce more waste than other waste flows; in fact, statistics show that it produces less waste than other products, but we must still build a sustainable future [38]. Waste management is, therefore, quite important. The article concludes that the circular economy is the most effective solution to address the waste management dilemma in the renewable energy sector. The government's policies and regulations will help the community become more aware of the renewable energy sector. Government involvement is especially vital in large-scale energy initiatives. The government can establish guidelines for preparing and selecting land for renewable energy projects, particularly solar and wind farms. Furthermore, the government plays a significant role in maintaining research and development unions to deploy cost-effective renewable energy technologies that are environmentally friendly [44],[45]. According to statistics, most countries use incredibly good rules and regulations to decrease the environmental impact of the renewable energy business. People are talking about a net-zero globe by 2030, but people are still preparing. For that, developing Sustainable Development Goals 7 and 12 in partnership with the circular economy would be game changers in creating a net-zero world by 2030 [41],[42].

Conclusion

Converting to renewable energy is a smart option in the fight against global warming and climate change, but it presents several environmental concerns. Examples include habitat destruction, overuse of resources in the construction of renewable energy equipment, and waste generation. To tackle these issues, circular economic concepts are critical, particularly in terms of waste management and resource efficiency. However, government laws and regulations have a significant impact in promoting these approaches to the public. Furthermore, adopting and extending research and development in these subject areas will aid in the discovery of novel, cutting-edge, and cost-effective solutions to meet energy demand.

References

- [1]M. R. A. Bhuiyan, "Overcome the future environmental challenges through sustainable and renewable energy resources," Micro & Nano Letters, Oct. 2022, doi: https://doi.org/10.1049/mna2.12148.
- [2]A. M. Omer, "Energy use and environmental impacts: A general review," Journal of Renewable and Sustainable Energy, vol. 1, no. 5, p. 053101, Sep. 2009, doi: https://doi.org/10.1063/1.3220701.
- [3]A. Q. Al-Shetwi, "Sustainable development of renewable energy integrated power sector: Trends, environmental impacts, and recent challenges," Science of The Total Environment, vol. 822, no. 822, p. 153645, May 2022, doi: https://doi.org/10.1016/j.scitotenv.2022.153645.
- [4]D. Streimikiene and G. Šivickas, "The EU sustainable energy policy indicators framework," Environment International, vol. 34, no. 8, pp. 1227–1240, Nov. 2008, doi: https://doi.org/10.1016/j.envint.2008.04.008.
- [5]I. Gunnarsdottir, B. Davidsdottir, E. Worrell, and S. Sigurgeirsdottir, "Review of indicators for sustainable energy development," Renewable and Sustainable Energy Reviews, vol. 133, p. 110294, Nov. 2020, doi: https://doi.org/10.1016/j.rser.2020.110294.
- [6]F. Cherubini, N. D. Bird, A. Cowie, G. Jungmeier, B. Schlamadinger, and S. Woess-Gallasch, "Energy-and greenhouse gas-based LCA of biofuel and bioenergy systems: Key issues, ranges and recommendations," Resources, Conservation and Recycling, vol. 53, no. 8, pp. 434–447, Jun. 2009, doi: https://doi.org/10.1016/j.resconrec.2009.03.013.
- [7]A. L. DREWITT and R. H. W. LANGSTON, "Assessing the impacts of wind farms on birds," Ibis, vol. 148, no. s1, pp. 29–42, Mar. 2006, doi: https://doi.org/10.1111/j.1474-919x.2006.00516.x.
- [8]V. Fthenakis, "Sustainability of photovoltaics: The case for thin-film solar cells," Renewable and Sustainable Energy Reviews, vol. 13, no. 9, pp. 2746–2750, May 2009, doi: https://doi.org/10.1016/j.rser.2009.05.001.
- [9]T. Katzner et al., "Challenges and opportunities for animal conservation from renewable energy development," Animal Conservation, vol. 16, no. 4, pp. 367–369, Jul. 2013, doi: https://doi.org/10.1111/acv.12067.
- [10]J. A. Smith and J. F. Dwyer, "Avian interactions with renewable energy infrastructure: An update," The Condor, vol. 118, no. 2, pp. 411–423, May 2016, doi: https://doi.org/10.1650/condor-15-61.1.
- [11]J. E. Keehn, K. T. Shoemaker, and C. R. Feldman, "Population-level effects of wind farms on a desert lizard," The Journal of Wildlife Management, vol. 83, no. 1, pp. 145–157, Sep. 2018, doi: https://doi.org/10.1002/jwmg.21565.
- [12]S. S. Kulkarni and D. J. Edwards, "A bibliometric review on the implications of renewable offshore marine energy development on marine species," Aquaculture and Fisheries, Nov. 2021, doi: https://doi.org/10.1016/j.aaf.2021.10.005.
- [13]B. Tilt, Y. Braun, and D. He c, "Social impacts of large dam projects: A comparison of international case studies and implications for best practice," Journal of Environmental Management, vol. 90, no. 3, pp. S249–S257, Nov. 2008, doi: https://doi.org/10.1016/j.jenvman.2008.07.030.
- [14]T. Tsoutsos, N. Frantzeskaki, and V. Gekas, "Environmental impacts from the solar energy technologies," Energy Policy, vol. 33, no. 2, pp. 289–296, 2005, doi: https://doi.org/10.1016/S0301-4215(03)00241-6.
- [15]United Nations, "Goal 7 | Department of Economic and Social Affairs," sdgs.un.org, 2024. https://sdgs.un.org/goals/goal7.
- [16]United Nations, "Goal 12 | Ensure Sustainable Consumption and Production Patterns," United Nations, 2023. https://sdgs.un.org/goals/goal12.
- [17]National Geographic Society, "Global Warming," education.nationalgeographic.org, Dec. 14, 2022. https://education.nationalgeographic.org/resource/global-warming/.
- [18]A. MacMillan and J. Turrentine, "Global Warming 101," NRDC, Apr. 07, 2021. https://www.nrdc.org/stories/global-warming-101#warming.
- [19]H. Lakeh, "What are the Pros and Cons of Renewable Energy?," www.greenmatch.co.uk, Dec. 17, 2021. https://www.greenmatch.co.uk/blog/2021/09/advantages-and-disadvantages-of-renewable-energy.
- [20]"Intermittent electricity Energy Education," energyeducation.ca. https://energyeducation.ca/encyclopedia/Intermittent_electricity#:~:text=Wind%20power%20is%20con sidered%20highly.

- [21]G. Ren, J. Liu, J. Wan, Y. Guo, and D. Yu, "Overview of wind power intermittency: Impacts, measurements, and mitigation solutions," Applied Energy, vol. 204, no. 204, pp. 47–65, Oct. 2017, doi: https://doi.org/10.1016/j.apenergy.2017.06.098.
- [22]"How can renewables deliver dispatchable power on demand? | Vision of Earth," www.visionofearth.org, Nov. 10, 2010. https://www.visionofearth.org/industry/renewable-energy-review/how-can-renewables-deliver-dispatchable-power-on-demand/
- [23] Energyeducation, "Tidal power Energy Education," energyeducation.ca, 2023. https://energyeducation.ca/encyclopedia/Tidal_power.
- [24]A. Gasparatos, C. N. H. Doll, M. Esteban, A. Ahmed, and T. A. Olang, "Renewable energy and biodiversity: Implications for transitioning to a Green Economy," Renewable and Sustainable Energy Reviews, vol. 70, pp. 161–184, Jul. 2024, doi: https://doi.org/10.1016/j.rser.2016.08.030.
- [25] "Moragolla Dam," Wikipedia, Aug. 20, 2021. https://en.wikipedia.org/wiki/Moragolla Dam.
- [26]USGS, "What materials are used to make wind turbines?," www.usgs.gov, 2018 https://www.usgs.gov/faqs/what-materials-are-used-make-wind-turbines#:~:text=According%20to%20a%20report%20from.
- [27]Solar Energy Technologies Office, "Solar Photovoltaic Cell Basics," Energy.gov, May 31, 2023. https://www.energy.gov/eere/solar/solar-photovoltaic-cell-basics#:~:text=Silicon (accessed Jun. 31, 2024).
- [28]Solar Materials, "SOLAR MATERIALS Home," SOLAR MATERIALS, 2023. https://solar-materials.com/.
- [29]CT.gov Home, "Introduction to Dams," CT.gov Connecticut's Official State Website, 2024. https://portal.ct.gov/DEEP/Water/Dams/Introduction-to-Dams#:~:text=Various%20materials%20are%20used%20for.
- [30]Britannica, "Three Gorges Dam | Facts, Construction, Benefits, & Problems," Encyclopædia Britannica. Feb. 25, 2019. Available: https://www.britannica.com/topic/Three-Gorges-Dam
- [31]H. Ritchie, "How much waste do solar panels and wind turbines produce?," www.sustainabilitybynumbers.com, 20, 2023. https://www.sustainabilitybynumbers.com/p/renewables-waste.
- [32]P. Liu and C. Y. Barlow, "Wind turbine blade waste in 2050," Waste Management, vol. 62, pp. 229–240, Apr. 2017, doi: https://doi.org/10.1016/j.wasman.2017.02.007.
- [33]USAID, "Promoting a Circular Economy," www.usaid.gov, Jun. 14, 2022. https://www.usaid.gov/energy/sure/circular-economy.
- [34]J. Pennington, "3 ways the circular economy is vital for the energy transition," World Economic Forum, Feb. 23, 2022. https://www.weforum.org/agenda/2022/02/3-ways-circular-economy-renewables-energy-transition/.
- [35]G. Grazieschi, "Overview Article Circularity and Low-Carbon Building Materials in Construction | BUILD UP," build-up.ec.europa.eu, Nov. 03, 2022. https://build-up.ec.europa.eu/en/resources-and-tools/articles/overview-article-circularity-and-low-carbon-building-materials.
- [36]A. G. Schmid and J. M. F. Mendoza, "Circular Economy and the Clean Energy Transition | Future Earth," Future Earth, Dec. 16, 2022. https://futureearth.org/2022/12/16/circular-economy-and-the-clean-energy-transition/.
- [37]H. Sanderson, "Battery technology gives China an opening in electric vehicles," Financial Times, Oct. 07, 2021. Accessed: Jul. 01, 2024. [Online]. Available: https://www.ft.com/content/fcbc860b-51cd-40d8-b65f-db97ce9adc57
- [38]E. Lucey, "What exactly is the role of renewable energy in a circular economy?," acehub.org.au, 2022. https://acehub.org.au/news/the-role-of-renewable-energy-in-a-circular-economy.
- [39]United States Environmental Protection Agency, "Basics of Climate Change," www.epa.gov, Apr. 15, 2021. https://www.epa.gov/climatechange-science/basics-climate-change
- [40]NASA, "What Is Climate Change?," science.nasa.gov, 2024. https://science.nasa.gov/climate-change/what-is-climate-change/.
- [41] Wikipedia, "Sustainable Development Goal 12," Wikipedia, Oct. 11, 2020. https://en.wikipedia.org/wiki/Sustainable Development Goal 12.

- [42]Wikipedia , "Sustainable Development Goal 7," Wikipedia, Feb. 08, 2021. https://en.wikipedia.org/wiki/Sustainable Development Goal 7.
- [43]N. E. Selin, "tidal power | Types & Facts," Encyclopædia Britannica. Apr. 04, 2019. Available: https://www.britannica.com/science/tidal-power
- [44]M. Jefferson, energy policies for sustainable development. UK: UNDP, 2024, pp. 416-452.
- [45]energy.gov, "Policies and Programs," Energy.gov, 2024. https://www.energy.gov/scep/slsc/policies-and-programs
- [46]Mygov.scot, "Environmental Impact Assessment (EIA)," www.mygov.scot, Jul. 21, 2022. https://www.mygov.scot/eia.
- [47] "Renewable Energy Zones," EnergyCo. https://www.energyco.nsw.gov.au/renewable-energy-zones.
- [48] "Integrating energy planning and land-use planning AIRE Protocol," QUEST Canada, 2024. https://questcanada.org/aire-protocol/land-use-planning/.
- [49]M. Jacoby, "How can companies recycle wind turbine blades?," Acs.org, Aug. 08, 2022. https://cen.acs.org/environment/recycling/companies-recycle-wind-turbine-blades/100/i27
- [50]B. Walsh, "Community Engagement Strategies for Renewable Energy Developers," Landgate, Dec. 11, 2023. https://www.landgate.com/news/community-engagement-strategies-for-renewable-energy-developers.
- [51]Benjamin, "Understanding the role of R&D in the renewable energy industry," Alexander Clifford, Dec. 05, 2023. https://alexanderclifford.co.uk/blog/role-of-r-and-d-in-renewable-energy-industry.
- [52]colorlib, "Research and Development," www.energy.gov.lk. https://www.energy.gov.lk/en/energy-management/research-and-developments.
- [53]C. Owen-Burge, "3 ways the circular economy is vital for the energy transition Climate Champions," Climate Champions, Mar. 03, 2022. https://climatechampions.unfccc.int/3-ways-the-circular-economy-is-vital-for-the-energy-transition.
- [54]Siemens, "Wind Works New York," Wind Works New York, Aug. 16, 2022 https://windworksny.org/press/siemens-gamesa-claims-worlds-first-recyclable-offshore-wind-turbine-blade.

Lifecycle Impact Analysis of a Traditionally Manufactured Cotton Batik Shirt in Sri Lanka– Case Study

K. M. G. L. Karunarathna, T. D. Amarasooriya*

Sri Lanka Institute of Information Technology qayath18@gmail.com, thilini.d@sliit.lk*

Abstract

The textile industry is famous for its high environmental impact, and the garment manufacturing sector in Sri Lanka is also responsible. Batik shirts are a popular traditional clothing item created in Sri Lanka, and their production includes numerous stages with varying environmental impacts, such as cotton cultivation, weaving, wax application, coloring, and finishing. Batik textile manufacturing originated in Sri Lanka and Indonesia, following a unique and traditional manufacturing method. This research has identified the environmental impacts from the traditional Batik manufacturing of Sri Lanka throughout its lifecycle, segmented into five main stages as fabric production, shirt production, usage, transportation, and disposal in a cradle-to-grave approach. It was identified that fabric production and shirt production stages are most impactful, where fabric production is highly impactful in climate change with 42.5% and human toxicity with 44.7% while the shirt production stage is highly impactful in acidification with 47.4%, eutrophication potential with 41.7% and photochemical oxidation with 41.4%.

Keywords: Environment, Ecofriendly, Hotspots, Manufacturing, Niche, Sustainability

1 Introduction

The textile manufacturing industry in Sri Lanka has expanded dramatically over the years, playing an essential part in the country's economy. However, as the sector expands, there is rising concern about its environmental impact, particularly in the production of textile goods, as the global population prioritizes sustainability. The textile manufacturers must examine the environmental effect of their goods and operations no matter it is large-scale manufacturing or small-scale manufacturing like Batik textile manufacturing. Lifecycle Assessment (LCA) is a useful tool for assessing a product's environmental performance throughout its life cycle.

Batik shirts are one-of-a-kind items that need a variety of raw materials and production procedures, each having its own environmental effect. Starting from cotton farming, which requires a large amount of water and chemicals, the dyeing and finishing procedures may generate a lot of waste and pollution. Furthermore, like any other textile product, the disposal of Batik shirts can accumulate textile waste in landfills. As a result, doing a life cycle assessment of Batik shirts is critical in identifying areas where the sector may minimize its environmental impact and transition to more sustainable practices. A comparison of past LCA studies of Batik shirts can provide valuable insights into the environmental impact of the product and identify areas for improvement, but it is very limited as Batik has a niche market share. An LCA can highlight the stages with the most significant environmental impact and help identify strategies for reducing this impact by assessing the entire life cycle of a Batik shirt, from the raw material extraction to the end-of-life treatment. This research aims to contribute to the existing knowledge of the environmental impact of Batik shirts and promote sustainable practices in the Sri Lankan textile industry. This Research on the life cycle assessment of Batik shirts in Sri Lanka is crucial for improving sustainability and lowering the environmental impact of the textile sector. The findings of this study may be used to drive sustainable product development, influence regulatory choices, and urge the sector to embrace sustainable practices. The significance of this research lies in offering insights on the environmental impacts of Batik shirts, which contributes to the larger objective of sustainable development and improving the planet's long-term health.

There are two approaches to conducting an LCA: Cradle-to-Grave and Cradle-to-Cradle. The Cradle-to-Grave approach has been considered for conducting research aimed at achieving the objectives below.

- 1. Conduct a comprehensive evaluation of the environmental impacts associated with the production of Batik shirts in Sri Lanka, including the use of energy, water, and raw materials, as well as emissions to air, water, and land, with the aim of identifying areas for improvement and developing strategies to minimize environmental harm.
- 2. Minimize water consumption and reduce wastage, such as implementing recycling and reusing practices, fixing leaks, and utilizing rainwater harvesting techniques.
- 3. Assess the amount of waste generated, including wastewater and solid waste, and to identify and recommend strategies to reduce waste and implement responsible disposal practices to minimize environmental impact and promote sustainability.

4. Improve the efficiency of Batik shirt production, explore innovative technologies and methods such as utilizing advanced machinery with high efficiency, enhance productivity, increase profitability and reduce the environmental footprint.

2 Literature background

Research conducted in China [1] provides insights into the environmental impact of cotton T-shirts through a Life Cycle Assessment (LCA) method. The study found that cotton cultivation, dyeing, makeup, and use phases contribute the most to the environmental impact of cotton T-shirts. More specifically, the study highlights the use of fertilizers, pesticides, and water in cotton cultivation, coal, dyes, and auxiliaries in dyeing, and electricity in making up as the main hotspots in the life cycle of cotton T-shirts [1]. Based on the research presented, it is suggested that the textile industry prioritize sustainability by adopting eco-friendly farming practices, using more sustainable dyeing and making-up technologies, and promoting environmentally friendly consumer habits by taking a proactive approach to sustainability, the industry can work towards minimizing the environmental impact of cotton T-shirts and promote sustainable textile production practices [1]. Based on the research findings, it suggests encouraging consumers to make more conscious and sustainable choices when purchasing textile cotton products, such as opting for eco-friendly options like the organically grown cotton Eco T-shirts [2]. Additionally, policymakers and industry leaders can consider implementing and promoting sustainable production practices in the textile industry to further reduce the environmental impact of cotton textile products [2]. The study of lifecycle assessment was done for apparel consumption in Australia, which evaluates the environmental impact of clothing from raw material extraction to disposal [3]. The study uses ISO 14040/14044:2006 methodology, the Eco Invent dataset, and the Australian life cycle assessment dataset. The environmental impact of apparel consumption is assessed based on climate change potential, acidification potential, water depletion, abiotic resource depletion potential, and land occupation [3]. Similarly, another study on the lifecycle assessment of cotton textile products in Turkey highlighted the importance of using sustainable raw materials and practices throughout the life cycle of cotton products. Eco T-shirts, made from organically grown cotton with green dyeing, showed lower environmental impact [2]. The study encouraged consumers to make sustainable choices and recommended policy and industry support for sustainable production practices [2].

Life Cycle Analysis (LCA) of a Cotton Woven Shirt methodology was applied to analyze environmental impacts throughout the production of cotton woven shirts. The study emphasized the need for systematic approaches to address environmental challenges in the textile sector, with recommendations to reduce water, auxiliaries, and electricity usage. Government and environmental organizations were urged to lead sustainability initiatives [4]. The same study [3] evaluated the entire life cycle of clothing, identifying the production stage as the most impactful. It stressed the interrelation of production and consumer use, calling for sustainable practices throughout the supply chain. Prioritizing renewable energy, mixed fiber apparel, and sustainable consumer behavior was suggested to reduce the overall environmental impact.

Overall, the literature review underscores that the production and use stages are the main contributors to environmental impacts in textile production. Sustainable materials, production methods, renewable energy, and eco-friendly dyes can significantly mitigate these impacts.

3 Methodology

The visit to a famous Batik factory in Maharagama, Sri Lanka, is well-known for manufacturing Batik clothing, not only for Sri Lanka but also for other countries. In order to gather data, a number of interviews were conducted with the management and workers of the company. Firstly, it was identified the process of Batik manufacturing was identified to identify the life cycle phases to consider in the LCA, as given in Fig. 1. Secondly, necessary data was collected regarding inputs and outputs of each stage of manufacturing to use in the OpenLCA software. This data includes materials use, waste management, and fuel and emission data. Further, data required for the conduct of LCA was collected through databases and literature. The single factory was chosen to conduct research due to the lack of data availability and literacy on environmental contributions in other Batik manufacturers that were reached out to gather data. Brief discussions and collection of data from those manufacturers were also in the same range as the selected manufacturer. Also, the selected manufacturer had a comparatively large-scale manufacturing facility, which provided sufficient data.

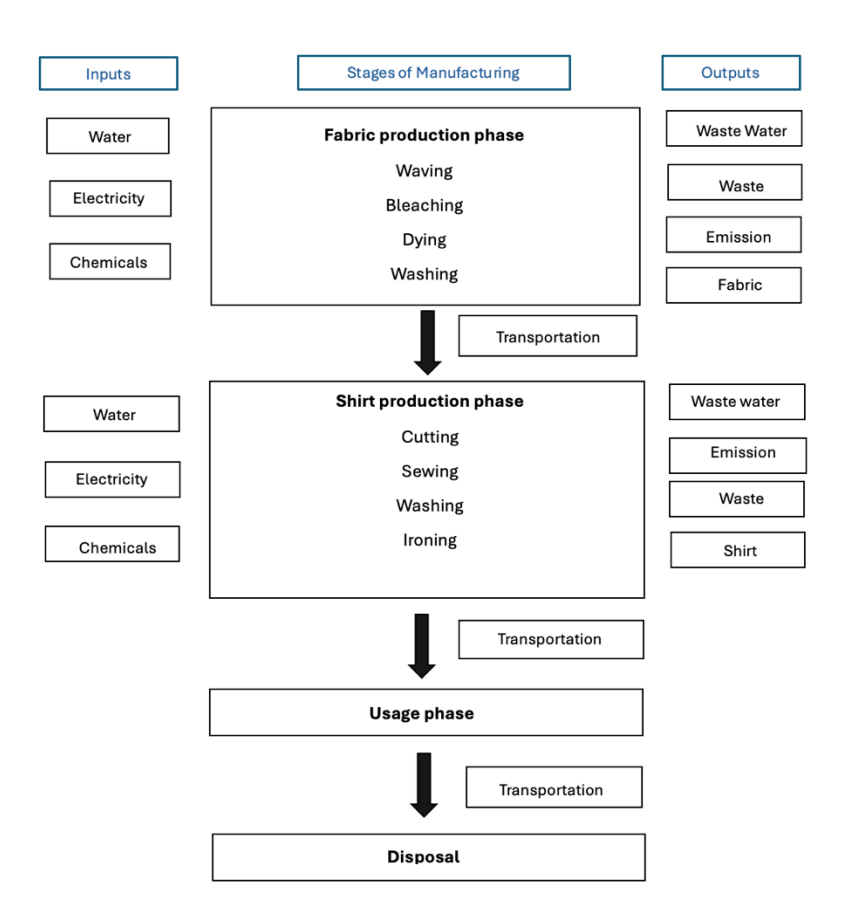


Fig. 1 Lifecycle stages of Batik shirt manufacturing

Inputs and outputs were categorized for the five stages of the lifecycle used in the lifecycle assessment, which are given in Tables 1 to 8 in the results and discussion section of this paper. The identified five lifecycle phases are Fabric production, shirt production, usage, disposal, and transportation, which are used to identify Climate change, Eutrophication potential, Human toxicity, Photochemical Oxidation, and Acidification potential at each stage. OpenLCA outputs are analyzed to identify what is most impactful in each stage.

The data used for this assessment has been collaboratively collected from a questionnaire shared among the general public to collect data on usage, transportation, and disposal stages. It's important to note that Batik shirts may not be equally popular throughout the year, with a notable surge in demand typically occurring during the April Avurudu season. This season-specific data can provide valuable insights into the environmental impact of Batik shirts during peak demand periods. But the LCA was not conducted specifically for the high seasonal demand, but average impacts per year from the total production, including the high-demand season.

The equations below were used to calculate input and output data for the unit of a single shirt used in the analysis.

CO₂ emissions associated with this LPG consumption (CO₂) = Volume of LPG (L) x Emission factor (kg CO₂ per L) (Eq 1)Energy consumption for sewing (kWh) = Power rating of sewing machine x number of hours (Eq 2)Energy consumption for ironing (kWh) = Power rating of iron x number of hours (Eq 3)Emissions per shirt (Sewing) = Electricity consumption per Sewing session (kWh) x Emission factor (kg CO₂/kWh) (Eq 4)Emissions per shirt (ironing) = Electricity consumption per ironing session (kWh) x Emission factor (kg CO₂/kWh) (Eq 5)Emissions per shirt (washing) = Electricity consumption per shirt (kWh) x Emission factor (kg CO2/kWh) (Eq 6)Total CO2 emissions per shirt = Emissions per shirt (Sewing) + Emissions per shirt (ironing) (Eq 7)

Nitrogen (N) emissions per shirt (Sewing) = Electricity consumption per sewing session (kWh) x N emission factor (kg/kWh)	(Eq 8)
Nitrogen (N) emissions per shirt (ironing) = Electricity consumption per ironing session (kWh) x N emission factor (kg/kWh)	(Eq 9)
Nitrogen (N) emissions per shirt (washing) = Electricity consumption per shirt (kWh) x N emission factor (kg/kWh)	(Eq 10)
Nitrogen Oxides (NOx) emissions per shirt (ironing) = Electricity consumption per ironing session (kWh) x NOx emission factor (kg/kWh)	(Eq 11)
Water consumption per kg = (Water usage per wash) / (Washing machine capacity)	(Eq 12)
Detergent consumption per kg = (Detergent usage per wash) / (Washing machine capacity)	(Eq 13)
Detergent consumption for 1 shirt = Detergent consumption kg x Weight of the shirt	(Eq 14)
Electrical energy consumption per kg = (Washing machine energy efficiency) / (Washing machine capacity)	(Eq 15)
Electrical energy consumption for 1 shirt = Electrical energy consumption per kg x Weight of the shirt	(Eq 16)
Total Petrol consumption = Distance traveled / Fuel efficiency.	(Eq 17)
CO2 emissions at transportation = Fuel consumption x CO2 emission factor	(Eq 18)
NOx emissions at transportation = Fuel consumption x NOx emission factor	(Eq 19)
CO2 emissions at disposal = Carbon content x Emission factor x Weight of waste pieces	(Eq 20)

4 Results and Discussion

4.1 Inputs and outputs considered for the analysis in each stage of the life cycle

4.1.1 Inputs and outputs for the Fabric production stage

Fabric production is a crucial stage in manufacturing the 'Batik Shirt' in Sri Lanka's apparel industry, where the analysis was done for the environmental impact of waxing, dyeing, and Boiling operations. In order to provide a thorough analysis, an average shirt produced per week was taken 15 and the average amount of cotton fabric used per shirt is 1.25m2. Table 1 shows the other amounts of materials used as inputs for the process. The analysis was done for wastewater generation, and the presence of toxic chemicals during the stages of dyeing and washing. By evaluating these factors in terms of wastewater and toxic chemicals, the research aimed to improve the sustainability of fabric production and promote eco-friendly practices for the 'Batik Shirt' in Sri Lanka. To calculate the emissions for the 12.5 kg Liquid Petroleum Gas (LPG) cylinder, we need to determine the volume of LPG consumed. 1 liter of LPG is approximately equal to 0.54 kg (density of LPG). So, for a 12.5 kg LPG cylinder the volume of LPG is closely equal to 23.15L. Calculating the CO2 emissions associated with this LPG consumption was found as 34.96 kg CO2 with the CO2 emission factor 1.51 kg per liter.

Batik, a renowned fabric-making technique known for its intricate patterns and vivid colors, has gained worldwide recognition. However, concerns have risen regarding potentially harmful substances in Batik dyes that could impact human health and the environment. To address these concerns, the International Organization for Standardization (ISO) has developed specific standards for Batik dye composition. Adherence to these ISO guidelines is crucial for the Batik industry to promote health and sustainability in its dyeing processes. According to ISO maximum allowable percentage of heavy metals is Chromium (Cr) 0.1%, Lead (Pb) 0.01%, Cadmium (Cd) 0.005% and Mercury (Hg) 0.001%.

Accordingly, input data and output data are calculated per month, and it is given in Tables 1 and 2.

Table 1 Input data for the Fabric production stage

Data Type	Description	Value Per shirt	Value per month	Units
Water	The average amount of water needed for dying in Fabric manufacturing per month	5	300	1
	The average amount of water needed for boiling per month	-	220	1

Chemicals	Average amount of HCl needed per month	50	3000	g
	Average amount of NaOH needed per month	25	1500	g
Wax	Average Amount of wax used in Fabric manufacturing per month	100	6000	g
Gas	Average Amount of gas cylinders used per month	_	4	Cylinder
Dye	Average Amount of dye used in fabric manufacturing per month	`25	1500	g

Table 2 Output data for Fabric production stage

Category Subcategory		Value per shirt Value per month		Unit
Waste water	Total Wastewater generated per month	60	520	1
	Pb	0.0025	0.15	g
Harmful chemicals	Hg	0.00025	0.015	g
	Cd	0.00125	0.075	g
	Cr	0.025	1.5	g
Emissions to Air	Carbon dioxide (CO2)	-	139.84	kg

4.1.2 Input and output Data for the Shirt production stage

This study assessed the environmental impact of the shirt production stages of cutting, sewing, washing, and finishing for the Batik Shirt. The input data for the sewing stage, as given in Table 3 electrical energy consumption by sewing is approximately 0.1 kilowatt-hours of electricity using a 100W machine for 1 hour and approximately 0.2 kilowatt-hours of electricity using a 1200W iron for 10 minutes. Emissions to air (CO2, N, SO2, NOx) are taken in grams per shirt (g/shirt). The emissions for CO2, with emission factor 0.71 kg CO2/kWh and total N, SO₂, NOx emissions per shirt, with Nitrogen (N) emission factor 0.002 kg/kWh, Sulfur Dioxide (SO2) emission factor 0.001 kg/kWh and Nitrogen Oxides (NOx) emission factor 0.0015 kg/kWh. Total Emissions per shirt are given in Table 4.

Table 3 Input data for the shirt production stage

Data Type	Amount	Per Shirt	Per Month	Unit
	The average amount of electricity needed for sewing in one month	0.1	6	kWh
Electrical Energy	The average amount of electricity needed for ironing in one month	0.2	12	kWh

Table 4 Output data for the shirt production stage

Category	Subcategory	Amount per Shirt	Amount per Month	Unit
	Carbon dioxide (CO ₂)	0.213	12.78	kg
Emissions 4s Air	Nitrogen (N)	0.0006	0.036	kg
Emissions to Air	Sulphur dioxide (SO ₂)	0.0003	0.018	kg
	Nitrogen oxide (NO _x)	0.00045	0.027	kg

4.1.3 Input and output data for Usage stage

In the usage phase evaluation took into account several key factors, including average water consumption (in liters per month), chemical usage (in grams per month), and electrical energy consumption (in kilowatt-hours per month) associated with washing and ironing. The research evaluated its environmental impact in terms of air emissions (CO2, N, SO2, NOx), wastewater generation, and the presence of water with toxic chemicals. Measurements are expressed in grams per shirt (g/shirt) for emissions and grams per shirt (g/shirt) and liters per shirt (L/shirt) for water-related factors.

Average input data for washing was collected by using a questionnaire among a sample of Batik shirt buyers during April. It was identified that, Batik shirt's Average Washing frequency per week is 1 (Batik shirt are washed once a week), Average Water usage per wash is 40 liters, Average Detergent usage per wash is 50 gram, Average Washing machine energy efficiency is 0.32 kWh per wash, Average Weight of the Batik shirt is 220 grams (0.22 kg), Washing machine capacity is 7.00 kg, Average amount of washing machine usage per week for Batik shirt is once from the data collected by the questionnaire. Therefore, the values for a unit of single shirt with the updated washing machine capacity of 7.00 kg, input data were included as given in Table 5. During Batik shirt washing, detergent powder in the washing machine effectively removes dirt and stains using primary surfactants like LAS (R-C6H4-SO3Na) and SLS (CH₃(CH₂)11OSO₃Na). Sodium percarbonate (2Na₂CO₃ · 3H₂O₂) and sodium perborate (NaBO₃ · H₂O₂) act as bleaching agents for tough stains without fading the vibrant Batik colors. Builders, STPP (Na₅P₃O₁₀) and sodium carbonate (Na₂CO₃), enhance cleaning efficiency and prevent dirt redeposition. This synergy preserves Batik's beauty and craftsmanship, delivering clean, vibrant shirts. The amount of each chemical in 1.57g of detergent powder composition might be as follows, Linear Alkylbenzene Sulfonates (LAS) 5%, Sodium Lauryl Sulfate (SLS) 5%, Sodium Percarbonate 2%, Sodium Perborate 2%, Sodium tripolyphosphate (STPP) 20%, Sodium carbonate (soda ash) 20%. Total emissions were calculated using the same emission factors used above and output data presented in Table 6.

	•	0 0		
Data Type	Amount	Per shirt/week	Per month	Unit
Water	The average amount of water needed for washing 1 shirt in the usage phase per month	1.2572	5.0288	1
Detergent	Average amount of Detergent needed for washing 1 shirt in the usage phase per month	1.5712	6.2848	g
E	The average amount of electricity needed for washing 1 shirt in the usage phase per month	0.010057	0.040228	kWh
Energy	The average amount of electricity needed for ironing 1 shirt in the usage phase per month	0.2	0.8	kWh

Table 5 Input data for the shirt usage stage

Table 6	Output	data	for	the	shirt	usage	stage
---------	--------	------	-----	-----	-------	-------	-------

Category	Subcategory	Value per shirt/week	Value per shirt/per month	Unit
	Carbon dioxide (CO ₂)	0.149	0.596	kg
Estate and Ata	Nitrogen (N)	0.00042	0.00168	kg
Emissions to Air	Sulphur dioxide (SO ₂)	0.00021	0.00084	kg
	Nitrogen oxide (NO _x)	0.00031	0.00124	kg
Waste water	Wastewater generated	1.2571	5.0284	1
Sodium Lauryl Sulphate-(SLS)- CH ₃ (CH ₂) ₁₁ OSO ₃ Na		0.0785	0.314	g
Harmful chemicals	Linear Alkylbenzene Sulfonates-(LAS)- R-C ₆ H ₄ -SO ₃ Na	0.0785	0.314	bIJ
	Sodium Percarbonate- 2Na ₂ CO ₃ · 3H ₂ O ₂	0.0314	0.1256	g

Sodium Perborate- NaBO ₃ · H ₂ O ₂	0.0314	0.1256	g
Sodium Tripolyphosphate- (STPP)-Na ₅ P ₃ O ₁₀	0.314	0.1256	g
Sodium Carbonate -(Soda Ash)- Na ₂ CO ₃	0.314	0.1256	g

4.1.4 Input and output data for the Transportation stage

The research meticulously examines the energy requisites for the transportation of clothes in the assessment of the Batik Shirt supply chain's transportation and distribution phase. The analysis found data that quantifies the energy consumption per kilogram of cloth, measured in joules per kilogram (kJ/month). It's noteworthy that the data used for this evaluation was meticulously gathered through an analysis of a reputed Batik company in Sri Lanka. Additionally, it is important to note that Batik Shirt predominantly retails its clothing through its store situated in the town of Maharagama. Furthermore, a portion of their clothing products were exported to international markets. This diversified distribution strategy necessitates thorough consideration of energy-related factors and the exploration of opportunities for improvement within the transportation and distribution phase.

Distance Traveled is taken as 2.5km in a car with a fuel efficiency of 12 km/ liter, Number of Shirts Transported by one car is taken as 15. Total Petrol Consumption is given in Table 7. Emission factors (per liter of diesel during burning) were considered as CO2 is 2.68 kg CO2/liter, NOx is 5 grams NOx/ liter, Nitrogen (N), and sulfur dioxide (SO2) emissions are typically negligible from petrol vehicles. Output emissions are as in Table 8.

Data Type	Description	Per shirt	Per month	Unit
Petrol consumption	The average amount of Petrol consumption during the transportation stage per	-	0.8334	1

Table 7 Input data for the shirt transportation stage

Table 8	Output	data f	for th	e shirt	transp	ortation	stage
---------	--------	--------	--------	---------	--------	----------	-------

Category	Subcategory	Per shirt	Per day	Per month	Unit
	Carbon dioxide (CO ₂)	-	557.7g	2230.8	g
	Nitrogen (N)	-	1	-	-
Emission to Air	Sulphur dioxide (SO ₂)	-	1	-	-
	Nitrogen oxide (NO _x)	-	1.0415	4.166	g

4.1.5 Input and output data for Disposal stage

The research assessed the waste generated in the disposal phase of the Batik Shirt from the data collected by the questionnaire from the monthly weighted quantity of shirts discarded measured in kilograms/month. The objective was to understand waste generation patterns and identify opportunities for waste reduction and proper disposal practices. Weight of Batik shirt waste pieces generated is 58g, Carbon content of the Batik shirt waste pieces is 45% To estimate the CO₂ emissions, where The emission factor for textiles material is commonly considered as 3.67 kilograms of CO₂ per kilogram of carbon burned. Therefore, it was found that CO₂ Emissions are 0.0764 kg/shirt. The nitrogen content in Batik cotton fabric is relatively low, and the emissions of nitrogen during combustion are generally minimal and considered negligible. Therefore, for the burning of Batik shirt waste pieces, we can assume negligible emissions of nitrogen (N). The sulfur content in cotton fabric is generally low, and the emissions of sulfur dioxide during combustion are also typically minimal. Therefore, for the burning of Batik shirt waste pieces, we can assume negligible emissions of sulfur dioxide (SO₂).

4.2 Results from the impact assessment done through OpenLCA software

The life cycle assessment of Batik shirts reveals significant environmental impacts across various categories. The top 5 impact categories were identified with OpenLCA software as Climate Change, Eutrophication Potential, Human Toxicity, Photochemical Oxidation, and Acidification Potential. These findings highlight the critical areas for environmental improvement in the Batik shirt life cycle, emphasizing the importance of addressing fabric and shirt production processes to reduce environmental footprints. Table 9 gives the category, a brief description of the category, and units of output.

Environmental Impact Categories				
Category	Description	Units		
Climate Change	Global warming potential of greenhouse gases released to the environment	kg CO ₂		
Water Consumption	Net freshwater taken from the environment minus water returned to thesame watershed at the same quality or better	liters		
Eutrophication	Oxygen depletion occurs because of nitrogen and phosphorus deposits into freshwater or marine environments	Kg NO _X		
Human Toxicity	Potential adverse effects on human health resulting from exposure to toxic substances throughout the life cycle of a product or process	Emission to the air urban air		
Acidification	Evaluates the potential harm to soil, vegetation, and terrestrial organisms caused by the deposition of acidifying substances from human activities.	$ m kg~SO_2$		

Table 9 Environmental impact categories

4.2.1 Contribution to climate change from the life cycle of the Batik shirt manufacturing.

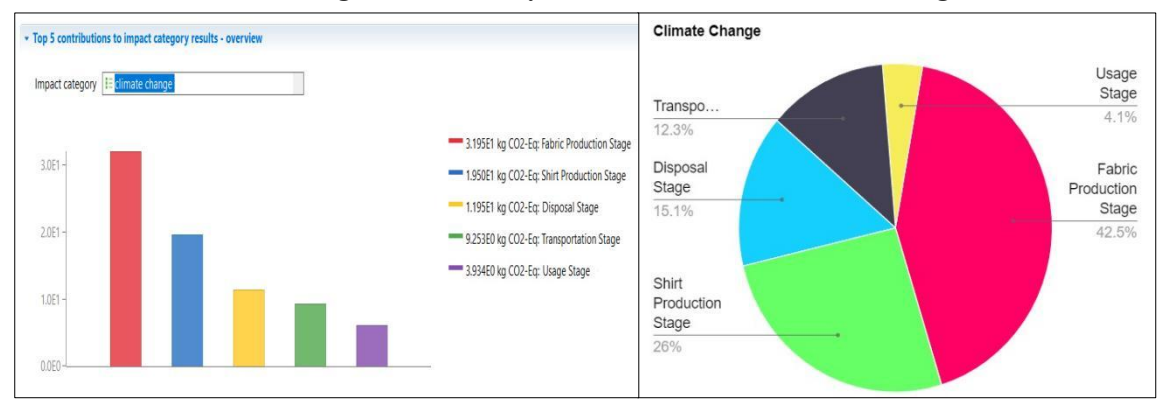


Fig. 2 OpenLCA results for Climate Change

Fabric production stands out with 31.95 kg CO₂ emissions, constituting 42.5% of the total, while it is least at the usage stage, with 3.93kg CO₂ emissions contributing to climate change by 4.1%. There is a significant impact on climate change at the shirt production stage with a contribution of 26%, 19.5kg of CO₂ emissions, as shown in Fig. 2. The least impact from usage is because the CO₂ emissions are the least from activities related to usage as impacts are from a few ironing and washing cycles. Fabric production and shirt production stage has more CO₂ emissions as they involve many sewing machines and heating while dying fabric.

4.2.2 Contribution to the Eutrophication Potential from the life cycle of the Batik shirt manufacturing

Eutrophication Potential data given in Fig. 3, the highest impact during the shirt production stage, with 15.12kg NOx emissions, representing 41.7%. The least impact is from the fabric production stage, which is 3.06kg NOx emissions, which is 8.3%. The shirt production stage has a higher use and release of chemicals than any other stage, which shows a high potential for harming water bodies. But looking into Fig. 3, it shows all stages are significantly contributing to the Eutrophication Potential.

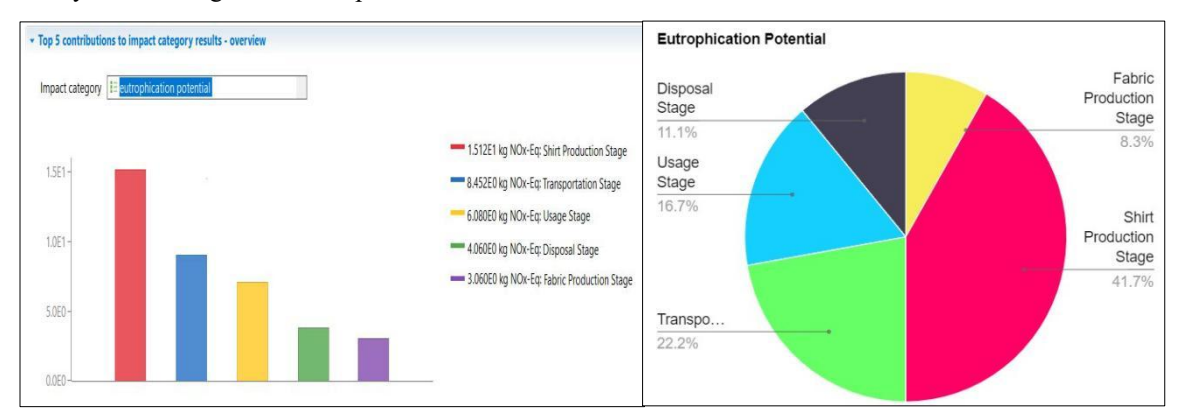


Fig. 3 OpenLCA results for Eutrophication Potential

4.2.3 Contribution to Human Toxicity from the life cycle of the Batik shirt manufacturing.

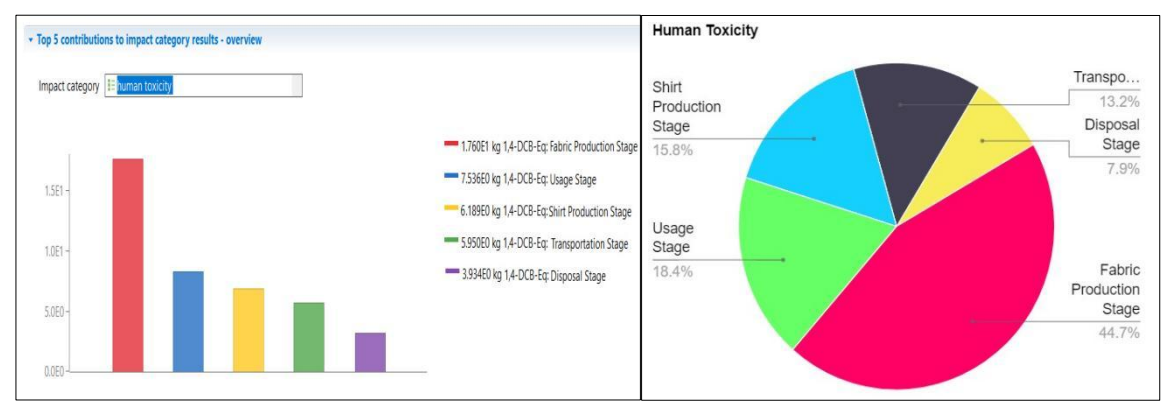


Fig. 4 OpenLCA results for Human Toxicity

Human Toxicity impact is primarily linked to fabric production, with 17.6 Kg 1,4 DCB emissions, making up 44.7% of the total is the highest as given in Fig. 4. Human toxicity is also considerable in each stage of manufacturing where the toxic substances resulting the total emissions from the total lifecycle are 41.13 kg 1,4 DCB emissions. This makes changes in the human living environment harmful, which may lead to health effects in humans in the environment.

4.2.4 Contribution to Photochemical Oxidation from the life cycle of the Batik shirt manufacturing

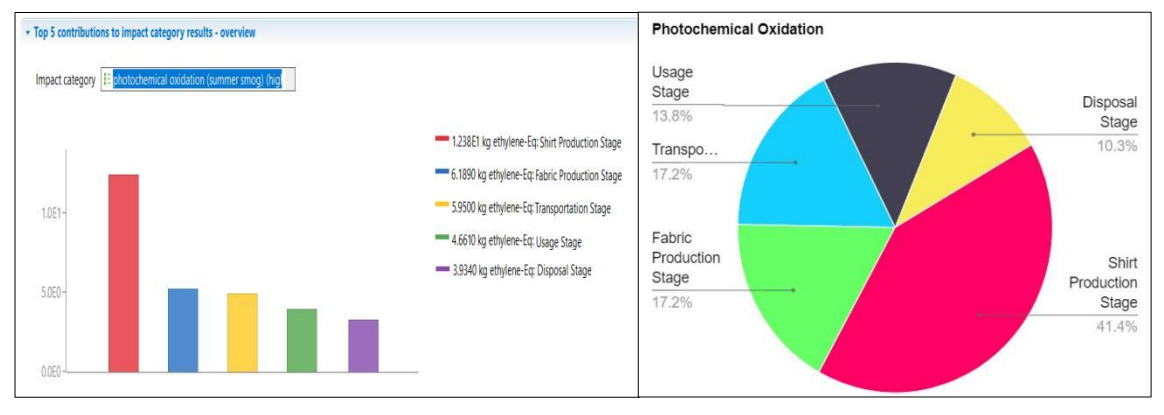


Fig. 5 OpenLCA results for Photochemical Oxidation

The Photochemical Oxidation impact is significant during shirt production, contributing 12.38 kg of ethylene emissions, or 41.4%. Photochemical Oxidation is in considerable amounts in each stage of Batik shirt manufacturing, where it is 17.2% in the fabric production stage, 17.2% in the transportation stage, 13.8% in the usage stage, and 10.3% at the disposal stage, as shown in Fig. 5.

4.2.5 Contribution to the Acidification Potential from the life cycle of the Batik shirt manufacturing

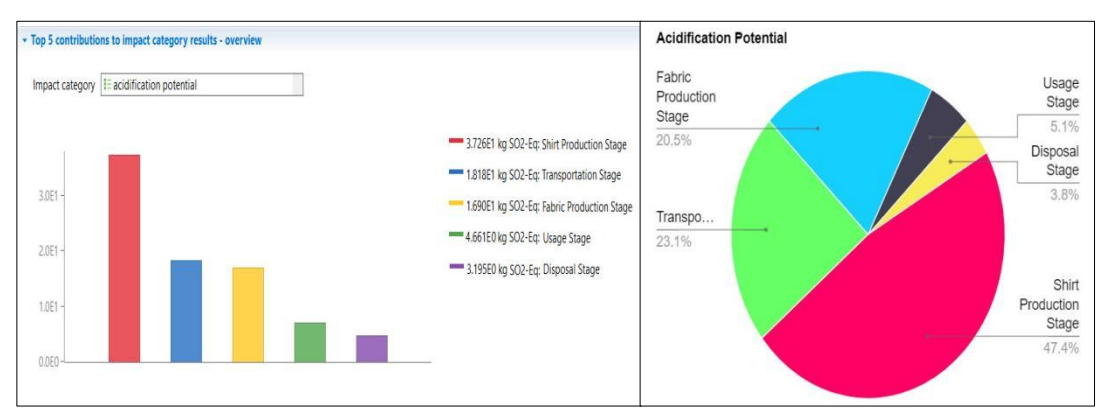


Fig. 6 OpenLCA results for Acidification Potential

Acidification potential, the shirt production stage dominates, contributing 37.26 kg SO2 emissions, or 47.4%. The transportation stage contributes 18.18k SO₂ emissions, or 23.1%. Fabric production stage contributes 16.9kg SO₂ emissions, or 20.5%. The usage stage and disposal stage have comparatively low impact with 4.66kg SO₂ emissions and 3.19kg SO₂ emissions respectively, as summarized in Fig. 6.

5 Conclusion

The identification of hotspots holds a very high importance with a focus on the manufacturing of Batik shirts, an iconic and culturally significant garment in Sri Lanka. Though the Batik manufacturing cater a niche market in the island and globally, the research found out there is a significant contribution to climate change with 76.58kg CO2 emissions in total, total eutrophication potential of 36.77kg NOx emissions, human toxicity total of 41.13kg 1,4 DCB emissions, total photochemical oxidation of 33.1kg ethylene emissions, and total acidification potential of 80.19kg SO2 emissions throughout the complete lifecycle of Batik shirt manufacturing. These mechanisms can vary across different environmental impact categories and different geographic specifications. Accordingly, they will have distinct implications for ecosystems, resources, and human factors. This study rigorously examines the lifecycle assessment (LCA) of Batik shirt production to identify these hotspots by dissecting primary contributors to environmental impact, analyzing elemental flows affecting these processes, and identifying key human activities responsible for these impacts. These hotspots provide a focus for potential improvements, offering a guide towards enhancing the sustainability profile of Batik shirt production in Sri Lanka.

These hotspots in the production process really ramp up the impact on the environment. They're the main reasons behind climate change, acidification, eutrophication, human toxicity, and photochemical oxidation. But if we focus on fixing these exact spots, we can seriously cut down on how much harm what manufacturing of Batik shirts does to the environment. The table below breaks down these critical spots and suggests smart ways to make them less damaging. It is possible to make the manufacturing of Batik shirts much more eco-friendly in the textile industry by working on these specific stages.

Environmental Impact Category	Hotspot Identified	Percentage Contribution	Recommendations
Climate Change	Fabric Production Stage	42.50%	Optimize manufacturing processes to lower energy consumption, use renewable energy sources for production, implement efficient transportation methods
Acidification Potential	Shirt Production Stage	47.40%	Reduce chemical usage in production processes, Implement eco-friendly

Table 11 Identified environmental impact hotspots

			manufacturing practices, Use of organic Cotton for shirt manufacturing.
Eutrophication Potential	Shirt Production Stage	41.70%	Implement better waste management practices, consider alternative dyeing methods to minimize water pollution
Human Toxicity	Fabric Production Stage	44.70%	Substitute toxic chemicals with safer alternatives
Photochemical Oxidation	Shirt Production Stage	41.40%	Implement air pollution control technologies, Use eco-friendly dyes and chemicals in the dyeing process

Future work

It is needed to explore sustainable practices, renewable energy sources, implement eco-friendly dyeing methods, optimize transportation, and invest in advanced wastewater treatment systems emerges as a roadmap towards a greener, more environmentally responsible manufacturing process of Batik manufacturing as this industry is also a part of textile industry which is one of the main industries in the country. The alternative methods can be compared in OpenLCA software to identify the difference in environmental impacts from the traditional method and the environmentally friendly, sustainable method, which can be used as a guide to future improvements. This study's findings emphasize the importance of informed decision-making and proactive measures to minimize environmental impact, where the pursuit of sustainable practices is not only an option but a necessity for preserving ecological balance, safeguarding human health, and fostering a more responsible industrial landscape. Ultimately, by implementing the suggested recommendations and embracing sustainable methodologies, the Batik shirt manufacturing sector in Sri Lanka can pave the way for a more environmentally conscious and sustainable future. The identification of exact economic methods and methods of providing environmentally sustainable solutions to the Batik industry is a possible future research area that can help this unique manufacturing technology.

Further financial feasibility and economic feasibility studies can be conducted to understand how society will be affected by the manufacturing process, which was not covered in this research due to the time limitation. Also, a sensitivity analysis will be valuable to address uncertainties and limitations inherent in this LCA study, such as assumptions, data quality, and methodological choices. In addition, conducting the same research from a collection of Batik manufacturers will improve the findings, and can also be expanded into many other clothing choices, such as dresses, sarees, decorations, etc., which use different amounts of resources.

References

- [1] Zhang, Y., Liu, X., Xiao, R. and Yuan, Z.: Life cycle assessment of cotton T-shirts in China. The International Journal of Life Cycle Assessment, 20(7), pp.994–1004, (2015).
- [2] Baydar, G., Ciliz, N. and Mammadov, A.: Life cycle assessment of cotton textile products in Turkey. Resources, Conservation and Recycling, 104, pp.213–223, (2015)
- [3] Moazzem, S., Crossin, E., Daver, F. and Wang, L.: Life Cycle Assessment of Apparel Consumption in Australia. Environmental and Climate Technologies, [online] 25(1), pp.71–111, (2021)
- [4] Ali A., Ara Z.A., Khan A. N., Rakib A. R.: Lifecycle Analysis (LCA) of a White Cotton T-shirt and Investigation of Sustainability Hot Spots: A Case Study, London Journal Press, vol. 18, pp 20-31, (2018)
- [5] Heavy metal concentration in the synthetic dyes used in Batik industry, Available at: https://www.researchgate.net/Fig./Heavy-metal-concentration-in-the-synthetic-dyes-used-in-Batik-industry-observed-in-the fig5 358479564. (Accessed: 25 July 2023).
- [6] How to calculate carbon dioxide equivalent emissions from different GHG sources?, Green Clean Guide. (Accessed: 25 July 2023).
- [7] Umar S. N. H. U., Akthar M. N., Bakar E. A., Kamaruddin N. M., Othman A. R.: Development of Heavy Metal Potentiostat for Batik Industry, MDPi journal of Applied Science, (2020)
- [8] Carbon Footprint Ltd using RADsite CMS (https://www.radsite.co.uk/) (no date) Household energy consumption. Available at: https://www.carbonfootprint.com/energyconsumption.html (Accessed: 25 July 2023).
- [9] Crenna, E. et al. (2019) Global Environmental Impacts: Data sources and methodological choices for calculating normalization factors for LCA the International Journal of Life Cycle Assessment, SpringerLink. Available at: https://link.springer.com/article/10.1007/s11367-019-01604-y (Accessed: 25 July 2023). [10] Hillege, L. (2023) Impact categories (LCA) Overview, Ecochain. Available at: https://ecochain.com/knowledge/impact-categories-lca/ (Accessed: 25 July 2023).

Evaluation of Traffic Flow Characteristics on Sri Lankan Expressways

K.V.D. Perera*, W.R.S.S. Dharmarathna

Department of Civil Engineering, University of Peradeniya, Kandy, Sri Lanka vperera1989@eng.pdn.ac.lk*

Abstract

Evaluating traffic flow characteristics, including speed, density, and volume, is essential for sustainable transport because it helps optimize traffic management and improve safety. Understanding these dynamics helps in designing infrastructure improvements and implementing policies that accommodate current and future traffic demands. In Sri Lanka, the usage of expressways is increasing day by day, and hence, accurate assessments of traffic flow are vital for enhancing road efficiency, minimizing travel times, and supporting sustainable transportation development. This study evaluates traffic flow characteristics on Sri Lankan expressways: Southern (E01), Outer Circular (E02), and Colombo - Katunayake (E03), by analyzing data collected from peak hour traffic surveys for different vehicle categories. The relationships between speed-density, volume, and speed-volume were modeled using the Greenshield model. Theoretical relationships derived from the model were compared with observed data and design data to assess the accuracy and applicability of the Greenshield model in the Sri Lankan context. Observed density values were found to be lower than predictions from the design. This research contributes to understanding traffic dynamics on expressways and informs sustainable transport planning by identifying discrepancies between design values and real-world observations.

Keywords: Greenshield Model, Peak Hour, Speed-Density, Volume-Density, Speed-Volume, Sustainable Transport

1 Introduction

Traffic flow characteristics are essential concepts in transportation engineering, describing the fundamental aspects of vehicular movement on roadways. Flow, speed, and density are the three characteristics of traffic and are used to describe various aspects of the operations of a highway facility. When describing and assessing traffic operations, normally concerned with the movement of a group of vehicles, or the traffic stream, rather than the movement of each vehicle [1]. In the planning, design, and establishment of various transportation system policies, the traffic flow theory of movement plays a very important role. To facilitate the application of traffic flow theory of movement, we used a mathematical approach which was used to analyze the phenomenon that took place in the traffic flow. One approach to comprehend the traffic behavior was by verifying it into mathematical and graphics relationships by observing to the relationship among speed, density, and volume [2].

There are two basic models of observing traffic behavior, namely, microscopic and macroscopic models. Microscopic models, such as car-following models, focus on individual vehicle behavior, while macroscopic models consider traffic flow characteristics such as speed, density, and volume. Density allows you to get an idea of how crowded a certain section of a road is and expressed in number of vehicles per kilometer. It totally ignores the effect of traffic composition and vehicle lengths, as it only considers the number of vehicles. Volume is expressed as several vehicles passing a specific point per hour [3].

Expressways are crucial to Sri Lanka's transport network, supporting the efficient movement of goods and passengers. With rising traffic volumes and diverse vehicle types on expressways such as E01, E02, and E03, accurate assessment of road capacity and traffic flow is essential for design and management. This study focuses on speed, density, and volume relationships, addressing gaps in understanding how unique vehicle types influence traffic flow. Normal weather and standard road conditions were assumed to simplify analysis, as their effects are minimal on well-maintained expressways. Geometric features like shoulder width are considered to have a limited impact based on prior research findings.

The Greenshield model (1934) assumes a linear speed-density relationship and a parabolic volume-density relation, offering a simple yet effective method for analyzing traffic flow, especially on expressways with minimal vehicle interactions than other models proposed by Greenberg (1959) and Underwood (1961) [4]. Its simplicity, ease of use, and reliance on limited data like free flow speed and maximum flow make it ideal for scenarios with stable traffic conditions or limited data availability. This study applies to the Greenshield model, assuming uninterrupted traffic flow and consistent weather and road conditions. In Sri Lanka, where the traffic flow characteristics of expressways remain unexplored, this research provides novel insights that will contribute significantly to the planning and design of future expressways in Sri Lanka.

1.1 Aim and Objectives

The aim of the study is to analyze and evaluate the traffic flow characteristics on selected expressways in Sri Lanka and hence contribute to future expressway designs. The objectives are to obtain the variations of traffic flow characteristics on selected expressways in Sri Lanka and to suggest plans for improving the infrastructure.

2 Methodology

Peak-hour traffic survey data were collected at specific locations along each expressway, focusing on areas where high traffic flow was anticipated. Three distinct locations were selected, one per expressway. For speed calculation, measurements, i.e., vehicle entry time and exit time for a particular road stretch, are necessary. However, due to non-functional CCTV cameras and the availability of interchanges, it was challenging to select the same locations used for collecting traffic survey data for speed calculation. The traffic flow can be influenced by factors such as school and work schedules, region type, public transportation, economic activities, land use patterns, driver behavior, and weather conditions. Therefore, the data were collected by selecting the dates and times, especially avoiding holidays. By considering the permission requirement for traveling on Sri Lankan expressways, the vehicles were classified into eight categories as follows.

- Passenger Car PC
- Passenger Car (Small) PCS
- Van
- Medium Bus MB
- Large Bus LB
- Light Goods Vehicle LGV
- Medium Goods Vehicle MGV
- Large/Heavy Goods Vehicle (3-axles, 4-axles, 5-axles, 6-axles) HGV

2.1 Design Free Flow Speed and Maximum Flow

To use Greenshield's model to calculate traffic density, it is required to find the free flow speed and maximum flow. For that, according to the design, the value 100 km/h was selected as the free flow speed, considering the assigned maximum speed limit for expressways in Sri Lanka. For the maximum flow, the value of 2000 passenger cars per hour per lane (pcphpl) was selected for three expressways [5].

2.2 Observed Free Flow Speed

To calculate observed traffic density, it is required to find observed speed and observed maximum flow. Data such as vehicle entry time, exit time, and fixed trap length were considered in each location for calculating free flow speed, as mentioned in Table 1. Vehicle entry time and exit time data were collected using CCTV camera recordings provided by the expressway operation, maintenance, and management divisions at Gelanigama (for E01 and E02) and Seeduwa (for E03). For this study, 1-way, 2-lane sections were considered. The data collection locations for calculating speed were selected based on the availability of CCTV cameras on the expressways, and locations are shown in Fig. 1. The fixed length was identified based on the locations of cameras (six locations). Vehicle travel time was noted at the entry and exit points of the trap length from the recorded video. The speed was then calculated by dividing the fixed trap length by the difference between exit and entry times.

Table 1 Locations and fixed trap lengths

Expressway	CCTV locations	Fixed trap length (km)
E01	Dodangoda and Gelanigama	24.6
E02	Athurugiriya and Kadawatha	16.2
E03	Ja-ela and Peliyagoda	17.3

Data collected locations are shown on Fig.1.



Fig. 1 Data Collected Locations

The percentage of vehicles with respect to the total number of vehicles observed is presented in Fig. 2.

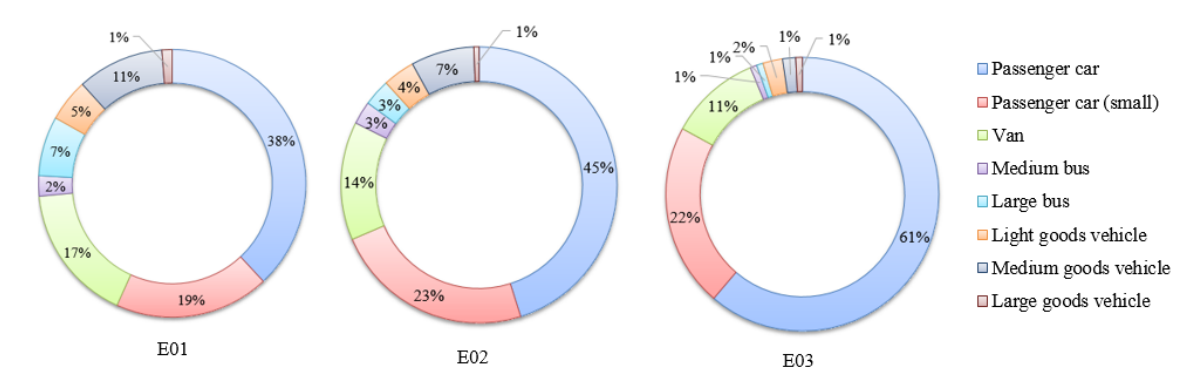


Fig. 2 Percentage of Vehicles

The speed distribution of three expressways is presented in Fig. 3. The median speeds of expressways lie in between 95-120 km/h. The Interquartile Range (IQR) for E01 expressway is relatively narrow, indicating less variability in speeds. The IQR of E02 and E03 expressways is wide, indicating more variability in speeds. The broad range of speeds in E03 suggests diverse driving conditions, due to less traffic enforcement.

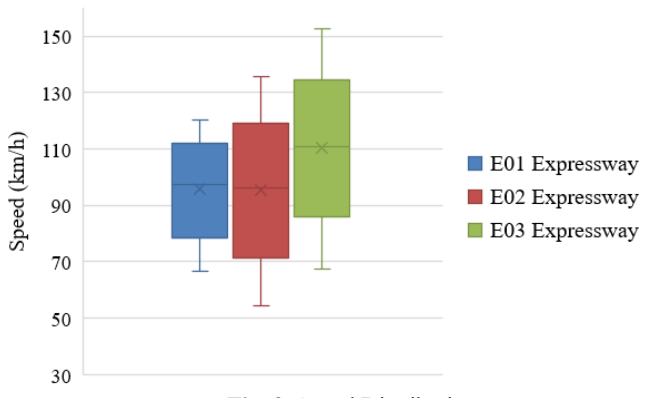


Fig. 3 Speed Distribution

2.3 Observed Maximum Flow

To obtain the maximum flow, peak hour traffic volumes were collected on E01 (at Kottawa), E02 (at Kadawatha), and E03 (at Peliyagoda) expressways, considering morning and evening peak hours for five consecutive weekdays.

3 Calculation

Calculation of average speed and peak hour traffic volumes of selected expressways is described in sections 3.1 and 3.2 to match the Greenshield model.

Calculation of Average Speed

Average speed values for each vehicle category for the selected three expressways are tabulated as mentioned in Table 2. Then, the average of all the categories of vehicles was considered to calculate densities.

Vahiala aatagami	Average speed (km/h)			
Vehicle category	E01	E02	E03	
PC	99.9	97.3	114.2	
PCS	96.3	95.2	106.0	
Van	92.5	96.0	104.5	
MB	96.8	95.3	97.7	
LB	103.0	99.9	84.0	
LGV	90.9	81.1	100.7	
MGV	88.9	80.7	85.4	
HGV	80.2	86.9	92.8	
Average	93.6	91.6	98.2	

Table 2 Average speeds of expressways

Average speeds for the selected three expressways are graphically presented as follows.

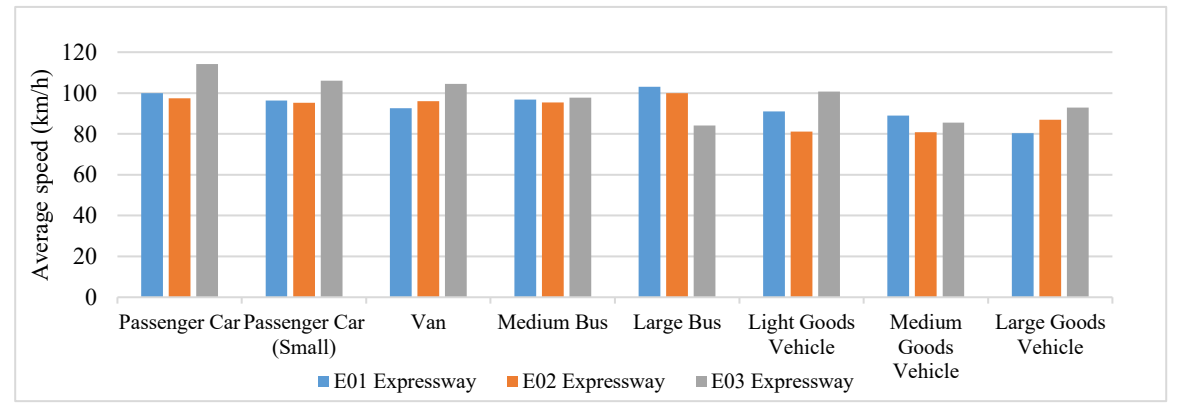


Fig. 4. Average Speeds

Fig. 4 shows that, for most vehicle categories, the average speed remains fairly consistent across the E01 and E02 expressways, with only slight variations. Passenger cars and passenger cars—small categories exhibit the highest average speeds. Large goods vehicles and medium goods vehicles show fewer average speeds compared to passenger cars and vans, which is expected due to their larger size and potentially heavier loads. The E03 expressway generally shows the highest average speeds across most vehicle categories. This indicates lower traffic conditions. The variation in average speed between different vehicle categories is relatively small, suggesting that the expressways are designed to facilitate uniform traffic flow.

3.1 Calculation of Peak Hour Traffic Volume

Peak hour traffic volumes on each expressway were obtained considering morning and evening peaks for five consecutive weekdays using video recordings provided by expressway management divisions. Peak hours were identified separately for morning and evening after obtaining a minute traffic count on each location to identify the peak hour. Likewise, peak hour volumes were obtained for five weekdays and the average. These volumes were converted using Passenger Car Unit (PCU) values mentioned in a previous study for the E02 expressway and

a two-lane road [6]-[7]. It is assumed that the vehicle types and proportions on E02 and a two-lane road are representative of those on E01 and E03, ensuring compatibility of PCU values across these routes. Driver behavior, including acceleration, deceleration, and lane usage, is presumed consistent across all expressways in Sri Lanka, owing to uniform traffic regulations and similar road-user characteristics. Additionally, E01, E02, and E03 share comparable geometric standards, such as lane widths, gradients, and curvature, making the previously derived PCU values applicable under these conditions. Uninterrupted flow conditions of all three expressways, characterized by controlled access and minimal external interference, further justify the use of values derived for E02 expressway for E01 and E03 expressways. The absence of expressway-specific PCU values for E01 and E03 makes the use of values from E02 and two-lane roads a practical alternative for traffic volume estimation. The used PCU values for different vehicle categories are mentioned in Table 3.

Vehicle category	PCU value	Average traffic volume (pcph) – E01	Average traffic volume (pcph) – E02	Average traffic volume (pcph) – E03
PC	1.00	402.60	370.80	1029.60
PCS	0.75	166.05	175.65	426.45
Van	1.11	95.46	89.02	163.17
MB	1.87	55.35	36.28	95.00
LB	3.57	77.11	52.12	89.25
LGV	1.04	43.47	34.53	29.74
MGV	1.90	55.10	60.80	38.38
HGV	3.33	16.65	13.99	13.32
Total		911.80	833.19	1884.91

Table 3 Average traffic flow volumes as pcph

3.2 Calculation of Density, Speed, and Volume

Based on the method proposed by Greenshield, the density of vehicles can be calculated as follows.

$$q = kv \tag{1}$$
 Where,
$$q = \text{Flow}$$

$$k = \text{Density}$$

$$v = \text{Speed}$$

$$k_{max} = \frac{q_{max}}{v_{max}} = 40pc/km$$

Based on the field data, the observed density was calculated using equation 1 and tabulated as follows. It can be seen that the observed density values are far beyond the design density value, indicating expressways have excess capacity. Lower density reduces wear and tear on road infrastructure, thereby decreasing the frequency of maintenance. E03 expressway shows a relatively higher density, indicating the need for careful monitoring. The actual density being lower provides scope for accommodating higher traffic in the future. Hence, authorities can attract more vehicles through strategies such as toll adjustments, incentives for commercial transport, or connecting expressways to other networks. Lower densities lead to environmental benefits such as reduced emissions, fuel consumption, and pollution, aligning with sustainability goals.

Observed flow Observed average **Observed density** Expressway speed (km/h) (pcph) (pc/km) E01 93.6 911.80 9.74 E02 91.6 833.19 9.10 E03 98.2 1884.91 19.19

Table 4 Observed density

To obtain the relationship of speed, density and volume, Greenshield's method was applied (equation 2) as presented below.

$$v = v_f - (\frac{v_f}{k_i})k \tag{2}$$

Where,

v = Mean speed at density k

vf = Free flow speed

kj = Jam density

Considering equations 1 and 2, the following expressions can be derived [4].

At maximum flow,

$$k = \frac{k_j}{2} \tag{3}$$

The maximum flow is.

$$q_{max} = \frac{v_f k_j}{4} \tag{4}$$

The speed at maximum flow is.

$$v = \frac{v_f}{2} \tag{5}$$

After finding free flow speed, maximum flow, and jam density, the relationship of speed-density, volume-density, and speed-volume was obtained. A sample calculation of speed, density, and volume related to the theory and E01 expressway is presented below.

Density, speed, and volume calculations for the design are presented below.

Since the free flow speed is 100 km/h and the maximum flow is 4000 pcph;

Design jam density is (equation 4).

$$k_i = 160 \, pc/km$$

If density is 10 pc/km, speed is (equation 2);

$$v = 100 - \left(\frac{100}{160}\right) x 10 = 93.75 \, km/hr$$

Then, volume is (equation 1).

$$q = 10 \times 93.75 = 937.50 pcph$$

Density, speed, and volume calculations for the E01 expressway are presented below.

The free flow speed of the E01 expressway is 93.6 km/h, and the maximum flow is 911.80 pcph.

Jam density is.

$$k_i = 38.97 \ pc/km$$

If density is 10 pc/km, speed is (referring to the Table 5);

$$v = 93.6 - \left(\frac{93.6}{38.97}\right) x 10 = 69.58 \, km/hr$$

Then, volume is.

$$q = 10 x 69.58 = 695.82 pcph$$

Density (pc/km)	Speed (km/h)	Volume (pcph)
0	100.0	0.00
10	93.75	937.50
20	87.50	1750.00
40	75.00	3000.00
60	62.50	3750.00
80	50.00	4000.00
100	37.50	3750.00
120	25.00	3000.00
140	12.50	1750.00
160	0.00	0.00

Table 5 Density, speed, and volume as per the design

Design values calculated for speed, density, and volume are tabulated in Table 5. Observed values calculated for speed, density, and volume on the E01 expressway are tabulated in Table 6.

Table 6 Density, speed, and volume as per the design

Density (pc/km)	Speed (km/h)	Volume (pcph)
0	91.60	0.00
5	79.01	395.05
10	66.42	664.21
15	53.83	807.48
18.19	45.80	833.10
20	41.24	824.85
25	28.65	716.33
30	16.06	481.92
35	3.47	121.61
36.38	0.00	0.00

Observed values calculated for speed, density and volume on E02 expressway is tabulated in Table 7.

Table 7 Density, speed, and volume values - E03 expressway

Density (pc/km)	Speed (km/h)	Volume (pcph)
0	100.0	0.00
10	93.75	937.50
20	87.50	1750.00
40	75.00	3000.00
60	62.50	3750.00
80	50.00	4000.00
100	37.50	3750.00
120	25.00	3000.00
140	12.50	1750.00
160	0.00	0.00

Observed values calculated for speed, density, and volume on the E03 expressway are tabulated in Table 8.

Table 8 Density, speed, and volume values - E03 expre
--

Density (pc/km)	Speed (km/h)	Volume (pcph)
0	98.20	0.00
10	85.41	854.10
20	72.62	1452.41
30	59.83	1794.92
38.39	49.10	1884.95
40	47.04	1881.63
50	34.25	1712.55
60	21.46	1287.68
70	8.67	607.00
76.78	0.00	0.00

Graphical relationship of speed and density according to Greenshield model is presented in Fig. 5.

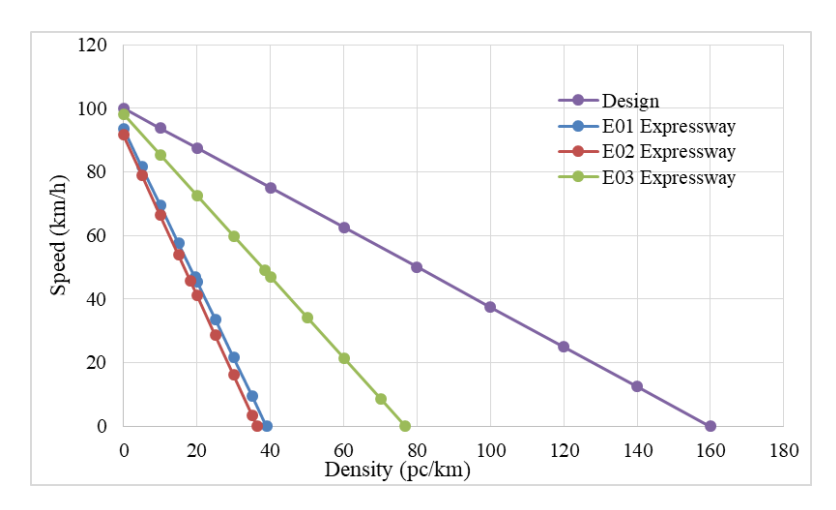


Fig. 5 Speed-Density Relationship

Lines in Fig. 5 represent the relationship where the speed decreases linearly as density increases. E01 and E02 expressways show similar speed-density behavior with a steep decline in speed as density approaches 40 pc/km. Observed maximum speed for these expressways is around 90 km/h, slightly lower than the design free flow speed of 100 km/h. E03 expressway displays a more gradual reduction in speed as density increases, with speeds decreasing at a slower rate compared to the E01 and E02 expressways. All expressways show lower maximum densities compared to design density, indicating that current traffic conditions on these expressways are far from their design capacity.

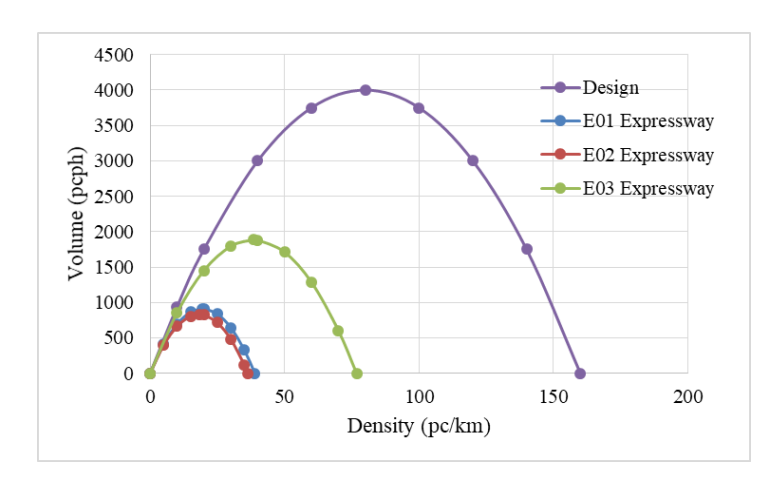


Fig. 6 Volume-Density Relationship

Fig. 6 shows the relationship of volume and density. Parabolic shapes of the curves indicate that volume increases as density increases reaching a maximum point, after which the volume decreases as density increases. Both E01 and E02 expressways show similar behavior with volume peaking around 950 pcph and at a density around 30-40 pc/km which is considerably lower than the design maximum. E03 expressway exhibits slightly higher peak volume than E01 and E02 expressways. All three expressways operate at volumes far below the design capacity of 4000 pcph.

Fig. 7 shows the relationship of speed and volume with wide curves. In low traffic volumes, speeds remain close to free flow conditions. As volume increases, speeds gradually decrease reaching a minimum at a certain volume (maximum flow) after which the curve sharply tapers. The design curve reflects a theoretical model, reaching maximum volume (4000 pcph) at a speed close to 50 km/h. It has a broad range of speeds across different volumes, with speeds up to 100 km/h for lower volumes, gradually decreasing as volume increases. E01 and E02 expressways exhibit a similar pattern, with speed dropping rapidly after volumes reach around 800-900 pcph. E03 expressway shows a broader curve compared to E01 and E02 expressways. Maximum volumes recorded for these expressways are below the design maximum volume, indicating a large gap with the design capacity.

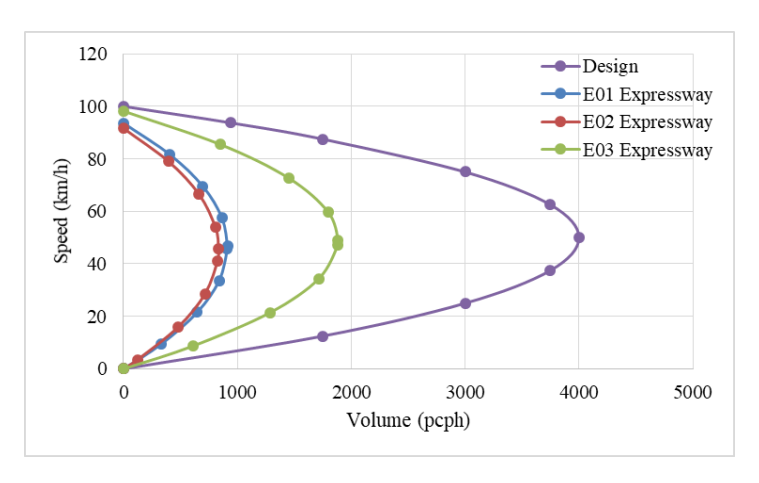


Fig. 7. Speed-Volume Relationship

All the curves and lines indicated in the above three figures suggest that the relationships of speed-density, volume-density, and speed-volume are closely matched with the Greenshield model. Hence, it can be applied to expressway designs in Sri Lanka.

3.3 Comparison of Traffic Volumes with Predicted Values

It is observed that the current traffic volumes of expressways are far below the design traffic volume. Therefore, it is required to calculate future traffic volumes to compare with the design volume. For that, predicted vehicle

growth rates are required. Predicted vehicle growth rates as percentages are presented in Table 9. These values were extracted from a study done for the E01 expressway at Kottawa interchange [8].

Vehicle category	2025	2030	2035	2040	2045	2050	2055	2060	2065	2070	2075	2080
PC	3.6	4.1	3.95	3.8	3.7	3.6	3.5	3.45	3.4	3.3	3.25	3.2
PCS	3.6	4.1	3.95	3.8	3.7	3.6	3.5	3.45	3.4	3.3	3.25	3.2
Van	2.1	2.21	2.19	2.12	2.11	2.1	2.0	2.04	2.01	2	1.99	1.95
МВ	2.1	2.21	2.19	2.12	2.11	2.1	2.0	2.04	2.01	2	1.99	1.95
LB	2.1	2.21	2.19	2.12	2.11	2.1	2.0	2.04	2.01	2	1.99	1.95
LGV	3.6	4.1	3.95	3.8	3.7	3.6	3.5	3.45	3.4	3.3	3.25	3.2
MGV	3.6	4.1	3.95	3.8	3.7	3.6	3.5	3.45	3.4	3.3	3.25	3.2
HGV	2.1	2.05	1.93	1.8	1.7	1.6	1.5	2.06	1.32	1.22	1.15	1.11

Table 9 Predicted vehicle growth rates

The vehicle growth rates for the E02 and E03 expressways were assumed to match those of the E01 expressway due to similarities in design standards, operational conditions, and regional factors affecting all three expressways. In the absence of specific growth rate data for E02 and E03 expressways, using E01 expressway growth rates serves as a practical approximation, reflecting trends from a comparable segment of the expressway network. Nonetheless, this assumption is recognized as a limitation, highlighting the need for future studies to gather specific vehicle growth rate data for E02 and E03 to enhance accuracy and reliability. The following equation is used to calculate future traffic volume. A sample calculation for the E02 expressway is presented below.

$$(Peak hour traffic volume)_{future} = (Peak hour volume)_{present} x (1+g)^n$$
 (6)

Where,

g = Annual growth rate

n =Number of years

Using equation 6,

Peak hour traffic volume at 2030 for passenger car category = $370.8 \times (1+0.041)^6 = 471.89 \text{ pcph}$

Likewise, future traffic volumes were calculated for all vehicle categories mentioned in Table 2, and the total traffic volume for all three expressways is tabulated in Table 10. A graphical representation of the traffic volume forecast is shown in Fig. 8.

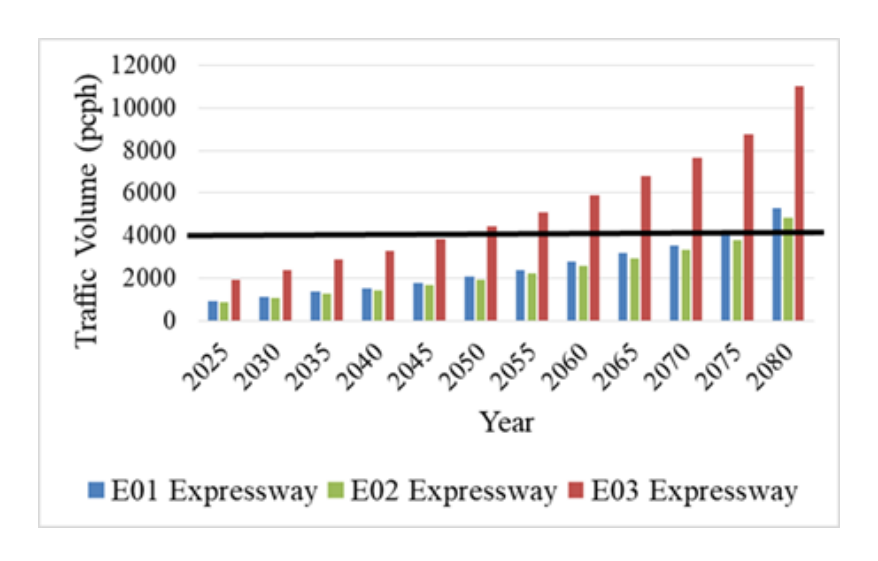


Fig. 8 Traffic Volume Forecast

<u></u>	1	1	ı	ı	1	1		ı	ı	ı	ı	1
Expressway	2025	2030	2035	2040	2045	2050	2055	2060	2065	2070	2075	2080
E01 expressway	940.95	1159.96	1396.25	1552.77	1808.03	2089.89	2385.81	2768.62	3171.81	3566.70	4061.72	5320.57
E02 expressway	860.31	1061.87	1275.89	1432.38	1671.38	1935.38	2214.39	2572.34	2952.86	3323.21	3789.01	4861.91
E03 expressway	1947.36	2376.60	2886.42	3271.87	3826.40	4439.35	5090.78	5914.63	6811.51	7673.70	8760.93	109999.0

Table 10 Future traffic volumes as pcph

Traffic forecasts for expressways show a significant increase in volume over time. By 2080, the traffic on E01 is expected to surpass 5320 pcph, E02 around 4862 pcph, and E03 close to 11,000 pcph. Traffic is predicted to exceed the design capacity after 2070 in E01, 2075 in E02, and 2045 in E03 expressways. The E01 and E02 expressways exhibit comparable traffic volumes, although the E02 expressway experiences slightly lower volumes in certain years. In contrast, the E03 expressway records the highest traffic volume. This trend underscores the importance of strategic capacity planning, particularly for the E03 expressway, to manage the growing demand effectively.

4 Conclusion

Traffic studies pose significant challenges due to the varied behavior of different vehicle types, influenced by factors such as speed, acceleration, road space utilization, and maneuvering abilities. To obtain the relationships of traffic flow characteristics, the Greenshield model was applied, assuming the linear relationship of speed and density, uninterrupted flow conditions, and consistent weather and road conditions. It was noted that the observed results were matched by the model, suggesting that the model can serve as a baseline for analyzing overall traffic behavior. Although the Greenshield model assumes homogeneous traffic, it was applied in this study to analyze heterogeneous traffic by converting vehicle flows into standardized passenger car units. This approach enables the model to approximate mixed traffic conditions while maintaining its theoretical simplicity. While recognizing its limitations, the model provided valuable insights into speed-density, volume-density, and speed-density relationships, on E01, E02, and E03 expressways, which are critical for identifying traffic management and infrastructure needs in Sri Lanka.

To obtain the maximum flow, peak hour traffic volumes were calculated in each expressway. Average peak hour traffic volumes obtained were 911.80, 833.19, and 1884.91 pcph for E01, E02, and E03 expressways, respectively. These values are less than the design volume of 4000 pcph. Observed density values of each expressway are also less than the design value of 40 pc/km. Design a free flow speed of 100 km/hr, and free flow speed values calculated for expressways are similar. It was observed that the relationships are highly matched with the Greenshield model, but actual values fall significantly below the design values. When considering the future traffic volumes, after 2070, 2075, and 2050, the design value of 4000 pcph is expected to surpass that for E01, E02, and E03 expressways, respectively.

Calculated traffic flow characteristics for above mentioned three expressways are beneficial for future expressway designs in Sri Lanka. There are ongoing expressway projects such as E04 (Kadawatha to Dambulla), E08 (Athurugiriya - New Kelani Bridge), and E09 (Port access elevated highway project). Outcomes of this study offer valuable insights for implementing proactive congestion management strategies on expressways such as E04, E08, and E09. These include the adoption of intelligent traffic systems (ITS), toll optimization, and efficient traffic control measures, such as lane management and diversions during peak hours. By analyzing the relationships of speed, density, and volume, planners can predict traffic behavior on the new expressways, aiding in efficient traffic management. The insights can guide policymakers in setting appropriate speed limits, developing of bypass routes, toll structures, lane expansion, maintenance, and access controls on expressways. Understanding current traffic patterns can inform environmental impact assessments, helping to design projects that minimize emissions and

environmental degradation. Currently, the effect of environmental pollution is less due to lower traffic volumes. In the future, promoting sustainable transportation is essential to reduce environmental pollution by implementing strict vehicle emission regulations, encouraging electric vehicle adoption, and developing green corridors along the expressways. In addition, it is necessary to address future traffic growth to reduce longer travel times and higher transportation costs. For that, it is recommended to implement long-term investments, such as constructing new expressways, upgrading existing expressways, and integrating public transportation systems to reduce pressure on road infrastructure. Further research on traffic flow analysis considering real-time data or technological advancement in traffic management systems on Sri Lankan expressways, incorporating larger survey lengths, would provide a solid base for future expressway designs.

Acknowledgement

The authors wish to acknowledge the assistance given by the expressway operation, maintenance, and management divisions at Gelanigama and Seeduwa attached to RDA for providing the required data to complete this study successfully.

References

- [1] Elefteriadou, L. (2003). Flow, Speed and density and their relationships. In *An introduction to traffic flow theory*. doi: 10.1007/978-3-031-54030-1 3
- [2] Sholahudin, F., & Rochim, A. (2019). The comparison of road capacity of Greenshield model, Greenberg model and Underwood model toward MKJI 1997 calculation on the Jendral Sudirman road, Batang. *ResearchGate*. doi:10.30659/pondasi.v24i1.4995
- [3] Maerivoet, S., & De Moor, B. (2008). Traffic flow theory. https://arxiv.org/pdf/physics/0507126
- [4] Mathew, T. (2023). Traffic stream models. Indian *Institute of Technology Bombay, India:* https://www.civil.iitb.ac.in/~vmtom/nptel/513 TrStream/web/web.html#x1-80004.1
- [5] Road Development Authority (RDA). (1998). Geometric design standards of roads.
- [6] Dhananjaya, D.D., Fernando, W.M., De Silva, M.M. and Sivakumar, T. (2023). Passenger car units for different midblock sections in Sri Lanka under mixed traffic conditions. *Journal of Applied Engineering Science*. 21(2), 375-383. https://scindeks-clanci.ceon.rs/data/pdf/1451-4117/2023/1451-41172302375D.pdf
- [7] Kumaratunga, P. (2018). Evaluation of PCU factors for two lane sub-urban roads. *MSc. thesis*. University of Moratuwa. http://dl.lib.uom.lk
- [8] Kumari, M.L.G.D., Priyadarshana, P.G.D. and Weeerasekara, K.S. (2015). Future impact of current toll gates on the capacity of the southern expressway. *OUSL Journal*. 9, 19-40. https://www.civil.iitb.ac.in/~vmtom/nptel/513 TrStream/web/web.html#x1-80004.1

Energy Management by Optimizing Operations and Resource Recovery in the Water Supply Sector

B.G.A. Dinesh, P.G.P.I. Dharmadasa, M.B. Mahanama

National Water Supply and Drainage Board, Sri Lanka bgadinesh@gmail.com, pgpid86@gmail.com

Abstract

The circular economy (CE) approaches minimizing environmental impact from all angles, focusing on resource efficiency and restorative solutions. The water sector will benefit from a CE, so we ought to seize the opportunity to establish closed loops for the recovery of resources like water, electricity, and materials. By increasing the energy efficiency of the pumps, it will deliver a significant reduction to the electricity consumption in the pumping station overall. Thus, load shading and the load shifting potential can be identified in the pumping station. The water sector, as a main carrier of materials and energy, should be shaped by the CE. In order to implement the formation of a CE, individuals and organizations move beyond their conventional prevention. This paper presents the outcomes of implementing CE concepts in the water supply sector in Sri Lanka by Technological Innovations in Water and Sanitation. The linear water sector infrastructure was shifted for the CE concept by integrating two drinking water systems at Pelenwatta and Makumbura pumping areas. The two pipe laying systems were reviewed, and the interconnection was done in the pipe laying systems. At the Makumbura Pump House (MPH), energy audits were completed, and data on energy consumption were gathered. Pumping capacity at Pelenwatta Pump House (PPH) wasn't increased significantly to cater to the requirement generated by the interconnection of additional area from MPH. A pump was de-energized at MPH according to the reduction performed by the strategic innovation. Financial gain and the environmental impact were evaluated to identify the CE impact by a strategic innovative plan using resource recovery. This was achieved by balancing the old tower, which was not utilized for about 10 years, with a cost renovation and utilizing as a balancing tank. The findings demonstrated that the financial gains outweighed the small cost of innovation, with a total of 298,602 kWh saved in energy in 2023–2024. An annual reduction in carbon dioxide of 212,008kg is projected.

Keywords: Energy Management, Sri Lanka Nationally Determined Contribution (SLNDC), Circular Economy, Demand Side Management (DSM), Optimize Operations

1 Introduction

Sri Lanka has implemented financial incentives, policy tools, and a number of proactive measures over the last five years to create a low-carbon pathway. Sri Lanka is putting a lot of effort into meeting the national policy targets for the power industry, which include generating 70% of the nation's electricity from renewable sources by 2030[1]. As of September 2022, the national power grid has a total installed capacity of 5,024 MW, comprising 42% derived from fossil fuels and 58% from renewable energy sources [2]. The majority of projects aim to increase the amount of renewable energy that is used in a business-as-usual environment and comply with the target of NDCs activity 1[1]. The goal of this project is to use Demand Side Management (DSM) strategies through the adoption of system enhancements in compliance with the NDCs activity 2[1].

The NWSDB's Makubura pumping station has three 55kW three pumps supplying approximately 7500 m3/day of clean drinking water to approximately 12600 homes and businesses. The facility is fed with a 400kVA bulk supply by the Ceylon Electricity Board (CEB) and includes a 305kVA standby generator alongside three 12.5kVAr capacitor banks which are deployed at the control panel. The pumping system was initially designed to operate with two pumps on duty and one on standby. However, driven by an increase in demand, the operating regime was adapted to use all three pumps on duty with a bypass valve at the water tank used to connect the incoming and distribution lines of the water tank.

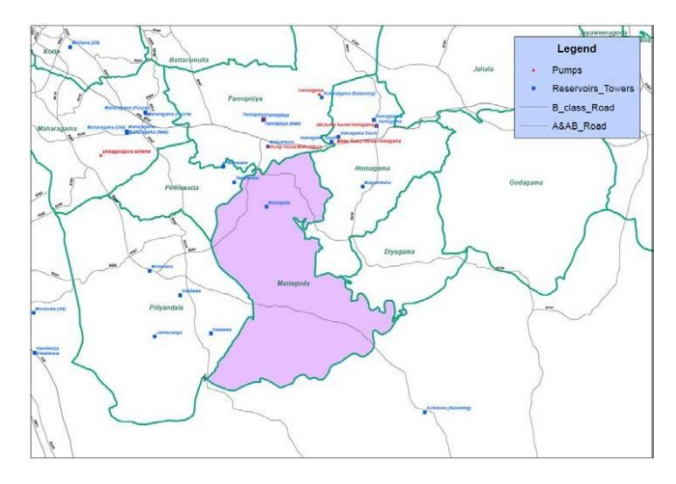


Fig. 1 Indicative Region Supplied by the Makubura Pump House

1.1 Problem Statement

A vital part of industrial and water distribution systems, the pump house usually uses a lot of energy because the pumps must run constantly to keep the community's water supply steady. Thus, peak energy demand in water distribution systems significantly increases operational costs due to higher tariffs and energy inefficiency. The abandonment of old water tanks, due to infrastructure upgrades, often leads to underutilized resources. Leveraging these tanks as supplemental reservoirs offers a potential solution to manage peak load and improve the energy efficiency of the pump operation. Inefficient operating patterns are due to excessive energy use, high operating expenses, and elevated carbon emissions in many urgent pump houses.

In order to improve the energy efficiency of pump house operations, it is necessary to integrate high-efficiency pumps, optimize operational patterns. By examining and putting into practice solutions that would lower total energy consumption, minimize environmental effects, and cut costs while preserving dependable performance and sufficient system capacity, this case study seeks to address the inefficiencies and resource reuse. Makumbura Pump House (MPH) was chosen for this study because it is one of the most important energy users in the NWSDB. The following actions will be taken at MPH to accomplish the goal.

1.2 Objectives

Assess the feasibility of re-integrating abandoned water tanks into existing systems.

Reduce energy waste during periods of low demand by modifying pump operation schedules to correspond with peak demand.

Setting up new energy-efficient Pumps to cut down on overall energy consumption, replacing old pumps with high-efficiency ones that provide the required capacity at reduced energy inputs.

Quantify the reduction in energy consumption and cost.

2. Methodology

2.1 System Overview

Current Setup: The Existing tank is connected to a pumping system serving a specific population.

Proposed Setup: Integrating an abandoned water tank as an auxiliary reservoir to store water during off-peak hours and distribute it during peak demand. By implementing this reduces the three-pump operation is reduced to the two-pump operation and energy consumption at peak time.

2.2 Data Collection

- Historical Water Demand Data
- Energy Consumption and Tariff Rates
- Pumping system performance metrics
- Energy Audit at the pump house and literature review of existing pumping system

2.3 Constrains

The tank capacity and operation limit can be identified as constraints to the project. This constraint ensures that the water level in the tanks (both abandoned and existing) stays within their physical and operational capacity during operation. The tank cannot store more than its total volume, and tanks must retain a certain minimum amount of water to maintain pressure or meet emergency requirements. The continuous water supply requirement is another constraint on the project. The system must operate such that the combined output from the active tanks always meets the real-time demand. However, flow rate management, coordination between tanks, and pump scheduling ensure the proper outcome of the energy-saving method. Through operation patterns, the Project Team identified that at present, all three pumps are operated to cater to the required demand, and the pumping station had an above-average consumption of electricity relative to other pumping stations of similar size and operational regimes. In addition to the implied waste of energy resulting from the leakages of the system, the current operational regime without a standby facility could result in a large portion of the customer base losing access to clean drinking water for extended periods of time.

Against this backdrop, the Project Team conducted an energy audit on June 16, 2022, and identified that the pumping station consumed approximately 100 MWhr for one month. Further, the team identified that an overwhelming majority of electricity consumption (~99%) could be attributed directly to the pumps, with lighting and dewatering consuming the remainder. Hence, an increase in the energy efficiency of the pumps will deliver a significant reduction in the electricity consumption in the pumping station overall.

The methodology used to calculate the energy consumption of the pumps was to first determine the existing system curve, followed by the pump curves with one, two, or all three pumps in operation. The results of this analysis are summarized in Fig. 2.

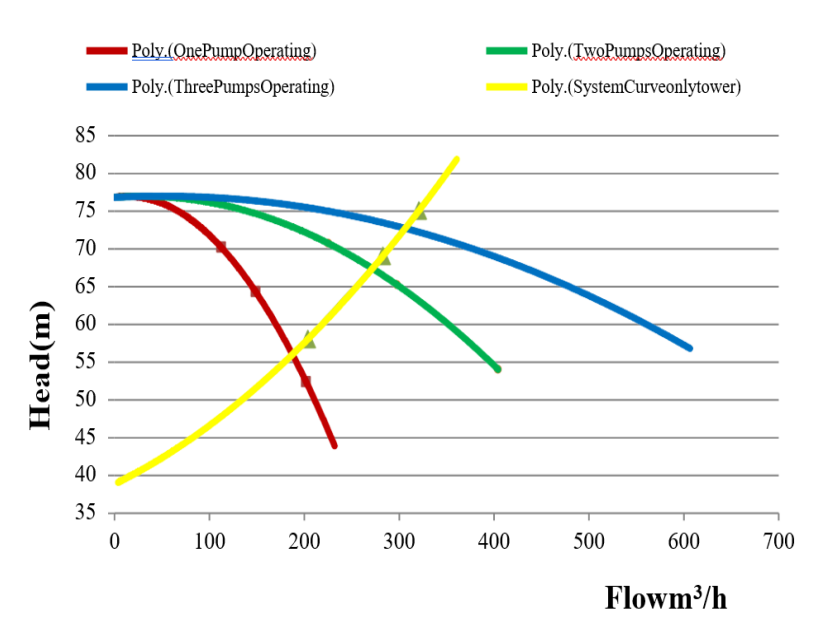


Fig. 2 System Curve and Pump Curves of Makubura Pump House

Table 1 summarizes the calculated efficiency and Specific Energy Consumption (SEC) for the existing pumping system.

Caamania	Flow	Demand	Efficiency	SEC
Scenario	(m3/h)	kVA	(%)	kW/m3
One Pump	202.24	69.5	44.05	0.32

45.92

43.34

0.39

0.45

126.6

164.6

Two

Pump Three

Pump

298

338.38

Table 1 Efficiency and SEC of the Existing Pumping System

Flow Demand Efficiency SEC

3. Analysis of 2021 to 2023 Operations

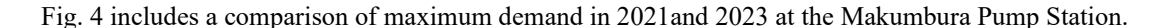
As per the data, in 2018 and 2019, two pumps were running continually, and the third pump was operated at peak time. But with the requirements, in 2020, the third pump was operated beyond peak hours. After 2020, the third pump was also operated continuously to feed the system. A strategic plan for energy savings was implemented in June 2023. Therefore, in this report, 2021 data were compared with 2023 (last 6months) data to identify the savings at the Makumbura pump station.

In the above energy audit, it was identified that SEC was considerably higher when three pumps were running. But production only increases in small amounts. Overall SEC is much higher when three pumps are running. The M&E team studied the availability of pumps to decrease the capacity requirements and enrolled in a strategic plan for running two pumps. In the study, it was identified that the area that feeds Makumbura pumps can feed Palanwatta Tower by merging the two systems. By implementing that proposal, the system pressure requirement can be maintained, and only two pumps can be operated at the Makumbura pumping station. This was implemented in May 2023, and energy savings were indicated in June 2023.

Specific Energy consumption for pump houses cannot be universally compared, as each pump house operates under unique conditions such as varying head, flow rate, and system configurations. Therefore, it is more meaningful to evaluate specific energy consumption by considering the characteristics of each pump house. The reduction in specific energy consumption at the Makumbura Pump House has been achieved with minimal risk to water supply reliability. Reduction of system operational activities has ensured that the water delivery meets demand without compromising the service levels. The operational changes were implemented with a reduction in the one pump requirement, and it enhances the equipment longevity and reduces the maintenance requirements. Fig. 03 includes a comparison of energy usage in 2021 and 2023 at the Makumbura Pump Station



Fig. 3 Energy Consumption in 2021 and 2023 of Makumbura Pump Station



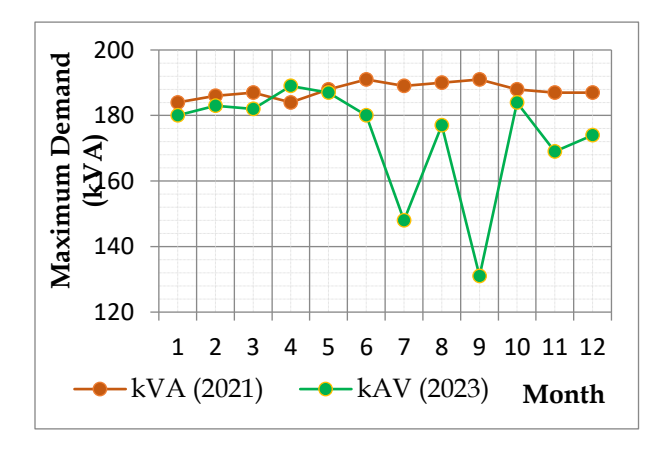


Fig. 4 Maximum Demand in 2021 and 2023 of Makumbura Pump Station

Fig. 5 includes a comparison of production data in 2021 and 2023 at the Makumbura Pump Station.

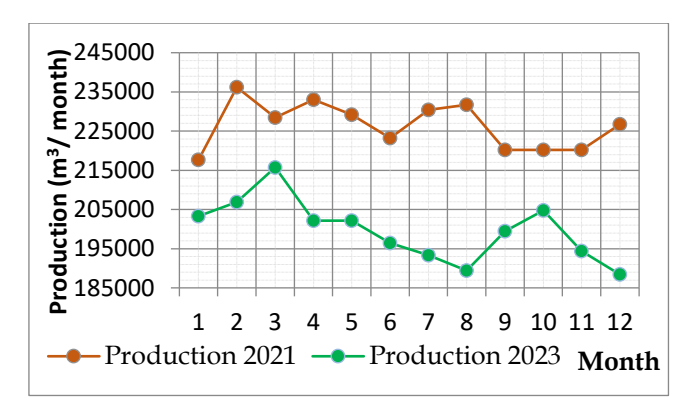


Fig. 5 Production Data in 2021 and 2023 of Makumbura Pump Station

According to Fig. 2, energy consumption in 2023 has been reduced compared to energy consumption in 2021. According to Fig. 3, the maximum demand in 2023 has been reduced compared to the maximum demand in 2021. According to Fig. 4, water production in 2023 decreased compared to water production in 2021.

3.1 Analysis of 2021 and 2023 Performances

Through energy efficiency improvements and the energy efficiency operations pattern that the M&E Team suggested, at present, the analysis of the Specific Energy Consumption of the Makumbura pumping station and the energy consumption over production indicate the energy savings of the project.

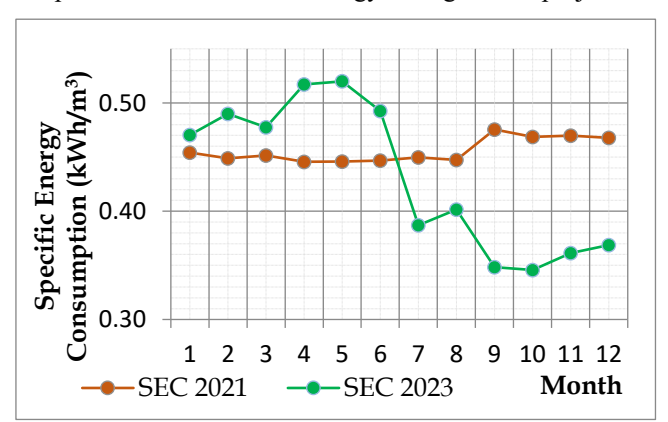


Fig. 6 Specific Energy Consumption in 2021 and 2023 of Makumbura Pump Station

Fig. 07 includes a comparison of energy vs. production in 2021 and 2023 at the Makumbura Pump Station.

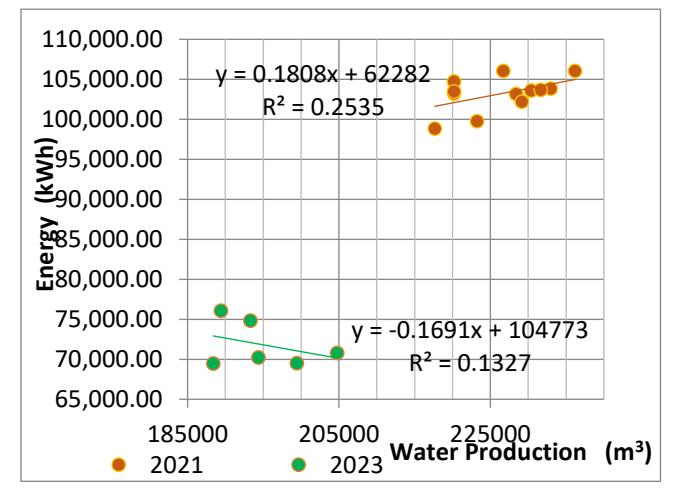


Fig 7 Energy vs. Production in 2021 and 2023 of Makumbura Pump Station

4. Expected Outcomes from the Project

The Project Team expects that the successful completion of this Project will:

- Unlock demand-side energy management by enabling the pump house to turn down to a lower load during peak electricity consumption periods
- Increase energy efficiency at the Makumbura Pump House from ~45% to 70%
- Reduce the maximum demand of the pumping station by ~25%
- Reduce the ongoing annual operating cost by:
 - o Decreasing the maximum demand (kVA) and maximum demand charges to the facility
 - o Decreasing energy consumption (kWh)
- Increase reliability by providing a standby pump facility

The Project Team determined, based on the above analysis, that replacing the existing outdated pumps with modern pumps operating under a 3X50% regime can significantly reduce the energy demand and consumption of the pumping station whilst simultaneously increasing the overall reliability of the pumping station due to the presence of a standby facility

In line with the requirements defined above, the Project Team developed a pumping system and identified a pump model that has the capability to meet the existing demand using two pumps with a third on standby. The Project Team intends to benchmark the performance of the new system against the existing system using three metrics. Namely, maximum demand (kVA), total energy consumption (kWh), and SEC (kW/m³).

Table 2 shows the Cumulative Energy Saving after the implementation of the Strategic Plan at the Makumbura pump house

Month	Production	Expected kWh	Actual kWh	Energy Saving	Cumulative Energy Saving
	2023	for 2023	2023	Actual - Expected	After implementing
	m ³	kWh	kWh	kWh	kWh
Jan	210,070.00	100,262.66	98,795.00	1,467.66	
Feb	193,098.00	97,194.12	94,583.00	2,611.12	
Mar	222,931.00	102,587.92	106,424.00	-3,836.08	
Apr	202,144.00	98,829.64	104,508.00	-5,678.36	
May	208,908.00	100,052.57	108,624.00	-8,571.43	
Jun	196,422.00	97,795.10	96,760.00	1,035.10	
Jul	199,750.50	98,396.89	77,303.00	21,093.89	21,093.89
Aug	195,753.00	97,674.14	78,608.00	19,066.14	40,160.03
Sep	199,448.00	98,342.20	69,491.00	28,851.20	69,011.23
Oct	211,601.00	100,539.46	73,150.00	27,389.46	96,400.69
Nov	194,366.00	97,423.37	70,216.00	27,207.37	123,608.06
Dec	194,685.00	97,481.05	71,788.00	25,693.05	149,301.11

Table 2 Cumulative Energy Saving in 2023 (6 months)

5 The Cost Saving Calculation

The following table shows the total electricity charge for 2023 production (6 months) calculated for the 2023 tariff rate and the 2023 total energy saving (6 months). Then the cost savings are calculated for 2023(12 months).

	Total Energy Saving	Total Cost Saving
	2023 kWh	LKR
Jul	21,093.89	452,200.28
Aug	19,066.14	408,730.43
Sep	28,851.20	618,497.57
Oct	27,389.46	587,161.57
Nov	27207.37	583,258.05
Dec	25,693.05	550,794.72
Total	Cost Saving in 2023 (for six months)	3,200,642.61
Total	Cost Saving in 2023 (for six months x 2)	6,401,285.22

Table 3 Cost Saving in 2023 compared to 2021

6 Conclusion

This Concept was implemented in June 2023 without any budget requirement at NWSDB. The main business process of NWSDB is supplying clean drinking water to the consumers. Doing this with efficient energy utilization which not losing any consumer for access to safe drinking water. The project is forecasted to utilize energy efficiently, as this gives a positive impact on the whole society, as the country is facing a huge energy crisis.

The NWSDB bears the moral responsibility to provide an uninterrupted supply of clean drinking water to homes and businesses while minimizing the impact of our operations on society. The extremely high energy consumption pump operation resulted in the consumption of excessive energy consumption. There is high potential in the organization to be addressed in the future. NWSDB has the potential for efficient energy use practice as follows.



Fig. 8 Demand Saving Potential of the Makumbura Pump House

However, implementing these solutions in different regions or systems may present challenges due to varying infrastructure, operational conditions, and resource availability. Future studies could explore regional-specific adaptations to address these variables effectively. Also, implementing these solutions to different regions or systems may present challenges, such as initial technical barriers, financial constraints, and system reliability concerns. These factors will be included in the iterations of the study to ensure a more comprehensive analysis.

Table 4 CO₂ Emission Reduction Calculation

Energy Saving in 2023 (Six	298,602.00	kWh
Months x2)		
Total CO ₂ emission reduction by	-	Kg/year
energy saving at the pump house		

References

- [1] Ministry of Environment, Nationally Determined Contributions (September 2021)
- [2] Ceylon Electricity Board, Sales, and Generation Data Book (2022)

Circular Economy Adaptation of Electric Vehicle Batteries in Sri Lanka

M A T M Kumara*1, H A K Hapuarachchi1, H A C Hapuarachchi1, R L K Lokuliyana2

¹National Engineering Research & Development Centre, ²Department of Mechanical Engineering, Faculty of Engineering Technology, ^{The} Open University of Sri Lanka

*tharangamuditha01@gmail.com, ashan.hapuarachchi@gmail.com, charithnerdc@gmail.com, rllok@ou.ac.lk

Abstract

Electric vehicles (EVs) are being adopted increasingly worldwide, which is also causing Sri Lanka to move towards EVs in the transportation sector. While the trend in EVs is ever-increasing in Sri Lanka, most overlooked concern related to EVs is the waste that EVs generate and standardized methods of managing that waste. The most critical waste that EVs generate is the batteries that are removed from EVs after their useful life. Electric vehicle battery waste will be a focal point in the future as the waste keeps accumulating without having a standardized process for managing it in the country. With the research carried out, it is analyzed that electric vehicles imported to Sri Lanka, along with electric vehicles manufactured in the country, have Lithium Ferrous Phosphate batteries. With the analysis of circular economy adaptation, which is currently practiced and planned by other countries on EV batteries, this research paper illustrates the most suited Lithium Ferrous Phosphate EV battery circular economy adaptation for Sri Lanka.

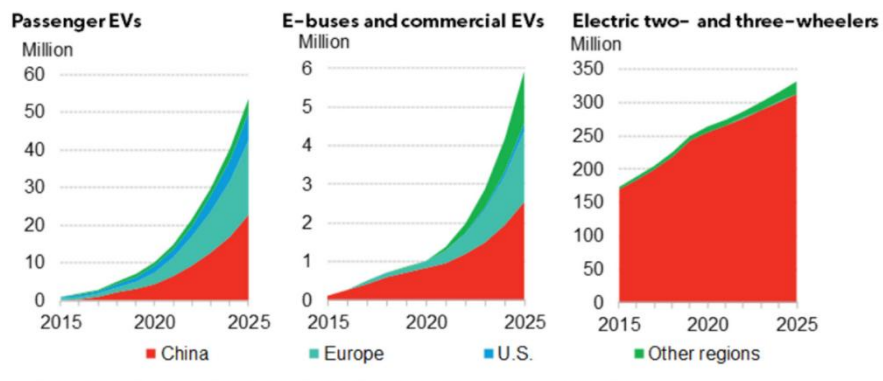
Keywords: Electric Vehicles, Circular Economy, Lithium Ferrous Phosphate battery technology, Recycling, Hydrometallurgy, Pyrometallurgy

1 Introduction

Most developed countries are now in the transition phase to electric vehicles (EV) because of the new policies on emission reduction. In Sri Lanka also EVs are also gaining momentum in the market, and there will be EV batteries as waste in the future. To reduce the amount of EV battery that enters to the environment, circular economy approaches reuse, repurposed, or recycling EV batteries for materials rather than continually relying on substances obtained through mining. In this study, we have done a market study on EV dealers and EV assemblers in Sri Lanka to find out the market segment in electric vehicle types, EV battery types used in those, and the warranty period of those EV batteries. Then, by using the data and reviewing the past research papers and applying the circular economy principles, we propose the most suitable approach for EV battery circular economy adaptation in Sri Lanka.

2. Global Context of EVs

Currently, electric vehicles are flooding the markets of Europe, the USA, China, and other developed countries due to actions taken by the governments to reduce traffic pollution and greenhouse gas emissions [9].



 $Source: BNEF.\ Note: Two-Wheelers\ includes\ mopeds, scooters\ and\ motorcycles,\ excludes\ e-bikes.$

Fig. 1 Global Electric Vehicle by segment and market [15]

Also, in 2040 the global EV market is expected to surpass 60 million according to several analyses.

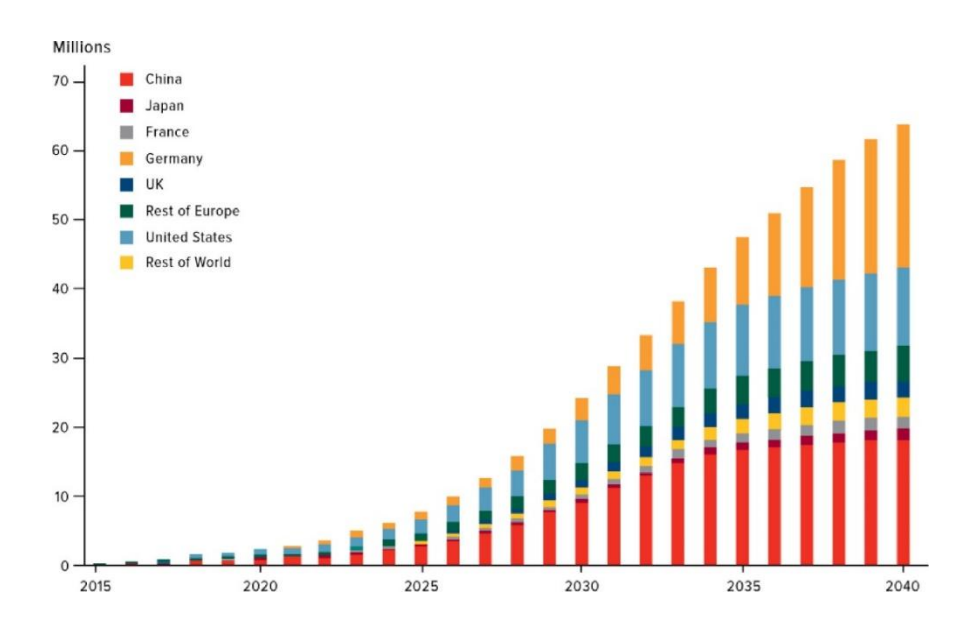


Fig. 2 Annual demand forecast for EVs in the world [19]

The electric vehicle battery market is also expanding due to the increasing demand for EVs. According to the surveys in 2021, around 85.5% of EV batteries came from seven major companies [26].

Cell Supplier	EV makers serve/ Under contract	GWH	Market Share (%)
Contemporary Amperex Technology Co.	Dongfeng Motor Corp., Stellantis, Tesla, BMW, Volvo Car Group, Honda, SAIC Motor Corp., Volkswagen Group	21.6	26
LG Energy Solution	Groupe Renault, Volvo, Stellantis, Tesla, VW Group, General Motors,	21.4	26
Panasonic	Toyota, Tesla	14.1	17
Samsung SDI	Stellantis, VW Group, BMW, Ford	5.5	7
BYD Co.	BYD, Ford	5.5	7
SK Innovation	Daimler, Ford, Hyundai, Kia	3.4	4
China Aviation Lithium Battery (CALB)	Zhejiang Geely Holding Group Co., GAC Motor	2.7	3
Others			14.5

Table 1 Market share of each major EV battery manufacturer [26]

There are different technologies used in EV batteries in different types of EV batteries. Those have different advantages and disadvantages among them. Those are as follows,

- Lithium-ion battery
- Lead-acid battery
- Nickel-Cobalt-Aluminum and Nickel-Manganese-Cobalt batteries
- Nickel-Metal Hydride battery
- Solid and semi-solid battery

2.1 Lithium-ion Battery

In the present world, Lithium-ion (Li-ion) Battery is a very popular battery type which can be found in EVs because of its high energy-to-unit mass compared to others [2]. It means these batteries can store more energy. Also, Li-ion batteries are thermally stable and have good safety, which means this is a safer option for EVs.

2.2 Lead-Acid Battery

Lead Acid battery was first developed in 1859 by Gaston Planté [25], and in the automobile industry, it was the most popular battery used in the world. Before the invention of the Li-ion batteries, the common battery type of EVs was lead-acid. But after the 80s, lead-acid batteries in EVs were replaced by Li-ion batteries. They are heavier and have a low energy density compared to Li-ion batteries

2.3 Nickel-Cobalt-Aluminum (NCA) and Nickel-Manganese-Cobalt (NMC) batteries

Lithium nickel manganese cobalt oxide (NMC) and lithium Nickel Cobalt Aluminum oxide (NCA) are the most commonly used Li-ion cathode chemistry for EVs today [5]. In both types, Lithium is used as a common material. These are ideal for EVs due to high energy density, longer range, and faster charging.

2.4 Nickel-Metal Hydride (NIMH) Battery

These have a good balance between cost and performance and a reliable option for the EVs. NIMH batteries exhibit greater energy density by weight and volume, have better high-rate capabilities, and can withstand excessive discharges more effectively [3]. NiMH batteries operate on the principle of hydrogen ion exchange between the electrodes, enabling energy to be stored and released efficiently.

2.5 Solid and semi-solid battery

Solid and semi-solid types of batteries are not commercially available on the EVs yet, but they are likely to come to the market in the near future. These batteries replace the liquid electrolyte with a solid and have increased energy density, improved safety and longer life. Because these batteries in solid state features it eliminates the risk of leakage and reduces the likelihood of fire and increases the safety of EVs.

When looking at the global battery market it is notable that the past was dominated by lead-acid batteries and now with the growth of the EVs Lithium-ion batteries market started rising. People are now choosing EVs over internal combustion engine vehicles and this trend increases the demand of batteries, such as Lithium-ion, Nickel Cadmium, and Nickel Metal Hydride.

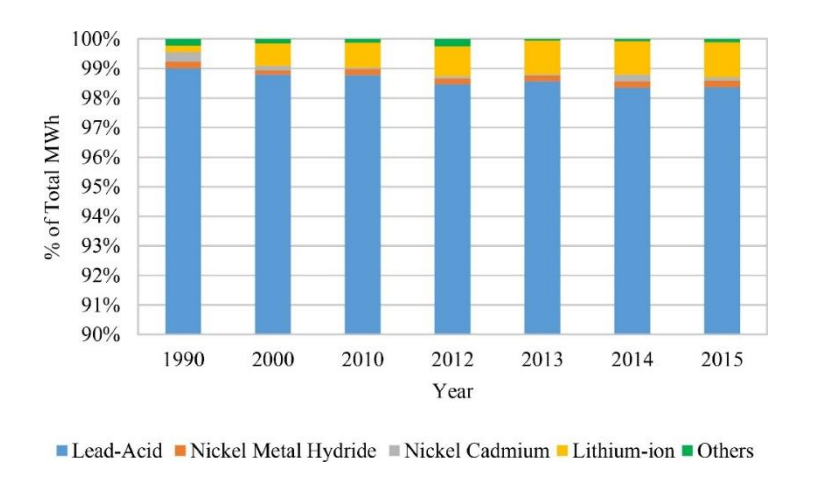


Fig. 3 The battery market growth over the years [19]

3 Global Circular Economy Approach for EV Batteries

The European Commission have included strategies and new approaches for the circular economy approach for EV batteries in their circular economy plan 2020 [13]. In that action plan they have more focused on the following segments,

Improving the collection and recycling rate for all batteries, securing valuable materials recovery and advising consumers.

- To deal with non-rechargeable batteries in such a way that their use shall be progressively phased out where alternatives exist.
- Requirements on batteries will take into consideration issues such as carbon footprint from manufacturing, ethical sourcing of raw materials and security of supply, reuse, repurposing, and recycling.

In this policy structure, they are more focused on sustainable battery and vehicle technologies for the EU countries.

China is another one of the major players in EV vehicles, and they use a lot of EVs inside the country; because of that, they are also promoting circular economy policies in the EV batteries [14]. In there, they are heavily forced into battery collection and material extraction processes.

The Netherlands also adopted the EU's circular economy policies on EV batteries, and they have taken actions to make the EV batteries as much as possible. In that policy framework, they focused much on EV battery collection, material extraction, reducing the carbon footprint of EV batteries, and increasing battery recycling efficiency [7].

4 Sri Lankan Context of EVs

In Sri Lanka, according to the data of the Department of Motor Traffic, the most popular vehicle type is motor bikes, followed by three-wheelers and motor cars [10].

Fuel Type	2017	2018	2019	2020	2021	2022
Diesel	34,989	31,617	20,822	15,865	15,440	7,376
Patrol	388,809	408,997	335,862	181,970	13,160	9,514
Hybrid	22,426	36,061	7,717	1,665	334	16
Electric	772	987	7567	272	273	746
Total	446,996	477,662	365,157	199,77	29,207	9,514

Table 2 Yearly registered vehicles according to fuel type [22]

The present Sri Lankan scenario of EVs is very similar to the world trend. The demand and popularity of EVs are rising. Also, the government is keen to introduce new policies to increase the EVs in Sri Lanka, Because of the government planning to reduce the transport sector emissions by introducing E-mobility in the country according to the 2050 Carbon Net Zero 2050 Roadmap and Strategic Plan [6]. That means there will be a huge EV market in Sri Lanka in the future, and because of that, there will be a lot of EV batteries as waste when their lifetime is over.

In Sri Lanka, there are around 15-20 companies that import and assemble EVs, and major vehicle types are electric bikes, electric cars, and electric three-wheelers. To find out the current Sri Lankan EV market, we carried out a survey among the 14 companies that import and assemble EVs to Sri Lanka. According to that, the majority of EV suppliers are electric cars (36%), followed by electric bikes (43%) and three-wheelers (21%).

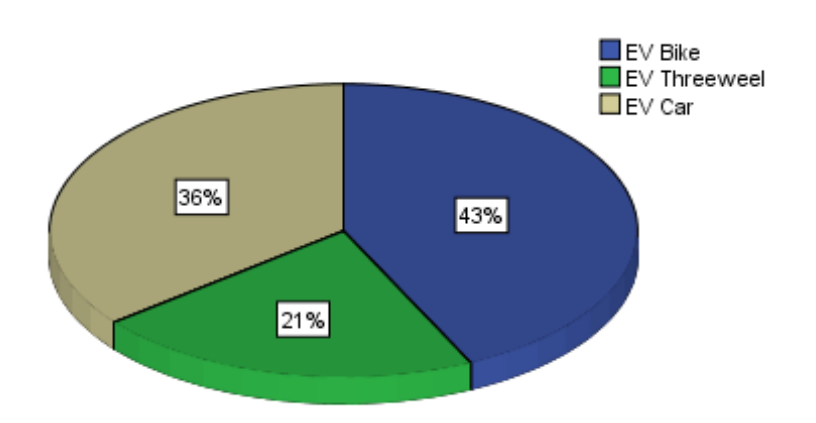


Fig. 4 Type of EV released to market by EV assemblers and EV dealers

In the survey conducted, the majority of the EV suppliers used the Lithium iron phosphate batteries (LiFePO), which is 71% followed by 21% of graphene batteries and 7% Lithium nickel manganese cobalt oxides (NCM Lithium) battery. In here graphene and NCM lithium batteries mainly used in the electric bikes and many times LiFePO batteries used in the electric cars, three-wheelers and bikes too.

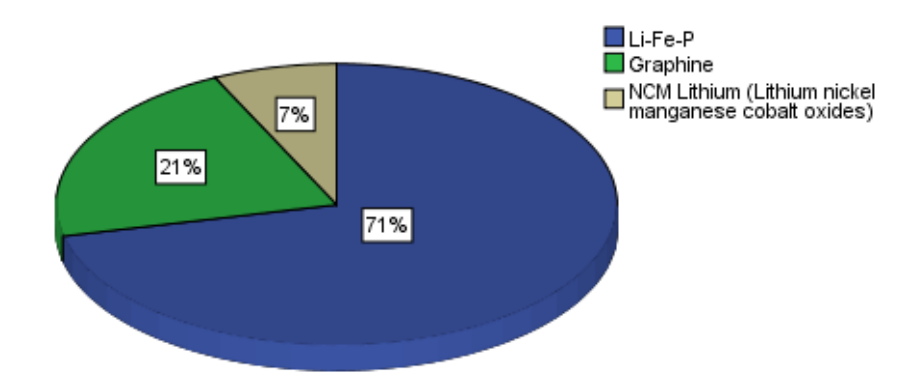


Fig. 5 Type of EV battery released to market by EV assemblers and EV dealers

When analyzing the most important case in EV battery warranty period it ranges from one year to eight years' period in Sri Lanka. According to the survey, the electric bike battery warranty varies from one year to 5 years, and nearly 30% of the suppliers give a 1.5-2-year warranty period. Also, electric three-wheelers are getting a 5-year warranty for their battery. Finally, the majority of electric cars have 8 8-year warranty period for the battery.

In this study almost all EV importers and assemblers do not have a clear idea about the proper disposal method of EV batteries. Also, when going through the above data, it can be seen that the main challenge of disposing EV batteries in Sri Lanka will come around in the next decade. The major battery type that is going to the disposal phase will be the lithium-iron-based batteries. Hence circular economy approach for Lithium-Ion batteries and selecting suitable circular economy policies for Sri Lanka are considered here.

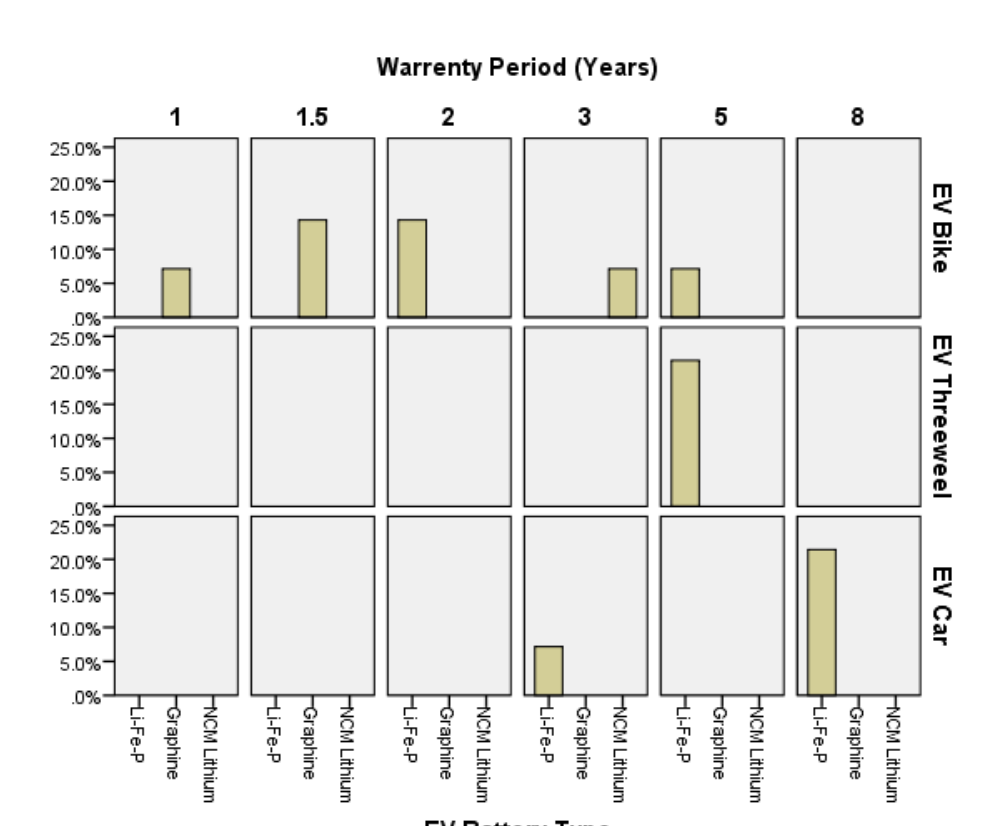


Fig. 6 Type of EV battery, Type of Vehicle vs market share percentage

5. Sri Lankan Context in Reduce Reuse Recycle Concept and the proposed plan

With the analysis carried out on EV batteries in this research, it is identified that lithium ion batteries used in EVs are material intensive and need mining and processing of ingredients resulting in environmental and social impacts. In overcoming these issues related to EV batteries, many countries like China, European Union and state of California have identified that reducing, reusing, and recycling (3R Method) the EV batteries at its end-of-life is required in mitigating the externalities of the transition to EVs [12]. This 3R process of Reduce, Reuse and Recycle concept in circular economy on EV batteries is analyzed from this part of the research paper by other countries in the world and identifies the most suitable 3R method suits to Sri Lanka on EV batteries.

5.1 Reduce Concept on LIBs to be adapted in Sri Lanka

The below aspects are currently being carried out and initiated in other countries in the world related to the Reduce Concept on LIBs in adaptation to the circular economy [4].

- Selection of a LIB technology that is currently used for EVs with minimum material usage
- Selection of a LIB technology that has the optimum energy density for the EVs
- Carrying out LIB technology design improvements, continuously focusing on reduced material usage on battery manufacturing, and increasing energy density

Considering the option of selecting LIB technology with minimum material usage, it is required to find out the available LIB technologies that are currently used in EVs. There are 6 major LIB types which are currently used in EVs, namely Lithium Nickel Manganese Cobalt Oxide (NMC), Lithium Nickel Cobalt Aluminum Oxide (NCA), Lithium Ferrous Phosphate (LFP), Lithium Cobalt Oxide (LCO), Lithium Manganese Oxide (LMO) and Lithium Titanium Oxide (LTO). Out of these 6 LIB types, the most widely used LIB types for EVs are Lithium Nickel Manganese Cobalt Oxide, Lithium Ferrous Phosphate, and Lithium Manganese Oxide due to reasons like specific energy capacity levels, performance, cost, specific power, life span, safety, etc. [18].

From these three most widely used LIB technologies for EVs, Lithium Ferrous Phosphate battery is the only battery type that does not use Nickel, Manganese, or Cobalt as battery ingredients. Nickel, manganese, and Cobalt extraction as virgin materials from the earth is recognized to be energy intensive and high cost, and these three materials are in the zone of rare earth materials, which make the material extraction process to be further affects the planet earth. Hence, going for Lithium Ferrous Phosphate batteries to be incorporated into EVs would mean that the rare earth materials to be extracted less from the earth. That makes the Reduce concept of the circular economic pathway to be positively addressed.

Considering the data analysis carried out in the research on the EV battery market in Sri Lanka, 71% of EVs coming into Sri Lanka are equipped with Lithium Ferrous Phosphate batteries. It is a good trend towards reducing the concept of circular economy adaptation into EV batteries in Sri Lanka. This can be further strengthened by implementing government-level policies on importing only Lithium Ferrous Phosphate used EVs into the country.

Considering the next option of selecting a LIB technology which has the optimum energy density for the EVs, out of the six LIB types mentioned above, Cobalt included LIBs have a greater energy density compared to others. Below Fig. illustrates the information on energy density of the six LIB types along with other characteristics.



Fig. 7 Comparison of different LIB types used in EVs [18]

According to the above Fig., NMC and NCA LIBs have the best energy density compared with other LIB types. Both NMC and NCA batteries are having materials like Nickel and Cobalt which require high energy intensive processes in mining which leads to deviate from the circular economic approach. Hence it is required to further analyze the energy density aspect of selecting a LIB type in focusing with Reduce Concept of circular economy adaptation.

Carrying out LIB technology design improvements, continuously focusing on reduced material usage in battery manufacturing and increasing energy density is another key aspect to be looked into in the Reduce Concept of circular economy adaptation. Continuous research and development related to battery technology innovation make new breakthroughs related to reduced material usage in battery manufacturing and the substitution harmful materials in battery manufacturing. This approach is evident through using less cobalt percentage in LIB manufacturing in high-capacity LIBs.

Another research area on LIBs is improving the design of electrodes to increase the battery capacity. Chemically related reactions are occurring at the electrodes of LIBs. Research on reducing the internal resistance of the electrodes will decrease the heat generated in using the LIB and thereby improve the lifespan and cell capacity of the LIB. In recent research carried out on LIB efficiency improvement, reducing the electrode size and showing improvement could be achieved. It was further identified that it has a limit on reducing the electrode size where electrode thickness reduction of 130 micrometers leads to an inability to reach the required energy specifications. Such research on LIB performance improvement with reduced material usage will positively affect the Reduce concept of circular economy adaptation into LIBs in EVs. Sri Lanka needs to be updated on such current trends in LIB research and adapt them accordingly.

5.2 Reuse Concept on LIBs to be adapted in Sri Lanka

Once the LIBs used in EVs have come to a stage of inability in charging to 70 – 80% of their rated capacity, such LIBs are required to be replaced. Such LIBs can be reused, refurbished, and repurposed before they are recycled. This incremental process is termed as the waste hierarchy, and this process follows the circular economic concept [23]. This way of reusing, refurbishing, and repurposing LIBs has environmental benefits, as it increases the use of a product that has already been designed and manufactured [12]. When LIBs are repurposed to aid renewable energy generation, they improve the low-carbon electricity generation and provide carbon abatement [4]. In reusing the LIB, the battery pack is placed into a new EV by removing it from the old EV. Considering the adaptation of this process into the Sri Lankan context, it is possible to remove old LIBs in electric cars and other higher capacity LIBs and use them in other smaller EVs like electric three-wheelers and electric two-wheelers. This process has possible entrepreneurship possibilities with government aid.

In refurbishing LIBs, the old battery of the EV is removed, and it is repaired and reused. For the refurbishing of LIBs, it is required to have the necessary LIB repairing technology in place, which is currently lacking in Sri Lanka. If the necessary infrastructure is provided via financing facilities, the refurbishing of LIBs in EVs in Sri Lanka would provide a path to the adaptation of LIBs into the circular economy implementation. Repurposing used LIBs is performed by removing old LIBs from EVs and repurposing them to be used in a stationary storage application, aiding in solar and wind energy-related renewable energy integration. Sri Lanka has widespread wind and solar energy generation in a widespread way, and this would help in repurposing LIBs used in EVs to be used

as energy storage establishments for solar and wind energy generating plants in Sri Lanka. This is yet to be implemented in Sri Lanka, and with the financial support from the government level.

5.3 Recycle Concept on LIBs to be adapted in Sri Lanka

Lithium-ion batteries (LIB) require multiple steps before recycling due to their complex structure and variety of materials [16]. The process starts with classification and pre-treatment, which includes discharging or subjecting to the inactivation of batteries, followed by disassembly and separation. After these steps, materials can be recycled using one of several methods mentioned below.

- Direct recycling
- Pyrometallurgy
- Hydrometallurgy
- Combinations of these approaches

The direct recycling method used in LIB recycling is in the laboratory stage and needs to be removed from the selection of ideal recycling methods for LIBs in Sri Lanka. The pyrometallurgy process of recycling requires expensive infrastructure establishment and causes adverse environmental effects when in operation, making it to be removed from the selection of an ideal recycling method for LIBs in Sri Lanka. Considering the hydrometallurgy process of recycling EV batteries, the three main steps in hydrometallurgy recycling are pretreatment, leaching, and metal deposition. Benefits and challenges in the hydrometallurgy process need to be looked at in further studies of this recycling method of LIBs.

5.3.1 Benefits of the hydrometallurgy process

Life Cycle Analysis results

Life cycle analysis (LCA) results related to hydrometallurgy EV battery recycling provide information on the impact of recycling EV batteries compared to dumping the end-of-life Lithium-Ion Batteries (EoL LIBs). In one such research, life cycle assessment was carried out with system boundaries including primary material mining, production of LIB cells, and end-of-life recycling processes, including emissions and wastewater disposal. The use phase of batteries was excluded from the LCA study. Findings from the LCA study were that the global warming impact of LIB is reduced by 25% when performing recycling of LIBs using the hydrometallurgy process [20].

Another LCA study has been carried out by one of the leading EV battery recycling companies [1]. The system boundaries of that LCA were the production of 1 ton of battery materials extracted from the recycling of EoL EV batteries with a hydrometallurgy process. The result of that LCA suggests that carbon dioxide emission reduction is 74%, nitrate and sulfates emission reduction is 92% and reduction in water usage is 97%. To achieve 97% water usage reduction, the company is performing a recycling process, and liquids in the process are recirculated and contained within the process.

In research carried out on LCA of LIBs, it used the functional unit of LCA was 1kg of EV battery waste. The system boundary of that LCA included the collection of EoL EV battery waste and its treatment to recover active materials. The system boundary excluded the production of EV batteries and the use phase of them. The findings of that LCA study were that recycling of EoL LIBs using hydrometallurgy reduced the greenhouse gas emission by 37% toxic emission by 81%, acidification by 94%, fossil fuel depletion by 14% and abiotic resource depletion by 78% when compared to utilizing virgin materials in producing LIBs [24].

Materials Flow Analysis

Research has been carried out on material flow analysis related to EV battery manufacturing. In one such research work [12], after carrying out a materials flow analysis, it was predicted that recycled EV batteries using the hydrometallurgy process could supply 60% of the cobalt requirement, 53% of the lithium requirement, 57% of the manganese requirement and 53% of nickel requirement worldwide in 2040. This provides the importance of recycling of EoL LIBs with the hydrometallurgy process.

Competitive advantage

Active materials extracted from recycling EoL LIBs are metals, including lithium, cobalt, nickel, manganese, graphite, etc. Since the recycled materials from LIBs are collected from using one source, that is, using EoL LIBs, battery recycling is cost-effective than extracting virgin materials by mining. The quality and performance of

recycled materials are at the same level of virgin materials, and hence, the recycled materials have the same competitiveness.

Easy adaptability in developing countries

Developing countries can be involved in the current EV battery boom in two ways. One way is to be a hub of EoL EV battery collection. Recycling companies around the globe face the issue of less collection of EoL EV batteries. Developing countries can supply EoL EV batteries to such recycling companies. The other way is that since the hydrometallurgy process can be scaled down, developing countries can establish local hydrometallurgy facilities with their technologies. India is an ideal example for this, where it has several hydrometallurgy plants such as Batx, LICO, Recyclekaro, etc., which are recycling EoL LIBs.

Considering these benefits and the fact that the hydrometallurgy process can be easily adapted to developing countries, the ideal method of recycling LIBs in Sri Lanka would be the hydrometallurgy method of recycling EoL LIBs.

5.3.2 Challenges in the hydrometallurgy process

Combining Hydrometallurgy with Smelting

In the LIB chemistry, there are five main types of cathode compounds that are commercially available. They are Lithium-Cobalt Oxide (LCO), Lithium-Nickel-Manganese-Cobalt (NMC), Lithium-Manganese Oxide (LMO), Lithium-Nickel-Aluminum Oxide (NCA), and Lithium-Iron Phosphate (LFP). NMC has a market share of around 29% while LCO is of 26% and LFP has around 23% [17]. A robust and resilient hydrometallurgical process will extract materials from all these LIB chemistries. Since the hydrometallurgy process can be implemented in multiple ways and forms, countries need to make sure that the process used by each of those LIB recycling companies is environmentally friendly. LIB recycling companies are combining smelting and hydrometallurgy in recycling LIBs where smelting is a harmful process to the environment, with emissions of organic volatile compounds and metal.

Emergence of Cobalt-free and nickel-free batteries

Cobalt-free and nickel-free EV battery manufacturing is emerging, and this has the benefit of reducing the requirement for mining scarce virgin materials in manufacturing LIBs and eventually reducing the production cost of LIBs. This new emergence in LIB manufacturing will replace the most expensive materials, like Cobalt and nickel, with other materials. That will make the recycling of EV batteries less attractive [21].

Non-availability of Regulations related to EV battery recycling

Countries like the United States and European countries still have not established firm regulations on the recyclability of EV batteries. The main requirement in establishing regulations on EV batteries is to ensure that EV batteries are designed and produced to suit easy end-of-life recyclability. For example, PTFE used for EV batteries as a binder is more difficult to extract in the recycling process. The design stage of EV battery manufacturing can mitigate such flaws. China released battery recycling regulations in 2018 to put responsibility on EV manufacturers in collecting and performing the recycling of EoL EV batteries. Developing countries can establish similar regulations to encourage EV battery recycling plants to be installed [8].

A summary of benefits and challenges in the Hydrometallurgy process of EV battery recycling is shown in the table below.

Table 3 Summary of benefits and challenges in the hydrometallurgy process of EV battery recycling

Benefits	Challenges
Reduced global warming Reduced GHG emissions, toxic emissions, and acidification Reduction in CO ₂ emissions and water usage	Combined processes like smelting with hydrometallurgy raise concerns
Materials flow analysis	Emergence of Cobalt-free and nickel-free batteries

• In the year 2040, more than 50%	Make recycling of EV batteries		
requirements of Lithium, Cobalt,	less attractive		
Manganese, and Nickel in EV battery			
manufacturing can be achieved using the			
hydrometallurgy process of EV battery			
recycling			
Competitive advantage	Non-availability of Regulations in EV		
 Recycled materials are equally competitive 	battery recycling		
in quality and performance			
Adaptability in developing countries	EoL EV battery collection		
The hydrometallurgy process can be scaled	Require specific transportation		
down to suit the requirements and financial			
capability of the country			

5 Conclusion

From the carried out EV market survey in Sri Lanka, the portion of the market segment for EV bikes is 43% while EV cars is 36% and EV three-wheelers are 21%. Out of the EVs in Sri Lanka, there are several EV battery technologies have been utilized for these EVs. LFP battery used EVs in Sri Lanka are around 71% while NMC used EVs are around 36% and graphene used EVs are 21%. Hence, it is evident that Sri Lanka needs to focus on EV battery circular economy adaptation, especially considering LIBs, since EV battery technology has more than 70% market share. In the Reduce concept of circular economy adaptation for LIBs, it was identified that Sri Lanka can implement policies on importing EVs which are having only Lithium Ferrous Phosphate batteries, which use less costly materials and have a greater lifespan than other LIB types. As a country, Sri Lanka can also focus on going for LIBs with better energy density and support for research and development in LIB technology advancement. In adapting the Reuse concept into the Sri Lankan context, it is possible to implement reuse, refurbish, and repurpose opportunities related to used LIBs in EVs, with the required technology infrastructure being established with the aid of government and financial backup. With the analysis carried out related to recycling of end-of-life LIBs in EVs, Sri Lanka can focus on the hydrometallurgy recycling process of LIBs and establish such recycling facilities with the technological support from neighboring countries like India, which have already established and are processing end-of-life LIB recycling using the hydrometallurgy recycling process.

Challenges in establishing hydrometallurgy-based LIB recycling plants in Sri Lanka are the high cost involved in establishing such facilities, difficulty in providing infrastructure requirements, such as allocating suitable lands for recycling plants, and regulatory barriers at the national policy level, etc. Government intervention is essential in sorting out most of the above-mentioned challenges. Hydrometallurgy processing of LIBs can be combined with other material extraction methods like pyrometallurgy and electrometallurgy. Optimizing these combinations to best extract materials from LIBs has future research potential. It is a must that Sri Lanka as a country needs to constantly update on current global trends in LIB circular economy adaptation and identify suitable arrangements that can be implemented in the country while establishing supportive regulations towards promoting circular economy in general, and specifically on LIB circular economy adaptation.

References

- [1] Ali, A., Manzan, M., & Adjoumane, A. (2022). *Hydrometallurgy for EV batteries*. Retrieved from https://sdgs.un.org/sites/default/files/2022-05/2.4.8-18-Ali-Hydrometallurgy%20for%20EV%20batteries.pdf
- [2] Anup KumarH S. (2022, September 15). Different Types of Batteries used in EV vehicles. Retrieved September 20, 2024, from Skill-Lync website: https://skill-lync.com/blogs/different-types-of-batteries-used-in-ev-vehicles
- [3] B. Hariprakash, Shukla, A. K., & S. Venugoplan. (2009). SECONDARY BATTERIES NICKEL SYSTEMS | Nickel–Metal Hydride: Overview. Elsevier EBooks, 494–501. https://doi.org/10.1016/b978-044452745-5.00158-1
- [4] Bobba, S., Fabrice Mathieux, Ardente, F., Gian Andrea Blengini, Maria Anna Cusenza, Podias, A., & Pfrang, A. (2018). Life Cycle Assessment of repurposed electric vehicle batteries: an adapted method based on modelling energy flows. *Journal of Energy Storage*, 19, 213–225. https://doi.org/10.1016/j.est.2018.07.008

- [5] Brand, M., Gläser, S., Geder, J., Menacher, S., Obpacher, S., Jossen, A., & Quinger, D. (2013). Electrical safety of commercial Li-ion cells based on NMC and NCA technology compared to LFP technology. World Electric Vehicle Journal, 6(3), 572–580. https://doi.org/10.3390/wevj6030572
- [6] Carbon Net Zero 2050 Roadmap and Strategic Plan. (n.d.). Retrieved from https://www.climatechange.lk/CNZ2050_Synthesis%20Report.pdf
- [7] Circular Batteries Charging the Future Collaborating for a Sustainable and Resilient Value Chain 3. (n.d.). Retrieved from https://english.rvo.nl/sites/default/files/2023-11/HCH-Circular-Batteries-Charging-the-Future-Brochure.pdf
- [8] China releases battery recycling regulations electrive.com. (2019). Retrieved September 23, 2024, from electrive.com website: https://www.electrive.com/2019/11/11/china-releases-battery-recycling-regulations/#:~:text=The%20Chinese%20Ministry%20of%20Industry,for%20some%20electric%20car%20 manufacturers.
- [9] Contribution of Li-Ion Batteries to the Environmental Impact of Electric Vehicles. (2010, August 9). Retrieved September 20, 2024, from ACS Publications website: https://pubs.acs.org/doi/10.1021/es903729a
- [10] Department of Motor Traffic NEW REGISTRATION OF MOTOR VEHICLES (2012-2023) CLASS OF VEHICLE. (2012). Retrieved frohttps://dmt.gov.lk/images/2023/total_population/Vehicle_Population_2010-2023.pdf
- [11] Dunn, J. (2022). Lithium-ion battery material circularity: material availability, recycling economics, and the waste hierarchy. Retrieved September 23, 2024, from Escholarship.org website: https://escholarship.org/uc/item/7h92v5td
- [12] Dunn, J., Slattery, M., Kendall, A., & Shen, S. (2021, March 25). Circularity of Lithium-Ion Battery Materials in Electric Vehicles. Retrieved September 23, 2024, from ResearchGate website: https://www.researchgate.net/publication/350390623_Circularity_of_Lithium Ion Battery Materials in Electric Vehicles
- [13] EUR-Lex 52020DC0098 EN EUR-Lex. (2020). Retrieved September 20, 2024, from Europa.eu website: https://eur-lex.europa.eu/legal-content/EN/TXT/?qid=1583933814386&uri=COM:2020:98:FIN#footnote26
- [14] Hu, Z., Yu, B., Ichiro Daigo, Tan, J., Sun, F., & Zhang, S. (2024). Circular economy strategies for mitigating metals shortages in electric vehicle batteries under China's carbon-neutral target. Journal of Environmental Management, 352, 120079–120079. https://doi.org/10.1016/j.jenvman.2024.120079
- [15] Kene, R., Olwal, T., & Wyk, van. (2021). Sustainable Electric Vehicle Transportation. Sustainability, 13(22), 12379–12379. https://doi.org/10.3390/su132212379
- [16] Kim, H.-J., Krishna, T., Zeb, K., Vinodh Rajangam, Chandu V. V. Muralee Gopi, Sangaraju Sambasivam, ... Obaidat, I. M. (2020). A Comprehensive Review of Li-Ion Battery Materials and Their Recycling Techniques. Electronics, 9(7), 1161–1161. https://doi.org/10.3390/electronics9071161
- [17] Larouche, F., Farouk Tedjar, Kamyab Amouzegar, Georges Houlachi, Bouchard, P., Demopoulos, G. P., & Karim Zaghib. (2020). Progress and Status of Hydrometallurgical and Direct Recycling of Li-Ion Batteries and Beyond. *Materials*, *13*(3), 801–801. https://doi.org/10.3390/ma13030801
- [18] Miao, Y., Hynan, P., Annette von Jouanne, & Alexandre Yokochi. (2019). Current Li-Ion Battery Technologies in Electric Vehicles and Opportunities for Advancements. *Energies*, *12*(6), 1074–1074. https://doi.org/10.3390/en12061074
- [19] Mohammadi, F., & Saif, M. (2023). A comprehensive overview of electric vehicle batteries market. E-Prime Advances in Electrical Engineering Electronics and Energy, 3, 100127–100127. https://doi.org/10.1016/j.prime.2023.100127
- [20] Mohr, M., Peters, J. F., Baumann, M., & Weil, M. (2020). Toward a cell-chemistry specific life cycle assessment of lithium-ion battery recycling processes. *Journal of Industrial Ecology*, 24(6), 1310–1322. https://doi.org/10.1111/jiec.13021
- [21] Mossali, E., Picone, N., Gentilini, L., Rodrìguez, O., Juan Manuel Pérez, & Marcello Colledani. (2020). Lithium-ion batteries towards circular economy: A literature review of opportunities and issues of

- recycling treatments. *Journal of Environmental Management*, 264, 110500–110500. https://doi.org/10.1016/j.jenvman.2020.110500
- [22] Randula. (2017). Department of Motor Traffic. Retrieved September 20, 2024, from Transport.gov.lk website:

 https://www.transport.gov.lk/web/index.php?option=com_content&view=article&id=26&Itemid=146&lang =en#vehicles-by-fuel-type
- [23] Richa, K., Babbitt, C. W., & Gaustad, G. (2017). Eco-Efficiency Analysis of a Lithium-Ion Battery Waste Hierarchy Inspired by Circular Economy. *Journal of Industrial Ecology*, 21(3), 715–730. https://doi.org/10.1111/jiec.12607
- [24] Rinne, M., Heini Elomaa, Antti Porvali, & Lundström, M. (2021). Simulation-based life cycle assessment for hydrometallurgical recycling of mixed LIB and NiMH waste. *Resources Conservation and Recycling*, 170, 105586–105586. https://doi.org/10.1016/j.resconrec.2021.105586
- [25] Selamat Muslimin, Zainuddin Nawawi, Bhakti Yudho Suprapto, & Tresna Dewi. (2022). Comparison of Batteries Used in Electrical Vehicles. Atlantis Highlights in Engineering/Atlantis Highlights in Engineering. https://doi.org/10.2991/ahe.k.220205.074
- [26] Ulrich, L. (2021, August 25). The Top 10 EV Battery Makers. Retrieved September 20, 2024, from IEEE Spectrum website: https://spectrum.ieee.org/the-top-10-ev-battery-makers

Optimizing Peer-to-Peer Energy Trading: Dynamic Pricing Model and Algorithm for Dispatching Battery Energy Storage System

R. H. G. Sasikala*1, K.A.C. Udayakumar² and Narendra de Silva³

^{1,2} Department of Electrical and Computer Engineering, The Open University of Sri Lanka, Nawala, Nugegoda, Sri Lanka
³Lanka Electricity Company Ltd, No. 411, Galle Road, Colombo 03, Sri Lanka

rhsas@ou.ac.lk

Abstract

The rise of distributed generation has introduced significant challenges to conventional grid-connected electricity distribution systems, especially with the integration of renewable energy sources. These changes have transformed traditional consumers into pros who produce and consume electricity. Peer-to-peer (P2P) energy trading platforms allow prosumers to exchange electricity with their neighbors, creating new decentralized energy markets supported by emerging technologies. This research explores the concept of P2P energy trading within grid-connected electricity networks, focusing on the role of dynamic pricing. Dynamic pricing adjusts based on real-time supply and demand, incentivizing efficient energy usage and reducing grid strain during peak periods. To enhance participation in P2P trading and maximize cost benefits through optimal resource utilization, this study proposes a simplified economic model incorporating dynamic pricing and resource flexibility, including Battery Energy Storage (BESS). The model developed a cost-based algorithm to optimize trading, with market prices determined by energy availability, storage levels, and time of day variables. Simulations in a grid-connected distribution network, with 15-minute intervals, show that the model effectively manages energy trading volumes while peers adjust their buying and selling quantities based on market price fluctuations. The results highlight the potential benefits of dynamic pricing in optimizing P2P energy trading.

Keywords: Algorithm, Battery Energy Storage System, Distribution Generation, Dynamic Pricing, Economic model

1 Introduction

The growing adoption of decentralized renewable energy sources, such as solar photovoltaics (PV), has spurred significant advancements in energy trading systems [1]. One prominent development in this realm is Peer-to-Peer (P2P) energy trading, which empowers prosumers—individuals who produce and consume energy—to trade electricity directly [2]. This approach contrasts with traditional utility models, offering enhanced flexibility, increased efficiency, and potential cost savings for participants. Integrating Battery Energy Storage Systems (BESS) further augments this model by allowing prosumers to store excess energy and utilize it during highdemand or low-renewable generation periods. Optimizing such systems requires sophisticated algorithms and dynamic pricing models to effectively balance energy supply and demand while minimizing costs [3]. In P2P energy trading, each prosumer's energy production, consumption, and storage capacity play a crucial role. Prosumers equipped with solar PV panels and BESS can generate surplus energy during peak sunlight hours and store it for later use. They can also sell excess energy to other prosumers or the grid when their own consumption is low. Conversely, prosumers can purchase energy from their peers or the grid during low-generation or highdemand periods to meet their needs. The challenge lies in optimizing these transactions to ensure economic efficiency and a reliable power supply. Dynamic pricing, which adjusts energy prices based on real-time supply and demand conditions, optimizes energy trading within these markets. It enables prosumers to make informed decisions about when to buy or sell energy, taking advantage of favorable price conditions to maximize financial benefits. During high solar generation and low demand periods, energy prices may drop, encouraging prosumers to charge their batteries or sell excess energy to their peers or the grid. Conversely, during peak demand periods, prices may rise, incentivizing prosumers to discharge stored energy or reduce consumption. Most existing literature uses different pricing structures that are not adjusted according to supply-demand dynamics in the peer market and other variables of resource availability in peer premises [4]. Therefore, participants are less interested in peer trading since pricing is not adjusted based on real-time dynamics [5]. It was learned that Dynamic Pricing Models are essential for managing P2P energy markets effectively. They reflect real-time changes in energy supply and demand, influencing prosumers' decisions regarding energy trading. Pricing models may vary based on the time of day, weather conditions, and battery state of charge (SOC). By adjusting energy prices dynamically, these models can incentivize prosumers to engage in trading activities that align with overall market efficiency [6].

Battery energy storage systems (BESS) further enhance the flexibility and reliability of P2P energy trading. By storing excess energy generated during periods of low demand, prosumers can shift their energy usage to times when prices are higher, or supply is constrained [7]. This helps stabilize the grid by reducing peak demand and allows prosumers to participate more actively in energy markets, increasing their profit potential. Dispatching algorithms for Battery Energy Storage Systems (BESS) are integral to optimizing P2P energy trading [8]. To make informed decisions, these algorithms must consider various factors, including energy availability, cost, and battery constraints. Optimizing energy trading through dynamic pricing and battery energy storage is essential for maximizing the economic and environmental benefits of P2P energy markets. It allows the efficient use of renewable energy, reduces the dependence on fossil fuels, and empowers prosumers to take control of their energy consumption and production. As the energy landscape evolves, these optimizations will become increasingly important for achieving a resilient and sustainable energy system. An economic model for P2P energy trading is proposed to address this, incorporating dynamic pricing and optimum resource utilization of Battery Energy Storage System (BESS). This model considers various factors to decide the peer energy trading prices in each trading interval, represented as a price function. Another cost function is introduced to manage the battery charging and discharging effectively, where both the peer market price function and battery storage cost function are embedded in an algorithm to formulate the trading process.

Algorithm development is crucial for effective P2P energy trading. A rule-based algorithm has been designed to streamline trading by evaluating predefined rules based on prosumers' priorities and constraints. This algorithm considers factors such as battery State of Charge (SOC), charging and discharging costs, and market prices. It allows prosumers to manage their battery usage flexibly, optimizing energy trading based on real-time conditions and individual preferences. Cost functions for battery storage and peer-to-peer market transactions are defined to quantify the economic aspects of energy trading within the proposed algorithm. These functions incorporate factors such as battery capacity, depth of discharge, charging efficiency, and operational costs. The proposed rule-based algorithm and dynamic pricing model aim to address the complexities of P2P energy trading by providing a structured approach to decision-making. The model also helps prosumers make informed decisions based on the state of each energy source for optimal financial gain. A dynamic pricing mechanism is integrated to effectively boost market participation and resource utilization. Through simulations and mathematical formulations, this research seeks to optimize energy trading processes, enhance market interactions, and contribute to developing efficient and sustainable energy systems.

2 Literature Review

2.1 Peer-to-Peer Energy Trading Systems

Peer-to-peer (P2P) energy trading allows prosumers more control over their energy resources, participates in bidding processes to exchange energy, and reduces dependence on centralized suppliers. In this model, the physical layer facilitates the actual energy flow, while the virtual layer handles the exchange of information, as shown in Fig. 1 [9].

2.2 Dynamic Pricing Models

Dynamic pricing is essential for incentivizing prosumers (producers/consumers) and consumers in a P2P network. The goal is to reflect real-time supply-demand conditions while maximizing efficiency and fairness [6]. Time-of-use, Real-Time, Locational Marginal, and Auction-based pricing models incentivize prosumers to optimize energy usage, promote local trades, and create competitive, decentralized marketplaces for efficient energy balancing and cost reduction

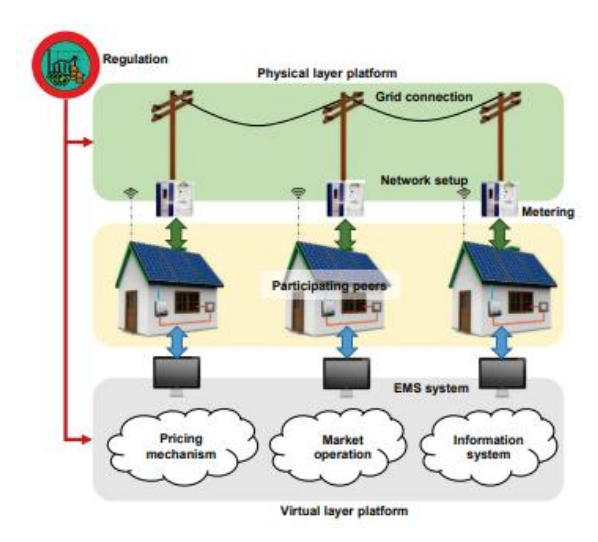


Fig. 1 P2P structure [9]

Dynamic pricing plays a critical role in enhancing the efficiency of energy trading, particularly in peer-to-peer (P2P) markets. By allowing electricity prices to fluctuate based on real-time factors such as supply, demand, and grid conditions, dynamic pricing aligns energy consumption and production more effectively, yielding several key benefits. Dynamic pricing in energy markets enhances load management, renewable energy utilization, and market efficiency by incentivizing consumers and prosumers to adjust their energy usage based on price signals. Additionally, dynamic pricing facilitates better trading strategies, market liquidity, and optimized resource allocation, leading to cost savings for consumers and more efficient energy distribution [5],[6].

Dynamic pricing introduces challenges such as price volatility, creating uncertainty for consumers and prosumers, necessitating advanced forecasting tools to optimize energy trading. Equity concerns arise, as consumers with limited flexibility to shift their energy usage may face higher costs, underscoring the importance of fair pricing models. Additionally, dynamic pricing must be carefully coordinated with grid stability mechanisms to prevent destabilization due to rapid, large-scale changes in consumption patterns [8].

2.3 Review Previous Work on Cost Functions and Optimization of BESS

Many studies have explored the market dynamics and price volatility in P2P energy trading. Authors Zhang [10] and Gao [11] highlight the potential benefits of P2P trading, with Zhang focusing on economic and technical benefits and Gao on reducing power purchase costs. Thomas [12] introduces a model for P2P trading, emphasizing the role of a policymaker in encouraging local generation or consumption. Ali provides a case study on the impact of variable spot prices on retailer income, finding that P2P trading can help reduce the impact of higher spot prices and improve network self-sufficiency [13]. These studies together emphasize the ability of P2P energy trading to reduce price fluctuations and enhance market dynamics. The research gap lies in developing an economic model that effectively motivates prosumers to engage in financially beneficial trading within P2P energy systems, particularly focusing on integrating solar PV systems with BESs. Most of the literature considered integrating BESS for effective P2P trading. Still, the literature does not fully address the cost associated with dispatching the batteries and managing battery charging and discharging according to consumer preference [8]. Furthermore, the existing literature emphasized the need for dynamic pricing for P2P trading. Das [4] and Lin [5] highlighted the need for a more comprehensive understanding of pricing mechanisms. However, this study lacks integration of BESS dynamics and time of energy trading into the pricing of the peer market. By dynamically adjusting prices based on supply and demand, consumers could be incentivized to use energy more efficiently and to reduce network strain during peak periods. The peer market price varies with the prosumer's battery SOC, reflecting the dynamic market pricing behavior throughout the day, which also requires further study [3]. Most of the literature on P2P models used flat tariff rates for grid selling/buying, and effective dynamic grid prices are not considered for evaluations, which could propose policy decisions in regulations in future P2P models [8]. Therefore, to address these research gaps, an economic model for P2P energy trading is proposed. This model incorporates dynamic pricing strategies and flexibility of resources (including BES) while considering prosumer preferences in BES utilization and achieving maximum cost benefit in P2P energy trading.

3 Methodology

3.1 Model for Multiple Prosumers' Energy Trading

This model describes the energy trading scenarios between multiple prosumers, where all prosumers and consumers are connected to the distribution grid. All prosumers have technological facilities to trade with the national electricity grid and trade with each other. It is assumed that all infrastructure is well maintained to establish secure transport of energy and transfer trading transaction information between prosumers. Fig. 2 illustrates such a system with prosumers installing solar PV on their premises with battery energy storage [14]. With the diverse energy sources, Fig. 3 illustrates potential measures that prosumers can undertake for energy trading while meeting their load demand. To improve market interactions, we devised an algorithm to optimize peer energy trading, minimize energy costs for participating prosumers, and maintain a reliable power supply. The developed algorithm uses the following proposed dynamic pricing structure to implement decision-making on the peer market prices of each peer involved in trading. This algorithm was then subjected to simulation using the MATLAB software, considering diverse constraints associated with the status of each entity involved.

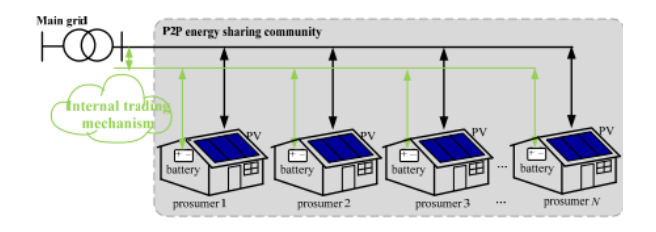


Fig. 2 Peer-to-peer energy sharing structure in a community grid [14]

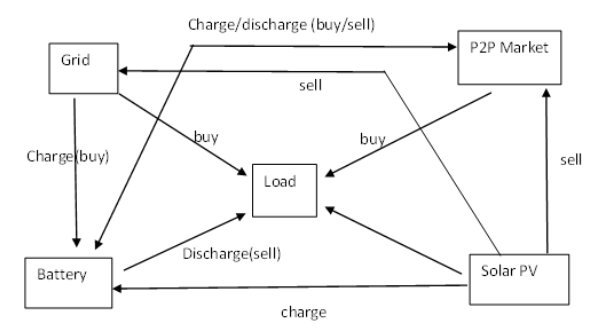


Fig. 3 Actions taken by prosumers engaging in peer energy trading

3.2 Dynamic Pricing Model Development

In a peer-to-peer energy trading environment, the selling price to the peer market is closely linked to the state of charge of the battery and the current demand and supply dynamics. Therefore, the pricing mechanism for peer-to-peer transactions depends on the energy levels stored in the battery and the availability of energy supply within the market. In this context, the cost of buying and selling is a function sensitive to the real-time state of the battery and the fluctuating dynamics of the peer market's energy supply and demand. The proposed cost function for peer-to-peer market selling price is given in Equation (1), representing real-time adjustments for the peer market prices.

$$C_{peer(h,t)} = C_{base(h,t)} + price \ adjustment \ due \ to \ weather + TOD \ price \ adjustment + SOC \ price \ adjustment(1)$$

 $C_{base(h,t)}$ is the base value determined by the selling consumer, comparing the existing grid price. When a consumer sells his excess energy to the peer market rather than to the grid, the base cost per unit can be determined by comparing it with the existing selling cost to the grid provided through power purchase agreements.

Price adjustment due to weather reflects the variation in peer market prices based on sunny or rainy conditions, influenced by the prosumer's willingness. On sunny days, the adjustment factor is negative, reducing prices. Conversely, on rainy days, the reduced energy availability from solar sources results in higher peer market prices, reflected by positive weather adjustment factors.

Time of Day (TOD) price adjustment reflects the variations in energy prices when sold to the peer market based on the time of day. Depending on demand during peak, off-peak, and daytime periods, this adjustment influences the overall peer market value differently. During peak hours, the adjustment has a positive value; during off-peak hours, it has a negative value; and during daytime periods, it also has a positive value, but lower than during peak hours. The prosumer's preferences determine the assigned values.

SOC price adjustment is crucial for determining peer market value. The state of charge of the prosumer's battery energy storage significantly influences the amount of energy sold to the peer market. When the battery is full, the

prosumer might sell excess energy at lower prices; however, with lower energy levels, the selling cost increases. This adjustment can be tailored to the prosumer's preferences across different SOC ranges. Consequently, the peer market price varies in each time slot based on the SOC levels of the prosumer's battery energy storage system.

The buying price from the peer market is derived from these interconnected selling prices. For house 'h,' the buying price will be the minimum selling price offered by other houses. Thus, when purchasing energy from the peer market, the consumer can search for peer-selling prices that are lower than the grid price.

3.3 Cost Function for Battery Energy Storage

The unit cost of battery energy storage is a critical component that directly affects the decision of the prosumer in the proposed algorithm. Several factors, such as battery type and technology, capacity, depth of discharge (DOD), charging and discharging efficiency, cycle life, Round Trip Efficiency (RTF), state of charge, operation and maintenance cost, and electricity prices in the grid, are involved in determining the cost of prosumer battery charging and discharging. The specific combination of these factors will vary based on individual circumstances, system configurations, and regional considerations.

Equation 2 calculates the cost of battery storage (UC(b)).

$$UC(b)\left(\frac{Rs}{kWh}\right) = \left(\frac{capital\ cost + 0\ \&\ M\ cost}{Battery\ capacity(kWh)*DOD*Cycles*RTF}....(2)\right)$$

Capital cost - the capital cost includes the cost of the battery system and the inverter.

O&M cost—Weniger suggested that annual operation and maintenance accounts for 1.5 % of the overall investment cost per year, considering the replacements of BESS [15]. Operation and Maintenance cost for household-level BESS is considered negligible for the proposed study since no such maintenance is required, indicating that it is considered insignificant for the calculation.

Equation 3 calculates the unit cost of the PV panel (UC ((pv)).

The actual daily operating hours of a solar PV system depend on the average sunlight hours on a particular day at its installed location. This can vary based on geographic location, weather conditions, seasonal change, etc. Energy from Solar PV is used to charge the BESS. Therefore, the unit cost of energy from solar PV is added when calculating the overall unit cost of BESS.

Equation 4 can be utilized to determine the overall unit cost of electricity for both battery charging and discharging. The prosumer needs to recover at least this unit cost of UC0 when dispatching one unit of his BESS to the peer energy market. According to the preference of the prosumer, the prosumer may add a profit margin to this unit cost to obtain profit in engaging in P2P energy trading. Therefore, this unit cost is the minimum cost of dispatching the BESS. Also, with higher SOC levels, the prosumer may sell his battery energy at a lower price, while the prosumer may increase his selling price when the SOC level decreases. Therefore, the optimal point for minimizing the unit cost occurs when the battery is charged up to its maximum SOC, highlighting the significance of SOC management in achieving cost-effective operation.

This research study considers the different charging and discharging willingness percentages of batteries (willingness of prosumers to manage their battery capacity) with different SOC levels. Therefore, for each combination unit cost of BESS should be defined. Equation 5 is proposed to calculate the unit cost with different SOC levels other than the maximum SOC. A maximum charging limit is introduced in this research to maintain the safe operation of the BESS. Otherwise, batteries can be fully charged up to 100%.

It was taken that K equals 1, therefore 1.00 rupees per 5% increase of SOC levels. The value of K may change according to consumer preference.

3.4 Algorithm for Optimization

In this research study, a rule-based algorithm has been developed to streamline energy trading among consumers. The algorithm relies on the consumer's choice of the most cost-effective energy source.

This system establishes pre-defined rules for prosumers based on their priorities and constraints. First, each prosumer meets their energy needs from their solar PV generation. Excess energy is used to charge their BESS or sold to the grid or peer market, depending on the associated costs. In case of energy deficits, prosumers prioritize discharging their BESS, considering costs and technical limits, or importing from the grid or market. Time-dependent factors such as grid prices, P2P market prices, BESS costs, storage capacity, solar availability, and demand are evaluated. The rules determine when to store, buy, or sell energy, and real-time P2P trading is executed based on these predefined rules. The proposed algorithm for energy trading among prosumers in a P2P market is based on factors such as battery energy levels, charging rates, prosumer preferences, peer market and grid prices, solar PV generation, and load demand. The main steps of the proposed algorithm are listed below.

Initialization: The algorithm initializes prosumer data, such as solar PV generation, load demand, battery capacity, willingness to charge/discharge, and cost components (grid and market prices) for each time interval of the day.

SOC and Charging Willingness Indexing: The algorithm identifies SOC and charging willingness indexes to calculate battery charging and discharging costs.

Cost Comparison: It calculates charging and discharging costs using a cost matrix(P_bat_cost) and compares them with peer market and grid prices.

Energy Trading Rules: If there's excess solar power, the battery is charged if costs are favorable. If the price is high, any extra energy is sold to the market or the grid.

If solar generation is insufficient, the algorithm prioritizes discharging the battery if the cost is lower than grid or market prices. If the battery can't cover the deficit, energy is purchased from the market or grid, depending on the prices.

Import and Export Handling: The algorithm manages energy imports from peers or the grid based on price and availability, seeking the lowest cost option for energy deficit.

SOC Update: Battery levels are updated according to charging and discharging actions, considering capacity limits.

Energy Trading Strategy Adjustment: Suggests adjusting peer market selling prices based on the battery's SOC, time of day, and weather conditions to optimize trading.

The energy balance equation defined in Equation 6 for prosumers in the proposed P2P energy trading algorithm ensures that energy supply matches demand at every interval.

```
\begin{split} P_{imp\_grid}(h,t) + P_{imp\_market}(h,t) + P_{pv}(h,t) + P_{bd}(h,t) \\ &= P_{exp\_grid}(h,t) + P_{exp\_market}(h,t) + P_{load}(h,t) + P_{bc}(h,t) \ for \ \forall \ h, \ \forall \ t \ ... \ ... \ ... \ ... \ ... \ ... \ ... \ ... \ ... \ ... \ ... \ ... \ ... \ ... \ ... \ ... \ ... \ ... \ ... \ ... \ ... \ ... \ ... \ ... \ ... \ ... \ ... \ ... \ ... \ ... \ ... \ ... \ ... \ ... \ ... \ ... \ ... \ ... \ ... \ ... \ ... \ ... \ ... \ ... \ ... \ ... \ ... \ ... \ ... \ ... \ ... \ ... \ ... \ ... \ ... \ ... \ ... \ ... \ ... \ ... \ ... \ ... \ ... \ ... \ ... \ ... \ ... \ ... \ ... \ ... \ ... \ ... \ ... \ ... \ ... \ ... \ ... \ ... \ ... \ ... \ ... \ ... \ ... \ ... \ ... \ ... \ ... \ ... \ ... \ ... \ ... \ ... \ ... \ ... \ ... \ ... \ ... \ ... \ ... \ ... \ ... \ ... \ ... \ ... \ ... \ ... \ ... \ ... \ ... \ ... \ ... \ ... \ ... \ ... \ ... \ ... \ ... \ ... \ ... \ ... \ ... \ ... \ ... \ ... \ ... \ ... \ ... \ ... \ ... \ ... \ ... \ ... \ ... \ ... \ ... \ ... \ ... \ ... \ ... \ ... \ ... \ ... \ ... \ ... \ ... \ ... \ ... \ ... \ ... \ ... \ ... \ ... \ ... \ ... \ ... \ ... \ ... \ ... \ ... \ ... \ ... \ ... \ ... \ ... \ ... \ ... \ ... \ ... \ ... \ ... \ ... \ ... \ ... \ ... \ ... \ ... \ ... \ ... \ ... \ ... \ ... \ ... \ ... \ ... \ ... \ ... \ ... \ ... \ ... \ ... \ ... \ ... \ ... \ ... \ ... \ ... \ ... \ ... \ ... \ ... \ ... \ ... \ ... \ ... \ ... \ ... \ ... \ ... \ ... \ ... \ ... \ ... \ ... \ ... \ ... \ ... \ ... \ ... \ ... \ ... \ ... \ ... \ ... \ ... \ ... \ ... \ ... \ ... \ ... \ ... \ ... \ ... \ ... \ ... \ ... \ ... \ ... \ ... \ ... \ ... \ ... \ ... \ ... \ ... \ ... \ ... \ ... \ ... \ ... \ ... \ ... \ ... \ ... \ ... \ ... \ ... \ ... \ ... \ ... \ ... \ ... \ ... \ ... \ ... \ ... \ ... \ ... \ ... \ ... \ ... \ ... \ ... \ ... \ ... \ ... \ ... \ ... \ ... \ ... \ ... \ ... \ ... \ ... \ ... \ ... \ ... \ ... \ ... \ ... \ ... \ ... \ ... \ ... \ ... \ ... \ ... \ ... \ ... \ ... \ ... \ ... \ ... \ ... \ ... \ ... \ ... \ ... \ ... \ ... \ ... \ ... \ ... \ ..
```

 $P_{imp\ arid}(h,t)$ – Electricity purchased from grid by h th prosumer at time t (kW)

 $P_{imp\ market}(h,t)$ – Electricity purchased from market by h th prosumer at time t (kW)

 $P_{pv}(h,t)$ – solar Pv generation at time t for h th prosumer (kW)

 $P_{bd}(h,t)$ — Battery discharging at time t for h th prosumer (kW)

 $P_{exp_qrid}(h,t)$ — Electricity sold to grid by h th prosumer at time t (kW)

 $P_{exp\ market}(h,t)$ – Electricity slod to market by h th prosumer at time t (kW)

 $P_{load}(h, t) - load$ at h th prosumer at time t (kW)

 $P_{hc}(h,t)$ – Battery charging at time t for h th prosumer (kW)

Three sets of constraints are imposed on the rules of P2P energy trading by solar PV generation, peer-to-peer market, and battery storage, which are also added to the algorithm formulation. Any P2P market should satisfy these constraints while participating in optimum energy trading. The algorithm ensures efficient P2P energy trading by balancing prosumer energy needs, solar PV generation, battery levels, and market/grid prices.

The proposed pricing model is simulated within multiple prosumer energy markets in a grid-connected distribution network.

4 Results and Discussion

4.1 Model Development and Simulation

Load data from different consumers in the existing LV distribution system is used for simulations. Fig. 4 illustrates the unit cost of selling and buying energy associated with the grid and the peer market for the data given in Table 1.

The unit cost of charging and discharging battery energy storage is calculated using Equation (5) and tabulated in a separate table as a matrix denoted as 'P_bat_cost'. The algorithm described in section 3.4 obtains and compares the exact unit cost (Rs/kWh) from this matrix based on the current SOC levels and desired charging and discharging willingness percentages at the exact time interval. In this work, lithium-ion batteries were considered. The energy cost in the peer market 'C_peer' varies with the current SOC levels and TOD adjustment for each simulation step; therefore, the cost variation in the peer market occurs with time and capacity of the battery.

Peers Identity	No SolarPV panels	Efficiency of Solar PV	BESS Capacity(k Wh)	Initial BESS Capacity (kWh)	Willingness to charge (%)	Willingness of discharging (%)
H1	4	0.2	5	1	100%	100%
H2	5	0.2	5	1	100%	100%
Н3	3	0.2	4	1	100%	100%
H4	4	0.195	5	1	100%	100%
S5	0	-	0	-	-	-
Н6	0	-	0	-	-	-
S7	0	-	0	-	-	-
Н8	4	0.195	5	1	100%	100%

Table 1 Details of prosumers in the P2P market

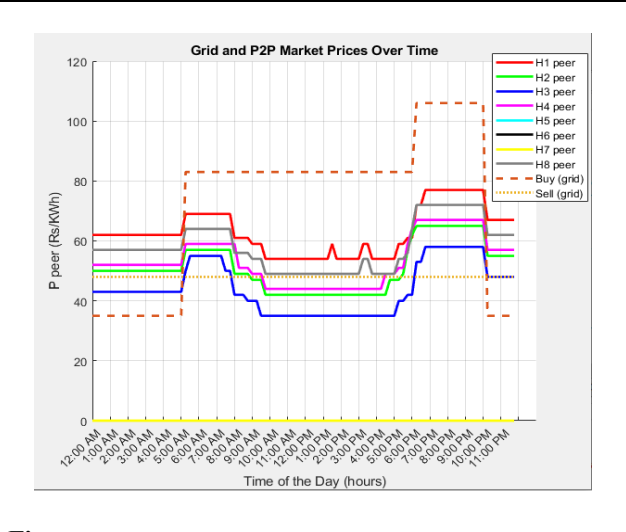


Fig. 4 Unit cost variation of the grid and peer market over time

4. Results

4.1 Simulation Results for Simultaneous Energy Sharing

According to the prosumer/consumer details provided in Table 1, the simulation results in Fig. 5 show the load demand and solar PV generation in each house throughout the day. The simulations were carried out considering that the market's spot pricing is changed every 15 minutes, so all the demand and generation variations are counted towards that interval. Fig. 5 shows that there is excess solar PV generation in 5 houses during the daytime, so that they can sell that excess energy to the grid or market or store it in a battery for future use. The decision depends

on the cost associated with each element and technical limitations such as SOC levels and energy demand from the peers.

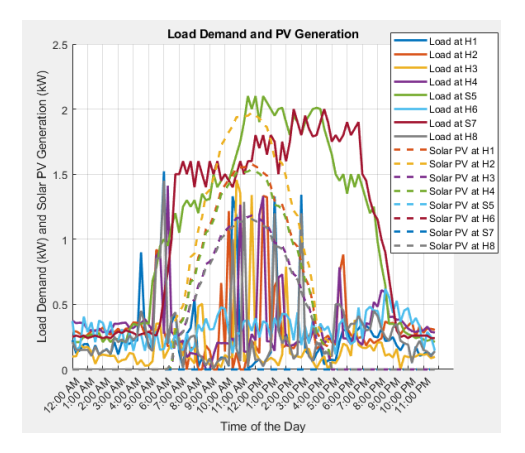


Fig. 5 Load demand and Solar PV generation in each household

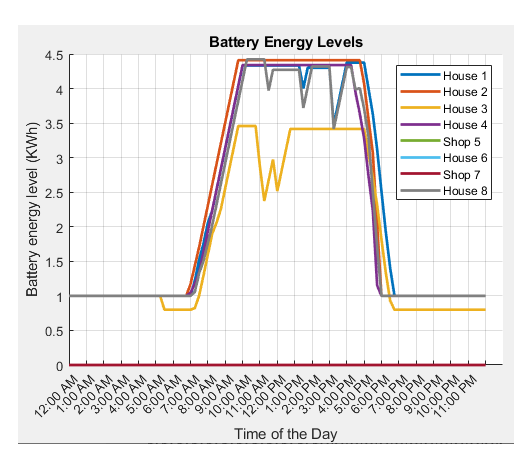


Fig. 6 Variation of battery energy status in each household

The proposed model can include prosumers' willingness to charge and discharge batteries as a percentage. Fig. 6 shows the variation of battery energy status for the battery capacities mentioned in Table 1 with 100% charging and discharging willingness of all prosumers. In specific households, it is observed that the demand is met by utilizing battery storage during the morning peak load, around 6.00 AM to 7.00 A.M.. This choice is influenced by the lower cost of utilizing battery storage compared to other sources, such as the grid and peer market. When Solar generation starts at around 7.00 AM, the batteries are charged and may reach their maximum capacity levels. At night, peak energy from the batteries can be dispatched to meet the demands. If surplus energy exceeds the demand, it can be sold on the peer market. Such decisions depend on the associated cost components at the given time.

Fig. 7 illustrates the surplus energy sold to the grid and the peer market, as determined by the rules outlined in the developed algorithm. Notably, the model enforces limitations on the amount of energy exported from battery storage to safeguard its integrity. This safeguarding mechanism assumes the implementation of a current-limiting circuit within the battery storage system during energy discharge to either the grid or the peer market.

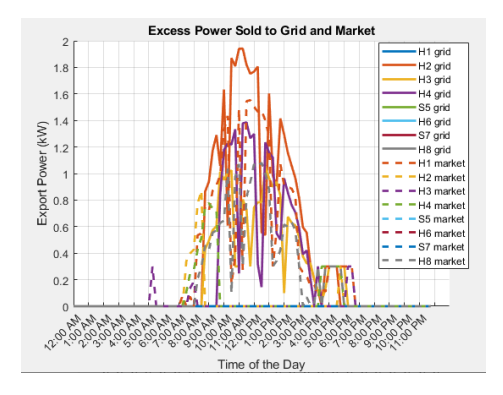


Fig. 7 Excess energy exported to the grid and peer market

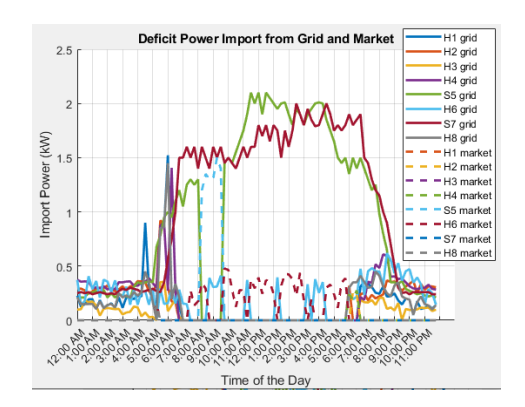


Fig. 8 Excess energy imported from the grid and peer market

During periods with insufficient solar generation available for sale, prosumers opted to share the surplus energy stored in their batteries with other prosumers, provided that their battery constraints allow it. In Fig. 6, particularly during the early morning, around 05:00 AM, and in the evening, around 05:00 PM to 07:00 PM, the excess energy sold originates from the batteries due to the absence of solar generation. Fig. 8 illustrates the energy imported by

each household prosumer to fulfill their load requirements during insufficient solar energy availability. The decision-making process relies on the associated cost components at that time and the energy availability from the peer market for importing. The data reveals that during the early morning period and late at night, following the peak demand time, prosumers rely entirely on energy imports from the grid or the peer market. This reliance is dictated by the energy availability and the unit cost considerations prevailing at that specific time.

Figs 9(a) to 9(h) present a comprehensive overview of the energy management strategies implemented by individual prosumer households within the peer energy trading framework, as outlined in Table 1. Including the representation of prosumers' battery status in the same graph provides valuable insights into understanding battery behavior alongside energy trading dynamics. This integrated visualization facilitates a comprehensive understanding of how battery storage is utilized in response to varying energy demands and market conditions. Houses H1, H2, H3, H4, and H8 show sudden load demand variations due to the usage of water heaters installed, and all prosumers can handle this sudden load variation either by taking energy from the grid or dispatching their BES, depending on the status of the battery. This highlights that the proposed model can effectively manage load variations within a peer-to-peer energy market, ensuring a balanced and reliable energy distribution system.

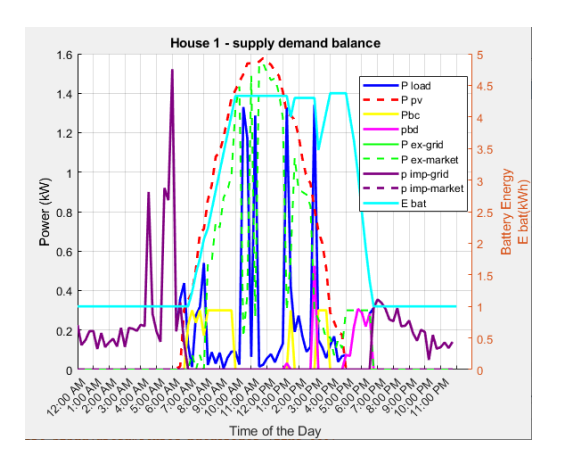


Fig. 9(a) Energy management in H1

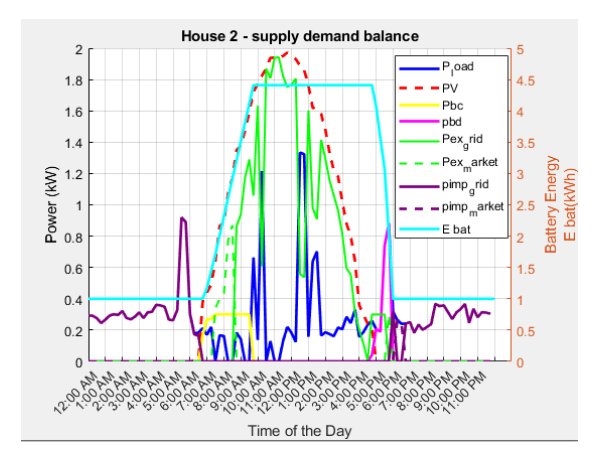


Fig. 9(b) Energy management in H2

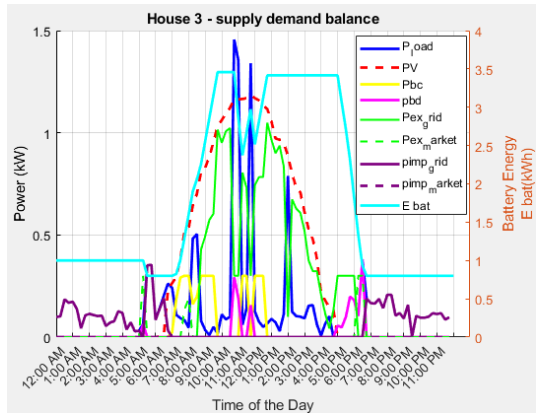


Fig. 9(c) Energy management in H3

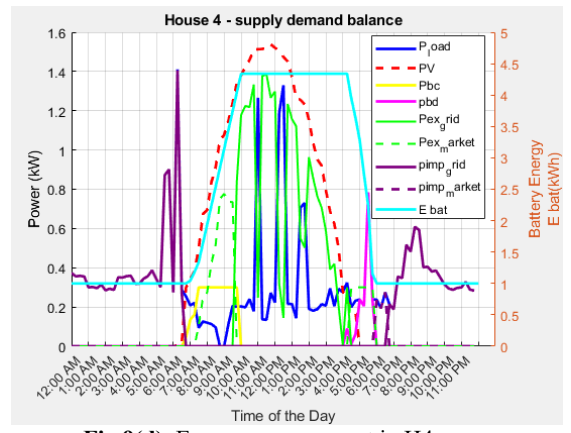


Fig.9(d) Energy management in H4

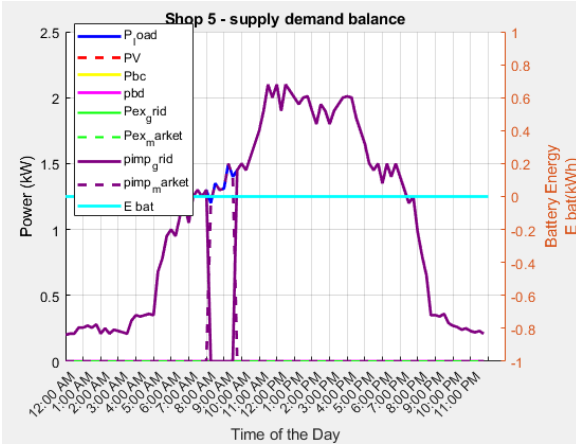


Fig.9(e) Energy management in S5

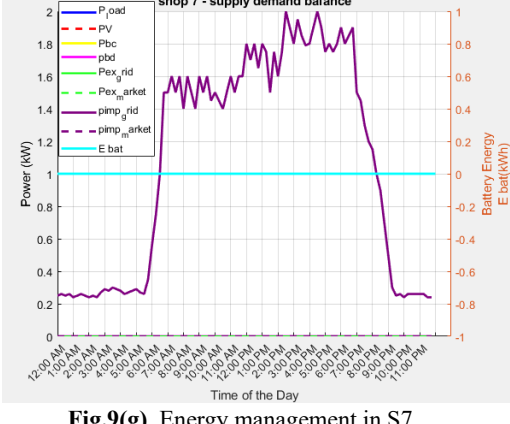


Fig.9(g) Energy management in S7

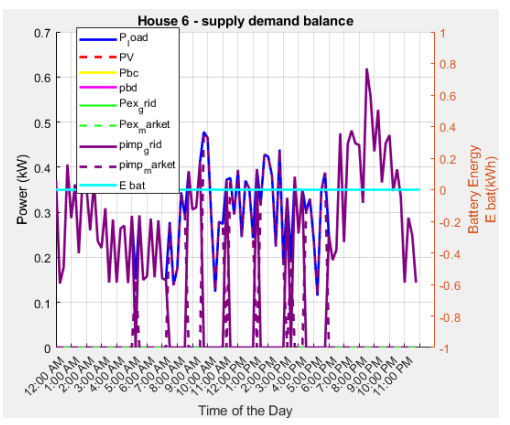


Fig.9(f) Energy management in H6

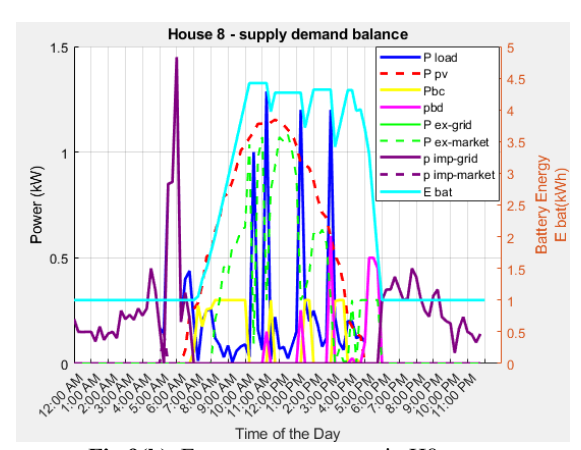


Fig.9(h) Energy management in H8

4.2 Simulations with Dynamic Peer-To-Peer Prices

The proposed algorithm undergoes testing with different peer energy selling rates. The selling rate at which each prosumer decides to sell one unit to the peer-to-peer market is characterized by his own decisions, such as energy availability and the prosumer's profit margin. Therefore, a fixed set of base prices is defined for each prosumer, which may be altered according to the prosumer's willingness. This defined base price for each prosumer, along with battery SOC levels and TOD adjustments, causes the selling price of prosumers to vary.

We assess the impact of peer market price fluctuations on export and import energy by adjusting the values of base prices within Equation (1) while keeping the other two adjustment variables constant during simulations. Fig.10 and Fig. 11 showcase the energy trading quantities corresponding to different selling prices for peers, achieved by altering the base prices of each prosumer as outlined in Table 2. After analyzing both Figures, it's apparent that the export energy quantities vary in response to the adjusted peer market selling rate. Consequently, there are fluctuations in the amount of imported energy as well.

Table 2 Variation of base prices in each prosumer

Prosumer	(case I) Initial base price (Rs/kWh)	(case II) Altered base price (Rs/kWh)		
H1	65	60		
Н2	53	45		

Н3	46	50
H4	55	65
S5	0	0
Н6	0	0
S7	0	0
Н8	60	85

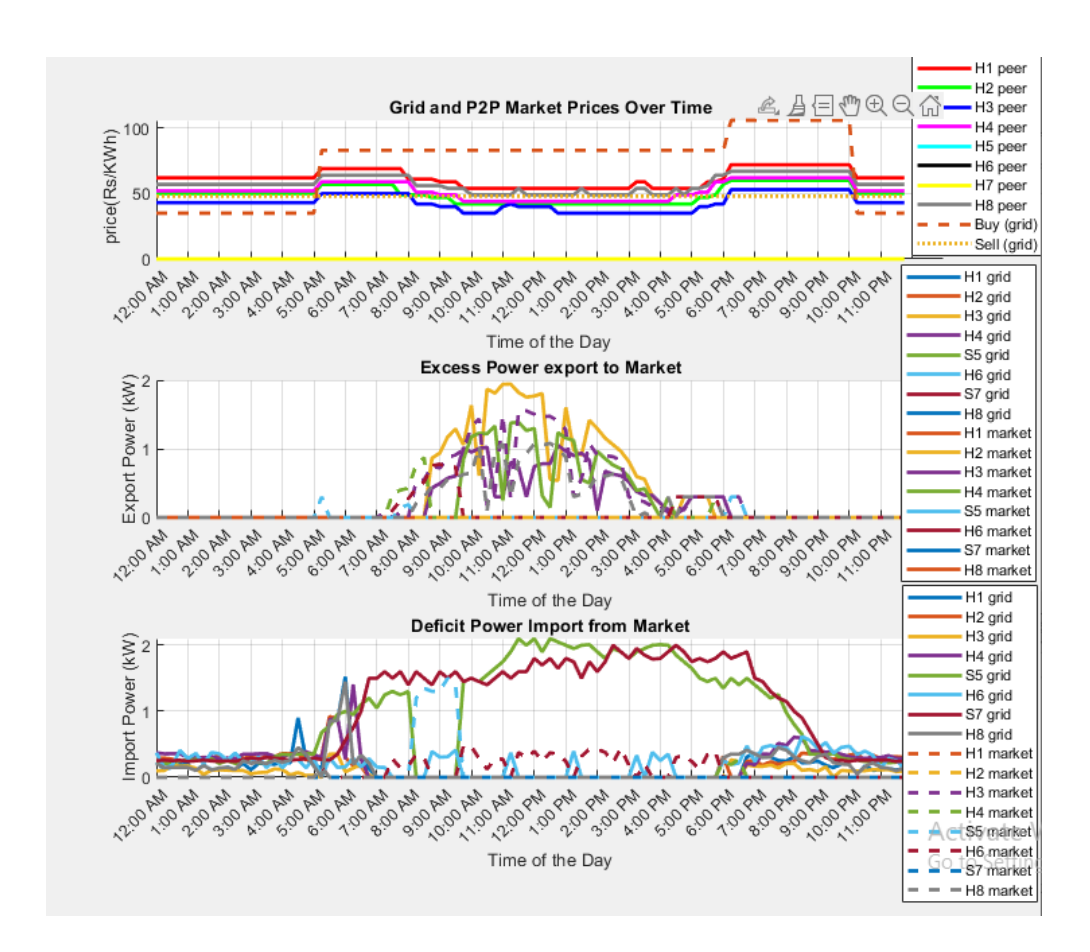


Fig. 10 Case I: Energy trading quantities

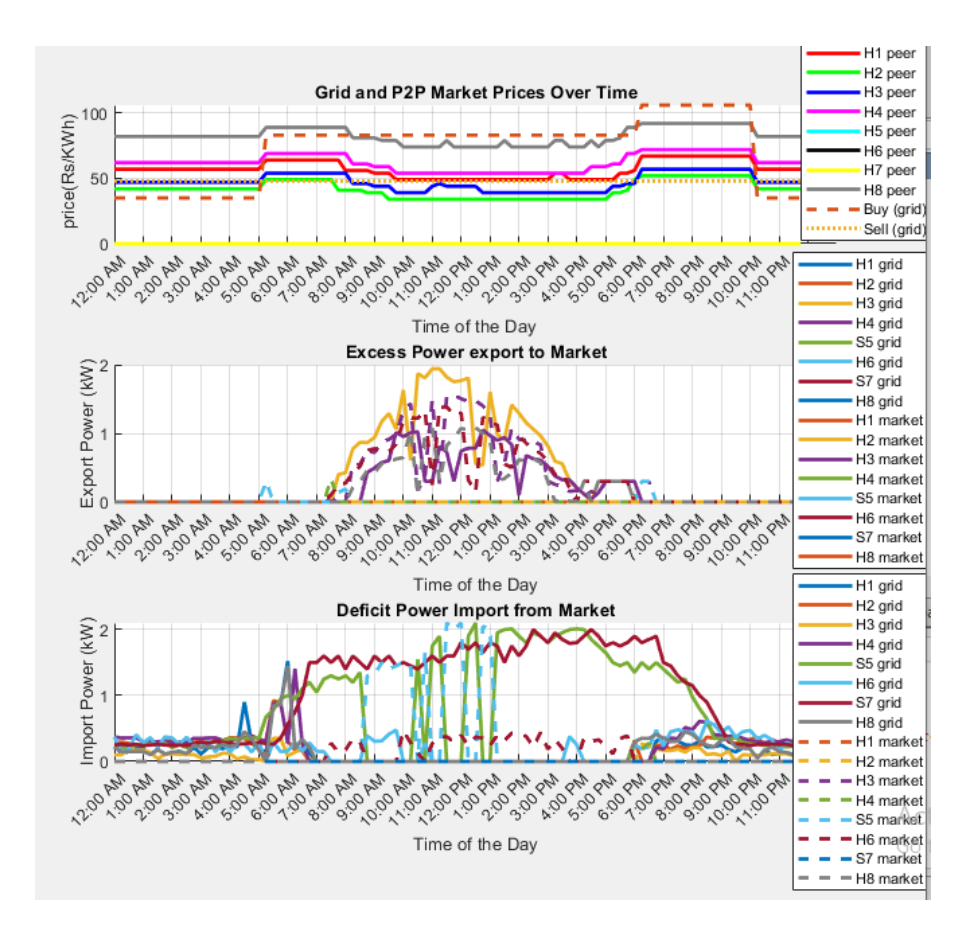


Fig. 11 Case II: Energy trading quantities

In Fig. 10, a significant exporter in the peer market during daytime is H3, where, with altered base prices, new suppliers appear in the markets as H1 and H8, as shown in Fig. 11. In Fig. 10, H6 and S5 import energy from the peer market in most periods, whereas in Fig. 11, with altered base prices, energy import from the peer market by S5 significantly increased during the 10.00 a.m. to 1.00 p.m. period.

The result demonstrates the export and import energy variations from each prosumer corresponding to the dynamics of market prices and resource availability, which are reflected in the quantities sold and bought. All peers adjusted their selling and buying energy in parallel with the new prices in each defined time interval.

5 Discussion

The proposed model facilitates energy's physical transmission and reception through the existing grid network. It is noted from simulations that energy transactions within the proposed P2P system comply with the current limits of energy transfer for LV-connected Solar PV systems. Consequently, the study does not evaluate grid stability variations, as these transactions are not expected to disrupt grid stability. However, it also recognized some limitations, like the absence of working peer-to-peer energy trading systems in Sri Lanka, which could affect how applicable the findings are in real-life situations. Prosumer and consumer behavior in this proposed market are incorporated into the model, such as the willingness to charge and discharge the battery as percentages that help prosumers actively participate in energy trading as desired. This helps regulate the peer energy market by controlling the prosumers. Also, by introducing a peer market price function, which depends on the SOC of each BES, the proposed model captures the market dynamics.

In the proposed algorithm, for each 15-minute spot pricing interval, the prosumer's BES status is updated, and batteries are dispatched to the peer market depending on their status. BES technical limitations are considered the maximum and minimum limits of battery capacity, and those rules are incorporated as constraints to the energy balance equation described in Eq (6). The RTF of each prosumer battery is considered to calculate the unit cost, as described in equation (3), which represents the integration of battery performance into the model. This research aims to develop a simplified economic model that incorporates dynamic pricing and effective battery management; therefore, a rule-based approach is used to develop the algorithm. Machine learning and complex optimization algorithms are used in different studies, which could lead to a more complicated and sophisticated formulation of

the trading environment, which needs a lot of data to fine-tune the models. Considering the absence of such data in the Sri Lankan Scenario, the proposed model limits the study to rule-based algorithm development, where the algorithm is developed based on the cost of energy.

This research mainly focuses on studying market dynamics based on dynamic pricing and incorporating flexibility through battery management; the study will not deeply investigate the framework for transactions and the bidding process, which could be developed in future research using trading platforms such as Blockchains.

6 Conclusion and Future Work

This study developed an economic model for peer-to-peer energy trading while participants get maximum benefits. Therefore, a cost-based algorithm enhanced P2P trading to maximize participants' benefit. Charging and discharging of BESS is determined based on the associated unit cost while taking SOC and prosumer willingness to use the batteries as indices. The developed algorithm also integrates dynamic peer market pricing into the model. The peer market price depends mostly on the availability of energy resources, storage status, and time of day. The simulation results proved that the proposed price function matches the real-world scenario, and price dynamics can change the pattern of energy trading quantities in defined time intervals.

The analysis highlights several policy implications for microeconomic markets where prosumers and consumers engage in energy trading. Policymakers should incentivize flexible energy storage and solar PV systems to encourage participation in P2P energy trading, offering financial incentives like subsidies or feed-in tariffs. Establishing clear regulatory frameworks is essential to ensure fair market operations, covering grid connection, pricing, metering, and consumer protection. Regulations should address grid connection, metering, pricing mechanisms, and consumer protection to develop trust and confidence in P2P energy markets. Additionally, policies regarding the technical upgrade of the existing system for two-way communication need to be addressed. Challenges may arise in developing these new regulations and frameworks. Still, the framework could align well with the country's goals of enhancing renewable energy adoption and transitioning towards a sustainable and decentralized energy system.

Future research in P2P energy trading could focus on advanced modeling techniques, such as machine learning and agent-based models, to better capture market dynamics. It could also explore novel market mechanisms, emerging technologies like blockchain and smart grids, and policy evaluation to address challenges in P2P trading. Additionally, bridging the gap between simulations and real-world applications through pilot projects would help validate the scalability and feasibility of P2P energy trading systems, contributing to sustainable and economically beneficial practices in the energy sector.

References

- [1] Huang, H., Nie, S., Lin, J., Wang, Y., and Dong, J. (2020). Optimization of peer-to-peer power trading in a microgrid with distributed PV and battery energy storage systems. Sustainability, 12(3), 923. https://doi.org/10.3390/su12030923
- [2] Dynge MF, del Granado PC, Hashemipour N, Korpås M.(2021). Impact of local electricity markets and peer-to-peer trading on low-voltage grid operations. Applied Energy, 301:117404. https://doi.org/10.1016/j.apenergy.2021.117404
- [3] Liu, Y., Zuo, K., Liu, X. (Amy), Liu, J., & Kennedy, J. M. (2018). Dynamic pricing for decentralized energy trading in micro-grids. Applied Energy, 228, 689–699. https://doi.org/10.1016/j.apenergy.2018.06.124
- [4] Das, A., Peu, S. D., Akanda, Md. A. M., & Islam, A. R. Md. T. (2023). Peer-to-Peer Energy Trading Pricing Mechanisms: Towards a Comprehensive Analysis of Energy and Network Service Pricing (NSP) Mechanisms to Get Sustainable Enviro-Economical Energy Sector. Energies, 16(5), 2198. https://doi.org/10.3390/en16052198
- [5] Lin, J., Pipattanasomporn, M., & Rahman, S. (2019). Comparative analysis of auction mechanisms and bidding strategies for P2P solar transactive energy markets. Applied Energy, 255, 113687. https://doi.org/10.1016/j.apenergy.2019.113687
- [6] Das, A., Peu, S. D., Akanda, Md. A. M., & Islam, A. R. Md. T. (2023). Peer-to-Peer Energy Trading Pricing Mechanisms: Towards a Comprehensive Analysis of Energy and Network Service Pricing (NSP) Mechanisms to Get Sustainable Enviro-Economical Energy Sector. Energies, 16(5), 2198. https://doi.org/10.3390/en16052198
- [7] Huang, H., Nie, S., Lin, J., Wang, Y., & Dong, J. (2020). Optimization of Peer-to-Peer Power Trading in a Microgrid with Distributed PV and Battery Energy Storage Systems. Sustainability, 12(3), Article 3. https://doi.org/10.3390/su12030923

- [8] Long, C., Wu, J., Zhou, Y., & Jenkins, N. (2018). Peer-to-peer energy sharing through a two-stage aggregated battery control in a community Microgrid. Applied Energy, 226, 261–276. https://doi.org/10.1016/j.apenergy.2018.05.097
- [9] Tushar, W., Saha, T. K., Yuen, C., Azim, M. I., Morstyn, T., Poor, H. V., Niyato, D., & Bean, R. (2020). A coalition formation game framework for peer-to-peer energy trading. Applied Energy, 261, 114436. https://doi.org/10.1016/j.apenergy.2019.114436
- [10] Zhang, B., Du, Y., Lim, E. G., Jiang, L., & Yan, K. (2019). Design and Simulation of Peer-to-Peer Energy Trading Framework with Dynamic Electricity Price. 2019 29th Australasian Universities Power Engineering Conference (AUPEC), 1–6. https://doi.org/10.1109/AUPEC48547.2019.211948
- [11] Gao, X., & Zhang, T. (2023). Peer-to-Peer Electricity Trading Strategy Considering Dynamic Network Fee. 2023 3rd International Conference on Energy, Power and Electrical Engineering (EPEE), 1395–1398. https://doi.org/10.1109/EPEE59859.2023.10351908
- [12] Thomas, A., Abraham, M. P., & G, A. M. (2021). Analysis of Peer-to-Peer Energy Trading in a Dynamic Environment Using Stackelberg Game. 2021 Seventh Indian Control Conference (ICC), 412–417. https://doi.org/10.1109/ICC54714.2021.9703159
- [13] Ali, L., Peters, J., Azim, M. I., Pashajavid, E., Bhandari, V., Menon, A., Tiwari, V., Ghosh, A., & Green, J. (2022). How P2P Trading Helps an Electricity Retailer Exposed to Volatile Spot Prices: A Case Study. 2022 IEEE Sustainable Power and Energy Conference (iSPEC), 1–5. https://doi.org/10.1109/iSPEC54162.2022.10033038
- [14] Long, C., Zhou, Y., & Wu, J. (2019). A game theoretic approach for peer-to-peer energy trading. Energy Procedia, 159, 454–459. https://doi.org/10.1016/j.egypro.2018.12.075
- [15] Weniger, J., Tjaden, T., & Quaschning, V. (2014). Sizing of Residential PV Battery Systems. Energy Procedia, 46, 78–87. https://doi.org/10.1016/j.egypro.2014.01.160

Optimal Placement of Multiple Distributed Generators Using Genetic Algorithm for Power Loss Minimization in the Distribution Networks

K.M.G.Y. Sewwandi 1*, K.A.C. Udayakumar¹, K.T.M.U. Hemapala²

¹Department of Electrical and Computer Engineering, the Open University of Sri Lanka ²Department of Electrical Engineering, University of Moratuwa, Sri Lanka

kmsew@ou.ac.lk, kauda@ou.ac.lk, udayanga@uom.lk

Abstract

This paper investigates optimizing Distributed Generators (DGs) in power distribution networks, focusing on minimizing power losses while improving voltage profiles. DGs are decentralized power generation systems that do not rely on long-distance transmission through a central grid, and their integration into distribution networks has increased significantly in recent years. The benefits of DGs, such as enhanced voltage profiles, improved reliability, stability, and power quality, are highly dependent on the proper placement and sizing of the units. In contrast, improper installation can lead to increased power losses and degraded voltage profiles, negatively impacting the overall performance of the distribution network.

To address these challenges, this study employs a genetic algorithm-based optimization technique to determine the optimal size and location of DG units to minimize power losses. The methodology is applied to a 33-bus system, analyzing four configurations with varying DG units. The results demonstrate the effectiveness of the proposed approach, achieving significant reductions in power losses and improvements in voltage profiles. Notably, the findings also indicate that adding more DG units does not justify the increased costs, as the incremental benefits in loss reduction become marginal with each additional unit. This highlights the importance of balancing the number of DGs and their associated costs to achieve optimal system performance.

Keywords: Distributed Generation (DG), Optimal DG Placement, Genetic Algorithm (GA), Distribution Loss Minimization, Voltage Profile Enhancement

1 Introduction

The current electricity supply structure, traditionally dominated by large, centralized power stations, is evolving into a more decentralized system with centralized and distributed generation [1] - [2]. In this changing landscape, distribution systems are critical, as their efficiency directly affects end consumers. Therefore, proper planning of distribution systems is crucial to enhance their performance and efficiency. With the continuous increase in load demand, expanding the existing power systems has become necessary to meet customers' needs. While effective, conventional expansion methods, such as transformer upgrades and feeder reconfigurations, are often complex and uneconomical. To address these challenges, Distributed Generators (DGs) have emerged as a favorable solution for distribution expansion planning [1], [3].

DGs are small-scale power generation systems near the point of use, bypassing the need for long-distance transmission through a central grid [4]. In recent years, the integration of DGs into distribution networks has grown rapidly due to their potential benefits, including enhanced voltage profiles, improved reliability, increased stability, and better power quality. However, the success of DG integration heavily depends on the correct placement and sizing of the units [4] - [10]. Improper installation can lead to undesirable outcomes, such as increased power losses and degraded voltage profiles, which ultimately harm the performance of the distribution network [11] - [16], [19] - [34].

These issues highlight the importance of careful planning and optimization in DG integration. Advanced optimization techniques can be applied to determine DGs' optimal size and location, maximizing their benefits while minimizing negative impacts on the system [34]. This paper explores these optimization techniques, demonstrating their effectiveness in enhancing system performance and addressing the challenges associated with DG placement and sizing in distribution networks.

2 Literature Review

2.1 Effects of Distributed Generation on the Distribution Network

Over the past two decades, the number of DG units has surpassed that of traditional large-scale power stations, significantly transforming the conventional structure of electrical supply systems. Traditional distribution networks, designed for unidirectional power flow from central generators to consumers, experience predictable voltage drops as the distance from the generator or transformer increases. These voltage drops are accounted for

in network design to ensure acceptable voltage levels under normal conditions. However, with the global demand for electricity rising rapidly, many distribution systems are now operating at or near their maximum capacity [2]. As more loads are connected, system losses tend to increase, making DG a practical solution for mitigating these losses [8].

Despite the benefits, integrating DG into radial distribution networks introduces challenges, especially when multiple DG units operate at high capacity, potentially causing reverse power flow [3]. Furthermore, improper placement of DG units can lead to increased network losses, surpassing those seen in the base case without DG integration. This highlights the importance of strategic planning in DG placement and sizing to prevent unintended consequences, such as inefficient energy distribution [5] – [9].

Additionally, different types of DG units exhibit distinct operational characteristics, which can lead to various power quality issues when incorporated into the distribution network. Common concerns include voltage fluctuations, harmonic distortions, and frequency variations, all of which must be carefully managed to maintain power quality within permissible limits [3]. Failing to do so can compromise grid reliability and negatively affect the performance of connected loads. Furthermore, load imbalances across phases can negatively impact the operation of DG units, cause inefficient power distribution, and accelerate equipment wear. As a result, addressing load balancing and power quality management is crucial for successfully integrating DG units into modern distribution networks [3], [8].

2.2 DG Placement Optimization

Although distributed generation offers numerous significant advantages for the distribution network, improper placement of DG units can lead to increased network losses beyond the base case. Most of the researchers highlighted that the random placement of DGs can result in heightened system losses, deteriorated voltage profiles, and other issues that may ultimately lead to increased operational costs [11] - [16], [19] - [34]. Therefore, careful consideration is essential when determining the capacity and location of these DG units. Optimal allocation and sizing of DGs are crucial for maximizing their operational efficiency and economic benefits, ensuring that the integration of DGs enhances overall system performance. To identify optimal configurations for DG placement, various algorithmic methods have been developed, focusing on minimizing or maximizing objective functions.

Analytical approaches are the earliest methods used in optimization problems [11] – [16]. They are known for their simplicity and offer a higher degree of accuracy compared to other categories. These techniques are commonly found in older research papers and often provide exact solutions within a reasonable time frame. Typically, these methods involve solving fewer equations based on relatively simple theoretical concepts. As a result, they require less computational time, leading to a high accuracy-to-computation time ratio. Despite these advantages, analytical approaches have a few notable limitations. A major drawback is that they cannot be applied when the distributed generation optimization problem involves multiple objectives or constraints. The primary focus of these methods is on minimizing power losses, and the constraints they address are generally limited to power flow-related factors, such as the relationship between power generation, demand, network losses, and voltage limits. However, when stability and reliability constraints must be considered, these approaches are unsuitable for DG optimization. Among the analytical methods, the exact loss formula-based techniques are considered the most reliable, as they achieve higher percentages of loss reduction.

In addition to the analytical approaches, which were predominantly used in earlier research, other DG optimization methodologies can be broadly classified into two main categories: metaheuristic and artificial intelligence-based approaches. The following metaheuristic algorithms have been widely employed in the literature for the strategic allocation of distributed generation in distribution networks: Particle Swarm Optimization (PSO), Genetic Algorithm (GA), Ant Colony Optimization (ACO), and Simulated Annealing (SA) [17] - [32]. All these metaheuristic methods are nature-inspired and effective for single-objective and multi-objective DG placement optimization problems. The accuracy of results obtained from these approaches is generally higher than other techniques. When the optimization problem involves many objectives and constraints, metaheuristic algorithms are the most suitable choice. However, the results can vary due to their iterative nature and dependence on initial random approximations, sometimes leading to lower convergence efficiency when approaching optimal solutions. Among these, genetic algorithm-based and particle swarm optimization-based methods are the most commonly used metaheuristic approaches in the literature [19] – [31].

This research aims to develop a genetic algorithm-based approach for optimizing DG placement in distribution networks. As per the existing literature, GA-based methods are one of the most effective methods of mathematical approaches, consistently producing reliable and accurate results in distributed generation optimization problems. The genetic algorithm is inspired by natural selection, where potential solutions evolve over successive iterations to find the optimal configuration [17] – [18]. This ability to simulate evolutionary processes allows GAs to efficiently explore large, multidimensional solution spaces. Additionally, GA adapts well to complex constraints, making it particularly well-suited for optimizing the placement and sizing of DG units, where multiple variables

such as location, capacity, power loss, and system reliability need to be considered. GA's advantage lies in its ability to perform well in single- and multi-objective optimization problems. For instance, when the main objective is the minimization of power loss, GAs can find configurations that achieve significant loss reductions while respecting operational constraints like voltage limits and power flow.

3 Proposed Optimization Approach

3.1 Genetic Algorithm

Genetic Algorithm is a popular nature-driven metaheuristic approach that is well-suited for formulating distributed generation sizing and sitting problems [19- [25]. When compared with the other popular metaheuristic approaches such as PSO, ACO, SA, and hybrid algorithms, GA utilizes a population of solutions, which improves their exploration of the search space while reducing the likelihood of premature convergence and increasing the ability to escape local optima, leading to more robust optimization outcomes [35]. However, when considering techniques like PSO, the optimization is biased towards swarm leaders, which can lead to premature convergence [36]. Also, Ant Colony Optimization (ACO) uses pheromone trails to guide ants, but this can cause stagnation if a suboptimal path gains excessive pheromone early on, limiting exploration. When this happens, the algorithm may overly exploit the favored path, reducing the exploration of alternative routes [37]. This limitation is not observed in approaches based on Genetic Algorithms. On the other hand, SA is a single-solution method, which requires careful tuning to escape local optima [38].

GA possesses a significant advantage in its inherent parallelizability, as each solution within the population can be evaluated independently. This characteristic makes GAs particularly well-suited for distributed computing environments, where multiple solutions can be processed simultaneously to expedite optimization [39]. In contrast, PSO and ACO offer limited potential for parallelization due to their reliance on collective interactions among particles or ants. SA has a sequential nature and encounters significant challenges in parallel implementation, as its iterative process relies on the results of preceding steps [40].

As mentioned earlier, GA performs a global search by evaluating multiple points within the search space, with each point representing a potential solution, or population [17]. Unlike traditional optimization methods, which may focus on local improvements, GAs maintain and evolve a population of solutions over successive iterations, using genetic operators such as selection, crossover, and mutation to explore new solutions and refine existing ones [17] – [18]. The use of these diverse genetic operators offers significant flexibility to the DG placement problem, while other metaheuristic approaches like PSO rely only on fixed velocity and position updates with limited customization capabilities. Also, the population of potential solutions is expected to converge towards an optimal solution through repeated application of these genetic operators. To implement genetic programming effectively, several preparatory steps are essential. The human user must define the problem in a structured manner, translating the high-level problem statement into parameters and constraints that the GA system can use. These preparatory steps form the foundation for developing the GA algorithm, ensuring it is well-suited to solving the specific problem of DG placement and sizing. Following these steps, the GA can efficiently search the solution space and find near-optimal configurations for integrating DG units into the distribution network.

3.2 Sizing & Placement of DG Using Genetic Algorithm

The problem of determining the optimal placement and sizing of Distributed Generators (DGs) can be formulated with a focus on minimizing power losses in the distribution network. The objective is to identify strategic locations for DGs that minimize power losses, ensuring the overall system operates economically. A DG's penetration level refers to the percentage of the total load demand that it supplies efficiently. The problem can, therefore, be framed as finding the most economically viable locations and corresponding sizes for different types of DGs to achieve maximum cost savings.

Proper DG placement within the power system is crucial to realizing their benefits. The goal is to determine the optimal size and location for DG units in the distribution network while ensuring that the voltage at each bus remains within the acceptable range of 1 ± 0.05 p.u. Additionally, the loading of transmission lines must be kept within specified MVA limits to maintain system stability and efficiency. Figure 1 presents the flowchart of the developed GA-based algorithm, which is designed to optimize the size and placement of DGs to meet these objectives effectively.

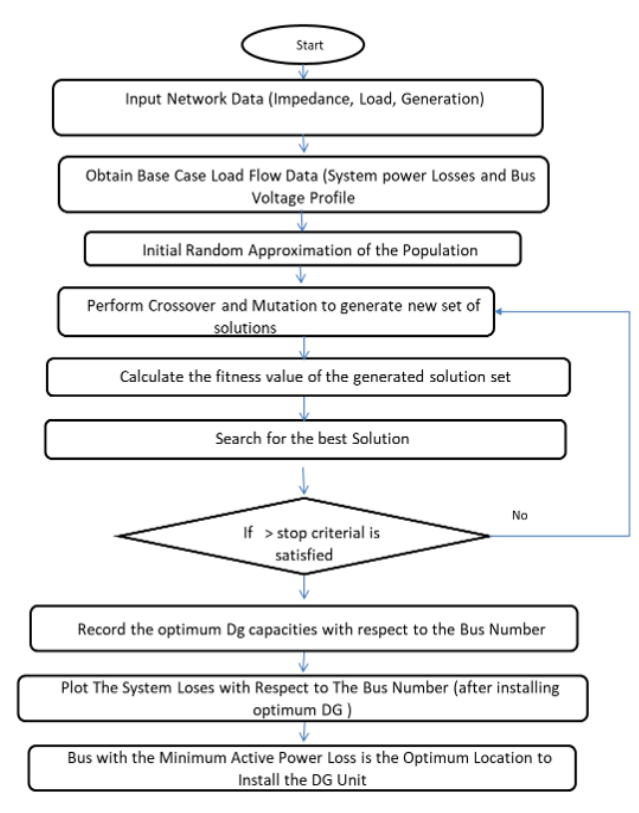


Fig. 1 Algorithm Flowchart

4 Model Development and Simulation

The IEEE 33-bus standard test system was selected for modeling and simulation to evaluate the proposed DG optimization approach's effectiveness. The IEEE 33 bus system is a widely used test network in power system studies, particularly for assessing the performance of optimization algorithms in distribution networks [29]. In this study, it was assumed that the renewable distributed generator produces both active and reactive power and a power factor of 0.9 was assumed.

4.1 Base Case Simulation

In this study, the IEEE 33-bus network was modeled under the Power World platform, and power flow analysis was conducted initially to determine the base case factors, such as initial power losses and the test system's initial voltage profile. The base case power flow simulation model is shown in Figure 02, and the base case bus voltage profile is shown in Figure 03.

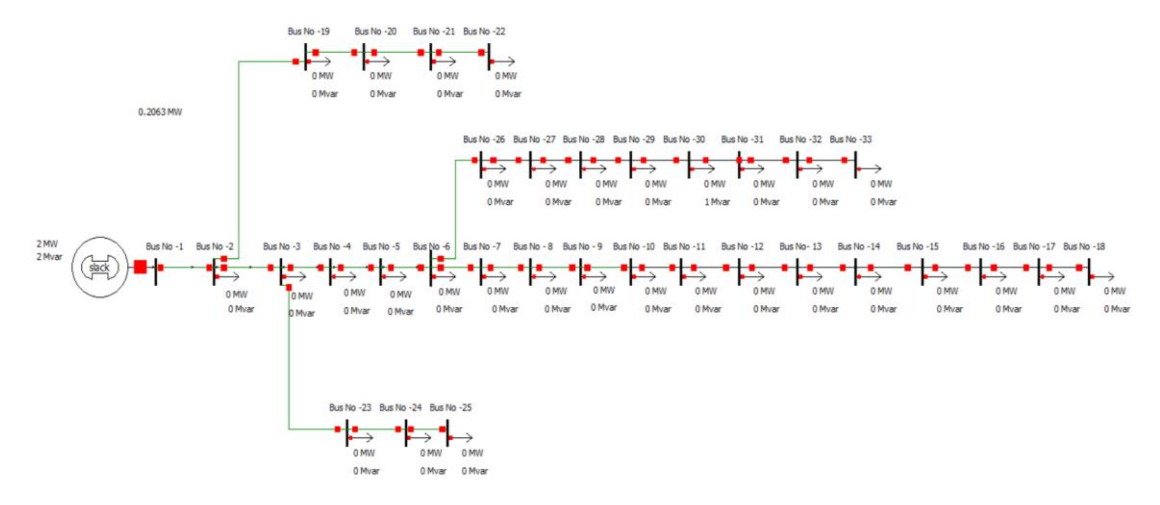


Fig. 2 Base Case Power Flow Simulation Model

In the base case, the active power losses are 211 kW, and the reactive power losses are 142MVar. In addition, 21 buses had voltages less than 0.95pu.

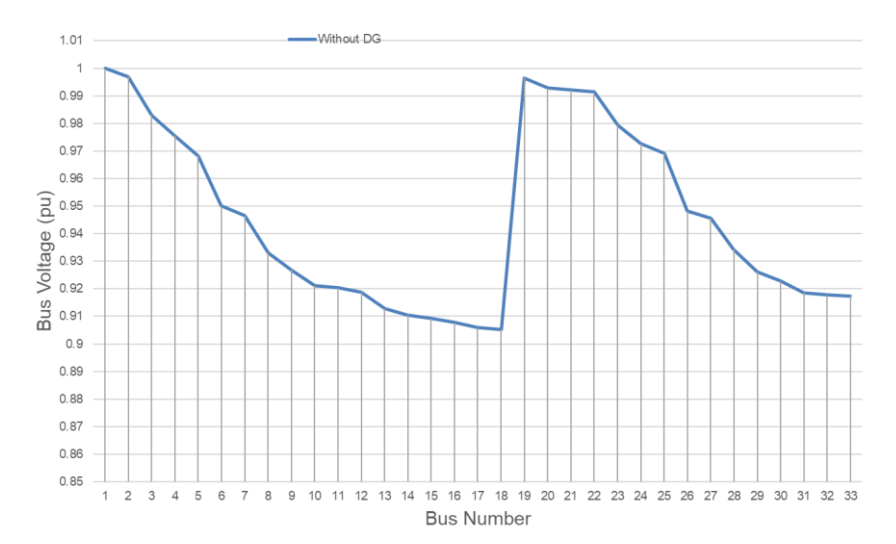


Fig. 3 Base Case Bus Voltage Profile

4.2 Simulation Results

After generating the base case results, the power flow algorithm for the IEEE bus system was implemented using MATLAB. Subsequently, the optimization algorithm was also developed within the same MATLAB directory and linked to the load flow algorithm. This setup allowed for the parallel execution of the load flow algorithms to obtain optimization results. Here, optimization was carried out considering four options. Option 01 focused on adding a single distributed generation unit, while Option 02 examined the integration of two DGs. Option 03 involved the incorporation of three DGs, and option 04 assessed the impact of four DGs on the network.

4.2.1 Option 01-Effect of Integrating Single DG Unit

As the first option, the optimization was carried out considering the integration of a single DG unit into the bus network. Based on the optimization performed, it was found that the optimal location is the 06th bus, and the DG capacity was obtained as 2664kW. The network losses after inserting DG into bus 06 were found to be 68.4kW. The bus voltage profile after adding the single DG unit is shown in Figure 4.

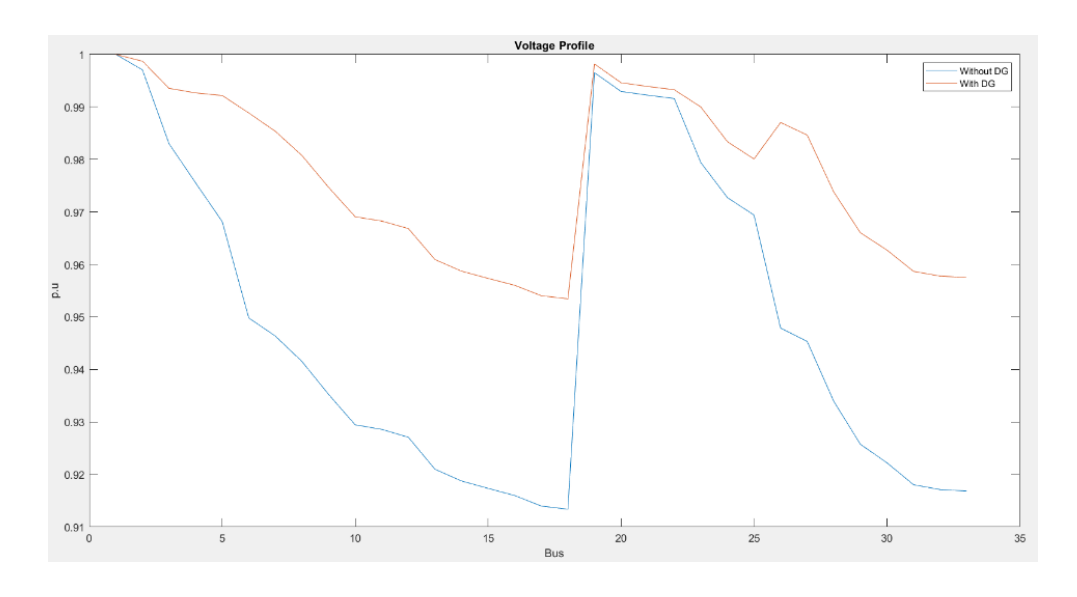


Fig. 4 Bus voltage profile before/ after adding a single DG unit into the Bus Network

4.2.2 Option 02-Effect of Integrating Two DG Units

As in the previous case, a similar procedure was carried out to integrate two DG units into the bus network. Based on the optimization performed, it was found that the optimal locations are the 13th and 30th buses, and DG capacities were obtained as 873kW and 1212kW, respectively. The network losses after inserting DGs into the bus system were found to be 30kW. The bus voltage profile after adding two DG units is shown in Figure 5.

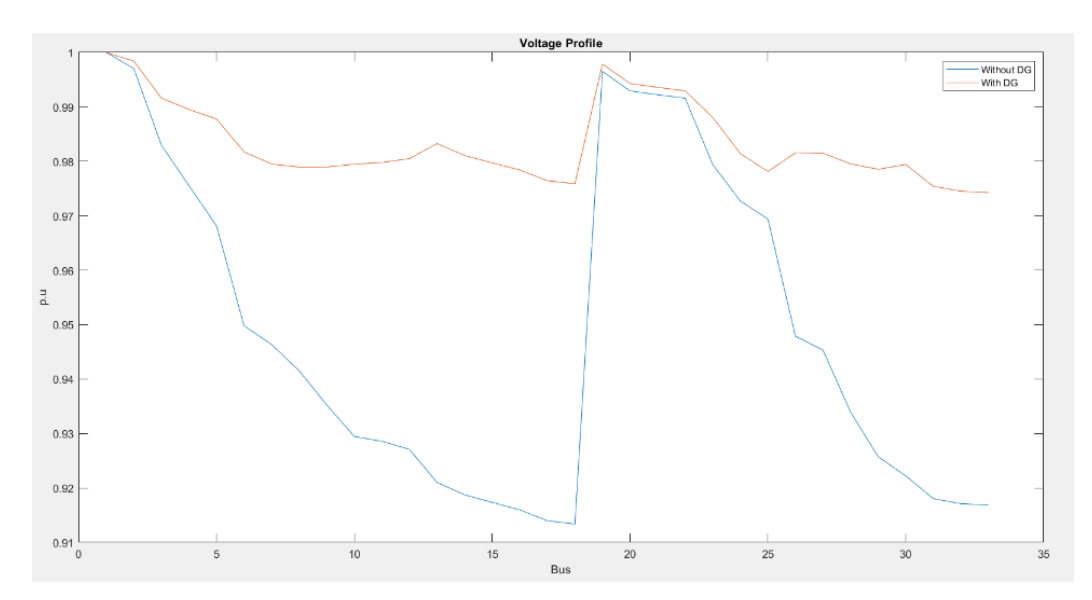


Fig. 5 Bus voltage profile before/ after adding two DG units into the Bus Network

4.2.3 Option 03-Effect of Integrating Three DG Units

The third option integrated three DG units into the bus network. However, the distribution losses were further decreased than in the previous two options. Based on the optimization performed, the optimal locations were the 14th bus, 24th bus, and 30th bus, and the DG capacities were obtained as 780kW,1075kW, and 1120kW, respectively. The network losses after inserting DGs into the bus system were 12.8kW. The bus voltage profile after adding three DG units is shown in Figure 6.

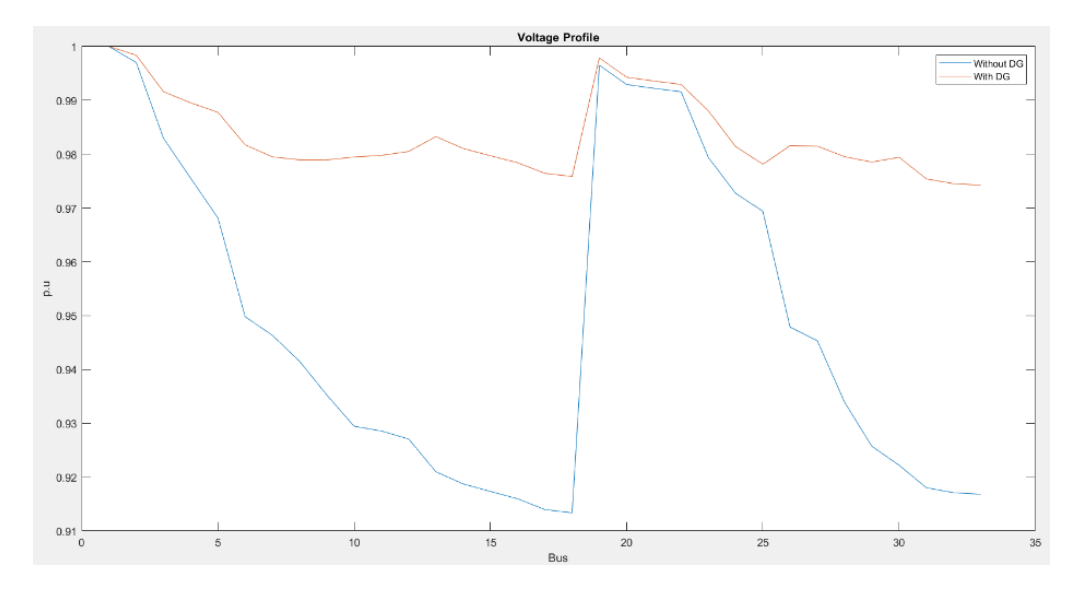


Fig. 6 Bus voltage profile before/ after adding three DG units into the Bus Network

4.2.4 Option 04-Effect of Integrating Four DG Units

Four DG units were integrated into the bus network in the fourth option. However, the distribution losses were further decreased than the previous three options. Although the distribution losses are minimized while adding more and more DGs, the loss reduction percentage is reduced significantly. Based on the performed optimization, it was found that the optimal locations are the 07th bus, 14th bus, 25th bus, and 31st bus, and the respective DG capacities were obtained as 907kW,622kW, 784kW, and 763kW. After inserting DGs into the bus system, the network losses were obtained as 9.8kW. The bus voltage profile after adding three DG units is shown in Figure 7.

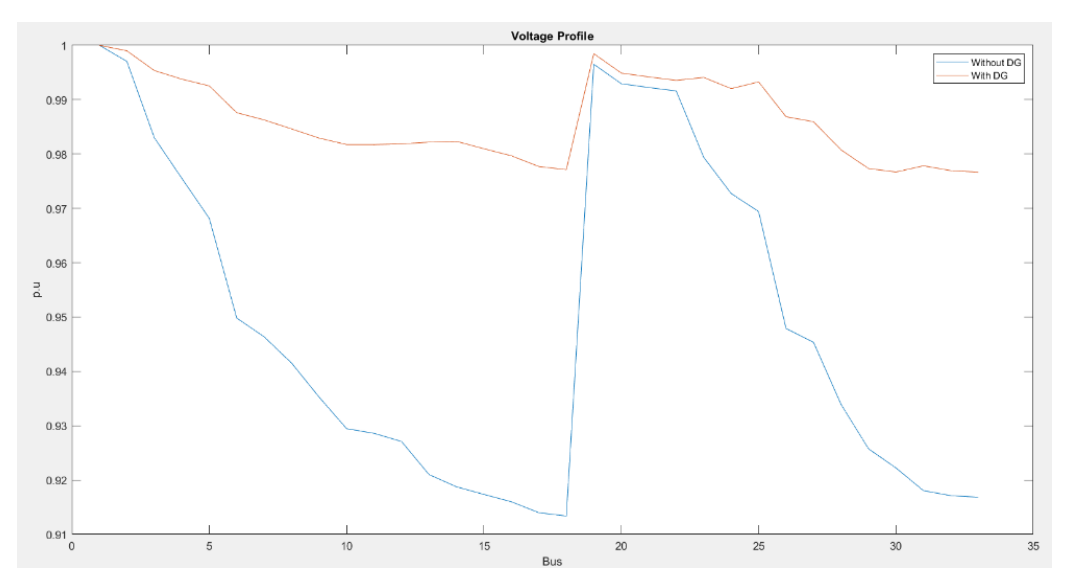


Fig. 7 Bus voltage profile before/ after adding four DG units into the Bus Network

4.3 Summary of the Results

The GA-based algorithm performed strongly in solving the distributed generation optimization problem, producing better results. Notably, the installation of a single DG unit reduced power losses by more than 60%. The summary of the obtained simulation results is shown in Table 01 below.

Option	Bus Location	DG Capacities	Network Power Loss (After installing DGs)	Loss Reduction Percentage
Single DG	06	2664kW	68.4kW	67.6%
Two DG Units	13,30	873kW, 1212kW	30. kW	85.8%
Three DG Units	14,24,30	780kW,1075kW and 1120kW	12.8kW	93.9%
Four DG Units	07,14,25,31	907kW,622kW,784kW,763kW	9.8kW	95.36%

Table 1 Summary of the obtained DG Optimization results

The results obtained were compared with those from other studies to evaluate the effectiveness of the proposed methodology. To maintain consistency across all referenced literature, only studies based on the IEEE 33-bus network were considered for benchmarking. Additionally, most reviewed studies focused on single DG allocation; thus, the results for integrating a single DG were considered for comparison. Table 2 below compares the results obtained from the proposed methodology against those from other studies.

Table 2 Comparison of Results with Other Optimization Methodologies

Optimization Technique	Test Case	Network Active Power Loss (After installing DGs)	Active Power Loss Reduction Percentage	Reference
Exact Loss Formula Based Analytical Approach	IEEE 33- bus	88.5kW	56.34%	[11]
SA and GA Combined Approach	IEEE 33- bus	201.8kW	26.1%	[25]
PSO Based Approach	IEEE 33- bus	110.99kW	47.39%	[30]
Neural Networks-Based Approach	IEEE 33- bus	108.99kW	48.34%	[33]
Proposed GA-Based Approach	IEEE 33- bus	68.4kW	67.6%	-

As shown in Table 02, the proposed GA-based approach yields better results than other approaches available in the literature. In all the studies considered for benchmarking, the sole objective was to minimize network power losses using a single distributed generator. These studies could not achieve more than a 60% reduction in power losses. However, the proposed GA-based approach achieves a 67.6% reduction in power losses, as demonstrated in Table 02. It is important to note that when applied to practical distribution networks and when integrating additional objectives, the loss reduction percentages are expected to decrease compared to the test case.

5 Scope for Future

5.1 Practical Implementation Challenges

The study proposed a GA-based technique for the optimal placement of renewable Generators in an IEEE 33-bus system. The results demonstrated that the algorithm performed as expected, achieving significant improvements in the test system. However, the proposed approach may face challenges when applied to real-world distribution networks, as it assumes static loads and uses average load values for each bus. However, the DG power delivery capability and load demand vary over time, especially when considering renewable energy sources. More advanced optimization algorithms would be needed to address all these complexities, and this proposed approach is most suitable for locations with stable load demands and for the DGs with fixed power delivery capability.

Additionally, the study primarily concentrated on power loss minimization objectives while considering fundamental operational constraints such as voltage limits. However, other critical objectives for real-world distribution networks must be incorporated, such as economic profit maximization, reliability enhancement, power quality improvement, and environmental impact reduction. These additional factors would introduce greater complexity to the optimization problem. The study incorporated basic operational constraints, such as voltage limits, in the optimization problem. However, in real-world applications, additional operational constraints related to capacity sizing, power quality, economic feasibility, and environmental impact should be considered to develop more realistic, practical, and effective optimization solutions. Furthermore, location-specific factors, such as space and infrastructure availability, must be carefully addressed to ensure optimization solutions are applicable and feasible in practical distribution networks. These considerations are crucial for achieving comprehensive and scalable DG optimization in real-world distribution systems.

5.2 Optimization Algorithm Enhancement

The Genetic Algorithm is a prominent member of the metaheuristic family, inheriting the common limitations associated with metaheuristic approaches. These include reliance on initial parameter settings, the risk of premature convergence, and high computational costs, especially for large-scale optimization problems. The application aims to determine the optimal size and location of Distributed Generation units to minimize power losses in the distribution network. While the study has utilized the IEEE 33-bus system to demonstrate the effectiveness of the proposed optimization algorithm, the limitations inherent to nature-inspired metaheuristic approaches may become more significant when applied to larger and more complex distribution networks with a more substantial number of buses. Combining GA with other techniques is recommended to mitigate dependency on initial parameter settings and reduce the likelihood of premature convergence. This hybridization can replace the initial random approximations with realistic approximations generated by alternative algorithms, improving the robustness and efficiency of the optimization process. This approach would be more useful if the number of buses in the distribution network is high.

6 Conclusion

According to the optimization results, as shown in the table above, adding more DG units continued to reduce power losses and improve the voltage profile of the system. However, it was observed that adding more DG units did not significantly enhance the loss reduction percentage beyond a certain point. This suggests that integrating additional DGs does not proportionally decrease power losses as their number increases. Additionally, integrating multiple DGs into the system can introduce other technical challenges, such as power quality issues, power system stability concerns, and protection coordination difficulties. This study did not consider these aspects, leaving room for future research to address these factors comprehensively.

Also, this study is primarily focused on low-voltage distribution networks. In the local context, the distribution transformer capacities are typically 160 kVA and 250 kVA. Given such networks' practical and technical limitations, the proposed methodology may not be directly applicable to large-capacity Distributed Generators (DGs) at low-voltage levels. This is due to the constraints in transformer capacity and the need for more robust infrastructure when dealing with larger DG installations

Regarding voltage profile improvement, the addition of the first DG unit had a substantial impact. After its installation, the voltage profile was significantly enhanced, with no under-voltage buses in any of the analyzed cases. While adding more DGs further improved the system, the gains in loss reduction were minimal, especially when considering the increased cost of capacity associated with installing additional DG units. Based on the results, it is evident that simply adding more DG units does not justify the higher benefits, as the incremental benefits in terms of loss reduction become marginal. Therefore, to optimize the overall profitability of a DG placement project, it is essential to find the right balance between system power losses and DG capacity costs. Achieving this balance depends heavily on the type and nature of the distributed generators integrated into the system.

Also, the proposed approach may encounter challenges when applied to real-world distribution networks, as it relies on assumptions of static loads and average load values for each bus. In reality, load demand and DG power output fluctuate over time. Addressing these dynamic conditions would require more sophisticated optimization algorithms. Consequently, this approach best suits scenarios with stable load demands and DGs with consistent power delivery capabilities.

References

- [01] Kang K., Singh R., Reilly J.T., and Segal N.: Impact of Distributed Energy Resources on the Bulk Electric System Combined Modelling of Transmission and Distribution Systems and Benchmark Case Studies, Technical Report (2017).
- [02] Zhang G., Yu S. S., Zou S., Iu H. H., Fernando T., and Zhang Y.: An Investigation into Cascading Failure in Large-Scale Electric Grids: A Load-Redistribution Approach, Appl. Sci. 2018, 8, 1033 (2018).
- [03] Sajadi and Amirhossein.: Integration of Renewable Energy Systems and Challenges for Dynamics, Control, and Automation of Power Systems, Wiley Online Library, John Wiley & Sons, Ltd, (2018).
- [04] Ackermann T., Andersson G., and Soder L.: Distributed generation: A definition, Electr. Power Syst. Res., vol. 57, no. 3, pp. 195–204, (2001).
- [05] Sharma K. K., Singh B.: Distributed Generation- A New Approach," International Journal of Advanced Research in Computer Engineering & Technology (IJARCET) Volume 1, Issue 8, (2012).
- [06] Sarabia A. F.: Impact of distributed generation on distribution system, Department of Energy and Technology, Faculty of Engineering, Science and Medicine, Aalborg University, (2011).
- [07] Kumar M., Samuel C., and Jaiswal A.: AN OVERVIEW OF DISTRIBUTED GENERATION IN POWER SECTOR, International Journal of Science, Technology & Management, Volume No 04, Special Issue No. 01, (2015).
- [08] Muhtazaruddin M. N. B., Bani N. A., Aris S. A. M., Kaidi H.M., Fatah A.Y.A., Jamia J.J., Muhammad-Sukki F., and Abu-Bakar S.H.: Distribution power loss minimization via distributed generation, capacitor and network reconfiguration, Indonesian Journal of Electrical Engineering and Computer Science (IJEECS), 5(3), pp 488-495, (2017).
- [09] Bhadoria V.S., Singh N., Shrivastava V.: A Review on Distributed Generation Definitions and DG Impacts on Distribution System, DOI: 10.13140/RG.2.1.4439.4328201, (2013).
- [10] Safari A., Jahani R., Shayanfar H. A., Olamaei J.: Optimal DG Allocation in Distribution Network, World Academy of Science, Engineering and Technology International Journal of Electrical and Computer Engineering, Vol:4, No:3, (2010).
- [11] Kumawat P., Sarfaraz and Tandon A.: An Analytical Approach for Optimal Allocation of DG unit in Distribution System, IEEE 7th Power India International Conference 978-1-4673-8962-4/16, (2016)

- [12] Hung D. Q., Mithulananthan N., and Bansal R. C.: Analytical Expressions for DG Allocation in Primary Distribution Networks, IEEE TRANSACTIONS ON ENERGY CONVERSION, VOL. 25, NO. 3, (2010).
- [13] Acharya N., Mahat P., Mithulananthan N.: An Analytical Approach for DG Allocation in Primary Distribution Network, Electric Power System Management, Energy Field of Study, Asian Institute of Technology, P.O. Box 4, Klong luang, Pathumthani 12120, Thailand, (2006).
- [14] Willis H. L.: Analytical Methods and Rules of Thumb for Modeling DG-Distribution Interaction, IEEE, Power Engineering Society Summer Meeting;3:1643–4 (2000).
- [15] Kumawat P., Sarfaraz, and Tandon A.: An Analytical Approach for Optimal Allocation of DG unit in Distribution System, IEEE 7th Power India International Conference 978-1-4673-8962-4/16, (2016).
- [16] Wang C., and Nehrir M. H.: Analytical Approaches for Optimal Placement of Distributed Generation Sources in Power Systems, IEEE TRANSACTIONS ON POWER SYSTEMS, VOL. 19, NO. 4, (2004).
- [17] Singh S.N., and Srivastava S.C.: Genetic Algorithm and its Applications in Power System Problems, Proceedings of tenth National Power System Conference NPSC, vol 1 pp. 289-296 (1998).
- [18] Goldberg D.E: Genetic Algorithms in Search, Optimization, and Machine Learning, Addison Wesley, Reading, Massachusetts, (1989)
- [19] Pisică, Bulac C., and Eremia M.: Optimal Distributed Generation Location and Sizing using Genetic Algorithms, IEEE, DOI: 10.1109/ISAP.2009.5352936, (2009).
- [20] Calderaro V., Piccolo A., and Siano P., Maximizing DG Penetration in Distribution Networks by means of GA based Reconfiguration, International Conference on Future power Systems, Amsterdam, pp.6 pp-6, DOI: 10.1109/FPS.2005204237 (2005).
- [21] Mardaneh M. and Gharephpetian G.B.: Siting and Sizing of DG Units Using GA and OPF Based Technique, IEEE Region 10 Conference TENCON 2004, Chiang Mai, pp. 331-334 Vol 3, DOI: 10.1109/TENCON.2004.1414774, (2004).
- [22] Shorman S.M, and Pitchay S.A.: Significance of Parameters in Genetic Algorithm, the Strengths, its Limitations and Challenges in Image Recovery, ARPN Journal of Engineering and Applied Sciences VOL. 10, NO. 2, (2015).
- [23] Subramanian R., Subramanian K., and Subramanian B.: Application of a Fast and Elitist Multi-Objective Genetic Algorithm to Reactive Power Dispatch, SERBIAN JOURNAL OF ELECTRICAL ENGINEERIN, Vol. 6, No. 1, 119-133, (2009).
- [24] Sattianadan D., Sudhakaran M., Dash S.S., Vijayakumar K. and Ravindran P, Optimal Placement of DG in Distribution System Using Genetic Algorithm, Panigrahi B.K., Suganthan P.N., Das S., Dash S.S. (eds) Swarm, Evolutionary, and Memetic Computing. SEMCCO 2013, Part II, LNCS 8298, pp. 639–647, (2013).
- [25] Gandomkar M., Vakilian M., and Ehsan M.: A Combination of Genetic Algorithm and Simulated Annealing for Optimal DG Allocation in Distribution Networks, IEEE CCECE/CCGEI, Saskatoon, (2005).
- [26] Abedini M., and Saremi H.: A Hybrid of GA and PSO for Optimal DG Location and Sizing in Distribution Systems with Load Uncertainty, J. Basic. Appl. Sci. Res., 2(5) pp 5103-5118, (2012)
- [27] Li M., Du W., and Nian F.: An Adaptive Particle Swarm Optimization Algorithm Based on Directed Weighted Complex Network, Mathematical Problems in Engineering, Article ID 434972, (2014).
- [28] Niazi G., and Lalwani M.: PSO based optimal distributed generation placement and sizing in power distribution networks: A comprehensive review, International Conference on Computer, Communications and Electronics (Comptelix), Jaipur, India, 2017, pp. 305-311, doi: 10.1109/COMPTELIX.2017.8003984, (2017).
- [29] Karunarathne E., Pasupuleti J., Ekanayake J. and Almeida D.: Optimal Placement and Sizing of DGs in Distribution Networks Using MLPSO Algorithm, Energies; 13(23):6185. (2020) https://doi.org/10.3390/en13236185
- [30] Prakash D. and Lakshminarayana C.: Multiple DG Placements in Distribution System for Power Loss Reduction Using PSO Algorithm, *Procedia Technology* 25: 785-792, (2016)
- [31] Adepoju G.A., Aderemi B.A., Salimon S.A., and Alabi O.J.: Optimal Placement and Sizing of Distributed Generation for Power Loss Minimization in Distribution Network using Particle Swarm Optimization Technique, European Journal of Engineering and Technology Research. 8, 1(Jan. 2023), 19–25, (2023).
- [32] Hadidian-Moghaddam M.J., Arabi-Nowdeh S., Bigdeli M., Azizian D.: A multi-objective optimal sizing and siting of distributed generation using ant lion optimization technique, Ain Shams Engineering Journal, Volume 9, Issue 4, Pages 2101-2109, ISSN 2090-4479, (2018).
- [33] Gupta S., Saxena A., Soni B.P.: Optimal Placement Strategy of Distributed Generators based on Radial Basis Function Neural Network in Distribution Networks, Procedia Computer Science, Volume 57, Pages 249-257, ISSN 1877-0509, (2015).
- [34] Rao, Gummadi & Obulesh, : Optimal location of DG for maintaining distribution system stability: A hybrid technique, Int. J. of Power and Energy Conversion. 4. 387 403. 10.1504/IJPEC.2013.057036, (2013).
- [35] Deepak M., Rustum R.: Review of Latest Advances in Nature-Inspired Algorithms for Optimization of Activated Sludge Processes, Processes 11, no. 1: 77 (2023)

- [36] Shami T. M., El-Saleh A. A., Alswaitti M., Al-Tashi Q., Summakieh M. A. and Mirjalili S. :Particle Swarm Optimization: A Comprehensive Survey, IEEE Access, vol. 10, pp. 10031-10061, (2022)
- [37] Wang M., Ma T., Li G., Zhai X. and Qiao S.: Ant Colony Optimization With an Improved Pheromone Model for Solving MTSP With Capacity and Time Window Constraint: IEEE Access, vol. 8, pp. 106872-106879 (2020)
- [38] Guilmeau T., Chouzenoux E. and Elvira V. :Simulated Annealing: a Review and a New Scheme, IEEE Statistical Signal Processing Workshop (SSP), Rio de Janeiro, Brazil, pp. 101-105, (2021)
- [39] Behera I. & Sobhanayak S.: Task Scheduling Optimization in Heterogeneous Cloud Computing Environments: A Hybrid GA-GWO Approach, Journal of Parallel and Distributed Computing, 183. 104766. 10.1016/j.jpdc.2023.104766, (2023)
- [40] Chen D.J., Lee C.Y. and Park C. H. : Parallelizing simulated annealing algorithms based on high-performance computer, J Glob Optim 39, 261–289, (2007)
- [41] Sivadilingam N. and Gukhool O.: HybridDNN-GA: A Genetic Algorithm to Optimize Layers of Hybrid Deep Neural Networks, 2024 IEEE 14th Symposium on Computer Applications & Industrial Electronics (ISCAIE), Penang, Malaysia, pp. 1-6, (2024)

Modern Approaches in Postgraduate Energy Technology Education: Active and Challenge-Based Learning Models

Jeevan Jayasuriya*1, Jordi Olivella2, Ruchira Abeyweera3, Nihal S. Senanayake3

¹KTH − Royal Institute of Technology Sweden, ²UPC- Universitat Politècnica de Catalunya Spain, ³OUSL − The Open University Sri Lanka

jeevan.jayasuriya@energy.kth.se

Abstract

This paper explores modern approaches in postgraduate energy technology education, focusing on Active Learning Techniques (ALE) and Challenge-Based Learning (CBL). As the energy sector evolves, there is a pressing need for educational frameworks that enhance student engagement and equip graduates with critical skills for the dynamic energy landscape. The study outlines the challenges in traditional teaching methods and emphasizes the importance of interdisciplinary collaboration and flexible learning environments. By integrating ALE and CBL, postgraduate programs can foster a deeper understanding of theoretical concepts through practical applications. This paper provides insights into effective curriculum design, faculty training, and industry partnerships to optimize learning outcomes. The findings indicate that these innovative teaching methodologies significantly improve student engagement, adaptability, and industry relevance, ultimately preparing graduates for the complexities of the energy sector.

Keywords: Active Learning Techniques, Challenge-Based Learning, Energy Technology Education, Student Engagement, Curriculum Development

1 Introduction

1.1 Overview of Postgraduate Education in Energy Technology

Energy technology is a rapidly evolving field, essential for addressing global energy challenges, such as the transition to renewable energy sources, energy efficiency, and the development of sustainable technologies. Postgraduate programs in this domain are designed to equip students with advanced knowledge, interdisciplinary skills, and the ability to innovate within complex, dynamic systems. As energy technologies continue to evolve, so must the approaches used to educate future leaders and experts in the field [1].

Challenges in Teaching Energy Technology

One of the primary challenges in teaching energy technology at the postgraduate level is its interdisciplinary nature, which spans engineering, environmental science, policy, and economics. This complexity demands educational strategies that go beyond traditional lecture-based teaching. Students must be able to apply theoretical knowledge to real-world problems, collaborate across disciplines, and engage in lifelong learning to keep pace with technological advancements [2].

The secondary challenge in postgraduate level programs is to maintain the sustainability of the program itself by teaching larger masses of students while keeping program budgets at optimal levels. This allows institutions to satisfy the growing demand for postgraduate education at an affordable price to applicants while ensuring that the quality of education remains high [3].

Moreover, with the increasing diversity of student backgrounds and learning preferences, there is a growing need for flexible educational models. On-campus students may benefit from hands-on laboratory work, while online and hybrid students require digital tools and interactive platforms to engage meaningfully with the content. Educators must therefore adopt innovative methods that are equally effective across different delivery modes—on-campus, online, and hybrid—to ensure that all students receive a high-quality education [4].

Purpose of the Paper

The purpose of this paper is to explore and analyze a range of modern teaching and learning methods applicable to postgraduate energy technology education. Special attention will be given to active learning in Engineering (ALE) and challenge-based learning (CBL), two approaches that have been shown to enhance student engagement, critical thinking, and problem-solving skills [5]. The paper will also address how these methods can be effectively integrated into on-campus, online, and hybrid programs, drawing on current pedagogical research and case studies [6].

By examining these innovative approaches, the paper aims to provide insights into how postgraduate energy technology programs can better prepare students for the challenges of the energy sector. It will highlight the benefits of combining theoretical knowledge with practical, real-world applications, ensuring that graduates are equipped not only with the necessary technical skills but also with the ability to think critically and work collaboratively in a rapidly changing field [7].

2 Literature Review

2.1 Active Learning in Engineering (ALE)

Active Learning in Engineering (ALE) refers to instructional methods that engage students in the learning process actively. This contrasts with traditional lecturing, where students passively receive information. Research shows that active learning in engineering promotes deeper understanding, retention of knowledge, and higher academic performance [8]. Common ALE methods include group discussions, problem-solving sessions, simulations, and hands-on projects [9].

2.2 Challenge-Based Learning (CBL)

Challenge-Based Learning (CBL) is a pedagogical framework that encourages students to address real-world challenges through collaborative projects. CBL fosters critical thinking, creativity, and problem-solving skills by placing students in authentic contexts [10]. In the energy sector, CBL can empower students to tackle pressing issues, such as energy access and sustainability, through innovative solutions [11].

2.3 The Need for Innovative Educational Approaches

As the energy landscape evolves, traditional teaching methods may no longer suffice. The increasing complexity of energy systems, coupled with the need for interdisciplinary collaboration, necessitates innovative educational approaches. Studies indicate that programs that embrace ALE and CBL produce graduates who are better prepared for the demands of the workforce [12].

3. Methodology

3.1 Research Design – Performance Evaluation

As reported in the literature, the evaluation of Active Learning in Engineering (ALE) and Challenge-Based Learning (CBL) in postgraduate energy technology education typically employs a mixed-methods approach. This combines qualitative and quantitative data to comprehensively assess their effectiveness. Studies in this field often utilize surveys and interviews targeting students and faculty involved in programs incorporating these methods [13].

3.2 Data Collection

Data collection is carried out through online surveys distributed to postgraduate students enrolled in energy technology programs across various institutions. Additionally, semi-structured interviews are proposed to be conducted with faculty members who have implemented ALE and CBL in their courses and industrial partners involved in CBL projects [14].

3.3 Data Analysis

Quantitative data is analyzed using statistical software to identify trends and correlations. Qualitative data from interviews is thematically analyzed to explore participants' experiences and perceptions of ALE and CBL [15].

4 Implementation Framework

4.1 Curriculum Design

Implementing ALE and CBL requires a thoughtful redesign of the curriculum. Course objectives should align with real-world challenges, encouraging interdisciplinary collaboration and critical thinking. Faculty should develop project-based assessments that allow students to apply theoretical concepts to practical scenarios [16].

4.2 Faculty Development

Educators must be trained in active learning strategies and CBL methodologies. Professional development programs should focus on effective facilitation techniques, assessment strategies, and the integration of technology in the classroom [17].

4.3 Technology Integration

Leveraging technology is essential for enhancing active learning experiences. Learning Management Systems (LMS) can facilitate collaborative projects and resource sharing. Additionally, simulation software and online collaborative platforms can support students in exploring complex energy systems [18].

4.4 Evaluation and Feedback

Regular assessment of student learning outcomes is crucial for continuous improvement. Institutions should establish feedback mechanisms that allow students to provide input on their learning experiences, fostering a culture of reflection and growth [19].

5 Discussion and Analysis

5.1 Effectiveness in Developing Essential Skills

- **5.1.1 Critical Thinking and Problem-Solving:** ALE and CBL significantly enhance students' critical thinking and problem-solving abilities. These methodologies engage students in real-world challenges that require them to analyze complex problems, evaluate multiple solutions, and make informed decisions. Research indicates that students engaged in ALE and CBL demonstrate superior critical thinking skills compared to those who experience traditional, lecture-based instruction [20]. For instance, in project-based assessments, students must develop innovative energy solutions, fostering a mindset that embraces complexity and creativity [21].
- **5.1.2 Collaboration and Communication:** The collaborative nature of ALE and CBL promotes essential teamwork and communication skills. As students work in groups to tackle challenges, they learn to articulate their ideas, listen to others, and negotiate solutions. This collaboration mirrors the interdisciplinary teamwork often required in the energy sector, preparing graduates to function effectively in diverse professional environments [22]. Research shows that students involved in collaborative projects report greater confidence in their communication skills, which are crucial for future career success [23].
- **5.1.3 Practical Application of Knowledge:** By engaging in hands-on projects, students can directly apply theoretical knowledge to practical situations. This application enhances retention and understanding of complex concepts. Programs that incorporate ALE and CBL report higher student satisfaction and perceived relevance of course material, as students see the direct impact of their learning on real-world energy issues [24]. The focus on practical applications not only prepares students for industry challenges but also instills a sense of agency in addressing global energy problems [25].

5.2 Adaptability to Diverse Student Needs

- 5.2.1 Inclusive Learning Environments: One of the strengths of ALE and CBL is their adaptability to diverse student backgrounds and learning preferences. These methodologies can be tailored to accommodate various learning styles, whether through hands-on activities for kinesthetic learners or digital tools for those who thrive in online environments. For instance, hybrid models can offer flexibility, allowing on-campus students to engage in laboratory work while online students participate in virtual simulations [26].
- **5.2.2 Addressing Varied Learning Preferences:** The use of digital tools and collaborative platforms facilitates engagement among students with differing levels of digital literacy. Instructors can provide varied resources, such as video tutorials, podcasts, and interactive modules, ensuring that all students can access content effectively [27]. This flexibility not only enhances learning outcomes but also fosters a sense of community among students, as they share diverse perspectives and collaborate on projects [28].
- **5.2.3 Lifelong Learning Skills:** ALE and CBL foster a culture of lifelong learning, essential in the rapidly evolving field of energy technology. By emphasizing self-directed learning and continuous improvement, these methodologies prepare students to seek out knowledge independently, a vital skill in an industry characterized by constant technological advancements [29]. Graduates who are adept at self-directed learning are more likely to remain competitive and innovative throughout their careers [30].

5.3 Impact on Program Sustainability and Scalability

5.3.1 Sustainability of Educational Programs: The integration of ALE and CBL can enhance the sustainability of postgraduate energy technology programs. By focusing on efficient teaching methods that leverage collaborative learning and technology, institutions can accommodate larger cohorts without compromising

educational quality. The scalability of these methods allows programs to expand while maintaining a high standard of education, essential in meeting the growing demand for skilled professionals in the energy sector [31].

- **5.3.2 Resource Optimization:** Implementing ALE and CBL can lead to optimized resource use, as these methods often require fewer traditional classroom hours while maximizing student engagement through active participation. Faculty can use their time more effectively by facilitating discussions and providing feedback rather than delivering lengthy lectures [32]. This optimization allows for more personalized learning experiences and enhances faculty-student interactions, further supporting student success [33].
- **5.3.3 Industry Partnerships:** Establishing partnerships with industry stakeholders is crucial for the sustainability of postgraduate programs. These partnerships can provide resources, real-world projects, and internships, ensuring that students gain practical experience while also supporting program development. Collaborative initiatives can attract funding and sponsorships, enhancing the overall educational offerings and sustainability of energy technology programs [34].

6 Conclusion and Recommendations

6.1 Conclusion

The landscape of postgraduate energy technology education is rapidly changing, driven by the need for innovative educational approaches. This paper has explored the integration of Active Learning in Engineering (ALE) and Challenge-Based Learning (CBL) as effective strategies for enhancing student engagement, developing critical skills, and preparing graduates for the complexities of the energy sector.

Key Findings:

- **6.1.1 Enhanced Learning Outcomes:** ALE and CBL methodologies significantly improve students' critical thinking, problem-solving, and collaboration skills. By engaging students in real-world challenges, these approaches foster a deeper understanding of theoretical concepts and their practical applications [35].
- 6.1.2 Adaptability and Inclusivity: These teaching methodologies are adaptable to diverse learning preferences, making them suitable for a wide range of students. The flexibility of delivery modes—whether on-campus, online, or hybrid—ensures that all learners have access to quality education [36].
- 6.1.3 Sustainability and Scalability: The incorporation of ALE and CBL can lead to more sustainable and scalable postgraduate programs. By optimizing resources and fostering industry partnerships, educational institutions can expand their offerings while maintaining high educational standards [37].
- **6.1.4 Industry Relevance**: By aligning curriculum with real-world challenges, ALE and CBL prepare students to meet the demands of the energy sector. Graduates emerge not only with the technical skills necessary for their careers but also with the adaptability and critical thinking abilities required in a rapidly changing industry [38].

6.2 Recommendations

To maximize the benefits of ALE and CBL in postgraduate energy technology education, the following recommendations are proposed:

6.2.1 Curriculum Development:

Institutions should redesign curricula to incorporate ALE and CBL principles. This includes developing project-based assessments that align with current industry challenges and promoting interdisciplinary collaboration among departments [39].

6.2.2 Faculty Training and Support:

Investing in professional development for faculty is crucial. Training programs should focus on effective implementation of active learning strategies, use of technology in education, and facilitation of collaborative learning experiences [40].

6.2.3 Leverage Technology:

Institutions should utilize digital tools and resources that support active and challenge-based learning. Learning Management Systems (LMS), simulation software, and collaborative platforms should be integrated into the educational framework to enhance student engagement [41].

6.2.4 Continuous Assessment and Feedback:

Implement formative assessments and peer feedback mechanisms to support ongoing learning and improvement. Regular feedback helps students gauge their progress and refine their skills in real-time [42].

6.2.5 Engagement with Industry:

Foster partnerships with industry stakeholders to create opportunities for real-world project involvement and internships. This collaboration ensures that the curriculum remains relevant and provides students with valuable insights into industry practices [43].

6.2.6 Focus on Lifelong Learning:

Embed self-directed learning components into the curriculum to encourage students to take ownership of their learning journeys. This approach prepares graduates to adapt to the evolving landscape of the energy sector and embrace continuous professional development [44].

References

- 1. Barrows, H. S. (1996). Problem-based learning in medicine and beyond: A brief overview. Inquiries into Teaching and Learning in Higher Education, 1(1), 3–11.
- 2. Bennett, N., & Brunner, I. (2015). The importance of collaboration in education. International Journal of Educational Management, 29(3), 212–223.
- 3. Brew, A., & Jones, R. (2018). The role of academic developers in leading educational change: The case of research-led learning. International Journal for Academic Development, 23(3), 224–236.
- 4. Candy, P. C. (1991). Self-direction for lifelong learning: A comprehensive guide to theory and practice. Jossey-Bass.
- 5. Dede, C. (2009). Immersive interfaces for engagement and learning. Science, 323(5910), 66–69.
- 6. Dewey, J. (1938). Experience and education. Kappa Delta Pi.
- 7. Freeman, S., Eddy, S. L., McDonough, M., Smith, M. K., Wenderoth, M. P., & Peregrin, T. (2014). Active learning increases student performance in science, engineering, and mathematics. Proceedings of the National Academy of Sciences, 111(23), 8410–8415.
- 8. Garrison, D. R., & Vaughan, N. D. (2008). Blended learning in higher education: Framework, principles, and guidelines. Jossey-Bass.
- 9. Gokhale, A. A. (1995). Collaborative learning enhances critical thinking. Journal of Technology Education, 7(1), 22–30.
- 10. Helle, L., Tynjälä, P., & Olkinuora, E. (2009). Project-based learning in post-secondary education: Theory, practice and rubber sling shots. Higher Education, 57(3), 245–265.
- 11. Kelley, T., Mazzurco, A., & McNair, L. (2013). Challenge-based learning: A model for engaged learning in higher education. Innovative Higher Education, 38(4), 1–10.
- 12. Klein, S. A., Beck, J. V., & Mitchell, D. (2004). EnergyPlus: Energy simulation software. EnergyPlus Documentation. U.S. Department of Energy.
- 13. Nicol, D. J., & Macfarlane-Dick, D. (2006). Formative assessment and self-regulated learning: A model and seven principles of good feedback practice. Studies in Higher Education, 31(2), 199–218.
- 14. Prince, M. (2004). Does active learning work? A review of the research. Journal of Engineering Education, 93(3), 223–231.
- 15. Rennie, L. J., & Duhs, R. (2015). The role of the teacher in implementing the Australian Curriculum: Science. Australian Curriculum, Assessment and Reporting Authority.
- 16. Trowler, V. (2010). Student engagement literature review. The Higher Education Academy.
- 17. Smith, M. K., & MacGregor, J. (2009). What is collaborative learning? Educational Resources Information Center.
- 18. Hattie, J., & Timperley, H. (2007). The power of feedback. Review of Educational Research, 77(1), 81–112.
- 19. Schunk, D. H. (2003). Self-efficacy for reading and writing: Influence of modeling, goal setting, and self-evaluation. Reading & Writing Quarterly, 19(2), 159–172.
- 20. Hattie, J. (2012). Visible learning for teachers: Maximizing impact on learning. Routledge.
- 21. Bransford, J. D., Brown, A. L., & Cocking, R. R. (2000). How people learn: Brain, mind, experience, and school. National Academy Press.
- 22. O'Donnell, A. M., & King, A. (2014). Cognitive perspectives on peer learning. In Handbook of Psychology: Educational Psychology (Vol. 7, pp. 307–339). John Wiley & Sons.
- 23. Johnson, D. W., & Johnson, R. T. (1994). Learning together and alone: Cooperative, competitive, and individualistic learning. Allyn & Bacon.
- 24. Chappell, C., & Hawke, M. (2005). Workforce development and the new skills agenda. Australian National Training Authority.
- 25. McKinsey & Company. (2016). The future of work: The impact of automation on employment.

- 26. Tharp, R. G., & Gallimore, R. (1988). The role of dialogue in learning: An educational perspective. The School of Education.
- 27. Wang, M. T., & Eccles, J. S. (2013). Family processes and student engagement: The role of parental involvement. The Journal of Educational Psychology, 105(3), 686–701.
- 28. Garrison, D. R. (2011). E-learning in the 21st century: A community of inquiry framework for online learning. Routledge.
- 29. Tough, A. M. (1979). The adult's learning projects: A fresh approach to theory and practice in adult learning. Ontario Institute for Studies in Education.
- 30. Knapp, M. S., & Copeland, S. (2006). The role of leadership in addressing the needs of all learners. The Leadership and Learning Center.
- 31. McGowan, J. J., & LaPorte, J. (2005). Faculty development: Critical ingredients for an effective academic program. Academic Medicine, 80(7), 617–619.
- 32. Hargreaves, A., & Fink, D. (2006). Sustainable leadership. The Education Forum.
- 33. Fullan, M. (2011). Change leader: Learning to do what matters most. Jossey-Bass.
- 34. Spencer, B. (2009). The role of industry partnerships in higher education. Journal of Industry Education Collaboration, 3(1), 47–55.
- 35. Bransford, J. D., et al. (2000). How people learn: Brain, mind, experience, and school. National Academy Press.
- 36. Grohmann, A., & Kauffeld, S. (2013). The impact of teaching styles on student engagement: The mediating role of cognitive and emotional engagement. Educational Psychology, 33(4), 389–401.
- 37. Wagner, T. (2008). The Global Achievement Gap: Why Even Our Best Schools Don't Teach the New Survival Skills Our Children Need—and What We Can Do About It. Basic Books.
- 38. DeZure, D., & Delaney, M. (2010). Creating effective university-industry partnerships. Academic Perspectives.
- 39. Dufresne, R. J., & Gerace, W. J. (2004). Student engagement in learning physics: A model of the learning process. American Journal of Physics.
- 40. Galbraith, M. W., & Cohen, N. (1995). The role of self-directed learning in postsecondary education. University Press of America.
- 41. Laird, T. F., et al. (2008). Learning and academic performance: The impact of college involvement. Journal of College Student Development, 49(3), 291–306.
- 42. Biggs, J. (1999). What the student does: Teaching for enhanced learning. Higher Education Research & Development, 18(1), 57–75.
- 43. Senge, P. M. (2006). The fifth discipline: The art and practice of the learning organization. Crown Business.
- 44. Schilling, J., & Kessler, E. (2004). Lifelong learning: A resource for higher education. Adult Education Quarterly.

Enhancing Boiler Efficiency through Waste Heat Recovery: A Feasibility Study in a Food Manufacturing Facility

A. Mohamed Rifnaz *, T.S.S. Jatunnarachchi, S.K. Dinusha Madurangi

Department of Mechanical Engineering, Faculty of Engineering Technology, The Open University of Sri Lanka, Nawala, Nugegoda

amrifnaz@gmail.com

Abstract

This research examines strategies to improve energy efficiency in a food manufacturing facility by utilizing waste heat recovery within the boiler steam generation system. Steam generation is critical in industrial food processing but poses high energy costs and environmental impacts when inefficiencies are present. This study specifically evaluates the feasibility of implementing a crossflow economizer to preheat feedwater using recovered heat, to optimize the steam-to-fuel ratio and reduce overall fuel consumption. Data from facility operations were collected, and computational modeling in ANSYS validated the design's performance. Results show that the economizer could increase feedwater temperature by an average of 35.1°C, leading to a projected efficiency improvement of 2.13% and monthly fuel savings of approximately 4,067 liters, with annual cost savings of around LKR 10 million. The economic analysis confirms the project's viability, with a payback period of 1.1 years. These findings illustrate that waste heat recovery in steam generation systems can yield significant energy, financial, and environmental benefits.

Keywords: Boiler Efficiency Optimization, Industrial Waste Heat Recovery, Heat Exchanger Design, Flue Gas Energy Utilization, Acid Dew Point Management

1 Introduction

Boiler systems are essential in many industrial processes, particularly in food manufacturing, where consistent steam generation is critical for operations like heating, cooking, and sterilization. However, steam generation is energy-intensive, making it a significant operational expense for facilities. Improving boiler efficiency is therefore a priority, as even marginal gains can lead to substantial cost savings and environmental benefits. For industries relying on fossil fuels, such as furnace oil, efficiency improvements can also contribute to lowering greenhouse gas emissions and reducing the overall environmental footprint.

Waste heat recovery (WHR) presents a valuable opportunity to enhance boiler efficiency. By capturing heat that would otherwise be lost through flue gases and reintroducing it into the system, WHR technologies can reduce fuel requirements, optimize steam-to-fuel ratios, and minimize energy wastage. Economizers are devices that preheat boiler feedwater using waste heat from exhaust gases and are widely recognized as effective WHR tools. An economizer can help achieve higher thermal efficiency by reducing the fuel required to reach the boiling point for steam generation, ultimately lowering operational costs and emissions. [1]

This study aims to assess the feasibility of implementing a crossflow economizer in the boiler system of a selected food manufacturing facility. Using a combination of data collection, computational modeling, and economic analysis, this research investigates the potential efficiency gains and fuel savings achievable with WHR. The outcomes of this study contribute actionable insights for the food industry and other sectors that rely on steam generation, promoting sustainable energy practices and operational cost reductions. Energy consumption of the plant is provided by electricity, furnace oil, and diesel, and the contribution of energy consumption is shown in Fig. 1.

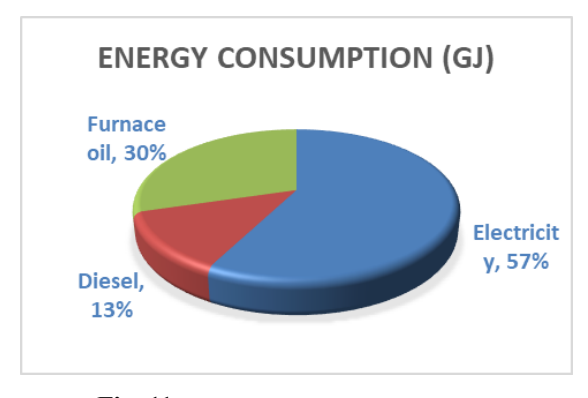


Fig. 11 Energy Consumption in the plant

2 Methodology

The methodology for this research involves a multi-step approach, including data collection, design and modeling of a waste heat recovery system, and a subsequent analysis of potential efficiency improvements and economic viability.

2.1 Data Collection and Site Assessment

The study began with a comprehensive assessment of the existing boiler system at the selected food manufacturing facility. Data collected included:

• Fuel Consumption and Type: The facility relies on Furnace Oil 800 for boiler operation. A calorific value of 10,258 kcal/kg was used as a basis for energy input calculations. It was decided to get the steam generation and fuel usage for 19 months with 2 2-month fuel exemption.

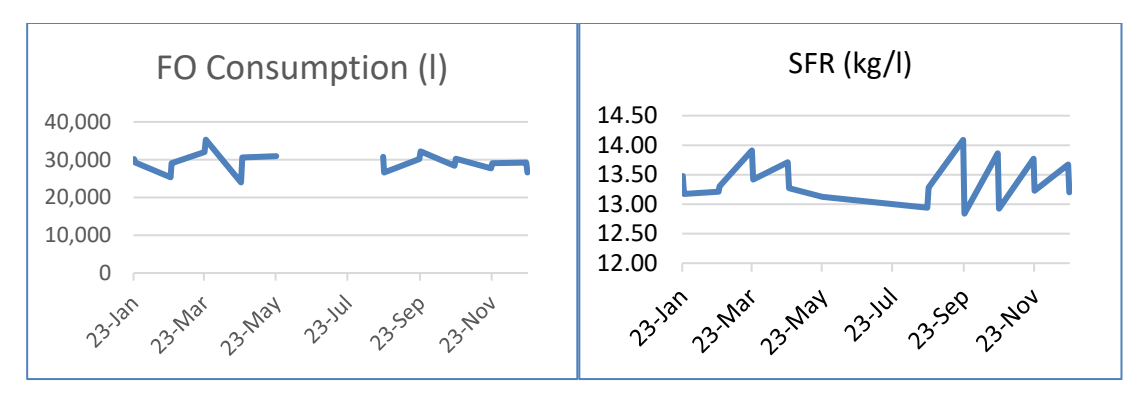


Fig. 22 Fuel Consumption and variation of SFR of 19 months

- Steam Demand and Flow Rates: The average steam-to-fuel ratio (SFR) was determined by observing operational data over 19 months, yielding an SFR of 13.95 kg steam per kg of fuel. Both fuel consumption and SFR variation of 19 months are shown in Fig. 2.
- Feedwater Characteristics: Feedwater flow rate was recorded at 536 kg/h, and its specific heat capacity was noted as 4.186 kJ/kg°C. The initial feedwater temperature averaged 92°C.
- Flue Gas Properties: Key parameters [2], such as flue gas temperature, oxygen content, and excess air levels, were monitored using a flue gas analyzer. The average flue gas temperature was recorded at 280.5°C, while the desired outlet temperature was set to 170°C to avoid corrosive condensation

2.2 Waste Heat Recovery Potential Calculation

To evaluate the waste heat recovery potential, calculations were performed based on the collected flue gas temperature and flow rate data. With the high temperature of flue gases exiting the boiler, there was considerable thermal energy available for recovery. Calculating the energy available:

$$Q = m_{flue \ gas} \ X \ c_{flue \ gas} \ X \ (T_{inlet} - T_{outlet})$$

Where flue gas represents the mass flow rate, cflue gas is the specific heat capacity (assumed to be 1.1 kJ/kg°C), and Tinlet and Toutlet are the flue gas temperatures in and out of the economizer, respectively. This calculation yielded an estimated recoverable energy of 78,635.59 kJ/h (21.84 kW)

2.3 Economizer Design

The design of the economizer was developed to maximize heat recovery from flue gases while ensuring compatibility with the existing boiler system at the food manufacturing facility. Key design considerations, including heat transfer efficiency, material selection, flow arrangement, and dimensional specifications, were rigorously evaluated to optimize performance. [3]

2.3.1 Design Objectives and Requirements

The primary objective of the economizer was to increase boiler efficiency by preheating feedwater using waste heat from flue gases. This process minimizes fuel consumption and reduces emissions. Specific design requirements included:

- Compatibility: The economizer was designed to integrate seamlessly with the existing boiler setup, requiring minimal modifications to the system.
- Safety and Reliability: The economizer needed to operate within safe temperature and pressure limits, avoiding condensation of acidic components in the flue gas, which could cause corrosion.

2.3.2 Tube Bundle Design

The economizer was designed as a crossflow heat exchanger with a tube bundle configuration to facilitate effective heat transfer between flue gases and feedwater. The following parameters were defined based on the facility's operational needs: [4]

- **Tube Diameter and Thickness:** Tubes with an outer diameter of 25 mm and a wall thickness of 1.6 mm were selected to ensure durability under high-temperature conditions. This configuration resulted in an inner diameter of 21.8 mm, allowing sufficient fluid flow while maintaining structural integrity.
- Tube Material Selection: Mild steel was chosen for the tubes due to its favorable thermal conductivity (around 50 W/m·K) and corrosion resistance. While stainless steel provides superior corrosion resistance, mild steel offers a cost-effective balance for non-condensing economizers where the risk of acidic condensation is controlled.
- Tube arrangements: In a crossflow type heat exchanger, a rod or tube bundle is an arrangement of parallel cylinders that heat, or are being heated by, a fluid that might flow normal to them. [4] For this study, it was decided to stick to aligned tube rows in tube bundles. The flow of water through tubes will be arranged in rows and columns as indicated in Fig.. [4]

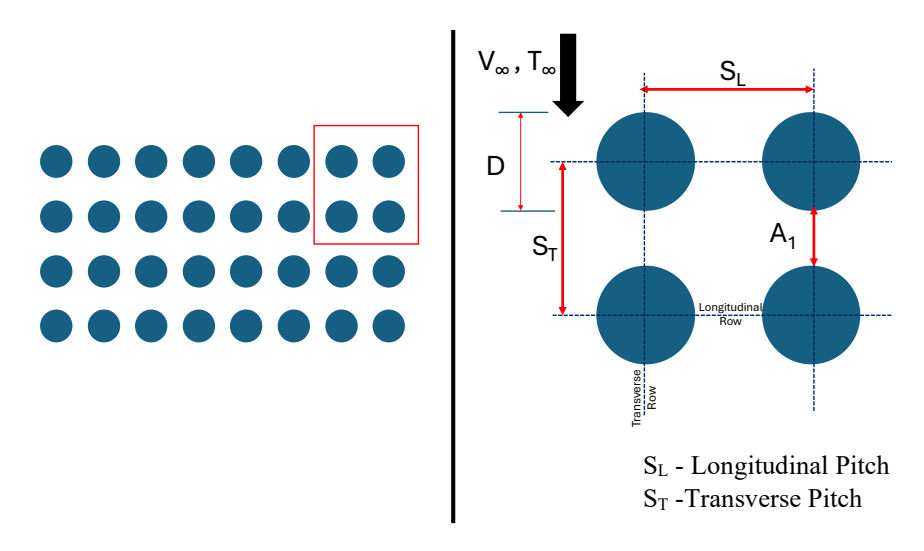


Fig. 33 Aligned tube arrangement

2.3.3 Calculating convective heat transfer coefficient of flue gas side (ho)and water side (hi)

Inlet flue gas velocity $(V\infty)$ is a crucial parameter for calculating the Reynolds number (Re), which is necessary to determine the flow type and ultimately the heat transfer coefficient on the flue gas side. Inlet flue gas velocity is calculated as below

Inlet flue gas velocity
$$(V\infty) = \frac{\text{Flue gas flow rate (Q)}}{\text{Area of the flue gas exhaust (Afe)}}$$

Mass flow rate of flue gas (m) of 0.498 kg/s, flue gas density of 0.748 kg/m³, and flue gas exhaust diameter (D) of 1.5 ft. are the parameters that were considered to find the inlet flue gas velocity

Inlet flue gas velocity (V
$$\infty$$
) =
$$\frac{\frac{0.498 \ kg/s}{0.748 \ kg/m^3}}{\pi \ * \ (1.5/2 * 0.3048)2 \ m^2}$$

Inlet flue gas velocity $(V\infty) = 4.06 \text{ m/s}$

The Reynolds number (Re) is a dimensionless quantity used in fluid mechanics to predict flow patterns in different fluid flow situations. It is defined as the ratio of inertial forces to viscous forces within a fluid. The maximum Reynolds number (ReD,max) for the foregoing correlations is based on the maximum fluid velocity (Vmax) occurring within the tube bank. For the aligned arrangement, Vmax occurs at the transverse plane, and from the mass conservation requirement for an incompressible fluid [4]

$$Vmax = \frac{ST}{ST - D} V \infty$$
$$Vmax = 5.41 \text{ m/s}$$

The heat transfer coefficient associated with a tube is determined by its position in the bank. The coefficient for a tube in the first row is approximately equal to that for a single tube in cross flow. [4] The various physical properties are calculated at the mean film temperature, which is 209.6 °C. From the Standard flue gas thermophysical properties table, the following properties of flue gas at 209 °C were obtained. [$p = 0.735 \text{ kg/m}^3$, Cp = 1.1 kJ/kg K, $k = 32.4 \times 10^{-3} \text{ W/mK}$, $v = 34.05 \times 10^{-6} \text{ m}^2/\text{s}$, and Pr = 0.683 (Prandtl Number)]

Reynolds number
$$(Re_{D,\text{max}}) = \frac{Vmax}{v}$$

Reynolds number $(Re_{D,\text{max}}) = \frac{5.4 \ m/s * 25 * 10^{-3} \ m}{34.05 * 10^{-6} \text{m2/s}}$
 $(Re_{D,\text{max}}) = 3,964.8$

The Nusselt number (NuD) is a dimensionless number used in thermal fluid dynamics to describe the ratio of convective to conductive heat transfer across a boundary in a fluid [4]. In a study published in 1972 by Zukhas, correlations for Nusselt number were described for different tube bank arrangements and listed in the table below. [5]

$$NU_D = F * C * Re_{D max}^{n} * Pr^{m}$$

In this Case Study, F = 1 (arrangement is aligned) $Re_{D,max} = 3,964.8$ (lies in the range of $1000 \le Re_{D,max} \le 2 \times 105$) $C = 0.27 \quad n = 0.63 \quad m = 0.36$

$$NU_D = 0.27 * Re_{D,max}^{0.63} * Pr^{0.36}$$

 $NU_D = 0.27 * (3.964.8)^{0.63} * (0.683)^{0.36}$
 $NU_D = 43.52$

Accordingly, the flue gas side heat transfer coefficient (h_o) can be calculated using the following formula.

$$ho = \frac{NU_D * k}{D_o}$$

$$h_o = \frac{43.52 * 32.4 * 10^{-3} \text{ W/mK}}{25 * 10^{-3} m}$$

$$h_o = 68.92 \text{ W/m}^2 \text{K}$$

Similarly, the water side heat transfer coefficient (hi) was calculated as 5,975.26 W/m² K

2.3.4 Calculating the Overall Heat Transfer Coefficient (U)

The overall heat transfer coefficient (U) is a key parameter in determining the heat transfer efficiency of the economizer. The coefficient (U) represents the combined resistance to heat flow across the various layers involved in the heat exchange process. It includes resistances due to the convection of fluids on both sides of the tube and conduction through the tube wall. Overall heat transfer coefficient can be characterized by the following equation,

where subscripts i and o refer to inner and outer tube surfaces, which may be exposed to either the hot or the cold fluid [4] [5] [6], where R" represents Fouling Factors.

$$\frac{1}{U} = \frac{D_o}{h_i D_i} + \frac{1}{ho} + \frac{D_o}{2\pi kL} \ln{(\frac{D_o}{D_i})} + R'' f, o + R'' f, i$$

The overall heat transfer coefficient is useful for finding the surface area for heat transfer. Since the convective heat transfer coefficient of the flue gas side ($h_o = 68.92 \text{ W/m}^2 \text{ K}$) is much lower than the water side ($h_i = 5,975.26 \text{ W/m}^2 \text{K}$). Therefore, the gas side coefficient is the governing parameter. In the plant, feedwater is taken from an in-house tube well, and the temperature is 92 °C. The Fouling factor is taken as $0.0002 \text{ m}^2 \text{K/W}$ for inside and $0.000179 \text{ m}^2 \text{K/W}$.

$$\frac{1}{U} = \frac{25}{5,975.26 * 21.8} + \frac{1}{68.92} + \frac{25}{2\pi * 50 * 1.83} \ln\left(\frac{25}{21.8}\right) + 0.0002 + 0.000179$$

$$\frac{1}{U} = 0.0150876 \, m^2 K/W$$

$$U = 66.28 \, W/m^2 K$$

The overall heat transfer coefficient would be defined as 66.28 W/m²K for this case study.

2.3.5 Use of the Log Mean Temperature Difference

To design or to predict the performance of a heat exchanger, it is essential to relate the total heat transfer rate to quantities such as the inlet and outlet fluid temperatures, the overall heat transfer coefficient, and the total surface area for heat transfer. [4] The appropriate average temperature difference is a log mean temperature difference for counterflow conditions, which can be written as follows.

$$LMTD = \frac{(T_{h_{in}} - T_{c_{out}}) - (T_{h_{out}} - T_{c_{in}})}{\ln\left(\frac{T_{h_{in}} - T_{c_{out}}}{T_{h_{out}} - T_{c_{in}}}\right)}$$

$$LMTD = \frac{(Th_{in} - Tc_{out}) - (Th_{out} - 92)}{\ln\left(\frac{280 - 186.55}{170 - 92}\right)}$$

$$LMTD = \frac{(280 - 186.55) - (170 - 92)}{\ln\left(\frac{280 - 186.55}{170 - 92}\right)}$$

$$LMTD = 85.49 \, ^{\circ}\text{C} \, (\text{/ K})$$

But for the crossflow, the result cannot be used directly. To correct the error, a correction factor should be introduced. That is, the appropriate form of LMTD is obtained by applying a correction factor to the value of LMTD that would be computed under the assumption of counterflow conditions. Algebraic expressions for the correction factor F have been developed for various shell-and-tube and crossflow heat exchanger configurations, and the results may be represented graphically.[4] To get the exact value for the correction factor (F), an online calculator [7] was used, and the average values of LMTD and F are as follows.

Table 1 LMTD & F values for the selected cases

	Case 1	Case 2	Case 3	Case 4	Case 5	Case 6	Case 7	Case 8	Case 9	Case 10
Tcin	90	90	90	90	90	90	60	70	80	85
Tcout	125.11	133.89	142.66	160.22	168.99	186.55	130.22	140.22	150.22	155.22
Thin	210	220	230	250	260	280	250	250	250	250
Thout	170	170	170	170	170	170	170	170	170	170
LMTD	82.42	83.02	83.61	84.80	85.38	86.55	114.82	104.82	94.81	89.80

P	0.2926	0.3376	0.3762	0.4389	0.4647	0.5082	0.3696	0.3901	0.4130	0.4256
R	1.1393	1.1393	1.1393	1.1393	1.1393	1.1393	1.1393	1.1393	1.1393	1.1393
F	0.9856	0.9785	0.9704	0.9514	0.9406	0.9166	0.9719	0.9669	0.9603	0.9562

Average values from the table

LMTD counterflow = 91.00 K

$$F = 0.9598$$

$$LMTD_{crossflow} = LMTD_{ccunterflow} * F$$

$$LMTD_{crossflow} = 91.0 \text{ K} * 0.9598$$

$$LMTD_{crossflow} = 87.35 \text{ K}$$

2.3.6 Heat Transfer and Surface Area Considerations

Maximizing the heat transfer area is essential for efficient energy exchange. The economizer's tube bundle was designed with staggered tube arrangements to increase the contact surface between flue gases and the tube walls, enhancing heat exchange. The staggered arrangement also disrupts laminar flow in the flue gases, promoting turbulence and improving convective heat transfer. The total heat transfer surface area (A) required was calculated using the equation:

Heat Transfer (Q) =
$$U * A * \text{LMTD}_{\text{crossflow}}$$

 $60.3 * 10^3 W = 66.28 \frac{W}{m^2 K} * A * 87.35 K$
 $A = 10.41 m^2$

2.3.7 Number of tubes in the Heat Exchanger

Surface area of the tubes depends on the number of tubes used and the length of each tube. Since the required surface area is known, it is required to select a suitable length of tube for the heat exchanger. According to Coulson & Richardson's Chemical engineering design, the preferred lengths of tubes for heat exchangers are: 6 ft (1.83 m), 8 ft (2.44 m), 12 ft (3.66 m), 16 ft (4.88 m), 20 ft (6.10 m), 24 ft (7.32 m). For a given surface area, the use of longer tubes will reduce the shell diameter, which will generally result in a lower cost exchange, particularly for high shell pressures. [3] For this study, it was decided to go for a 6 ft (1.83 m) tube was arbitrarily selected, and the required number of tubes is calculated using the following equation, where N is the number of tubes.

Surface area (A) =
$$(\pi * D * L) * N$$

 $10.41 m^2 = (\pi * 25 * 10^{-3} m * 1.83m) * N$
 $N = 72.45$

2.4 Economizer Modeling

The software used for the analysis was Ansys 2024 R2 (Student version) under this study. Ansys provides a series of analysis systems under the toolbox. In this study, the purpose is to study the fluid flow; it was decided to select the Fluid Flow (Fluent) analysis. The first step of the analysis is designing the proposed economizer as per the measurements and results obtained from the calculations in DesignModeler of ANSYS. [8]

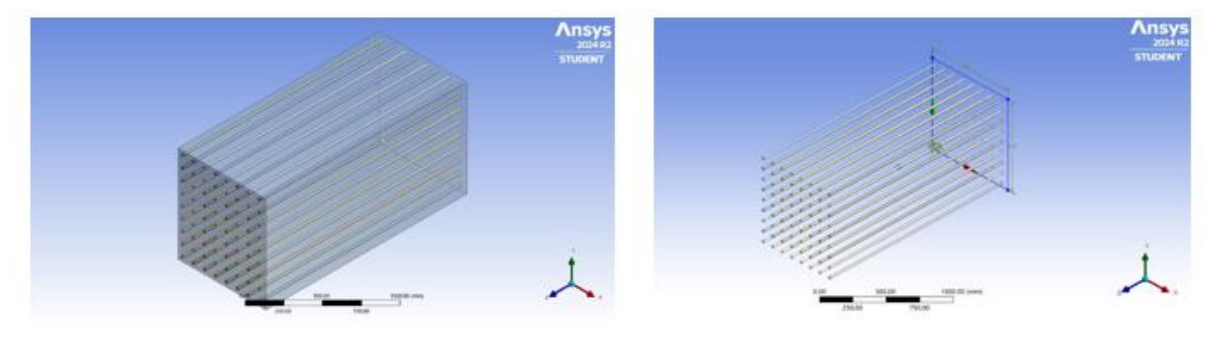


Fig. 44 3D model of tube arrangement

2.5 Results and Analysis

The final part of the analysis was to analyze the results. Under this, results, analysis of various aspects of different domains, streamlines, contours, vectors, and volume rendering as per the requirements. Since the main parameter of consideration is the temperature of the water pipe outlets, more analysis was done on the water side analysis. Also, the flue gas output temperature variation was also monitored to make sure the temperature doesn't drop below the acidic dew point. Some of the screenshots of the analysis results are listed below.

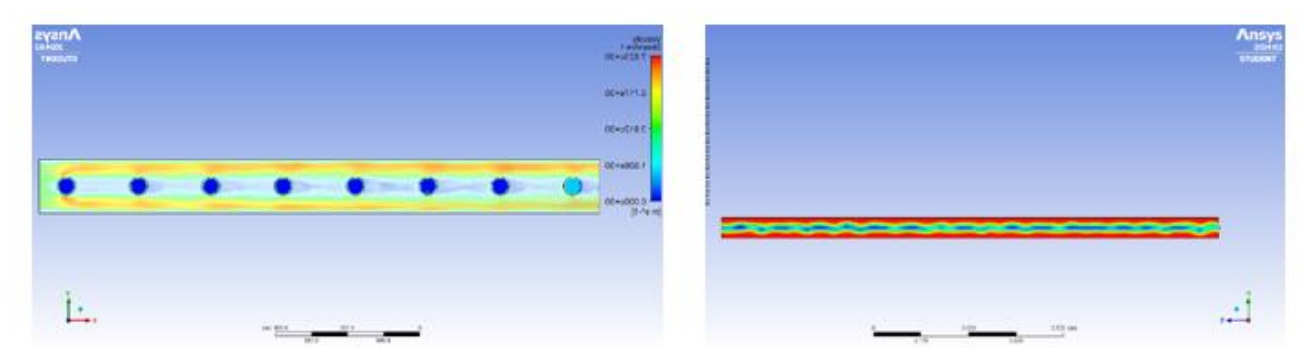


Fig. 55 Temperature contours of the water pipe outlet and the flue gas outlet face

The variation of each tube is tabulated, and the variation is further illustrated in a graph, and to show the variations clearly, the axis range for temperature was selected from 350 K to 470 K. The variation is shown in Fig. 6.

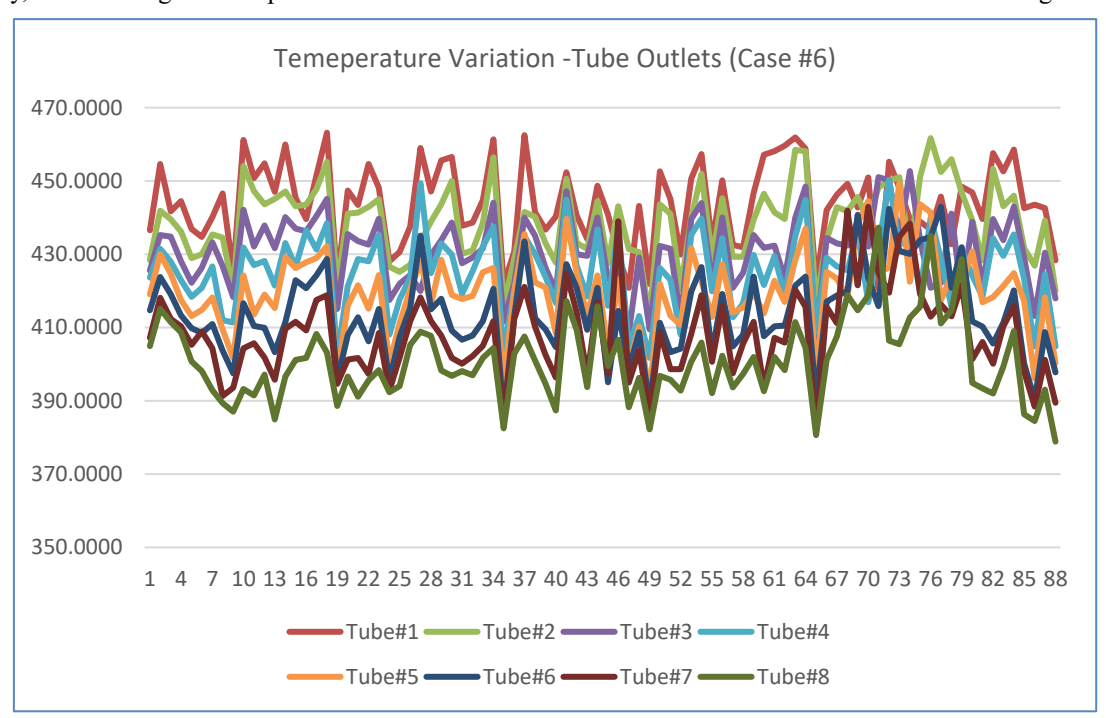


Fig. 66 Variation of temperatures in the tube's outlets

2.6 Boiler Efficiency Improvement Calculation

The efficiency improvement due to feedwater preheating was calculated by quantifying the energy saved per unit time:

$$E_S = m_{feedwater} X c_{water} X \Delta T$$

where $m_{feedwater}$ =536 kg/h, c_{water} =4.26 kJ/kg°C, and ΔT is the increase in feedwater temperature, approximately 39.5 °C.

The improved boiler efficiency was then calculated as [3]:

$$Efficiency\ Improvement = \frac{E_S}{Total\ Energy\ Input\ from\ Fuel}\ X\ 100$$

This approach allowed for a direct comparison between pre- and post-economizer energy use, showing a projected efficiency improvement of 2.13%.

2.7 Economic Feasibility Analysis

To assess economic viability, a cost-benefit analysis was performed. Monthly fuel savings were calculated using the reduced fuel consumption rate, estimated at approximately 4,067 liters. Given the current cost of furnace oil, these savings translate into a monthly financial saving of around LKR 833,847.

The payback period was calculated as:

$$Payback \ Period = \frac{Initial \ Investment \ Cost}{Annual \ Savings}$$

The initial cost of installing the economizer was budgeted at 4.5 million LKR, resulting in a projected payback period of 1.1 years, confirming the financial feasibility of the project. The sensitivity analysis further validated this feasibility under varied flue gas temperatures and feedwater flow rates, confirming consistent fuel savings across different operational scenarios.

3 Results

The study's results highlight the effectiveness of the waste heat recovery economizer in improving boiler efficiency, reducing fuel consumption, and delivering substantial cost savings. This section provides detailed insights into the feedwater temperature increase, boiler efficiency gains, monthly and annual fuel savings, economic feasibility, and performance robustness under varying operational conditions.

3.1 Increase in Feedwater Temperature

The implementation of the economizer resulted in a significant increase in feedwater temperature, improving preheating efficiency. With an initial average feedwater temperature of 92°C, the economizer was able to raise the temperature to approximately 127.1°C. This temperature increment of 35.1°C was achieved by effectively recovering waste heat from the flue gases, which entered the economizer at 280.5°C and exited at a controlled temperature of 170°C. This preheating reduced the energy required to bring the feedwater to the boiling point, directly impacting fuel efficiency.

The rise in feedwater temperature was consistently maintained across various steam loads, validating the economizer's capability to provide stable heat transfer under fluctuating operational conditions. The sustained temperature increase indicates that the economizer design, including tube arrangements and material selection, met the required thermal transfer objectives.

3.2 Improvement in Boiler Efficiency

The preheating of feedwater using recovered heat led to a quantifiable improvement in boiler efficiency. The economizer raised the boiler efficiency by an estimated 2.13%, from a baseline of 77.8% to approximately 79.9%. This efficiency gain was calculated based on the energy saved per hour due to the economizer and total energy input. The improved efficiency directly contributes to reducing fuel consumption and operational costs, underscoring the value of waste heat recovery in industrial settings.

This efficiency increase aligns with industry standards for economizer performance, validating the design and implementation strategy. The gain in efficiency not only reduces fuel dependency but also contributes to lowering greenhouse gas emissions, thereby supporting sustainability goals.

3.3 Monthly and Annual Fuel Savings

The efficiency improvements facilitated by the economizer translated to substantial monthly and annual fuel savings. With the economizer in operation, the boiler system demonstrated an average reduction in furnace oil consumption of approximately 4,067 liters per month. This reduction was calculated by comparing fuel usage before and after economizer implementation, factoring in the decreased energy required to heat the preheated feedwater.

Annually, this equates to a fuel saving of approximately 48,804 liters. Given the current cost of furnace oil, the monthly savings amount to LKR 833,847, translating into an annual cost reduction of nearly LKR 10 million.

These savings represent a significant financial impact, reducing the operational burden of fuel expenses and contributing to overall profitability.

3.4 Economic Feasibility Analysis

A cost-benefit analysis was conducted to assess the project's financial viability. The initial investment cost for the economizer system, including installation, materials, and labor, was budgeted at approximately LKR 4.5 million. Based on the calculated annual savings, the payback period was estimated to be 1.1 years. This rapid payback period demonstrates the project's economic feasibility, providing a strong return on investment for the facility.

The short payback period is advantageous for industrial applications, where capital investment decisions are often influenced by quick returns. With continued operational savings beyond the payback period, the economizer installation is expected to deliver long-term cost benefits while supporting energy efficiency objectives.

3.5 Sensitivity Analysis and Robustness of Performance

To ensure the reliability of the economizer's performance under varying conditions, a sensitivity analysis was conducted. This analysis assessed the economizer's effectiveness under different operational scenarios, including fluctuations in flue gas temperatures and feedwater flow rates. Key findings from the sensitivity analysis include:

- Variation in Flue Gas Temperature: When flue gas inlet temperatures varied by ±10°C, the economizer continued to achieve effective preheating, with feedwater temperature increases ranging from 33.5°C to 36.8°C. This result indicates the economizer's ability to perform consistently even when the waste heat input fluctuates.
- Fluctuations in Feedwater Flow Rate: Changes in feedwater flow rate by ±5% impacted the economizer's efficiency, slightly altering the exit temperature of feedwater. However, these variations had a minimal effect on the overall fuel savings, confirming that the economizer's performance remains stable under normal operational variability.

The sensitivity analysis highlights the robustness of the economizer design, ensuring reliable performance across a range of conditions typical of industrial steam generation systems. This adaptability further reinforces the system's suitability for industrial applications, where operational demands may vary.

3.6 Environmental Impact

In addition to economic benefits, the fuel savings achieved through improved boiler efficiency contribute to significant environmental gains. By reducing fuel consumption, the facility can lower its greenhouse gas emissions, aligning with sustainability and environmental compliance standards. The economizer's ability to reduce fossil fuel dependency supports corporate environmental goals, contributing to a reduction in the facility's overall carbon footprint.

In summary, the results indicate that the economizer provides substantial financial, operational, and environmental benefits. Its impact on boiler efficiency, fuel savings, economic feasibility, and environmental sustainability establishes a strong case for the adoption of waste heat recovery systems in industrial settings.

3.7 Summary of Analysis

A summary of results and analysis is tabulated in the table below.

Table 2 Summary of analysis and results

Parameter	Before Installing the	After Installing the	
	Economizer	Economizer	
Average Feedwater temperature (°C)	92	131.5	
Average SFR (kg steam/ l fuel)	13.39	15.54	
Boiler Efficiency (%)	77.8	80.03	
Average Monthly Fuel Saving (Liters)	-	4,067	
Average Annual Fuel Saving (LKR)	-	10 million	
Payback Period (years)	-	1.1	

4 Discussion

The findings of this study emphasize the substantial benefits of waste heat recovery for improving boiler efficiency in an industrial setting. By implementing a crossflow economizer, the facility achieved a notable reduction in fuel consumption, alongside financial and environmental gains. This section interprets the results in light of industry practices and explores the broader implications of these improvements.

4.1 Efficiency Improvement and Environmental Impact

According to the thumb rule of the industry, 6 °C rise in feed water temperature brought about by economizer recovery corresponds to a 1% saving in boiler fuel consumption. In the study, it was observed around 35 °C increment in feedwater temperature. According to the thumb rule, there should be an increment of 5% boiler efficiency. But in this study, there was a 2.13% increment in boiler which is lower than the thumb rule. Since the average feedwater temperature was studied only with four selected cases among the ten initially selected cases, the obtained value would not be the actual average. Hence further analysis is required to fine tune the boiler efficiency. In the commercial version of the analysis software, it is possible to design the boiler itself and do the analysis. It is recommended to do the same analysis in future studies.

4.2 Practical Implications for Industrial Energy Management

This study reinforces the practical feasibility of adopting waste heat recovery measures in steam generation systems. By integrating an economizer, the facility aligns with best practices in industrial energy management, optimizing resource use while achieving sustainability goals. The findings suggest that similar facilities could achieve comparable benefits by implementing waste heat recovery solutions tailored to their specific operational requirements.

4.3 Consideration of Pressure Drop

While this study primarily focused on improving boiler efficiency through thermal performance analysis of the economizer, the pressure drops across the system were not explicitly considered. Pressure drop is a critical factor in heat exchanger design, as excessive resistance to fluid flow can impact the overall system performance, requiring additional energy to maintain flow rates. Future iterations of this study could incorporate pressure drop calculations to refine the economizer design further. This would involve analyzing the fluid flow dynamics on both the flue gas and feedwater sides to ensure minimal resistance while maintaining efficient heat transfer. Specifically, the following aspects should be evaluated:

- Impact on boiler feedwater pumps
- Flue gas flow resistance
- Optimized tube and bundle configuration

Incorporating pressure drop analysis into future designs would provide a more comprehensive assessment of the economizer's performance and ensure that both thermal and mechanical efficiencies are optimized.

5 Conclusion

This study demonstrated the significant benefits of implementing a waste heat recovery economizer to improve boiler efficiency in an industrial food manufacturing facility. By capturing waste heat from flue gases to preheat feedwater, the economizer effectively enhanced the steam generation process, leading to an estimated 2.13% increase in boiler efficiency. This efficiency gain corresponded to a monthly fuel saving of approximately 4,067 liters, resulting in an annual cost reduction of around LKR 10 million. The economic analysis confirmed the project's financial feasibility, with a payback period of just 1.1 years, underscoring the strong return on investment for the facility. Moreover, the sensitivity analysis revealed the economizer's adaptability to operational fluctuations, highlighting its reliability under various steam demand scenarios.

In conclusion, the implementation of an economizer represents a viable, economically sound solution for reducing energy costs and emissions in steam generation systems. This study not only supports the adoption of waste heat recovery practices in the food manufacturing sector but also serves as a model for similar facilities aiming to improve energy efficiency and sustainability.

References

[1] X. Qian, S. W. Lee and Y. Yang, "Heat Transfer Coefficient Estimation and Performance Evaluation of Shell and Tube Heat Exchanger Using Flue Gas," *Processes*, 2021.

- [2] A. Bahadori, "Estimation of combustion flue gas acid dew point during heat recovery and efficiency gain," *Applied Thermal Engineering*, vol. 31, no. 8, pp. 1457-1462, 2011.
- [3] R. K. Sinnott, Coulson & Richardson's chemical engineering. Vol. 6, Chemical engineering design, Oxford: Elsevier Butterworth-Heinemann, 2005.
- [4] F. P. Incropera, D. P. Dewitt, T. L. Bergman and A. S. Lavine, Fundamentals of heat and mass transfer, John Wiley & Sons, 2007.
- [5] A. Zukauskas, "Heat Transfer from Tubes in Crossflow," *Advances in Heat Transfer*, vol. 8, pp. 93-160, 1972.
- [6] "Mild Steel Density Strength Hardness Melting Point," [Online]. Available: https://material-properties.org/mild-steel-density-strength-hardness-melting-point/.
- [7] "Flue gases properties table," 15 10 2024. [Online]. Available: https://www.pipeflowcalculations.com/tables/flue-gas.xhtml.
- [8] ANSYS, "16.5. Modeling Heat Exchangers," 26 October 2024. [Online]. Available: https://ansyshelp.ansys.com/public/account/secured?returnurl=/Views/Secured/corp/v242/en/flu_ug/flu_ug sec bc hex.html.
- [9] "Heat Transfer LMTD Correction Factor Charts," [Online]. Available: https://checalc.com/solved/LMTD_Chart.html#google_vignette.

FIRST

International Conference on Circular Economy and Sustainable Ecosystem

2024

Unlocking the Potential for Green Recovery

November 21 and 22, 2024 Colombo, Sri Lanka

www.eusl.edu.lk/ic2ese/











